An Endeavor in Receptor Design for Solid State Recognition of Anions/Hydrated Anions

A Dissertation Submitted for Partial Fulfillment for the Degree of

Doctor of Philosophy

by

Md. Najbul Hoque

(Roll No. 10612226)

Thesis Supervisor

Prof. Gopal Das

Department of Chemistry

Indian Institute of Technology Guwahati

May – 2015

This thesis is dedicated to my

Grandmother and my wife.

For their endless love, support and

encouragement

INDIAN INSTITUTE OF TECHNOLOGY GUWAHATI

Department of Chemistry

STATEMENT

I do hereby declare that the matter embodied in this thesis is the result of investigations carried out by me in the Department of Chemistry, Indian Institute of Technology Guwahati, India, under the guidance of Dr. Gopal Das, Professor (Department of Chemistry), Indian Institute of Technology Guwahati, India.

In keeping with the general practice of reporting scientific observations, due acknowledgements have been made wherever this work is based on the findings of other investigators.

May, 2014 (**Md. Najbul Hoque**)

IIT Guwahati

INDIAN INSTITUTE OF TECHNOLOGY GUWAHATI

Department of Chemistry

CERTIFICATE

This is to certify that Md. Najbul Hoque has been working under my supervision since July, 2010 as a regular registered Ph. D. student. His thesis entitled **"An Endeavor in Receptor Design for Solid State Recognition of Anions/Hydrated Anions"** is an authentic record of the results obtained from the research work carried out under my supervision in the Department of Chemistry, Indian Institute of Technology Guwahati, Assam, India. I am forwarding his thesis to submit for the award of degree of Doctor of Philosophy, from this institute. I certify that he has fulfilled all the requirements according to the rules of this institute regarding the investigations embodied in his thesis and this work has not been submitted elsewhere for a degree.

Dr. Gopal Das
(Thesis Supervisor)
Professor
Department of Chemistry
IIT Guwahati
Assam - 781 039, India

Acknowledgement

While writing this section after much exhausted period hoping to be refreshed, but practically I have become more mentally tired as I had to go through all the memories (almost all alive) left throughout the journey where each acquaintances put a brick to make stairs to which I have climbed up to this level. First of all I would like to recognize my parents who has been a source of encouragement and inspiration to me throughout my life. I specially thanks my parents for not having any pre-planned ambitions about me for what I enjoyed every aspect of my childhood by skipping traditional education process. To my mom who has no education, took me to school in unorthodox manner as she had to fight for it with others. I wish to express sincere gratitude towards my PhD supervisor Prof. Gopal Das. His wide experience, deep understanding and personal guidance have given me freedom to think, plan and execute my ideas to develop the quality of work throughout the process. Specially I would like thank him for unique style in leading the group which are reflected in happy faces of the group members.

Besides my supervisor, I would like to thank my doctoral committee members, Prof. Manabendra Roy, Dr. Lal Mohan Kundu, Dr. Chandan Mukherjee for their meaningful comments and suggestions. I owe my gratituted to head of department of chemistry of IIT Guwahati, Professor A. Chattapadhya (ex-head) and B. K. Patel for providing me necessary facilities. I wish to acknowledge departmental stuff for their cooperation.

I really had wonderful time working very friendly in lab where passing millions of hours was just simply matter of few cup of tea, many jaw cracking jokes and discussing many baseless topics. I have always felt very lucky that I got wonderful seniors like Bimlesh da, bedo da, Sandeep da, Arghya da, Jiban da, Chirantan da, amazing friend like Romen, Abhijit and extraordinary juniors like Barun, Soham, Nilotpal, *Utsab, Rupinder*. It will be incomplete if I do not mention Sandeep da and Arghya da like mentor and friend who taught me the basics of lab techniques and contributed to the work in greater extent from many aspects, without your support I would have given this up a long time ago.

I also owe my obligations to my other seniors, batch mate and juniors of PhD fraternity of chemistry department for their help and support. I will always appreciate rarely observed the friend like sukhamoy Gorai with big heart and sensible thoughts that cherished me the togetherness for few years.

I take this opportunity to thank my friends Jhony, Baby, Belly, Saddam, Masadul, Asraful, pinki, Sajbul, Rajbul, Amzad, Romen, Atanu, polash, Santunu, Joshi, Pryiobrata, Surjendu, Sourov, Main Mustafi, Koushik, Rakib, Ezaz, Hasan, Azim, Alimuddin for being a source of encouragement and love throughout the time. No word would suffice to thank my M. Sc friends like Jayanta, Kashi, Soumen, Bijoy, Arun and Aritra for their unconditional support and love during the tough hurdle in IIT-Delhi.

A great momentum is waved after meeting my friend, lover and wife pinki, who suddenly brought huge flash in my life and I discovered many hidden joys. I hold her faithful hands and crossed many toughest phases of my life. Her calm heart, soft voice and smiley face makes me happy even in frustrating times. All these will be meaningless, if I do not express my dedication to the best gift in the world, my ten months old son *RAVIV*. His smiley face, soft fingers and loud shout keeps me away from any stresses and tensions. Interestingly every evening two-three hours running with high level of energy irrespective of any situation washed away all the laziness I gained from the whole day.

I would like pay my appreciation to my *Bhabi* (Ity) who is the actual cause of everything what I have archived till today. As my carrier turned surprisingly in new direction just after her suggestion in opting science group in place of arts group (that I studied already for 2 months) in 12^{th} standard. It is impossible to me to cost that kindness.

To my parent-in-law, known only briefly but loved and missed. They has been continually supportive and gave me very homely staying with great care.

I extend my feelings for my teachers to whom I owe debt for their kindness and benevolence; Azad Sir, Laltu sir, Abhijit sir, Paltu sir, Debprasad sir, Safollo sir, Nittya Gopal Sir, Partha sir, Subhajs sir and many others from my school, college and university who gave me the direction and insightful information to march forward in this field. I am highly indebted to Laltu sir who taught me and gave many books with free of cost; Debprasad sir who helped in cracking *JAM* by economically and mentally.

People from my village who are the main source of all inspiration and motivation; I am greatly indebted to them for affection and bless.

I have been benefited by many extended hands and difficult to summarize within few pages. So I am sorry that still many names are missing whose contribution and help is worth mentioning.

najbul

SYNOPSIS

The contents of this thesis entitled **"An Endeavor in Receptor Design for Solid State Recognition of Anions/Hydrated Anions"** have been divided into seven chapters based on the results of experimental work carried out during the research period.

Chapter 1: Introduction

This chapter provides a brief introduction on '*supramolecular host-guest chemistry*' of ionic species with special reference to recognition of anions or hydrated anions. Supramolecular chemistry offer many possible avenues like recognition, catalysis and transport. Anions are ubiquitous in nature. Hence, molecular recognition of anionic species has attracted great interest during the last decades because of the imperative role in various biological and environmental processes. Extensive research effort has been expended toward understanding how host structure influences anion binding with the goal of discovering more effective and more selective anion receptors. A very large number of artificial systems for recognition and sensing of anions have been designed and synthesized by properly exploiting supramolecular concepts. One successful approach for preparing anion hosts has been to synthesize molecules that offer an array of H-bonding sites to the guest. Because H-bonds exhibit directionality, it should be possible to achieve a structure-based recognition for anions of particular shape and size. The binding of anion guests within preorganized macrocyclic systems is relatively more predicated easy to understand supramolecular association but the binding processes of acyclic receptors is unpredictable and very tough to control due to freedom of many conformation. Hence it is great challenge to study receptor-anion assembly of flexible acyclic receptor. Sometimes specially design acyclic receptor forms capsular assemblies which have shown a number of interesting properties e.g. encapsulation of anion/anion–water clusters, capturing aerial CO_2 as carbonate, selective salt extraction and anion transportation. On the other hand, Understanding the hydration of anions at the molecular level is thus important as the surface speciation and reactivity of aerosols, which play a key role in atmospheric and oceanic chemical cycles. The characterization of an isolated solvated ion serves to add to information about the solvation properties. As the properties of hydrated ions are quite

different from those of isolated ions (in the gas phase) or ions in nonpolar media and are governed by the nature of the surrounding hydration network.

Chapter 2: Experimental Methods and Characterization

Chapter **2** describes detailed report of the various reagents used in the synthesis of the receptors, their synthetic procedures, crystallization details, binding study and specifications of analytical instruments employed in the characterization of synthesized receptors and their various complexes.

Chapter 3: Linear Pyridine-Urea Receptor and Its Interaction with Hydrated Anions: Effect of positional isomer

In this chapter, the preparation of three isomeric pyridine-urea based receptors (^{o}**L$_1$**, ^{m}**L$_1$** and ^{p}**L$_1$**) and their anion complexation study in presence of inorganic acid has been described. The receptor is enriched with urea as H-bonding site and pyridine as a protonation site. Three isomers behave distinctively on treatment with acids. Upon acidification with H_3PO_4 results three different assembles of anion or anion-water cluster. Formation of stable discrete water hexamer and hybrid iodide-water cluster $[I_4\text{-}(H_2O)_6]^{4-}$ containing a tetrameric core of either water or iodide water respectively, infinite sulfate-water chain containing chair like sulfate-water hexamer $[(SO_4)_2\text{-}(H_2O)_4]_\infty^{4-}$, infinite chain of dihydrogen phosphate–water trimer $[(H_2PO_4)_2\text{–}H_2O]_\infty^{2-}$ and a simple perchlorate-water chain has been observed by *ortho* isomer. Whereas *meta* isomer gave simple 1-D infinite $[HPO_4]_\infty^{2-}$ chain. The *para* isomer stabilizes infinite chain of 1-D tetrameric cluster $[(SiF_6^{2-})_2\text{-}(H_2O)_2]_\infty^{4-}$, nitrate-water cluster $[(NO_3)_2\text{-}(H_2O)_6]_\infty^{2-}$ containing two fused rings, assembly of phosphate-water with minimum repeating unit $[(HPO_4^{2-})_2\text{–}(H_2O)_3]^{4-}$ and perchlorate-water cluster. Depending upon position of N-atom in the pyridine moiety, it offers various types of anion-water combination. Notably various conformation of the receptor and projection of urea hydrogen is observed while binding of anions occured. In all cases the anions are stabilized by N–H···O (urea NH and PyH^+), O···H_2O (lattice water), C–H···O and anion···π^+ interactions. Moreover other supramolecular interactions like anion···anion/anion–π^+ and π^+···π/ π^+···π^+ also play an important role in complexation and packing of molecules in the solid state.

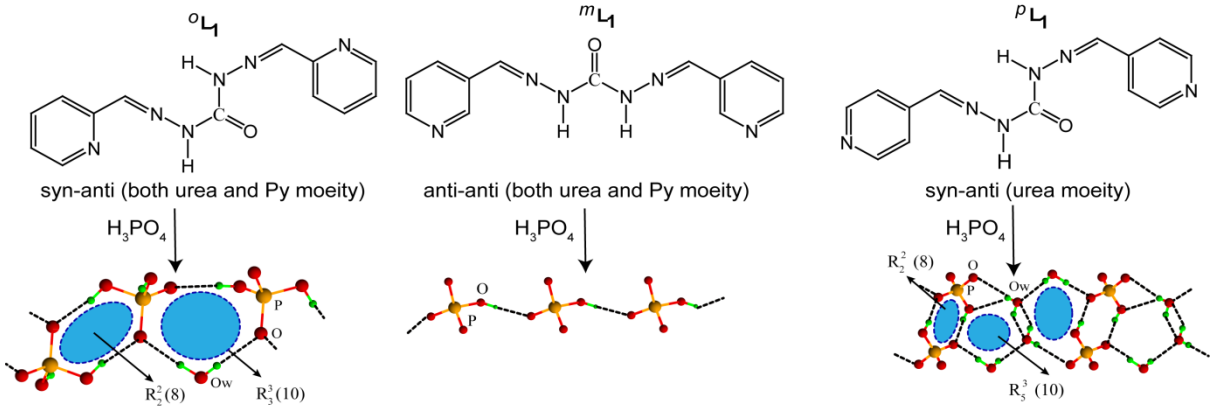

Scheme 1. A comprehensive representation of the research work presented in chapter 3.

Chapter 4: Aliphatic and Aromatic Capped Tripodal Receptors for Hydrated Anion Recognition: Effect of Ligand Flexibility

The key approach of this chapter is generating of multiple anions within a ligand framework and ligand structure directed anion-water assembly. Mercapto-benzimidazole substituted apical N-atom and benzene capped tripodal receptor **L2** and **L3** has been synthesized with three protonate site per molecule. The bowl shape and benzimidazole NH of the tripodal host offers suitable place and binding site favoring the formation of anion-water cluster. Two types platform remarkably affects the formation of anionic complex as well as anion-water aggregation. The N-atom based tripodal **L2** exclusively generate isostructural hybrid halide-water cluster ($[X_3(H_2O)_4]^{3-}$, X = Cl^-, Br^-) having cyclic pentameric puckered ring. The halide-water cluster is mainly stabilized by O–H···X^- and N–H···X^- H-bonds. Whereas benzene capped bowl shaped tripodal **L3** stabilizes infinite 1D water chain $[H_2O]_\infty$ and fluoride-water trimer $[F_2\text{-}(H_2O)_{0.5}]^{2-}$ or cyclic chloride water tetramer $[Cl_2\text{-}(H_2O)_2]^{2-}$ engulfed by the receptor and is governed by multiple non-covalent (hydrogen/halogen bond, CH···π and π···π) and electrostatic interactions. It is diprotonated (in spite of being three protonation sites) and form non-isostructural complex.

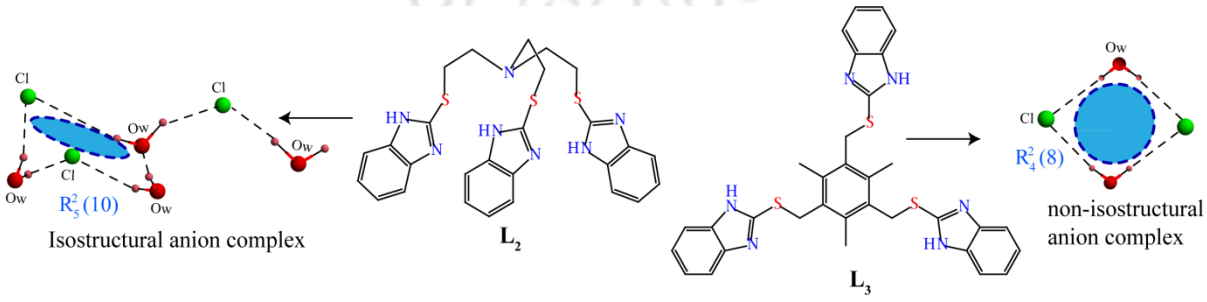

Scheme 2. A comprehensive representation of the research work presented in chapter 4.

Chapter 5: Hydrated Anion Glued Capsular and Non-capsular Assembly of a Tripodal Receptor

Chapter 5 describes the formation of capsular and non-capsular assembly of a newly synthesized polyammonium tripodal receptor **L_4**. The attachment of large number of H-bonding sites for the successful recognition of anions was introduced in this polyammonium based receptor.Highly effective anion receptors can be produced by combining electrostatics and hydrogen bonding; in fact our N_4 based receptor has multiple protonation sites able to contribute both. The receptor is highly efficient and form anion complex of widely spread like halide ions (F^-, Cl^-, Br^- and I^-) and oxyanions (NO_3^-, ClO_4^-, SO_4^- and $H_2PO_4^-$). Fluoride-water cluster and chloride ion belt mediated supramolecular assembly in bimolecular capsular fashion is established. On the other hand formation of non-capsular supramolecular association of the receptor is observed by chloride-water, bromide-water and iodide-water clusters. Moreover our observations underscore extended polymeric bromide-water cluster $[Br_5\text{-}(H_2O)_6]^{5-}$ having defined cyclohexane like chair conformation and discrete iodide-water cluster $[I_2\text{-}(H_2O)_4]^{2-}$ containing water tetramer in solid state. In case of oxyanion, infinite decameric dihydrogen phosphate cluster $[H_2PO_4^-]_{10}$ is reported. In addition, octahedrally arranged discrete anionic cluster $[Na(ClO_4)_6]^{5-}$, isolated discrete sulfate-hydrogen sulfate trimer $[SO_4\text{-}(HSO_4)_2]^{4-}$ and sulfate-water tetramer $[(SO_4)_2\text{-}(H_2O)_2]^{4-}$ is also described in solid state.

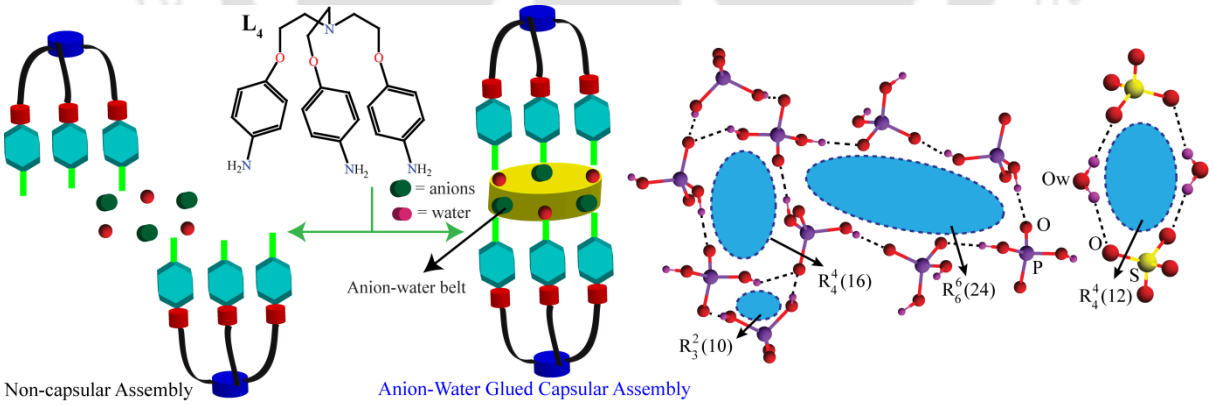

Scheme 3. A comprehensive representation of the research work presented in chapter 5.

Chapter 6: Anion Complexation with Cyanobenzoyl Substituted Tripodal Amide Receptors: A Comparative Study between First and Second Generation Receptor

Tripodal cyanobenzoyl appended triamide receptors with different length have been studied in this chapter. First generation tripodal receptor (**L_5**) and elongated second

generation tripodal (**L6**) was synthesized. Two receptors were exploited for comparative study of anion binding was also carried out in solid and solution state. The dimensionality and nature of the anions play a crucial role in making various molecular interactions possible in complexation of various anions in both receptors. The self-alignment and orientation of the flexible second generation tripodal is greatly influenced by the size and shape of the anion. The X-ray structure shows **L5** is internally locked and could not welcome anions into its C_{3v} symmetric cavity, shows side cleft anions binding. Positioning of amide functionality to a distant position with respect to apical N-atom results a bigger cavity and subsequently intimidate the N–H···O=C intramolecular H-bond unlike in **L5**. The receptor form quasi-planar arrangement of the arms, with two arms close each other while third arm pointing to opposite direction giving pseudo capsular complex during H-bonding interaction. Finally comparison of the recognition of anionic guests of different shapes/geometry and solid state organization of the two kind of receptor of varying podal length is done successfully. Interestingly anion induced reorientation of the receptor **L6** was observed during recognition of octahedral SiF_6^{2-} anion. In the solid state –CN group provide further stabilization to the supramolecular complexes through C–H···π and anion···π interactions. Moreover the solution state interaction phenomena of two receptors in neutral form with the anions of various shape and size like spherical (F^-, Br^-, I^-), planner (NO_3^-), tetrahedral (ClO_4^-) and octahedral (SiF_6^{2-}) by detailed ^1H NMR studies along with their molecular binding was thoroughly analyzed.

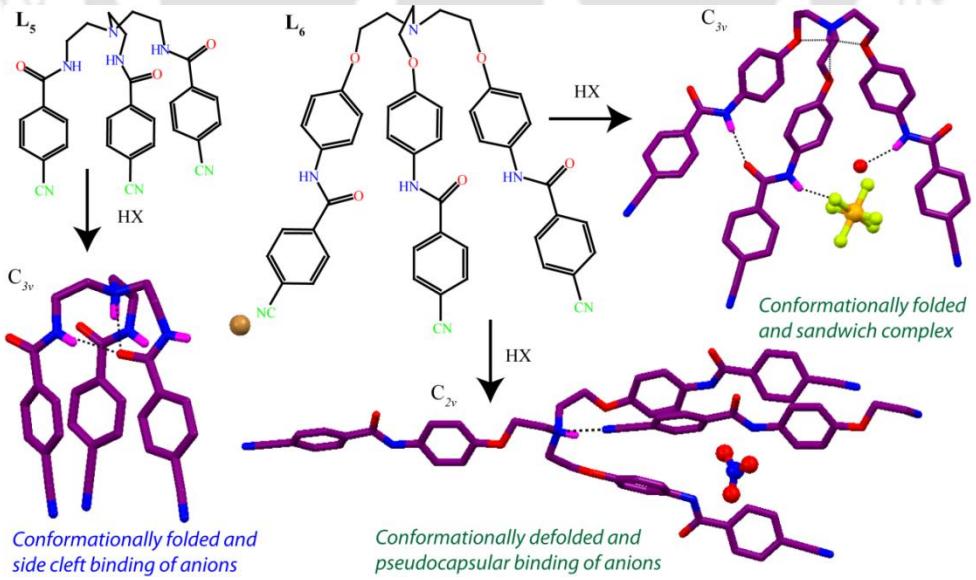

Scheme 4. A comprehensive representation of the research work presented in chapter 6.

Chapter 7: Hybrid Anion-Water Cluster Mediated Self-Assembly of Tripodal Polyammonium Receptor: Effect of Length of the Receptor

This chapter showed two polyammonium functionalized tripodal receptor for encapsulation of anions. Once observing the effect of length in the amide based receptors, subsequently two amine based receptors of different length has been synthesized. The amine group increase presence of multiple anions and acts as H-bonding source. These two receptors trap anions within its C_{3v} symmetric cavity. The first generation tripodal **L**$_7$ owing to have smaller inner space, it encapsulate the small anions like fluoride [F⊂**L**$_7$], whereas second generation tripodal **L**$_8$ allows bigger oxyanion like sulfate. The specially designed C_{3v} symmetric tripodal of having enough cavity, on protonation with sulfuric acid, successfully encapsulates hydrogen sulfate dimer in a unimolecular capsular fashion [$(HSO_4)_2$⊂**L**$_8$]. Such a big dimer inside the cavity is favored by H-bonding (NH···O) and electrostatic interactions among HSO_4^- and NH_2^+ ions. Moreover, by virtue of multiple anions exterior HSO_4^- ions and crystallized water molecules assembled into unique hybrid $[(HSO_4)\text{-}(H_2O)]_4^{4-}$ cluster having different cyclic motifs. The $[(HSO_4)\text{-}(H_2O)]_4^{4-}$ cluster and Cl···Cl halogen bond act as a template in the formation of unimolecular capsule [$(HSO_4)_2$⊂**L**$_8$].

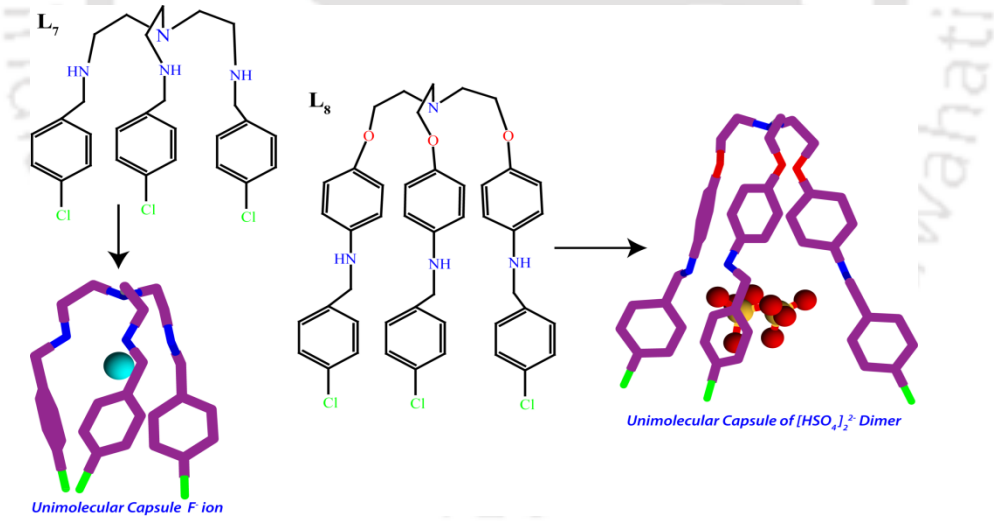

Scheme 5. A comprehensive representation of the research work presented chapter 7.

Conclusion

The concluding remarks on overall experimental works presented here may sound as the contribution to a vast wealth of anion recognition event. Solid state recognition of naked as well as hydrated anion by various synthetic receptors is relevant to biological systems which may open the opportunity of study of complex behavior of anions. Additionally it is

also instructive to know structural relationship of anion-water as solvated anion plays many roles in atmospheric chemistry and biology. All organic receptors contain at least one basic nitrogen atom which allows anion complexation with acid in protic solvent. Hence most of the anion complexes have inherent tendency to crystallize with at least one water molecule. This phenomenon renders the recognition of anion as a hydrated form with fascinating anion-water supramolecular architectures. Firstly pyridine-urea based three isomeric planar receptors $^{o}\mathbf{L_1}$, $^{m}\mathbf{L_1}$ and $^{p}\mathbf{L_1}$ which generate three different anion cluster $[(H_2PO_4)_2\text{-}H_2O]_\infty^{2-}$, $[HPO_4]_\infty^{2-}$ and $[(HPO_4)_2\text{-}(H_2O)_3]^{4-}$ respectively on treatment with H_3PO_4 acid. These receptors also stabilize other hydrated anions like $[(SO_4)_2\text{-}(H_2O)_4]_\infty^{4-}$, $[(SiF_6)_2\text{-}(H_2O)_2]_\infty^{4-}$ and $[(NO_3)_2\text{-}(H_2O)_6]_\infty^{2-}$ by N–H···O, O···H_2O, C–H···O and anion···π^+ interactions. The next receptors $\mathbf{L_2}$ and $\mathbf{L_3}$ were able to form capsular or noncapsular assembly in protonated state upon recognition of anion or hydrated anions. Thereafter synthetic modification of $\mathbf{L_4}$ lead to $\mathbf{L_5}$ and $\mathbf{L_6}$ having different length and cavity, effectively show side cleft and pseodu-capsular anion binding. Selective anion induced conformational change of $\mathbf{L_6}$ was observed in solid state. Secondly the ultimate outcome of ligand synthesis aiming of making big cavity for anions are done with $\mathbf{L_8}$ and $\mathbf{L_7}$ shows comparative study of effectiveness of cavity size. The $\mathbf{L_7}$ successfully encapsulate big anion like hydrogen sulfate dimer. Additionally the receptor stabilizes a big hydrogen sulfate-water cluster $[(HSO_4)\text{-}(H_2O)]_4^{4-}$. Small pocket of $\mathbf{L_8}$ is capable of encapsulating small anion like F^-.

Contents

Chapter 1

Introduction

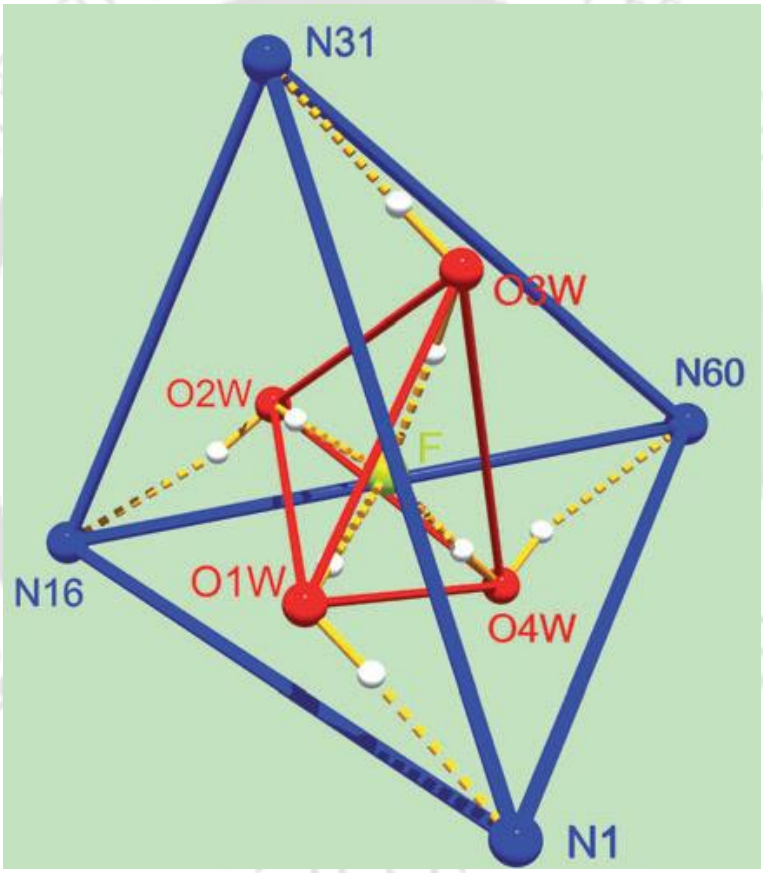

1.1 Supramolecular chemistry: An introduction

Supramolecular chemistry is the chemistry of the intermolecular bond, covering the structures and functions of the entities formed by association of two or more chemical species. Supramolecular chemistry may be defined as "chemistry beyond the molecule", bearing periodic assembly or regular arrangement of entities of higher complexity that result from the association of two or more chemical species held together by intermolecular forces.[1] Other definitions include phrases such as 'the chemistry of the non-covalent bond' and 'non-molecular chemistry'. It is concerned with the next step in increasing complexity beyond the molecule towards the supermolecule and organized polymolecular systems, held together by non-covalent interactions. While traditional chemistry focuses on the covalent bond, supramolecular chemistry examines the weaker and reversible non-covalent interactions between molecules. Many important aspect of chemistry have been nicely demonstrated that include self-assembly, folding, molecular recognition, host-guest chemistry. The emergence of supramolecular chemistry has a profound effect on how efficiently chemists prepare structures of different sizes and shapes. For the host-guest supramolecular chemistry there must be complementary interaction sites or host must have preorganized orientation for efficient guest binding. When host is preorganized, readjustment is needed to maximize complementarity. Host preorganization is a key concept because it represents a major enhancement in the overall free energy of guest complexation.[2] The study of non-covalent interactions is crucial to understanding many biological processes from cell structure to vision that rely on these forces for structure and function. Biological systems are often the inspiration for supramolecular research.

Supramolecular interactions (non-covalent interactions) might be roughly classified in the following categories like hydrophobic interaction, electrostatic interaction, H-bond interaction, van der Waals interaction, Ion–ion interactions and π···π stacking interactions. Among them the mostly discussed is hydrogen bonding interaction as the Hydrogen bonding is the most important directional interaction in molecular crystals.

1.2 Building Blocks and Concepts in Supramolecular Chemistry

Supramolecular systems are rarely designed from the principles. Rather, chemists have a range of well-studied structural and functional building blocks that they are able to use to build up larger functional architectures. Many of these exist as whole families of similar

units, from which the analog with the exact desired properties can be chosen. For example, use of crown ether binding with metal or ammonium cations, use π-electron and carboxylic acid for H-bonding. The complexation of bipyridines or tripyridines for construction of complex architectures. Cyclodextrins, calixarenes, cucurbiturils for supramolecular systems. Macrocycles are very useful in supramolecular chemistry, as they

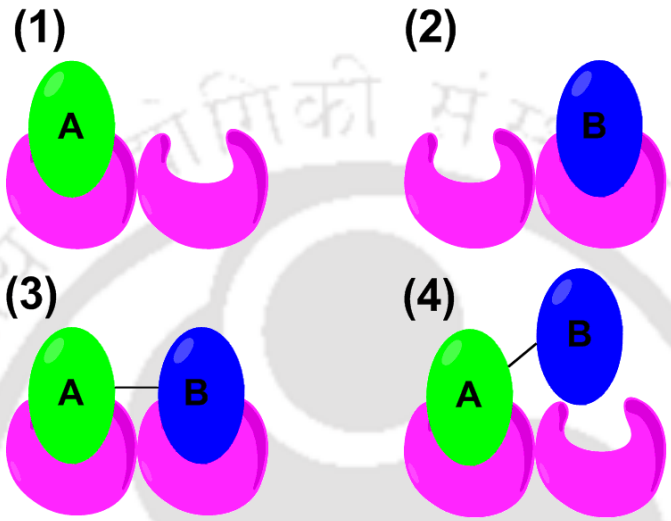

Scheme 1.2 General Host-Guest Binding. (1.) Guest A binding (2.) Guest B binding. (3.) Positive Cooperativity Guest A-B binding. (4.) Negative Cooperativity Guest A-B binding.

provide cavities for selective guest encapsulation. These building blocks have successfully been exploited in generating many aspect of supramolecular chemistry. Molecular self-assembly is the process where the molecules are directed to assemble through non-covalent interactions. Molecular self-assembly also allows the construction of larger structures such as micelles, liquid crystals, and is important to crystal engineering.[4] Molecular recognition is the particular binding of a guest molecule to a complementary host molecule to form a host-guest complex. The non-covalent interactions play big role in selective binding. Molecular recognition and self-assembly in ambient condition lead to template-directed synthesis which is considered special case of supramolecular catalysis.

1.3 Concepts in Anion Host Design

Anion coordination by synthetic receptors is a current research trend in supramolecular chemistry because of the vital roles in many natural, chemical, biological, and industrial

processes.[5] There are between 70-75% of enzyme substrate and cofactors contains anions (ATP and ADP). They play vital structural roles in many proteins, and are very important for manipulation and storage of genetic information (DNA and RNA are polyanions). Mobility of ions in ion channel through cell phospholipid bilayers is known to be mediated by a variety of channels and anion transport proteins with at least 14 mitochondrial anion transport system have been identified so far. These systems responsible for the trafficking of ADP, ATP, phosphate, citrate maleate, oxaloacetate, sulphate, glutamate, fumarate and halide anions. This "Hofmeister series" that ranks how ions affect protein solubility is remarkably reproducible for a wide variety of proteins and salts, with anions generally having a stronger effect than cations. Recently, several X-ray crystal structures have been solved that have allowed the direct visualization of enzyme–anionic substrate complexes

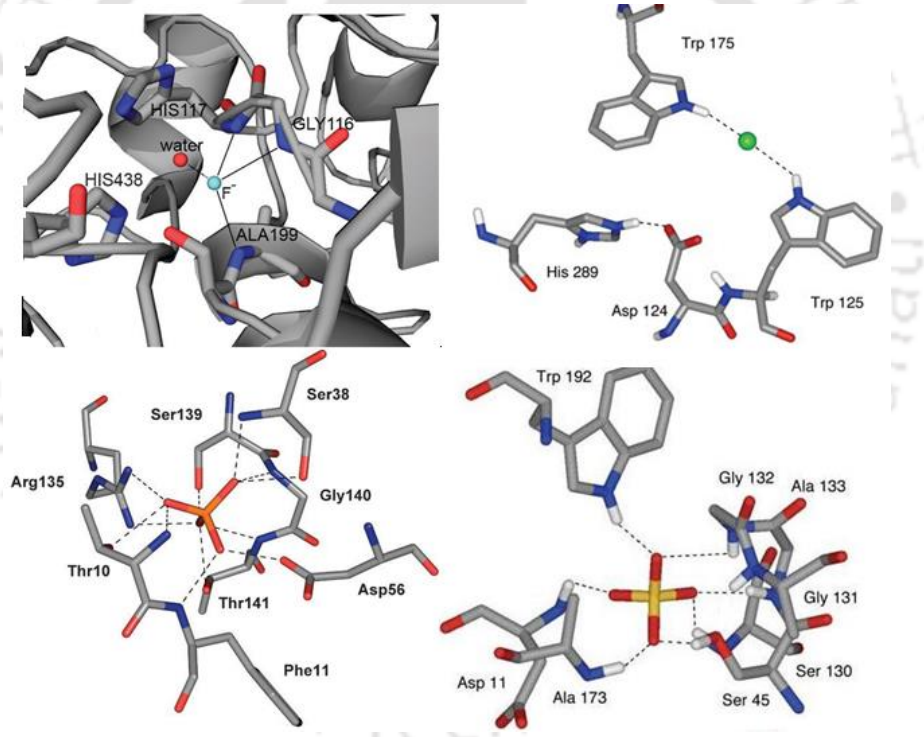

Figure 1.1 Anion binding in biology (a) Showing bound mono hydrated fluoride anion in human butyrylcholinesterase complex (PDB code = 2XMC). (b) Enzymatic active site of haloalkane dehalogenase the presence of a bound chloride anion. X-ray crystal structure of sulfate-binding protein. The sulfate anion is bound by seven hydrogen bonds from NH and OH bond donor group. (c) Showing binding mode of phosphate anion in phosphate-binding protein. (d) The sulfate anion is bound by seven hydrogen bonds from NH and OH bond donor group.

that are stabilized *via* multiple hydrogen-bonding interactions (Figure 1.1).[6] On the other hand recent developments in the field of new receptors for modes of binding, transport and extraction of anions, and sensing mechanisms has become important area in

supramolecular chemistry. Extensive research effort has been expended toward understanding how host structure influences anion binding with the goal of discovering more effective and more selective anion receptors to achieve these much needed goals. Among the numerous design choices, organic frameworks has led practical developments concerning anion binding. As anions are inherently negatively charged, an intuitive way of achieving anion binding is by the employment of positively charged species and ammonium groups have been widely used for this purpose. However, pyrrole, indole, amide and urea functions have been the subject of intensive investigations for its performance in the construction of neutral anion receptors *via* favourable hydrogen bonding interactions.[7]

1.4 Solid State Recognition of Anions/Hydrated Anions

Although Nature exemplify how proteins can selectively and efficiently bind anions by being fundamental in determining binding selectivity *via* topological complementarity. Due to larger size and variety in shape and geometry attracts special attention for design of receptors. In particular, recognition of discrete ordered anion-water clusters is more challenging, because anions in their hydrated form are highly random and display a wide range of complicated interactions due to spontaneous formation of strong stable hydrogen bonds in an aqueous environment. Many natural processes occur in aqueous media. Hydration of inorganic anions has been an interesting subject in solution chemistry and biochemistry.[8]

1.4.1 Benzimidazole based acyclic receptors for anions/hydrated anions

A simple benzimidazole based receptor **1** designed with protonation sites is found to stabilize a chloride-water chain by N−H···O, C−H···π and π···π interactions (Figure 1.2a).[9] Another reports highlight a MOF of copper-pyridine carboxylic acid encapsulate a square pyramidal shaped discrete chloride-water cluster $[Cl\text{-}(H_2O)_4]^-$ within its channel.[10] The carboxylic groups do not coordinate the copper centers. The channels of the cationic framework are occupied by $[Cl\text{-}(H_2O)_4]^-$ clusters (Figure 1.2b) and anchored to the channel walls by strong hydrogen bonds between the free COOH groups and the water molecules. The chloride sits on the 4-fold rotation axis passing through the center of the channel and interacts with the four water molecules within the cluster. The isomeric metal complex shows the stabilization of the 1D water–chloride chain assembly in the ion channel of the supramolecular hosts.[11] The network involves three lattice water molecules

together with the chloride ion to form a cyclic hydrogen-bonded water trimer (Figure 1.2c). Safari and coworkers have also isolated a hydrated discreet bromide-water cluster in a metal complex.[12] The cubane like bromide-water cluster $[Br_2\text{-}(H_2O)_6]^{2-}$ where the bromide ions occupy opposite vertices of the cube. The striking feature of this cluster is

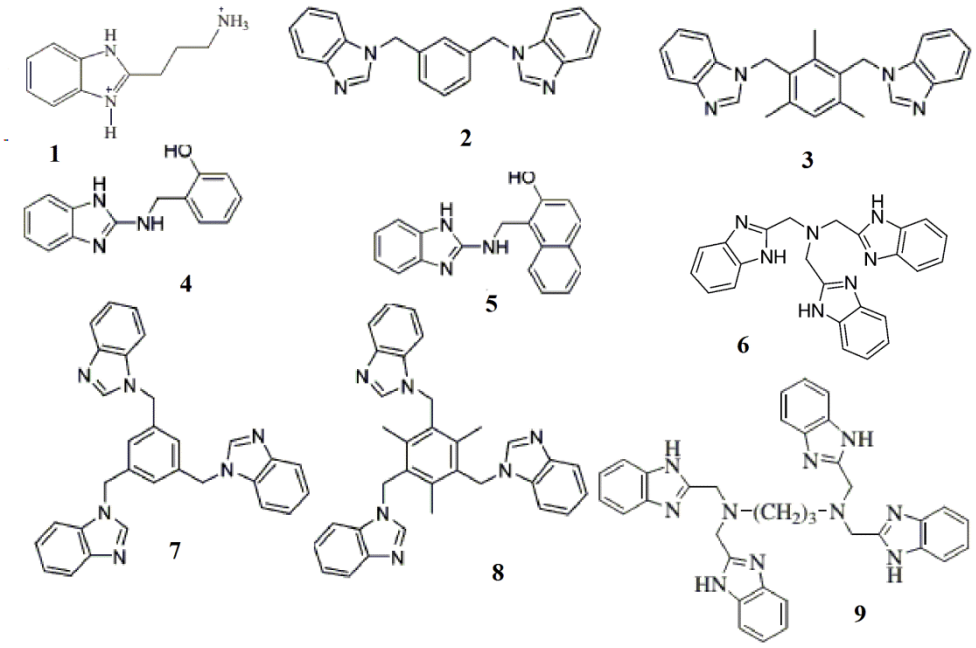

Scheme 1.3 Molecular structures of receptor containing benzimidazole as a protonation and H-bonding site.

that every bromide anion connects with three water molecules and every water molecule is linked by two bromide anions and two H_2O *via* H-bonds. Each oxygen atom has two hydrogen bonds to an oxygen atom and a bromide ion and one hydrogen bond from an adjacent oxygen atom on the same edge. A Chair-like $[(ClO_4)_2\text{-}(H_2O)_2]^{2-}$ cluster is formed by two symmetric equivalent free water molecules and two perchlorate anions.[13] A great deal of attention has especially been paid to understanding for solid state recognition of anions as well as hydrated anions. P. Ghosh and coworkers have shown an interesting example of anion binding by the mixture of **3** and **7** forms a new assembly of these receptors by encapsulating 14 water molecules and 8 ClO_4^- ions (Figure 1.2f).[14] Detailed structural analysis showed that protonated benzimidazolium units are hydrogen bonded with water molecules rather than perchlorate ions. The tripodal receptor **8** stabilize I^-, NO_3^-, and ClO_4^- anion. Two benzimidazole-based receptors **4** and **5** form crystalline salts on treatment with various acids. Structural analyses show that the anion binding in complexes is attributable entirely to $NH^+\cdots$anion, NH$\cdots$anion, and multiple CH$\cdots$anion hydrogen bonding interactions. The tetrahedral dihydrogen phosphate anion

forms a polymeric inter anionic chain structure with **4**, and the other tetrahedral hydrogen sulfate anion forms hydrogen sulfate–(water)$_2$–hydrogen sulfate adducts with charged receptor **5** (Figure 1.2g and 1.2h).[15] Another benzimidazole based tripodal **6** form supramolecular complexes with various organic acids.[16] A organic receptor **9** having four benzimidazole

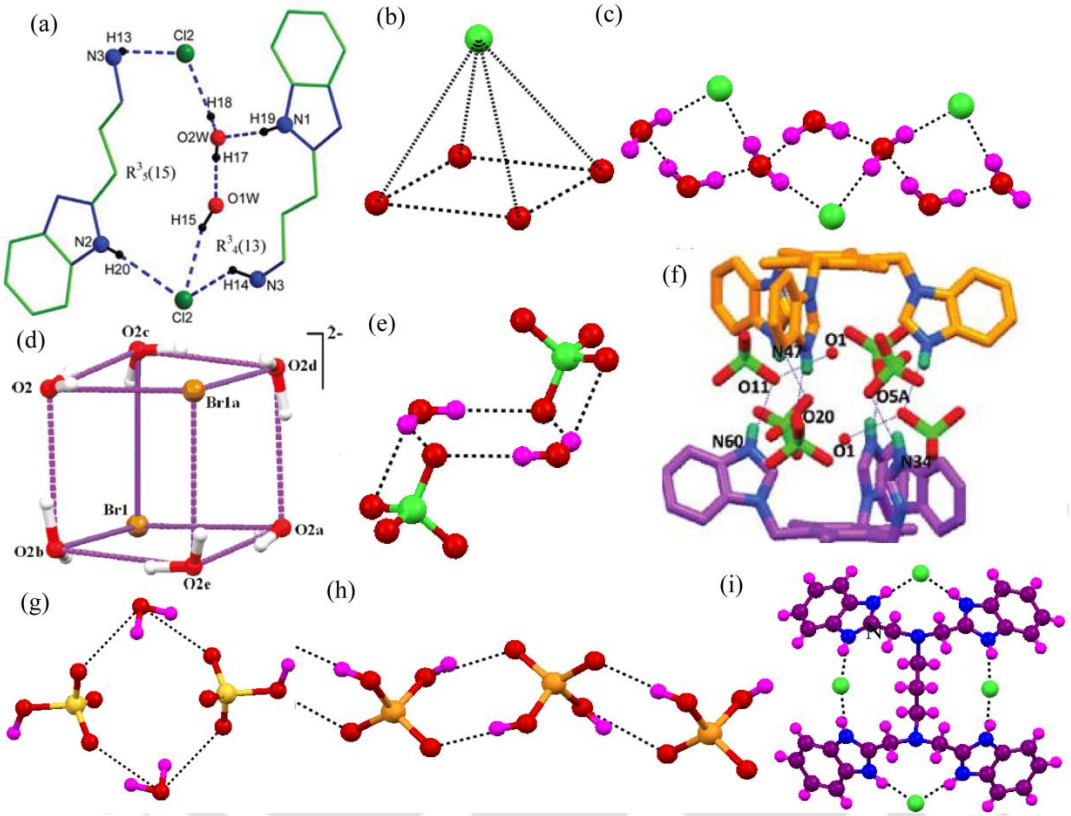

Figure 1.2 (a) A chloride-water chain found in complex of **1**. (b) square pyramidal shaped chloride-water cluster $[Cl\text{-}(H_2O)_4]^-$. (c) 1D water–chloride chain assembly. (d) cubane like bromide-water cluster $[Br_2(H_2O)_6]^{2-}$ (e) Chair-like $[(ClO_4)_2\text{-}(H_2O)_2]^{2-}$ cluster. (f) Perchlorate-water assisted capsular assembly of receptor **8**. (g) $HSO_4\text{-}(H_2O)_2\text{-}HSO_4$ cluster in complex of **5**. (h) infinite $[H_2PO_4]$ dimer assembly in receptor **4**. (i) Chloride coordination by tetrapodal receptor **9**.

moiety generates highly ionic environment on acidification and generates various organic salts with spherical to tetrahedral anions.[17] They have reported the anion directed supramolecular framework. The work demonstrates that the variation of anion plays a significant role in controlling the structure of the salts. The benzimidazole NH as well as the protonated NH are mainly involved in the extensive H-bonding and various NH···π, CH···π are also key contacts around anions (Figure 2i).

1.4.2 Polyammonium functionalized acyclic and cyclic receptors for anions/hydrated anions

Amine functionalities have been shown to coordinate with anions of different dimensionality in its protonated form. In this section, we take into account of two such amine based receptors (Scheme 1.4) bearing peripheral aromatic functions to discuss the structural aspects of anion-water assemblies in their protonated forms. Few reduced Schiff bases **10** contain both H-bond donor and acceptor (primary amine, $–NH_2$, secondary amine, –NH– and $–NO_2$) ideal receptors for anions.[18] These molecular systems are designed with self-complementary H-bond donors and acceptors, which is very suitable to interact with the anion like phosphate. The dihydrogen phosphate complex of **10a** contains one crystallized water molecule which interacts with $H_2PO_4^-$ ion. Two $H_2PO_4^-$-H_2O is related to inversion center forming a discrete $[H_2PO_4^-\text{-}H_2O]_2$ cluster having dihydrogen phosphate dimer $[H_2PO_4^-]_2$ (Figure 1.3a). The amino NH_2 , NH and ring N-atom actively participate in the stabilization of the cluster. The crystal packing of dihydrogen phosphate complex of **10b** shows that the oxygen atom of dihydrogen phosphate ion is H-bonded with the next molecular unit forming dihydrogen phosphate dimer $[H_2PO_4^-]_2$. The water oxygen atom acts as H-bond acceptor and oxygen atom of dihydrogen phosphate acts as H-bond donor and water molecules act as a bridging agent between two dihydrogen phosphate dimers. Such dimers with the help of two water molecules form infinite 1D assembly of $[H_2PO_4{\cdot}H_2O]_n^{n-}$ further stabilized by amino function (Figure 1.3b). A similar interaction pattern with anions and anion-water assembly is also noticed in the dihydrogen

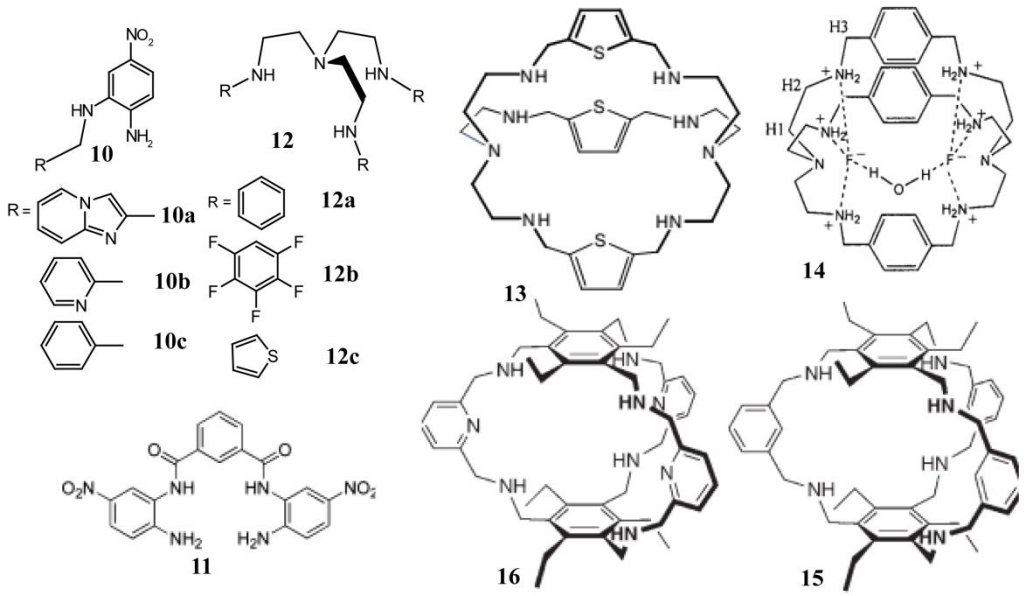

Scheme 1.4 Polyammonium functionalized acyclic and cyclic receptors for anions/hydrated anions.

phosphate complex of **10c**. A cleft-shape molecular receptor **11** having amine binding sites with an electron withdrawing nitro group help to form pseudo-encapsulated fluoride and a fluoride-water cluster.[19] The crystal structure shows that two fluoride ions occupy two diiffernet sites. The F1 atom is situated at the centre of the two amide (–CONH–) groups and two amine ($–NH_2$) groups and are strongly H-bonded. The F2 fluoride ion is hydrogen bonded with the amine ($–NH_2$) group and 1.5 units of the water molecules, such two structure assembled into a discrete fluoride-water cluster $[F_2\text{-}(H_2O)_3]^{2–}$ (Figure 1.3c). Solid state recognition of anions by multiple amine functionality is carefully investigated due to obvious presence of multiple anions and ample H-bonding sites. Such as a polyamine-based system were recently, probably the most widely studied systems. The tren-based acyclic or cyclic tripodal amines and benzene capped cyclic amines have been exploited for systematic perusal of anion binding. Bowman-James and cowokers reports a simple phenyl substituted tren based acyclic tripodal on treatement with acid forms non-cpsular with anions.[20] The bromide complex of **12a** triprotonated with three bromide ions and quasi-planar arrangement of arms with C_{2v} symmetry (Figure 1.3d). all three ammonium hydrogen are H-bonded with bromide ions. Among three one bromide ions Br1 is H-bonded by two close arms. Very interestingly, pentafluoro phenyl substituted tripodal in place of phenyl behaves distinctly from **12a**.[21] The receptor in this case make a bowl

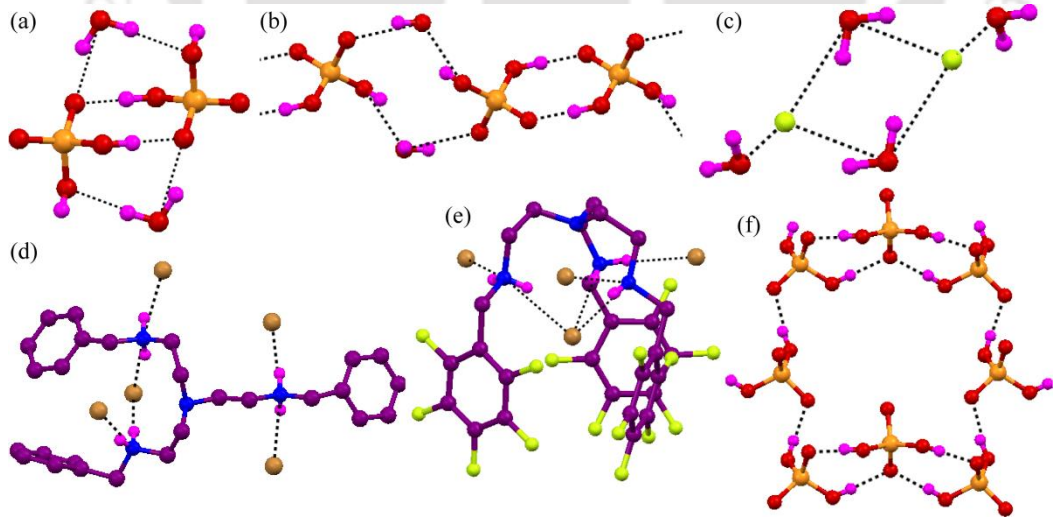

Figure 1.3. (a) Discrete dihydrogen-water cluster $[H_2PO_4^{–}\text{-}H_2O]_2$ in complex of **10a**. (b) Infinite dihydrogen-water cluster $[H_2PO_4{\cdot}H_2O]_n^{n–}$ in complex of **10b** and **10c**. (c) fluoride-water cluster $[F_2\text{-}(H_2O)_3]^{2–}$ in complex of **11**. (d) Coordination of bromide ion by polyammonium tripodal of **12a**. (e) unimolecular capsule of bromide ion in complex of **12b**. (f) octameric hydrogen phosphate cluster$(H_2PO_4^{–})_8$ assembly in complex of **12c.**

shaped cavity. The crystal structures of bromide complex of **12b** revealed that one bromide ion is encapsulated inside the tripodal cavity (Figure 1.3e). Structural analysis showed that encapsulation of bromide inside the receptor cavity is governed by $N^+–H\cdots Br^-$ interactions. This receptor also form isostructural complex with chloride ion. Another thiophenyl based tripodal reported by A. Hossain results very important aspect to anion chemistry. The compound **12c** on treatment phosphoric acid generates three dihydrogen phosphate anion leaving the receptor in triprotonated state.[22] one $H_2PO_4^-$ selectively encapsulated in its pseudo cavity. Structural analysis shows that other two $H_2PO_4^-$ anion are found to be involved in strong H-bonding interactions between H-bond donors and acceptors resulting in the formation of a cyclic phosphate octamer $(H_2PO_4^-)_8$ (Figure 1.3f). Two identical trimers (from two asymmetric units) are further linked *via* two $H_2PO_4^-$ anion from both sides, forming the octameric dihydrogen phosphate as $(H_2PO_4^-)_8$. Crystallographic analysis of the complex suggests that all three secondary amines in protonated state and H-bonded with oxygen of phosphate anions.

A thiophene-based cryptand having tren as a building block reported by the same group shows the tosylated salt of the receptor **13** form of a hybrid amine-water cyclic pentamer composed of four water molecules.[23a] The secondary amines are protonated and these H-bonding interactions facilitate the formation of a pentamer which adopts a puckered conformation (Figure 1.4a). When the receptor **13** treated with hydrobromic acid, it generates a well-defined hydrated bromide cluster. [23b] The receptor is hexaprotonated as expected and among six one bromide ion is located inside the cavity. The internal bromide is hexacoordinated with three "water tetramers," forming a C_3 symmetric propeller-shaped hydrated $[Br\text{-}(H_2O)_{12}]^-$ (Figure 1.4b). The encapsulated bromide is directly linked to three pairs of water molecules. Each pair of water molecules is further connected to dimeric water (O4 and O1) with two strong hydrogen bonds, completing the bromide-water

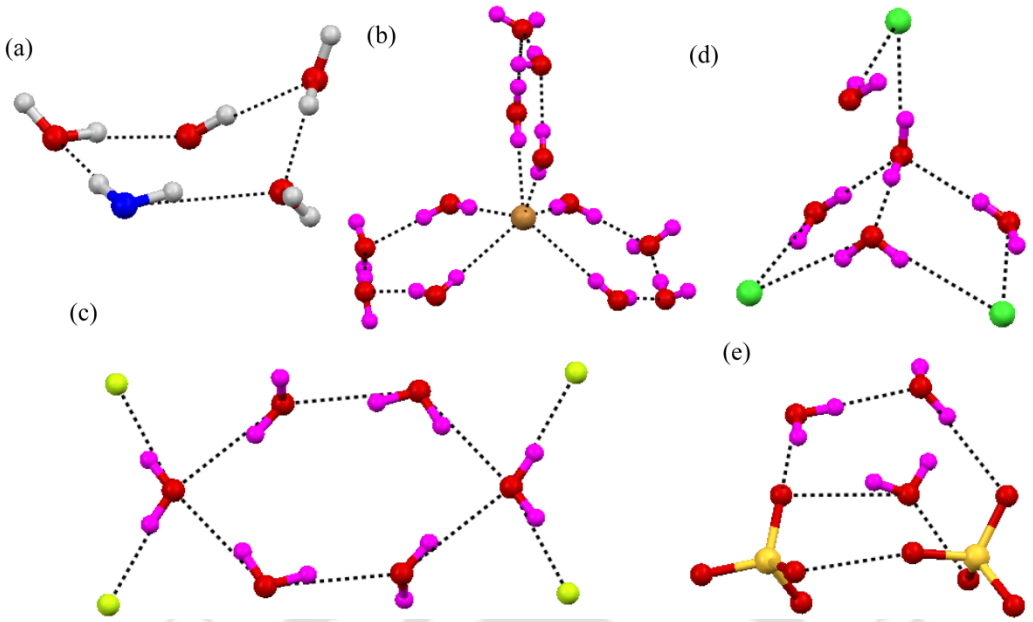

Figure 1.4 (a) Ammonium-water pentamer encapsulated in complex of **13**. (b) A bromide-water cluster $[Br\text{-}(H_2O)_{12}]^-$ encapsulated in complex of **13**. (c) A fluoride-water trimer of the cluster is encapsulated in complex of **14**. (d) A chloride-water cluster $[Cl_3\text{-}(H_2O)_5]^{3-}$ is stabilized in complex of **15**. (e) A sulfate-water cluster $[(SO_4)_2\text{-}(H_2O)_3]^{4-}$ is observed in complex of **16**.

pentameric cycle. Bowman-James and coworkers shows tren based macrocyclic receptor **14** on treatment with hydrofluoric acid encapsulate a hydrated fluoride anions.[24] The cavity is big, successful in capturing two fluoride ions inside the cavity bridged by a water molecule forming a *anion-based cascade complex*, where two spherical anions play the topological role of the two metal ions in traditional cascade complexes. Two encapsulated fluoride-water clusters $[F_2\text{-}H_2O]^{2-}$ is further linked with four exterior water molecules transforming big fluoride-water cluster (Figure 1.4c). Recently P. Ghosh establishes A C_3 symmetric drum-shaped homoditopic haxaamino bicyclic receptor **15** was successfully executed for halide ions.[25] A benzene cap having three $–NH_2$ is used as a building block. Hexachloride and hexaiodide complexes of **15** shows encapsulation of an iodide inside its cavity, and in hexachloride complex, chloride is recognized as $Cl\cdots H_2O$ in each of the three side pockets which are in extensive H-bonding interactions with the water and chloride ions. All six nitrogen atoms are protonated as expected and shows binding of the water-chloride network in the cavity. The chloride-water cluster is composed of three chlorides and five water molecules $[Cl_3\text{-}(H_2O)_5]^{3-}$ (Figure 1.4d). The chloride and water guests are in H-bonding interactions with the receptor *via* N−H···Cl and N−H···O interactions. Another similar type macrocyclic polyamines reported **16** by Delgado and coworkers was extensively studied for solid state recognition of hydrated

planar and tetrahedral anions.[26] The crystal structure shows one nitrate anion among six nitrate inserted into the macrobicyclic cage and stabilized by π···π interactions with addition of H-bonds with four bridging water molecules and NH_2 binding groups. The analysis of H-bonds is consistent with the existence of a $[NO_3\text{-}H_2O]_3^{3-}$ cluster with a nitrate embedded into the cage and stabilized by various H-bonds and electrostatic interactions. very interesting the receptor also capable of stabilizing The $[(SO_4)_2\text{-}(H_2O)_3]^{4-}$ and $[H_2O]_3$ entities through multiple and cooperative N-H···O H-bonds with the receptor (Figure 1.4e). The water molecule that bridges both sulfate anions, is completely encapsulated into the macrobicyclic cage and H-bonded to two N-H binding sites of NH_2^+.

1.4.3 Amide based acyclic and cyclic receptors for anions/hydrated anions

Tren has also been studied as an important building block in the design and syntheses of receptors capable of binding anionic. In some cases benzene cap was used to have more for anions/hydrated anions. In all these cases, anion binding by amide based receptors is exclusively by H-bond formation. Recent theoretical investigation by Hay et al. showed that the effect of electron withdrawing substituents on the aryl moiety significantly enhances the stability of anion complexes.[27] Structural information from these receptors

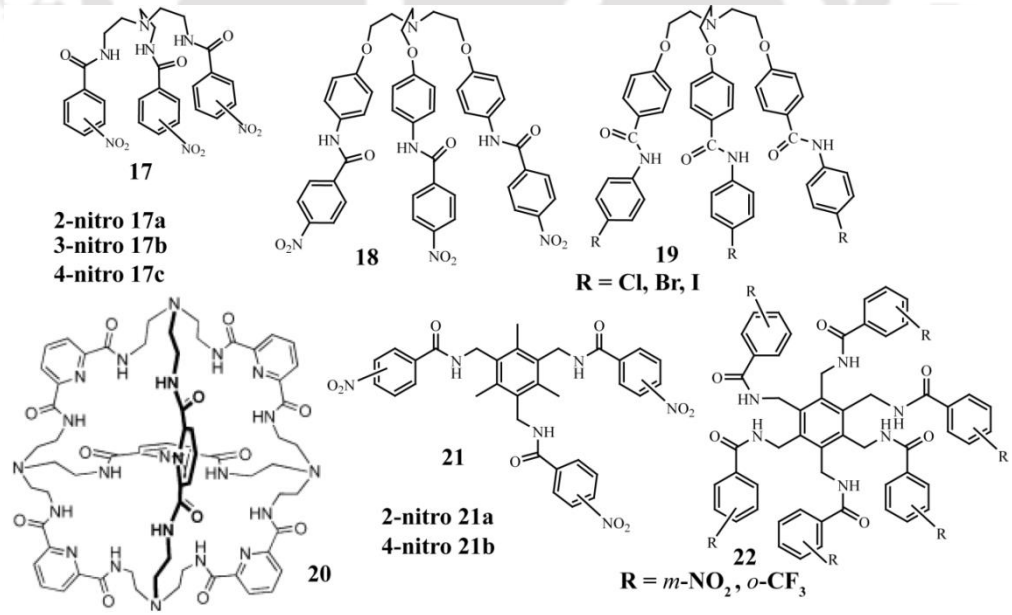

Scheme 1.5 Tren and benzene capped amide tripodal and hexapodal receptors for anion/hydrated anions.

can provide insight on the proper binding topology of anions with these tripodal amide receptors. Most recently P. Ghosh and coworker's periodically synthesized tren based

three isomeric nitrophenyl substituted amide receptors **17**.[28] All receptors in protonated state form C_{3v} symmetry and apical N-atom is protonated. None of the receptors form any suitable cavity for anion encapsulation irrespective of size, shape, and charge of the anions. In fact they shows side cleft anion binding via N−H···anion and C−H···anion interactions. The perchlorate and silicon hexafluoride complexes of ortho-isomer **17a** shows the active participation of amide, aromatic and aliphatic hydrogen while anion binding. The meta-isomer **17b** behaves with spherical, planar and tetrahedral anions almost in similar pattern only in varied number H-bondings around anions. Inorganic anionic salts of para-isomer **17c** as example iodide complex shows a side cleft anion binding and it is tri-coordinated by accepting one N−H···I^- and two aromatic C−H···I^- H-bonds. Another nitro functionalized second generation tripodal amide reported **18** by G. Das and A. Basu to study anion binding.[29] A clever design of the receptor lies to create larger cavity for what anion binding H-bonding site moved to distant position. A successful outcome obtained on treatment with halo acid. The receptor forms a bimolecular capsule of chloride/bromide-water tetramer. The hybrid cluster $[Cl_2\text{-}(H_2O)_2]^{2-}$ is formed via strong chloride–water interactions and possesses a planar cyclic tetrameric arrangement. Probably the H-bonding amidic functions of the receptor are too widely placed to offer an appropriate binding pocket for a single chloride anion, resulting in the formation of the interesting $[Cl_2\text{-}(H_2O)_2]^{2-}$ cluster encapsulated within a dimeric capsular assembly of a protonated receptor (Figure 1.5b and 1.5c). A series of neutral C_3-symmetric acyclic receptors **19** incorporating amide functionality has been designed for anion coordination.[30] These conformationally flexible tripodals forms in situ cone shape conformation and is capable of entrapping nitrate anions through the amide N−H bonds to form discrete nitrate complexes in unimolecular capsular fashion (Figure 1.5d). The crystal structures of three nitrate complexes of three halide substituted tripodals **19a, 19b** and **19c** are isostructural. The amide N−H bonds of each branch are directed inside toward center in plane with the nitrate anion. The nitrate anion is bound inside the cavity by strong H-bonds between oxygen atoms of the nitrate anion and three amide N−H protons. Their study shows unique example of neutral receptor for encapsulation of highly hydrated and weakly coordinated nitrate anion in polar solvent media. a tricyclic organic molecular capsule **20** having tren as a building block was reported by Bowman-James that provides an ideal docking site for tetrahedral H-bond coordination.[31] The capsule incorporates a tetrahedron of water molecules that holds (solvates) a small guest inside, either a single molecule of water or fluoride ion (Figure 1.5e and 1.5f). The

tetrahedrally positioned bridgehead amine H-bonding sites promote the tetrahedral orientation of the solvation sphere. The central water molecule of the encapsulated pentamer, H_2O(5w), forms four H-bonds, two acceptor and two donor. The geometry of encapsulated $F{\cdot}4H_2O$ complex is to the water pentamer. However, because F^- is a four hydrogen bond acceptor, the orientation of two of the water molecules is changed, with O2w and O4w now forming O−H···F^- H-bonds with the central F^-. The finding shows the acquisition of an isomorphous structure with F^- replacing the central water allows for a closer examination of an isolated sphere of a single halide, providing structural insight to solvation effects. A series of bowl-shaped tripodal receptor with appropriately positioned amide functionality on the benzene platform having various substituted has been synthesized and characterized by P. Ghosh's group for solid state recognition of various hydrated anions. *Ortho*-nitro substituted benzene cap tripodal receptor **21a** revealed all the three arms of projected in one direction to form a bowl shaped cavity.[32a] The dimeric capsular assembly of the receptor with encapsulated hydrated fluoride, $[F_2(H_2O)_6]^{2-}$ as a guest in the capsule which acted as a template in the formation of the dimeric capsule. This template is formed *via* strong fluoride–water and two N–H···F and four N–H···O interactions. The cluster possesses a tricyclic arrangement where two fluoride ions are in the apex of the tricycle and are bridged by two water dimers and two molecules of water (Figure 1.5g). The *para*-isomer of the tripodal also formed similar type fluoride-water cluster mediated bimolecular

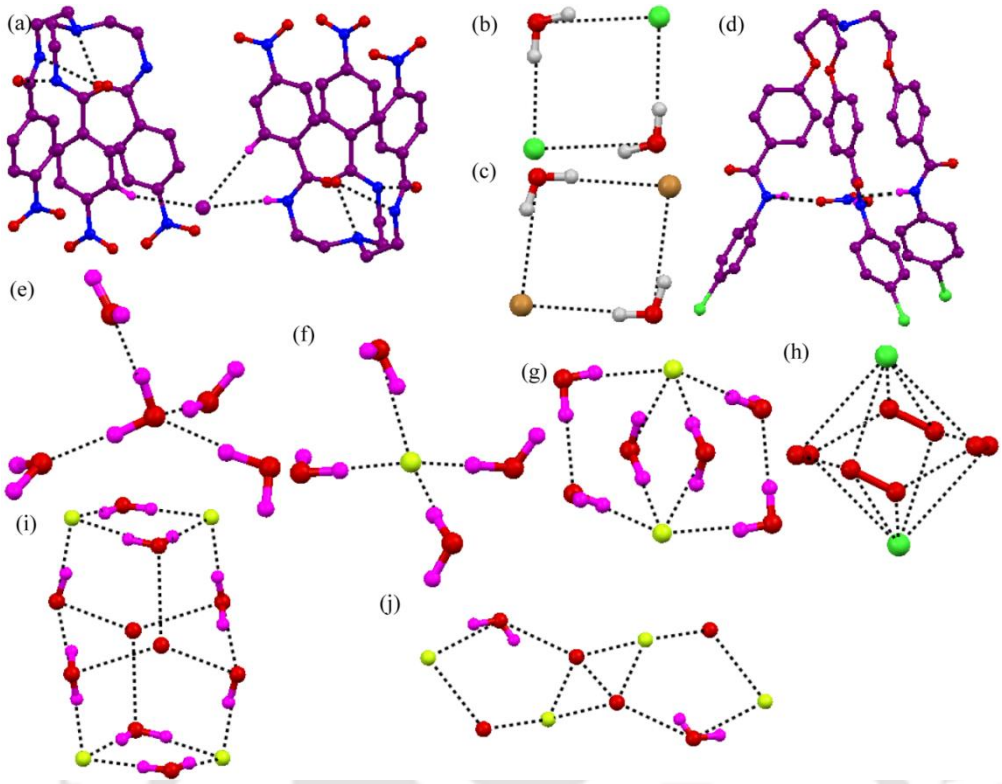

Figure 1.5 (a) Iodide coordination in complex of **17**. (b) and (c) Square shaped chloride-water $[Cl_2\text{-}(H_2O)_2]^{2-}$ and bromide-water cluster in the dimeric capsular assembly of **18**. (d) Nitrate encapsulation in unimolecular complex of **19**. (e) and (f) Encapsulation of tetrahedrally hydrated water $H_2O{\cdot}4H_2O$ and $F{\cdot}4H_2O$ fluoride ion in a tetrahedral host of **20**. (g) Encapsulation fluoride-water cluster $[F_2\text{-}(H_2O)_6]^{2-}$ within bimolecular capsule of **21a**. (h) Encapsulation octahedral chloride-water cluster $[Cl_2\text{-}(H_2O)_4]^{2-}$ within bimolecular capsule of **21b**. (i) Encapsulation fluoride-water cluster $[F_4(H_2O)_{10}]^{4-}$ inside the dimer of **22a**. (j) Encapsulation of chloride-water cluster $[Cl_2\text{-}(H_2O)_4]^{2-}$ in **22b**.

capsular assembly.[32b] additionally a acetate-water cluster $[(AcO)_2\text{-}(H_2O)_4]^{2-}$ and chloride-water cluster $[Cl_2\text{-}(H_2O)_4]^{2-}$ is found within bimolecular complex of the **21b**. The water-chloride cluster $[Cl_2\text{-}(H_2O)_4]^{2-}$ is in octahedral arrangement formed *via* strong H-bonding interactions (Figure 1.5h). 4-pyridine substituted benzene capped tripodal reported from the same group shows the formation of discreet fluoride-water cluster $[F_2\text{-}(H_2O)_4]^{2-}$ and chloride water cluster $[Cl_2\text{-}(H_2O)_4]^{2-}$ encapsulated in dimeric capsule. The geometry of the clusters is more like a parallelogram.[32c] Another fascinating ligand design on the benzene platform was done by the same group shows hydrated anion induced capsular assembly. In this case the hexapodal amide receptor **22a**, where all six arms are projected in one direction (an unfavorable conformation) along with the binding of other anions in solution and solid states.[33a] The solid state structure of1revealed the encapsulation of an unusual fluoride-water cluster, $[F_4\text{-}(H_2O)_{10}]^{4-}$ inside the dimer of **22a** with the highly unfavorable *aaaaaa* conformation of the hexapodal receptor. The cluster contains four, five and six membered rings, constructed by H-bonding interactions (Figure 1.5i). Three

water molecules (O3, O4 and O5) in the asymmetric unit form a symmetry induced cyclic hexameric water cluster with a chair conformation. A fluoride-water dimer is held by strong N–H···F and N–H···O interactions with the half capsule. All of the six amide protons are engaged in hydrogen bonding with the encapsulate guest $[F_4\text{-}(H_2O)_{10}]^{4-}$. Same group reported recognition of $[F_4\text{-}(H_2O)_6]^{4-}$ cluster in the dimeric capsular assembly of *ortho*-trifluoride methyl phenyl substituted hexaamide where all the six arms are in unidirectional conformation.[33b] Upon changing the guest from planar anions (acetate, nitrate) to spherical anion fuoride, they have observed trapping of very unusual conformer of the receptor **22a** i.e. *aaaaaa* that has recognized $[F_4\text{-}(H_2O)_6]^{4-}$ in the large cavity of the dimeric capsular assembly. The receptor form the cluster by various fluoride-water structures like, a encapsulated $[F_2\text{-}(H_2O)_2]^{2-}$ is further hydrogen bonded to another $[F_2\text{-}(H_2O)_2]^{2-}$ unit through two bridging water molecules (O15) to form $[F_4\text{-}(H_2O)_6]^{4-}$ cluster in the cavity of a dimeric capsular assembly. Encapsulation of $[F_4\text{-}(H_2O)_6]^{4-}$ cluster is assisted by multiple N–H···F, O–H···F and N–H···O strong interactions.

1.5 Objective of the thesis

From the above literature survey it is evident that selective recognition of anions/hydrated anions has attracted a great deal of attention. Carefully designed molecular receptors can provide suitable environments capable of trapping targeted guests inside their cavities. In particular, recognition of discrete ordered anion–water clusters is more challenging, because structure of anions in their hydrated form is highly unpredictable. As most of the anions remains in hydrated state, therefore structural characterization of anion–water clusters is also important. From the foregoing overview it emerges that receptors functioning as polyamine and amide hydrogen (specially containing one or more basic nitrogen) preferably dominates the recognition of anions/hydrated anions. The presence of basic nitrogen would actually register the occurrence of anions (on treatment with inorganic acid) and generates kind of organic salts which shows general tendency to crystallize with water molecules. Such situation is very much favourable to study anion-water structure relationship. Accordingly stabilization of such structural motif is also benefited by electrostatic interaction along with non-covalent interactions. Therefore fundamental goal of this thesis is the endeavour in decoration of suitable receptors preferably having multiple protonation sites and/or conventional H-bonding motifs which allow the study of structural aspect of anions/hydrated anions and trapping them within molecular cavity and their impact on supramolecular assembly of receptors.

References

1. (a) Whitesides, G. M.; Mathias, J. P.; Seto, C. T. *Science* **1991**, *254*, 1312. (b) Lehn, J.M. *Supramolecular Chemistry Concepts and Perspectives*; VCH: New York, **1995**. (c) Philp, D.; Stoddart, J. F. *Angew. Chem. Int. Ed. Engl*. **1996**, *35*, 1154. (d) Batten, S. R.; Robson, R. *Angew. Chem. Int. Ed*. **1998**, *37*, 1460. (e) Reinhoudt, D. N.; Stoddart, J. F.; Ungaro, R. *Chem. Eur. J*. **1998**, *4*, 1349.
2. Cram, D. J. *Angew. Chem., Int. Ed*. **1986**, *25*, 1039.
3. Steiner, T. *Angew. Chem., Int. Ed*. **2002**, *41*, 48.
4. Ariga, K.; Hill, J. P.; Lee, M. V.; Vinu, A.; Charvet, R.; Acharya, S. *Science and Technology of Advanced Materials*, **2008**, 9, 014109.
5. (a) Schultz, P. G. *Angew. Chem., Int. Ed. Engl*. **1989**, *28*, 1283. (b) Anslyn, E.V.; Smith, J.; Kneeland, D. M.; Arigaand, K.; Chu, F. *Supramol. Chem.* **1993**, *1*, 201. (c) Beer, P. D.; Gale, P. A. *Angew. Chem., Int. Ed.*, **2001**, *41*, 486.
6. Sessler, J.; Gale, P. A.; Cho, W. S. Anion Receptor Chemistry, *The Royal Society of Chemistry, Cambridge*, **2006**.
7. (*a*) Gale, P. A. *Chem. Commun*. **2008**, 4525. (*b*) Caltagirone, C.; Gale, P. A. *Chem. Soc. Rev***. 2009**, *38*, 520. (*c*) Gale, P. A. *Acc. Chem. Res.* **2006,** 39, 465. (d) Li, A.F.; Wang, J. H.; Wang, F.; Jiang, Y. B. *Chem. Soc. Rev.*, **2010**, *39*, 3729.
8. (a) Marcus, Y. Ion Solvation ~Wiley-Interscience, New York, **1985**. (b) Kirk, K. L. Biochemistry of Halogens and Inorganic Halides~Plenum, New York, **1991**.
9. Zhao, H. Y.; Ma, J. J.; Han, Z. G.; Yang, X. D.; Yang, M. L. *Synthesis and Reactivity in Inorganic, Metal-Organic, and Nano-Metal Chemistry*, **2015**, *45*, 621.
10. Custelcean, R.; Gorbunova, M. G. *J. Am. Chem. Soc*. **2005**, *127*, 16362.
11. Saha, R.; Biswas, S.; Steele, I. M.; Dey, K.; Mostafa, G. *Dalton Transactions* **2011**, *40*, 3166.
12. Bakhoda, A.; Khavasi, H. R.; Safari, N. *Cryst. Growth Des*. **2011**, *11*, 933.
13. Li, Z. Y.; Yang, J. S.; Liu, R. B.; Zhang, J. J.; Liu, S. Q.; Ni, J.; Duan, C. Y. *Dalton Trans*. **2012**, *41*, 13264.
14. Arunachalam, M.; Chakraborty, S.; Marivel, S.; Ghosh, P. *Cryst. Growth Des.* **2012,** *12*, 2097.
15. Gogoi, A.; Das, G. *Cryst. Growth Des*. **2012**, *12*, 4012.
16. Ji, B. M.; Deng, D. S.; Ma, N.; Miao, S. B.; Yang, X. G.; Ji, L. G.; Du, M. . *Cryst. Growth Des.* **2010**, *10*, 3060.
17. Singh, U. P.; Maurya, R. R.; Kashyap, S. *Struct Chem*. **2014,** *25*, 733.
18. Dalapati, S.; Alam, M. A.; Jana, S.; Guchhait, N. *CrystEngComm*. **2012**, *14*, 6029.
19. Dalapati, S.; Alam, M. A.; Saha, R.; Jana, S.; Guchhait, N. *CrystEngComm*. **2012**, *14*, 1527.
20. Hossain, M. A.; Liljegren, J. A.; Powell, D.; Bowman-James, K. *Inorg. Chem*. **2004**, *43*, 3751.
21. Lakshminarayanan, P. S.; Ravikumar, I.; Suresh, E.; Ghosh, P. *Inorg. Chem*. **2007**, *46*, 4769.
22. Hossain, M. A.; Isiklan, M.; Pramanik, A.; Saeed, M. A.; Fronczek, F. R. *cryst. Growth Des*. **2012**, *12*, 567.
23. (a) Saeed, M. A.; Wong, B. M.; Fronczek, F. R.; Venkatraman, R.; Hossain, M. A. *cryst. Growth Des*. **2010**, *10*, 1486. (b) Saeed, M. A.; Pramanik, A.; Wong, B. M.; Haque, S. A.; Powell, D.R.; Chand, D.K.; Hossain, M. A. *Chem Commun.* **2012,** *48*, 8631.
24. Hossain, A.; Llinares, J.M.; Mason, S.; Morehouse, P.; Powell, D.; Bowman-James, K. *Angew. Chem. Int. Ed.* **2002**, *41*, 2335.
25. Arunachalam, M.; Ravikumar, I.; Ghosh, P. *J. Org. Chem*. **2008**, *73*, 9144.
26. Mateus, P.; Delgado, R.; Brandao, P.; Felix, V. *J. Org. Chem.* **2009**, *74*, 8638.
27. Bryantsev, V. S.; Hay, B. P. *Org. Lett*. **2005**, *7*, 5031.
28. Ravikumar, I.; Lakshminarayanan, P. S.; Ghosh, P. *Inorganica Chimica Acta.* **2010**, *363*, 2886.
29. Basu, A.; Das, G. *Chem. Commun.*, **2013**, *49*, 3997.
30. Singh, S. A.; Sun, S.-S. *J. Org. Chem.* **2012**, *77*, 1880.
31. Wang, Q-Q.; Day, V. W. Bowman-James, K. *Angew. Chem. Int. Ed*. **2012**, *51*, 2119.
32. (a) Arunachalam, M.; Ghosh, P. *Chem. Commun*., **2009**, 5389. (b) Arunachalam, M.; Ghosh, P *Inorg. Chem.*, **2010**, *49*, 943. (c) Chakraborty, S.; Dutta, R.; Arunachalam, M.; Ghosh, P. *Dalton Trans.*, **2014**, *43*, 2061.
33. (a) Arunachalam, M.; Ghosh, P. *Chem. Commun.*, **2011**, *47*, 6269. (b) Chakraborty, S.; Dutta, R.; Wong, B. M.; Ghosh, P. *RSC Adv*., **2014**, *4*, 62689.

Chapter 2

Experimental Methods and Characterization

In this chapter, synthetic procedures (for **L_1-L_8**) characterization, crystallization details and specifications of instruments are presented.

2.1 Materials and Methods

All reagents and solvents were obtained from commercial sources and used as received without further purification. Solvents for synthesis and crystallization experiments were dried using standard procedures, wherever mentioned in the synthetic procedures. ^{1}H NMR was recorded on a Varian FT-400 MHz instrument and chemical shifts were recorded in parts per million (ppm) on the scale using tetramethylsilane (TMS) or residual solvent peak as a reference and ^{13}C spectra were obtained at 100 MHz at 298 K. FT-IR spectra were recorded on a Perkin-Elmer-Spectrum One FT-IR spectrometer with KBr disks in the range 4000-450 cm^{-1}. Powder X-ray diffraction patterns of dried crystalline powder were recorded using a Bruker-D8 Advance X-ray diffractometer with Cu-*Kα* radiation at λ = 0.15418 nm. Thermal analysis (TGA and DSC) of dried samples was performed using an SDTA 851-E TGA thermal analyser (*Mettler Toledo*) with a heating rate of 5-10^{o}C/min in a N_2 atmosphere.

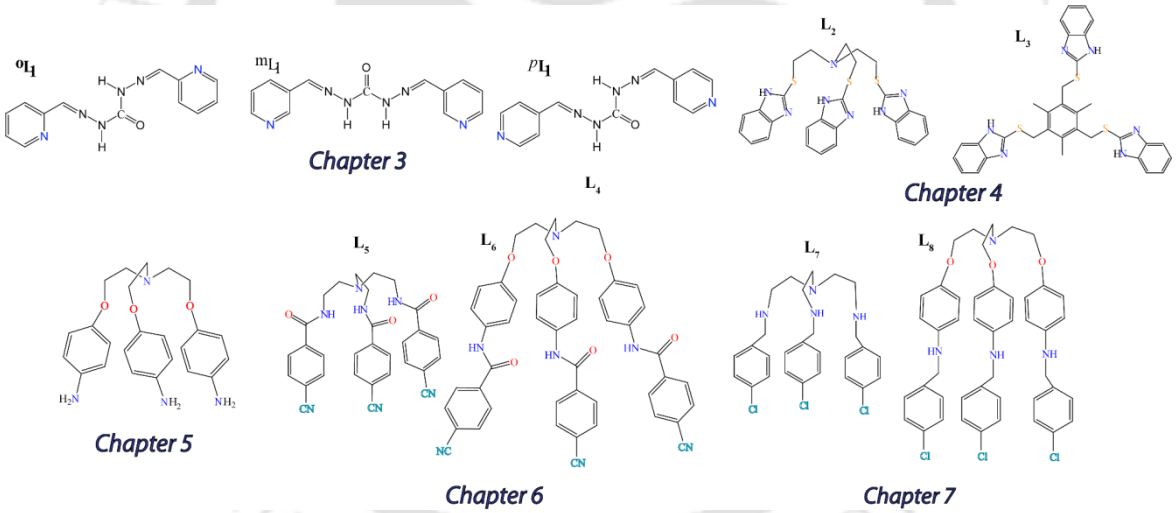

Scheme 2.1 Molecular structures of acyclic receptors studied in this thesis.

2.2 Single crystal X-ray diffraction

In each case, a crystal of suitable size was selected from the mother liquor and immersed in silicone oil, and it was mounted on the tip of a glass fiber and cemented using epoxy resin. The intensity data were collected using a Bruker SMART APEX-II CCD diffractometer, equipped with a fine focus 1.75 kW sealed tube Mo-K_α radiation (λ = 0.71073 Å) at 298(3) K, with increasing ω (width of 0.3^o per frame) at a scan speed of 5 s/ frame. The SMART software was used for data acquisition. Data integration and reduction were undertaken with SAINT and XPREP software.[1] Multi-scan empirical absorption

corrections were applied to the data using the program SADABS.[2] Structures were solved by direct methods using SHELXS-97[3] and refined with full-matrix least-squares on F^2 using SHELXL-97.[4] All non-hydrogen atoms were refined anisotropically and hydrogen atoms were geometrically fixed and refined isotropically. Hydrogen atoms attached with the amide, urea and nitrogen atoms were located from electron Fourier map and refined isotropically. Usually, temperature factors of hydrogen atoms attached to carbon atoms are refined by restraints -1.2 or -1.5 U_{iso} (C), although the isotropic free refinement is also acceptable. PLATON/SQUEEZE[5] was also applied some cases to exclude disordered solvent electron densities. Structural illustrations have been drawn with MERCURY-3.0[6] for Windows. Parameters for data collection and crystallographic refinement details of the complexes of the receptors (**L_1-L_8**) are summarized in the respective chapters.

2.3 Synthesis and characterization of receptors L_1-L_8 and their anion complexes

2.3.1 Isomeric pyridine-urea receptors $^{o}L_1$, $^{m}L_1$, and $^{p}L_1$

The *ortho* isomer **$^{o}L_1$** was synthesized as following procedure. White crystalline carbohydrazide (0.180 g, 2 mmol) was taken in round bottom flask containing 2 mL of water and heated to dissolve the solid powder.[7] Then 40 mL methanolic solution of pyridine-2-aldehyde (0.380 mL, 4 mmol) was added and stirred for 8 hrs. Light yellow semi-solid product obtained after solvent evaporation. The other isomers also prepared same way, only by changing corresponding pyridine aldehyde.

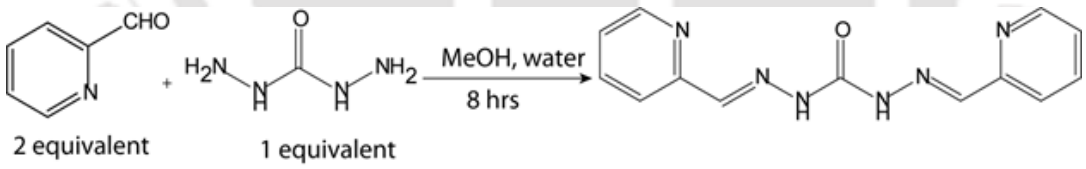

Scheme 2.2 Synthesis of the receptor $^{O}L_1$.

$^{o}L_1$: Yield = 95%, M. P: 190-191 °C. ^{1}H NMR (400 MHz, DMSO−d_6) δ (ppm): 11.084 (s, 1H, N–H_{urea}), 8.586(d, J = 4.4 Hz, 1H, C–H_{ar}), 8.251(s, 1H, C–H_{imine}), 8.152 (s, 1H, N–H_{urea}), 7.866 (t, J = 7.6, 1H, C–H_{ar}), 7.394 (t, J = 6.0, 2H, C–H_{ar}). ^{13}C NMR (400 MHz, DMSO−d_6) δ (ppm): 151.67, 148.56, 144.59, 143.83, 126.01, 123.88. IR spectra (KBr pellet): 3398 cm^{-1} *vs*(N−H), 3194 cm^{-1} *vs*(N−H), 1685 cm^{-1} *vs*(−C=O), 1537 cm^{-1} *vs*(−C=N). ESI mass spectrometry: calc for 269 [M + H$^+$]; found 269 [M + H$^+$]

2.3.2 Anion complexes of the receptors $^{o}L_1$, $^{m}L_1$, and $^{p}L_1$

[$^{O}L_1$·3H_2O](1): The ortho isomer **$^{O}L_1$** (0.137 g, 0.5 mmol) was dissolved in a test tube containing 5 ml methanol-water solution. Block shaped colourless crystal were gown within 7-10 days.

[^{o}L$_1$H$_2$·2I·3H$_2$O](2): Iodide complex was obtained by adding 0.5 mL of HI to a 5 mL methanolic solution of **^{o}L$_1$** (0.137 g, 0.5 mmol). Block shaped colourless crystal were gown via slow evaporation within 1-2 weeks.

Yield = 60 %, M. P: 210-212 °C. ^{1}H NMR (400 MHz, DMSO−d_6) δ (ppm): 11.503 (s, 1H, N–H$_{urea}$), 8.782 (d, *J* = 5.1 Hz, 1H, C–H$_{ar}$), 8.40 (t, *J* = 6.9 Hz, 1H, C–H$_{ar}$), 8.390 (s, 1H, C–H$_{imine}$), 7.84 (t, *J* = 6.9 Hz, 2H, C–H$_{ar}$). IR spectra (KBr pellet): 3432 cm^{-1} *vs*(O−H), 3244 cm^{-1} *vs*(N−H), 1716 cm^{-1} *vs*(−C=O), 1535 cm^{-1} *vs*(−C=N), 1112 cm^{-1} *vs*(−S=O).

[^{O}L$_1$H$_2$·SO$_4$·3H$_2$O](3): The preparation of complex **3** was similar to that of **2** except that H_2SO_4 was used instead of HI. Colorless crystals were obtained within 1-2 weeks.

Yield = 60 %, M. P: 210-212 °C. ^{1}H NMR (400 MHz, DMSO−d_6) δ (ppm): 11.525 (s, 1H, N–H$_{urea}$), 8.792 (d, *J* = 5.2 Hz, 1H, C–H$_{ar}$), 8.409 (t, *J* = 6.8 Hz, 1H, C–H$_{ar}$), 8.390 (s, 1H, C–H$_{imine}$), 7.854 (t, *J* = 6.8 Hz, 2H, C–H$_{ar}$). IR spectra (KBr pellet): 3435 cm^{-1} *vs*(O–H), 3240 cm^{-1} *vs*(N–H), 1712 cm^{-1} *vs*(–C=O), 1538 cm^{-1} *vs*(–C=N), 1110 cm^{-1} *vs*(–S=O).

[2^{o}L$_1$H·2H$_2$PO$_4$·3H$_2$O](4): The preparation of complex **4** was similar to that of **2** except that H_3PO_4 was used instead of HI. Colorless crystals were obtained within 1-2 weeks.

Yield = 65%, M. P: 185-186 °C. ^{1}H NMR (400 MHz, DMSO−d_6) δ (ppm): 11.507 (s, 1H, N–H$_{urea}$), 8.779 (d, *J* = 4.8 Hz, 1H, C–H$_{ar}$), 8.393 (t, *J* = 7.2 Hz, 1H, C–H$_{ar}$), 8.382 (s, 1H, C–H$_{imine}$), 7.841 (t, *J* = 6.8 Hz, 2H, C–H$_{ar}$). IR spectra (KBr pellet): 3440 cm^{-1} *vs*(O–H), 3231 cm^{-1} *vs*(N–H), 1711 cm^{-1} *vs*(–C=O), 1537 cm^{-1} *vs*(–C=N), 1120 to 1157 cm^{-1} *vs*(–P=O).

[^{O}L$_1$H$_2$·ClO$_4$·2H$_2$O](5): The preparation of complex **5** was similar to that of **2** except that $HClO_4$ was used instead of HI. Light yellow crystals were obtained within 1-2 weeks.

Yield = 90%, M. P: 250-252 °C. ^{1}H NMR (400 MHz, DMSO−d_6) δ (ppm): 11.529 (s, 1H, N–H$_{urea}$), 8.788 (d, *J* = 5.6 Hz, 1H, C–H$_{ar}$), 8.407(t, *J* = 8.0 Hz, 1H, C–H$_{ar}$), 8.388 (s, 1H, C–H$_{imine}$), 7.849 (t, *J* = 6.4 Hz, 2H, C–H$_{ar}$). IR spectra (KBr pellet): 3444 cm^{-1} *vs* (O—H), 3200 cm^{-1} *vs*(N—H), 1705 cm^{-1} *vs*(—C=O), 1520 cm^{-1} *vs*(—C=N), 1083 to 1138 cm^{-1} *vs*(—Cl=O).

[^{m}L$_1$H$_2$·HPO$_4$·H$_2$O](6): The preparation of complex **6** was similar to that of **2** except that H_3PO_4 was used instead of HI. Light yellow crystals were obtained within 1-2 weeks.

Yield = 75%, M. P: 230-232 °C. ^{1}H NMR (400 MHz, DMSO−d_6) δ (ppm): 11.528 (s, 1H, N–H$_{urea}$), 8.802 (d, *J* = 5.1 Hz, 1H, C–H$_{ar}$), 8.419 (t, *J* = 6.8 Hz, 1H, C–H$_{ar}$), 8.420 (s, 1H, C–H$_{imine}$), 7.859 (t, *J* = 6.8 Hz, 2H, C–H$_{ar}$). IR spectra (KBr pellet): 3437 cm^{-1} *vs*(O–H), 3243 cm^{-1} *vs*(N–H), 1719 cm^{-1} *vs*(–C=O), 1548 cm^{-1} *vs*(–C=N), 1110 cm^{-1} *vs*(–P=O).

[2^{p}L$_1$H·SiF$_6$·4H$_2$O](7): The preparation of complex **7** was similar to that of **2** except that HF was used instead of HI. Light yellow crystals were obtained within 1-2 weeks.

Yield = 60 %, M. P: 222-223 °C. ^{1}H NMR (400 MHz, DMSO−d_6) δ (ppm): 11.526 (s, 1H, N–H$_{urea}$), 8.797 (d, *J* = 5.2 Hz, 1H, C–H$_{ar}$), 8.423 (t, *J* = 6.8 Hz, 1H, C–H$_{ar}$), 8.40 (s, 1H, C–H$_{imine}$), 7.858 (t, *J* = 6.8 Hz, 2H, C–H$_{ar}$). IR spectra (KBr pellet): 3436 cm^{-1} *vs*(O–H), 3243 cm^{-1} *vs*(N–H), 1716 cm^{-1} *vs*(–C=O), 1539 cm^{-1} *vs*(–C=N).

[^{p}L$_1$H$_2$·2NO$_3$·3H$_2$O](8): The preparation of complex **8** was similar to that of **2** except that HNO_3 was used instead of HI. Colorless crystals were obtained within 1-2 weeks.

Yield = 65%, M. P: 195-198 °C. ^{1}H NMR (400 MHz, DMSO−d_6) δ (ppm): 11.517 (s, 1H, N–H$_{urea}$), 8.78 (d, J = 4.8 Hz, 1H, C–H$_{ar}$), 8.398 (t, J = 7.2 Hz, 1H, C–H$_{ar}$), 8.386 (s, 1H, C–H$_{imine}$), 7.848 (t, J = 6.8 Hz, 2H, C–H$_{ar}$). IR spectra (KBr pellet): 3440 cm^{-1} *vs*(O–H), 3231 cm^{-1} *vs*(N–H), 1711 cm^{-1} *vs*(–C=O), 1537 cm^{-1} *vs*(–C=N), 1120 to 1057 cm^{-1} *vs*(–N=O).

2.3.3 Tripodal receptors L$_2$ and L$_3$

The acyclic tripodal host **L$_2$** has been synthesized following Scheme 2. To a solution of 2-mercaptobenzimidazole (2 g, 12 mmol) in 20 ml ethanol crushed NaOH (0.80 g, 20 mmol) was added, and the solution was stirred at room temperature for 1h.[8] To the resulting suspension, Tris(2-chloro-ethyl)amine hydrochloride (1.071 g, 4 mmol) was added at once, and the reaction mixture was stirred for another 1 hr at room temperature. For the completion of the reaction, the mixture was refluxed for 8 hrs. The expected product was extracted with ethylacetate.

Yield 80% Mp 134°C, ^{1}H−NMR (400 MHz, d_6−DMSO) δ (ppm): 12.52(s, N−H), 7.40(m, arom), 3.46(t, NCH_2), 3.10(t, SCH_2). ^{13}C-NMR (100 MHz, d_6-DMSO) δ (ppm): 29.28, 52.83, 110.19, 113.24, 117.26, 121.51, 135.49, 143.75 and 150.58.

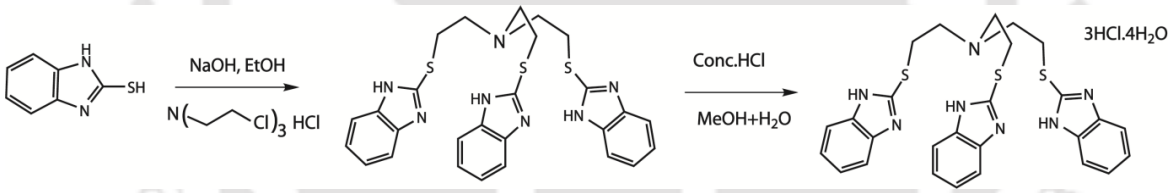

Scheme 2.3 Synthesis of the receptor **L$_2$**.

2.3.4 Anion complexes of L$_2$

[L$_2$H$_3$·Cl$_3$·4H$_2$O](2a): Methanolic solution of **L$_2$** was acidified to pH 1-2 with dilute HCl and resulting solution was stirred for 1 hr at room temperature. Block shaped colourless crystal was obtained by slow evaporation at room temperature after 1-2 weeks.

Yield 85%. Mp 160-162°C, ^{1}H−NMR (400 MHz, d_6−DMSO) δ (ppm): 7.5(m, arom), 7.3(m, arom), 5.076 (s, N−H) 3.87(t, NCH_2), 3.57(t, SCH_2). ^{13}C−NMR (100 MHz, d_6-DMSO) δ (ppm): 27.70, 52.00, 113.47, 124.01, 135.00, and 149.74.

[L$_2$H$_3$·Br$_3$·4H$_2$O](2b): The preparation of complex **2b** is similar to **2a** where HBr is used in place of HCl.

Yield = 85%. Mp 205 °C, ^{1}H-NMR (600 MHz, d_6-DMSO) δ (ppm): 7.572 (d 1H, C–H$_{ar}$), 7.345 (dd 2H, C–H$_{ar}$), 5.191 (broad 1H, N–H), 3.865 (t 2H, C–H$_{alp}$), 3.612 (t 2H, C–H$_{alp}$). IR spectra (KBr pellet): broad band at 3405 cm^{-1} *vs*(O–H), 3042 cm^{-1} *vs*(C–H), 2964 cm^{-1} *vs*(C–H), 2916 cm^{-1}, 2861 cm^{-1}, 1620 cm^{-1}, 1509 cm^{-1} *vb*(C=N), 1450 cm^{-1} *vs*(C=C), 1222 cm^{-1}.

2.3.5 Tripodal receptor L_3

To a solution of 2-mercaptobenzimidazole (0.900 g, 6.0 mmol) in 30 ml acetone:ethanol (3:1) crushed NaOH (0.240 g, 6.0 mmol) was added, and the solution was refluxed for 1h.[9] A 20 ml acetone containing 1,3,5-Tris(bromomethyl)-2,4,6-trimethylbenzene (0.800 g, 2.0 mmol) was added at once, and the reaction mixture was further refluxed for another 24 h at 80 °C. After completion of reaction the white precipitate was filtered off and washed several times with cold water followed by acetone-ethanol (3:1) mixture. The white mass then dried over vacuum.

Yield = 65%, M. P: 345 °C. ^{1}H-NMR (600 MHz, d_6-DMSO) δ (ppm): 7.457 (d 1H, C–H_{ar}), 7.130 (dd 2H, C–H_{ar}), 4.643 (s 2H, C–H_{alp}), 4.587 (s 1H, N–H), 2.479 (s 3H, C–H_{alp}). ^{13}C−NMR (150 MHz, d_6-DMSO) δ (ppm): 16.53, 32.24, 109.44, 121.48, 123.25, 132.87, 136.87 and 149.62. IR spectra (KBr pellet): 2962 cm^{-1} *vs*(C–H), 1500 cm^{-1} *vb*(C=N), 1445 cm^{-1} *vs*(C=C), 1268 cm^{-1}, 1231 cm^{-1}. ESI-mass in methanol: m/z 607.23.

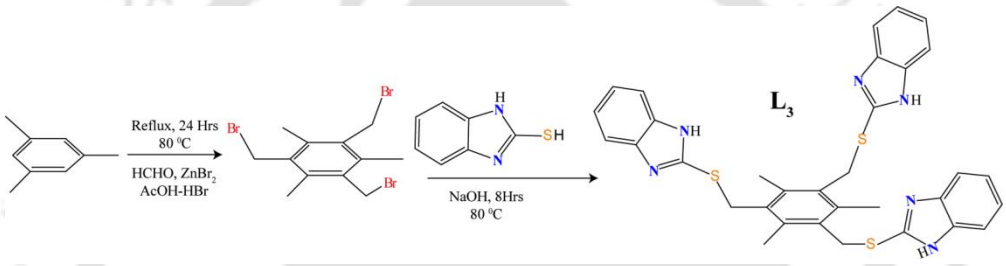

Scheme 2.4 Synthesis of the receptor L_3.

2.3.6 Anion complexes of L_3

[L_3H_2·2F·H_2O](3a): To a methanol solution containing **L_3** (0.060 g, 1.0 mmol) in plastic container 0.1 mL of HF was added and stirred for 1h.

Yield = 70%, M. P: 360 °C. ^{1}H-NMR (600 MHz, d_6-DMSO) δ (ppm): 7.567 (d 1H, C–H_{ar}), 7.264 (dd 2H, C–H_{ar}), 4.726 (s 2H, C–H_{alp}), 3.687 (broad 1H, N–H), 2.549 (s 3H, C–H_{alp}). IR spectra (KBr pellet): broad band at 3202 cm^{-1} *vs*(O–H), 2965 cm^{-1} *vs*(C–H), 1503 cm^{-1} *vb*(C=N), 1435 cm^{-1} *vs*(C=C), 1270 cm^{-1}, 1222 cm^{-1}.

[L_3H_2·2Cl·2H_2O] (3b): Preparation of complex **3b** was identical to that of complex **3a,** except that HCl was added in place of HF acid.

Yield = 80%, M. P: 381 °C. ^{1}H-NMR (600 MHz, d_6-DMSO) δ (ppm): 7.565 (d 1H, C–H_{ar}), 7.252 (dd 2H, C–H_{ar}), 4.714 (s 2H, C–H_{alp}), 3.587 (br 1H, N–H), 2.537 (s 3H, C–H_{alp}). IR spectra (KBr pellet): broad band at 3205 cm^{-1} *vs*(O–H), 2972 cm^{-1} *vs*(C–H), 1508 cm^{-1} *vb*(C=N), 1440 cm^{-1} *vs*(C=C), 1265 cm^{-1}, 1222 cm^{-1}.

2.3.7 Tripodal receptor L_4

Prior reduction crystalline product of tris[2-(4-nitrophenoxy)ethyl]amine (1.0 g) was prepared and yellow crystals was taken into flask containing 50 ml ethanol and heated for 1 hr to dissolve the yellow crystals. The solution was allowed to reach room temperature

and to this mixture 2 mL hydrazine and 0.02 g Pd/C was added and finally the whole mixture was refluxed at 80 °C for another 24 hrs for the completion of reaction. The Pd/C was filtered off and the filtrate was kept into beaker which afforded the colorless crystals of tripodal amine **L_4** within 24 hrs.

Yield = 95%, M. P: 141-143 °C. ^{1}H-NMR (600 MHz, CD_3OD) δ (ppm): 6.668 (d, *J* = 6.2 Hz, 2H, C–H_{ar}), 6.630 (d, *J* = 6.0 Hz, 2H, C–H_{ar}), 4.510 (s, 2H, –NH_2), 3.972 (t, *J* = 5.4 Hz, 2H, C–Halp), 3.004 (t, *J* = 6.0 Hz, 2H, C–H_{alp}). ^{13}C-NMR (150 MHz, CD_3OD) δ (ppm): 153.57, 142.07, 118.36, 116.94, 68.51 and 55.72. IR spectra (KBr pellet): 3430 cm^{-1} *vs*(N—H), 3350 cm^{-1} *vs*(N—H), 2972 cm^{-1} (C–H_{ar}), 2916 cm^{-1} (C–H_{alp}), 1620 cm^{-1} *vb*(N—H), 1518 cm^{-1} *vs*(C=C), 1222 cm^{-1}, 824 cm^{-1}.

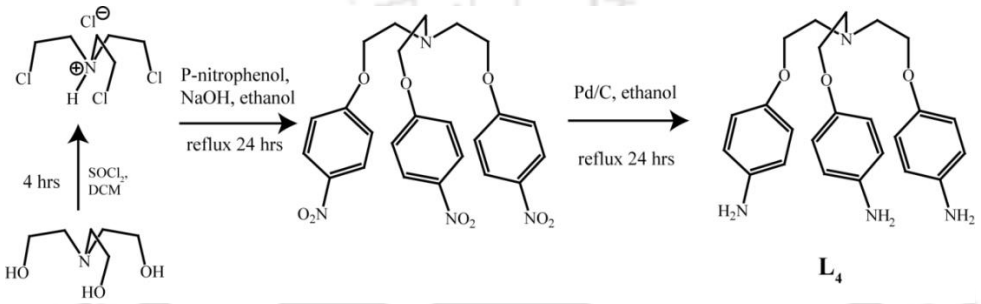

Scheme 2.5 Synthesis of the receptor **L_4**.

2.3.8 Anion complexes of L_4

[L_4H_4·4F·5H_2O](4a): To a 1 ml water of **L_4** in a small plastic container (0.052 g, 0.125 mmol) was added 1-2 drops HF and stirred for 1 hr to obtain the clear solution. Finally the aqueous mixture kept for crystallization in open atmosphere. After rapid evaporation it afforded colorless X-ray mountable single crystal just within a day.

Yield = 90%, M. P: 175-177 °C. ^{1}H-NMR (600 MHz, CD_3OD:D_2O, 1:2) δ (ppm): 7.401 (d, *J* = 6.6 Hz, 2H, C–H_{ar}), 7.142 (d, *J* = 6.6 Hz, 2H, C–H_{ar}), 4.578 (t, *J* = 4.2 Hz, 2H, C–H_{alp}), 4.011 (t, *J* = 4.2 Hz, 2H, C–H_{alp}). IR spectra (KBr pellet): broad and sharp band at 3435 cm^{-1} *vs*(N—H and O—H), 3140 cm^{-1} *vs*(C—H), broad band at 2875 cm^{-1} (N–H), 2590 cm^{-1} (C–H), 1620 cm^{-1} *vb*(N—H), 1510 cm^{-1} *vs*(C=C), 1259 cm^{-1}, 1222 cm^{-1}, 833 cm^{-1}, 740 cm^{-1}.

[L_4H_4·4Cl](4b): To a 1 ml DMF of **L_4** in a glass vial (0.052 g, 0.125 mmol) was added 1-2 drops HCl and stirred for 1 hr. Colorless blocked shape crystal obtained after 1-2 weeks.

Yield = 70%, M. P: 255-256 °C. ^{1}H-NMR (600 MHz, CD_3OD:D_2O, 1:2) δ (ppm): 7.367 (d, *J* = 9.0 Hz, 2H, C–H_{ar}), 7.069 (d, *J* = 9.0 Hz, 2H, C–H_{ar}), 4.545 (t, *J* = 3.6 Hz, 2H, C–H_{alp}), 3.985 (t, *J* = 3.6 Hz, 2H, C–H_{alp}). IR spectra (KBr pellet): broad band at 3440 cm^{-1} *vs*(N—H and O—H), 3150 cm^{-1} *vs*(C—H), broad band at 2882 cm^{-1} (N–H), 2580 cm^{-1} (C–H), 1611 cm^{-1} *vb*(N—H), 1510 cm^{-1} *vs*(C=C), 1259 cm^{-1}, 833 cm^{-1}.

[2L_4H_4·8Cl·5H_2O](4c): Preparation of complex **4c** is similar to **4a** and HCl was added in place of HF. Plate shape crystals were separated within 12 hrs.

Yield = 90%, M. P: 238-240 °C. ^{1}H-NMR (600 MHz, CD_3OD:D_2O, 1:2) δ (ppm): 7.319 (d, *J* = 8.4 Hz, 2H, C–H_{ar}), 7.021 (d, *J* = 8.4 Hz, 2H, C–H_{ar}), 4.492 (t, *J* = 4.6 Hz, 2H, C–H_{alp}), 3.938 (t, *J* = 4.8 Hz, 2H, C–H_{alp}). IR spectra (KBr pellet): broad band at 3440 cm^{-1} *vs*(N—H and O—H), 3150 cm^{-1} *vs*(C—H), broad band 2882 cm^{-1} (N–H), 2580 cm^{-1} (C–H), 1611 cm^{-1} *vb*(N—H), 1510 cm^{-1} *vs*(C=C), 1259 cm^{-1}, 833 cm^{-1}.

[L_4H_4·4Br·5H_2O](4d): Preparation of complex **4d** is similar to **4a** and HBr was added in place of HF.

Yield = 85%, M. P: 282-284 °C. ^{1}H-NMR (600 MHz, CD_3OD:D_2O, 1:2) δ (ppm): 7.401 (d, *J* = 6.6 Hz, 2H, C–H_{ar}), 7.142 (d, *J* = 6.6 Hz, 2H, C–H_{ar}), 4.578 (t, *J* = 4.2 Hz, 2H, C–H_{alp}), 4.011 (t, *J* = 4.2 Hz, 2H, C–H_{alp}). IR spectra (KBr pellet): broad band at 3435 cm^{-1} *vs*(N—H and O—H), 3145 cm^{-1} *vs*(C—H), broad band at 2882 cm^{-1} (N–H), 2585 cm^{-1} (C–H), 1611 cm^{-1} *vb*(N—H), 1510 cm^{-1} *vs*(C=C), 1259 cm^{-1}, 833 cm^{-1}.

[4L_4H_4·16I·7H_2O](4e). Preparation of complex **4e** is similar to **4a** and HI was added in place of HF.

Yield = 80%, M. P: 288-289 °C. ^{1}H-NMR (600 MHz, CD_3OD:D_2O, 1:2) δ (ppm): 7.355 (d, *J* = 7.5, Hz 2H, C–H_{ar}), 7.098 (d, *J* = 7.3 Hz, 2H, C–H_{ar}), 4.541 (t, *J* = 4.3 Hz, 2H, C–H_{alp}), 4.980 (t, *J* = 4.5 Hz, 2H, C–H_{alp}). IR spectra (KBr pellet): broad band at 3420 cm^{-1} *vs*(N—H and O—H), 3138 cm^{-1} *vs*(C—H), broad 2879 cm^{-1} (N–H), 2550 cm^{-1} (C–H), 1611 cm^{-1} *vb*(N—H), 1509 cm^{-1} *vs*(C=C), 1268 cm^{-1}, 824 cm^{-1}.

[L_4H_4·4H_2PO_4·H_2O](4f): Preparation of complex **4f** is similar to **4a** and H_3PO_4 was added in place of HF.

Yield = 80%, M. P: 232-234 °C. ^{1}H-NMR (600 MHz, CD_3OD:D_2O, 1:2) δ (ppm): 7.387 (d, *J* = 8.5 Hz, 2H, C—H_{ar}), 7.071 (d, *J* = 8.6 Hz, 2H, C—H_{ar}), 4.549 (t, *J* = 4.9 Hz, 2H, C–H_{alp}), 3.982 (t, *J* = 4.9 Hz, 2H, C–H_{alp}). IR spectra (KBr pellet): broad band at 3444 cm^{-1} *vs*(N—H and O—H), 3138 cm^{-1} *vs*(C—H), broad band 2907 cm^{-1} (N—H), 2580 cm^{-1} (C—H), 1611 cm^{-1} *vb*(N—H), 1515 cm^{-1} *vs*(C=C), 1259 cm^{-1}, 1129 cm^{-1} *vs*(P=O), 1102 cm^{-1} *vs*(P=O), 935 cm^{-1}.

[2LH_4·9ClO_4·Na·6H_2O](4g): Preparation of complex **4g** is similar to **4a** and $HClO_4$ was added in place of HF.

Yield = 80%, M. P: 274-275 °C. ^{1}H-NMR (600 MHz, CD_3OD:D_2O, 1:2) δ (ppm): 7.321 (d, *J* = 8.2 Hz, 2H, C—H_{ar}), 7.033 (d, *J* = 8.2 Hz, 2H, C—H_{ar}), 4.489 (t, *J* = 4.8 Hz, 2H, C—H_{alp}), 3.956 (t, *J* = 4.7 Hz, 2H, C—H_{alp}). IR spectra (KBr pellet): broad band at 3430 cm^{-1} *vs*(N—H and O—H), 3140 cm^{-1} *vs*(C—H), broad band 2888 cm^{-1} (N—H), 2574 cm^{-1} (C—H), 1611 cm^{-1} *vb*(N—H), 1509 cm^{-1} *vs*(C=C), 1259 cm^{-1}, 1138 cm^{-1} *vs*(Cl=O), 1101 cm^{-1} *vs*(Cl=O), 1083 cm^{-1} *vs*(Cl=O), 833 cm^{-1}.

[L_4H_4·2HSO_4·SO_4](4h): Complex **4h** was obtained by adding 1-2 drops H_2SO_4 acid to the 1 ml aqueous solution of **L_4** (0.052 g, 0.125 mmol) and stirred for 1 hr. Colorless crystal obtained within 12 hrs.

Yield = 80%, M. P: 255-256 °C. ^{1}H-NMR (600 MHz, CD_3OD:D_2O, 1:2) δ (ppm): 7.325 (d, *J* = 8.5 Hz, 2H, C—H_{ar}), 7.032 (d, *J* = 8.5 Hz, 2H, C—H_{ar}), 4.501 (t, *J* = 4.8 Hz, 2H, C—H_{alp}), 3.941 (t, *J* = 4.8 Hz, 2H, C–H_{alp}). IR spectra (KBr pellet): broad band at 3416 cm^{-1} *vs*(N—H), 3138 cm^{-1} *vs*(C—H), broad band 2880 cm^{-1} (N—H), 2583 cm^{-1} (C—H), 1612 cm^{-1} *vb*(N—H), 1509 cm^{-1} *vs*(C=C), 1259 cm^{-1}, 1205 cm^{-1} *vs*(S=O), 1175 cm^{-1} *vs*(S=O), 833 cm^{-1}.

[$LH_4{\cdot}2SO_4{\cdot}H_2O$](4i): Complex **4i** was obtained by adding 1-2 drops H_2SO_4 acid to the 1 ml aqueous solution of **L** (0.052 g, 0.125 mmol) and stirred for 1 hr. Colorless crystal obtained after 1-2 weeks.

Yield = 85%, M. P: 258-260 °C. ^{1}H-NMR (600 MHz, CD_3OD:D_2O, 1:2) δ (ppm): 7.363 (d, *J* = 8.3 Hz, 2H, C—H_{ar}), 7.021 (d, *J* = 8.3 Hz, 2H, C—H_{ar}), 4.498 (t, *J* = 4.5 Hz, 2H, C—H_{alp}), 3.943 (t, *J* = 4.5 Hz, 2H, C—H_{alp}). IR spectra (KBr pellet): broad band at 3425 cm^{-1} *vs*(N—H and O—H), 3138 cm^{-1} *vs*(C—H), broad band 2880 cm^{-1} (N—H), 2583 cm^{-1} (C—H), 1611 cm^{-1} *vb*(N—H), 1509 cm^{-1} *vs*(C=C), 1259 cm^{-1}, small 1195 cm^{-1} *vs*(S=O), 1120 cm^{-1} *vs*(S=O), 833 cm^{-1}.

2.3.9 Tripodal receptor L_5

Tripodal amide-based receptor **L_5** was synthesized by the reaction of tris(2-aminoethyl)amine (TREN) with three equivalents of 4-cyanobenzoyl chloride in presence of triethylamine in dry CH_2Cl_2 at 0 °C.[23] After stirring for 8 hrs the reaction mixture was filtered off and the precipitate was washed with plenty of water and methanol to remove the triethylammonium chloride and dried under vacuum to yield the colorless solid of **L_1** (Yield = 86%). Block shaped crystals of **L_1** were grown from DMF solution.

Yield = 80%, M. P: >300 °C. ^{1}H-NMR (600 MHz, DMSO-d_6) δ (ppm): 8.712 (br, 3H, NH), 7.951 (d, 6H, ArH, *J* = 7. 0 Hz), 7.942 (d, 6H, ArH, *J* = 7.0 Hz), 3.33 (m, 6H, NCH_2), 2.81 (m, 6H, $NHCH_2CH_2$). ^{1}H-NMR (150 MHz, DMSO-d_6): 164.98, 138.36, 132.30, 127.92, 118.28, 113.47, 52.96 and 37.2. IR spectra (KBr pellet): 3277 cm^{-1} *vs*(N–H), 2983 cm^{-1} *vs*(C–H), 2824 cm^{-1} (C–H), 2228 *vs*(C≡N), 1640 *vs*(CO), 1538 cm^{-1} *vs*(C=C). ESI mass [M+1] m/z = 534.2230 (calcd 534.590)

2.3.10 Anion complexes of L_5

All Complexes were obtained by stirring **L_5** (0.05 mM) in 5 mL of DMF in a glass beaker (or plastic vial for complex 6) and 1.2 equiv. of corresponding acid like HF, HBr, HI, HNO_3 and $HClO_4$. After a stirring for an hour, the solution was kept for crystallization.

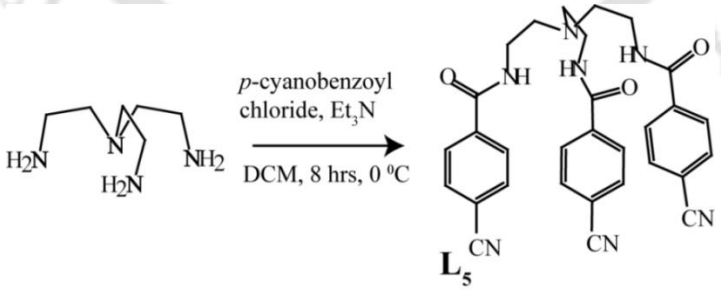

Scheme 2.6 Synthesis of the receptor **L_5**.

[$L_5H{\cdot}Br$](5a): Yield = 75%, M. P: >300 °C. ^{1}H-NMR (600 MHz, DMSO-d_6) δ (ppm): 8.995 (br, 3H, NH), 7.939 (d, 6H, ArH, *J* = 6.8 Hz), 7.889 (d, 6H, ArH, *J* = 7.1 Hz) 3.733 (m, 6H, NCH_2), 3.419 (m, 6H, $NHCH_2CH_2$). IR spectra (KBr pellet): 3342 cm^{-1} *vs*(N–H), 2983 cm^{-1} *vs*(C–H), 2824 cm^{-1} (C–H), 2231 *vs*(C≡N), 1648 *vs*(CO), 1541 cm^{-1} *vs*(C=C).

[L_5H·I](5b): Yield = 70%, M. P: >300 °C. ^{1}H-NMR (600 MHz, DMSO-d_6) δ (ppm): 8.992 (br, 3H, NH), 7.935 (d, 6H, ArH, J = 6.9 Hz), 7.882 (d, 6H, ArH, J = 7.0 Hz) 3.730 (m, 6H, NCH_2), 3.413 (m, 6H, $NHCH_2CH_2$). IR spectra (KBr pellet): 3277 cm^{-1} *vs*(N–H), 2983 cm^{-1} *vs*(C–H), 2824 cm^{-1} (C–H), 2231 *vs*(C≡N), 1640 *vs*(CO), 1538 cm^{-1} *vs*(C=C).

[$(L_5H)_2$·2NO_3·H_2O](5c): Yield = 65%, M. P: >300 °C. ^{1}H-NMR (600 MHz, DMSO-d_6) δ (ppm): 8.990 (br, 3H, NH), 7.933 (d, 6H, ArH, J = 6.8 Hz), 7.884 (d, 6H, ArH, J = 7.1 Hz) 3.728 (m, 6H, NCH_2), 3.409 (m, 6H, $NHCH_2CH_2$). IR spectra (KBr pellet): 3342 cm^{-1} *vs*(N–H), 3014 cm^{-1} *vs*(C–H), 2901 cm^{-1} (C–H), 2231 *vs*(C≡N), 1648 *vs*(C=O), 1537 cm^{-1} *vs*(C=C), 1379 cm^{-1} *vs*(N=O).

[L_5H·ClO_4](5d): Yield = 65%, M. P: >300 °C. ^{1}H-NMR (600 MHz, DMSO-d_6) δ (ppm): 8.990 (br, 3H, NH), 7.930 (d, 6H, ArH, J = 6.9 Hz), 7.883 (d, 6H, ArH, J = 7.0 Hz) 3.725 (m, 6H, NCH_2), 3.406 (m, 6H, $NHCH_2CH_2$). IR spectra (KBr pellet): 3350 cm^{-1} *vs*(N–H), 3046 cm^{-1} *vs*(C–H), 2901 cm^{-1} (C–H), 2231 *vs*(C≡N), 1646 *vs*(C=O), 1537 cm^{-1} *vs*(C=C), 1324 and 1287 cm^{-1} (Cl=O).

2.3.11 Tripodal receptor L_6

Receptor **L_6** was synthesized by following reported procedure.[10] The nitro tripodal was obtained from the treatment of tris(2-chloroethyl)amine hydrochloride by SN^2 substitution with 4-nitrophenol in EtOH (Yield 65%) followed by reduction of nitro group to yield corresponding triamine (Yield 72%). Subsequently, triamine solution in CH_2Cl_2 was slowly added to a mixture of three equivalents of 4-cyanobenzoyl chloride in presence of triethylamine in dry CH_2Cl_2 and stirred for 8 hrs at 0 °C. The reaction mixture is filtered off and the precipitate is washed with water and methanol to remove the triethylammonium chloride and dried under vacuum to yield the gray solid of **L_6**.

Yield = 85%, M. P: 175-177 °C. ^{1}H-NMR (600 MHz, DMSO-d_6) δ (ppm): 10.364 (s, 3N–H), 8.079 (d, 6H, ArH, J = 7.1 Hz), 8.004(d, 6H, ArH, J = 7.3 Hz), 7.654 (d, 6H, ArH, J = 7.0 Hz), 6.940 (d, 6H, ArH, J = 7.2 Hz), 4.087 (t, 6H, -OCH_2, J = 5.4) and 3.05 (t, 6H, -NCH_2, J = 5.8). ^{13}C-NMR (150 MHz, DMSO-d_6): 163.73, 155.08, 149.27, 139.07, 132.47, 131.87, 128.47, 122.14, 118.40, 115.56, 114.57, 113.73, 66.51 and 53.71. IR spectra (KBr pellet): 3287cm^{-1} *vs*(N–H), 3074 cm^{-1} *vs*(C–H), 2870 cm^{-1} (C–H), 2240 *vs*(C≡N), 1640 *vs*(CO), 1515 cm^{-1} *vs*(C=C). ESI mass [M+1] m/z = 810.3070 (calcd. 810.870).

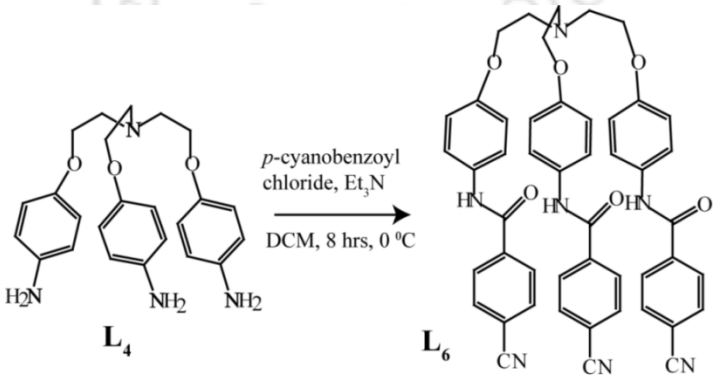

Scheme 2.7 Synthesis of the receptor **L_6**.

2.3.12 Anion complexes of L_6

All Complexes were obtained by stirring **L_6** (0.05 mM) in 5 mL of DMF in a glass beaker (or plastic vial for complex 6) and 1.2 equiv. of corresponding acid like HF, HBr, HI, HNO_3 and $HClO_4$. After a stirring for an hour, the solution was kept for crystallization. **$[L_6H{\cdot}F{\cdot}2H_2O]$(6a)**: Yield = 65%, M. P: 180-181 °C. ^{1}H-NMR (600 MHz, DMSO-d_6) δ (ppm): 10.383 (s, 3N–H), 8.080 (d, 6H, ArH, *J* = 6.9 Hz,), 8.010 (d, 6H, ArH, *J* = 7.0 Hz,), 7.669 (d, 6H, ArH *J* = 6.8 Hz), 6.961 (d, 6H, ArH, *J* = 7.1 Hz,), 4.387 (t, 6H, -OCH_2, *J* = 5.3) and 3.810 (t, 6H, -NCH_2, *J* = 5.5). IR spectra (KBr pellet): broad band at 3425 *vs*(O–H and N–H), 3083 cm^{-1} *vs*(C–H), 2910 cm^{-1} (C–H), 2231 *vs*(C≡N), 1648 *vs*(CO), 1518 cm^{-1} *vs*(C=C).

$[L_6H{\cdot}Br]$(6b): Yield = 70%, M. P: 195-196 °C. ^{1}H-NMR (600 MHz, DMSO-d_6) δ (ppm): 10.397 (s, 3N–H), 8.083 (d, 6H, ArH, *J* = 7.0 Hz), 8.011 (d, 6H, ArH, *J* = 7.2 Hz,), 7.945 (s, DMF solvent) 7.701 (d, 6H, ArH, *J* = 6.8 Hz), 6.961 (d, 6H, ArH, *J* = 7.1 Hz,), 4.389 (t, 6H, -OCH_2, *J* = 5.3) and 3.821 (t, 6H, -NCH_2, *J* = 5.5) 2.886 (s, DMF solvent) and 2.727 (s, DMF solvent). IR spectra (KBr pellet): broad band at 3425 *vs*(O–H and N–H), 3083 cm^{-1} *vs*(C–H), 2910 cm^{-1} (C–H), 2231 *vs*(C≡N), 1648 *vs*(CO), 1518 cm^{-1} *vs*(C=C).

$[L_6H{\cdot}NO_3{\cdot}H_2O]$(6c): Yield = 65%, M. P: 205-207 °C. ^{1}H-NMR (600 MHz, DMSO-d_6) δ (ppm): 10.395 (s, 3N–H), 8.080 (d, 6H, ArH, *J* = 7.3 Hz,), 8.009 (d, 6H, ArH, *J* = 7.0 Hz,), 7.705 (d, 6H, ArH, *J* = 6.5 Hz), 6.966 (d, 6H, ArH, *J* = 7.3 Hz,), 4.383 (t, -OCH_2, *J* = 5.3 6H) and 3.819 (t, 6H, -NCH_2, *J* = 5.5). IR spectra (KBr pellet): broad band at 3435 *vs*(O–H and N–H), 2983 cm^{-1} *vs*(C–H), 2910 cm^{-1} (C–H), 2230 *vs*(C≡N), 1657 *vs*(CO), 1528 cm^{-1} *vs*(C=C), 1380 cm^{-1} *vs*(N=O).

$[L_6H{\cdot}ClO_4]$(6d): Yield = 70%, M. P: 211-212 °C. ^{1}H-NMR (600 MHz, DMSO-d_6) δ (ppm): 10.396 (s, 3N–H), 8.082 (d, 6H, ArH, *J* = 7.0 Hz,), 8.010 (d, 6H, ArH, *J* = 7.1 Hz), 7.946 (s, DMF solvent) 7.699 (d, 6H, ArH, *J* = 6.9 Hz), 7.00 (d, 6H, ArH, *J* = 7.0 Hz,), 4.421 (t, -OCH_2, *J* = 5.3 6H,) and 3.816 (t, -NCH_2, *J* = 5.5 6H) 2.885 (s, DMF solvent) and 2.726 (s, DMF solvent). IR spectra (KBr pellet): broad band at 3435 *vs*(O–H and N–H), 3093 cm^{-1} *vs*(C–H), 2962 cm^{-1} (C–H), 2230 *vs*(C≡N), 1657 *vs*(CO), 1520 cm^{-1} *vs*(C=C) 1259 and 1240 cm^{-1} (Cl=O).

$[(L_6H)_2{\cdot}SIF_6{\cdot}4H_2O{\cdot}2DMF]$(6e): Yield = 60%, M. P: 229-230 °C. ^{1}H-NMR (600 MHz, DMSO-d_6) δ (ppm): 10.397 (s, 3N–H), 8.084 (d, 6H, ArH, *J* = 7.3 Hz), 8.013 (d, 6H, ArH, *J* = 7.0 Hz), 7.945 (s, DMF solvent) 7.701(d, 6H, ArH, *J* = 6.8 Hz), 7.01 (d, 6H, ArH, *J* = 7.0 Hz,), 4.396 (t, 6H, -OCH_2, J = 5.5) and 3.814 (t, 6H, -NCH_2, J = 5.6) 2.884 (s, DMF solvent) and 2.725 (s, DMF solvent). IR spectra (KBr pellet): broad band at 3440 *vs*(O–H and N–H), 3120 cm^{-1} *vs*(C–H), 2963 cm^{-1} (C–H), 2222 *vs*(C≡N), 1656 *vs*(CO), 1518 cm^{-1} *vs*(C=C).

2.3.13 Tripodal receptor L_7

Methanolic solution of 3 equivalent of *p*- chlorobenzaldehyde (0.840 g, 6 mM) was added slowly to nethanolic solution of TREN (0.300 g, 2 mM) in RB flask with constant stirring. The mixture was stirred for another 8 hrs. Oily product was obtained after solvent evaporation. The oily product further dissolved in methanol and one-fourth times $NaBH_4$ added by portions with interval of time and left for 24 hrs for the completion of the reaction. The light brown oily product was obtained after water-chloroform work up.[11]

Yield = 75%. ^{1}H-NMR (600 MHz, DMSO-d_6) δ (ppm): 7.284 (d, 6H, ArH, *J* = 7.3 Hz), 7.213 (d, 6H, ArH, *J* = 7.0 Hz), 4.527 (s, 3N–H), 3.596 (t, 6H, -NCH_2, J = 5.5 Hz) and 3.414 (t, 6H, -NCH_2CH_2, J = 5.6 Hz). ^{13}C-NMR (150 MHz, DMSO-d_6): 139.87, 131.07, 129.21, 127.8, 62.13, 53.6, 52.12. IR spectra (KBr pellet): broad band at 3440 *vs* (N–H), 3217 cm^{-1} *vs*(C–H), 2963 cm^{-1} (C–H), 1518 cm^{-1} *vs*(C=C). ESI mass: m/z 521.1330 (L_7+H).

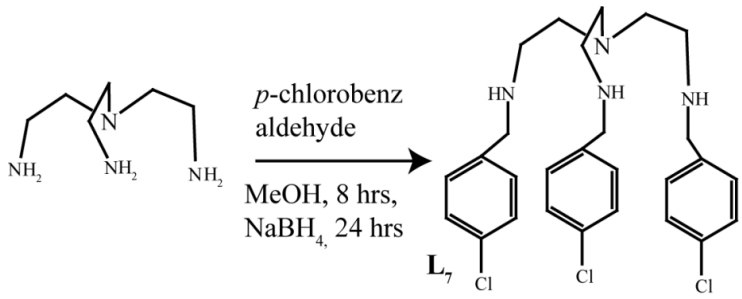

Scheme 2.8 Synthesis of the receptor **L_7**.

2.3.14 Anion complex of L_7

[L_7H_3·F_3](7a): 1.2 equivalent of HF was added to a plastic vial containing methanolic solution of **L_7** (0.05 mM, 0.026 g) and stirred for one hour. Colourless blocked shaped crystals were grown from clear solution in a week.

Yield = 60%. M.P- 215 °C ^{1}H-NMR (600 MHz, DMSO-d_6) δ (ppm): 8.636 d, 7.911 d 7.421 7.546 d, 7.28 s, 6.969 d, (d, 6H, ArH, *J* = 7.4 Hz), 7.36 (d, 6H, ArH, *J* = 7.1 Hz), 8.617 (s, 3N–H), 3.626 (t, 6H, -NCH_2, J = 5.6 Hz) and 3.520 (t, 6H, -NCH_2CH_2, J = 5.6 Hz).

2.3.15 Tripodal receptor L_8

Preparation of second generation tripodal receptor **L_8** was similar to that of **L_7** except that the triamine **L_4** (Chapter 5) is used in place of TREN.

Yield = 70%. ^{1}H-NMR (600 MHz, DMSO-d_6) δ (ppm): 7.284 (d, 6H, ArH, *J* = 7.3 Hz), 7.213 (d, 6H, ArH, *J* = 7.0 Hz), 4.527 (s, 3N–H), 3.596 (t, 6H, -NCH_2, J = 5.5 Hz) and 3.414 (t, 6H, -NCH_2CH_2, J = 5.6 Hz). ^{13}C-NMR (150 MHz, DMSO-d_6): 156.9, 149.9,143.6, 139.6, 135.2, 130.9, 129.0, 128.0, 122.3, 115.1,113.2, 67.2, 53.81, 46.21. IR spectra (KBr pellet): broad band at 34280 *vs* (O–H and N–H), 3229 cm^{-1} *vs*(C–H), 2958 cm^{-1} (C–H), 1516 cm^{-1} *vs*(C=C). ESI mass: m/z 765.15 (L_8+H).

2.3.16 Anion complex of L_8

[L_8H_4·$4HSO_4$·$2H_2O$](8a): Dilute H_2SO_4 (1.2 equivalent) acid was added to methanolic solution of **L_8** (0.05 mM, 0.026 g) and stirred for one hour. Colourless blocked shaped crystals were grown from clear solution in a week.

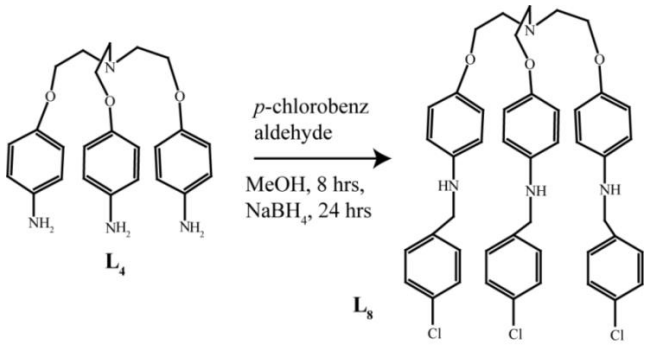

Scheme 2.9 Synthesis of the receptor $\mathbf{L_8}$.

Yield = 65%, M. P: 288-290 °C. ^{1}H-NMR (600 MHz, DMSO-d_6) δ (ppm): 7.380 (d, 6H, ArH, *J* = 7.1 Hz,), 7.32 (d, 6H, ArH, *J* = 7.0 Hz,), 7.205 (d, 6H, ArH, *J* = 6.5 Hz), 6.966 (d, 6H, ArH, *J* = 7.3 Hz,), 5.395 (s, 3N–H), 4.383 (t, -OCH_2, *J* = 5.3 6H) and 3.819 (t, 6H, -NCH_2, *J* = 5.5) 3.616 (t, 6H, -NCH_2, J = 5.5 Hz). IR spectra (KBr pellet): broad band at 3435 *vs*(O–H and N–H), 2983 cm^{-1} *vs*(C–H), 2910 cm^{-1} (C–H), 2230 *vs*(C≡N), 1657 *vs*(CO), 1528 cm^{-1} *vs*(C=C), 1380 cm^{-1} *vs*(N=O).

References

1. SAINT and *XPREP*, 5.1 ed.; Siemens Industrial Automation Inc.: Madison, WI, **1995**. Sheldrick,G. M.
2. *SADABS, empirical absorption Correction Program*; University of Göttingen: Göttingen, Germany, **1997**.
3. Sheldrick, G. M.; *SHELXTL Reference Manual: Version 5.1*; Bruker AXS: Madison, WI,
4. **1997**.
5. Sheldrick, G. M.; *SHELXL-97: Program for Crystal Structure Refinement;* University of Göttingen: Göttingen, Germany, **1997.**
6. Mercury 2.3 Supplied with Cambridge Structural Database; CCDC: Cambridge, U.K., **2011 -2012**.
7. Van der Sluis, P.; Spek, A. LActa Crystallogr., Sect. A: Found. Crystallogr., **1990**, *46*, 194.
8. Barragán, F. J.; Rosa, d. l.; J. L. Ariza, Gómez.; Pino, F. *Mikrochim. Acta*, **1984,** *82*, 171.
9. Dey, S. K.; Das, G. *Cryst. Growth. Des*. **2010**, *10*, 754.
10. Fan, C.; Ma, C.; Chen, C.; Chen, F.; Liu, Q. *Inorg. Chem. Commun*. **2003**, *6*, 491.
11. Basu, A.; Das, G. *Chem. Commun*., **2013**, *49*, 3997.
12. Bose, P.; Ravikumar, I.; Ghosh, P. *Inorg. Chem*. **2011**, *50*, 10693.

Chapter 3

Linear Pyridine-Urea Receptor and Its Interaction with Hydrated Anions:

Effect of positional isomer

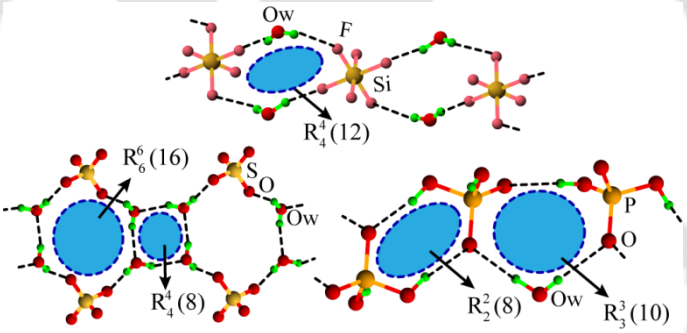

3.1 Back ground and focus on this chapter

Ion solvation is one of the most important subjects in solution chemistry. In recent times recognition of anions in hydrated forms has attracted a great deal of attention due to their occurrence in natural and biological environments.[1] Hydrated anions show a wide range of complicated interactions due to spontaneous formation of strong stable hydrogen bonds in an aqueous environment. As a consequence recognition of ordered anion-water clusters is a challenging task for researcher. Further, the formation of ordered anion-water clusters within chemical receptors allows an unique occasion to understand detail molecular interactions in these confined environments.[2] In particular, there has been significant attention on understanding the ordered water clusters in hydrophobic environments[3] due to their vast importance in chemical and biological interfaces.[4] Various types of anion-water clusters have been reported in synthetic.[5,6]

The design and study of suitable organic receptors is fundamental while studying supramolecular aspect of anions. The urea H-bonding functionalities may be used for anion binding as it is widely used. In this case, pyridine substituted urea have been chosen, where anion binding urea function along with two pyridine units (suitable for protonation). The pyridyl units not only act as protonation site, but they also enhances the solubility and anion binding efficiency of the receptor in aqueous medium. Urea containing receptors have general tendency of self-assosciation.[7] Though presence of water molecule sometimes disrupts self-aggregation through H-bonding.[8] By virtue of pyridine moiety anions are further stabilized by electrostatic interaction in protonation state. There are few linear urea have been exploited for anion binding,[9] few of them resulted self-associated interactions in presence of less basic anions.[10] Hence our attempt will be to avoid such incident by forcing them to bind with anions. The urea moiety is best known for binding of specially oxyanions. In this chapter anion complexation study in presence of inorganic acid of three isomeric pyridine-urea based receptors is discussed. Anion complex gives additional information about anion-water aggregation. Depending upon position of N-atom in the pyridine moiety, it offers various types of anion-water combination which finally manifest anion-water structure relationship.

3.2 Structural aspect of anion binding with the isomeric pyridine-urea receptors $^{o}L_1$ (*ortho*), $^{m}L_1$ (*meta*) and $^{p}L_1$ (*para*)

All three isomeric receptors were synthesized in good yield by reacting carbohydrazide with pyridinealdehyde following the reported literature procedure.[11] All the reported anion

complexes were obtained by slow evaporation of H_2O-CH_3OH (9:1) solution in presence of respective inorganic acids. Here the solid state structures of three isomers and their anion complexes will be discussed. It is observed that the orientation of the protonation sites generate very unique anion-water clusters.

3.3 Structural description of [^{o}L$_1$·3H$_2$O](1)

The *ortho* isomer ^{o}**L$_1$** crystallized in *P-1* space group as a colourless solid and asymmetric unit contains one ^{o}**L$_1$** and three water of crystallization. Solid state structure shows the receptor adopts *anti-anti* conformation (the N-atom of pyridine moiety either syn or anti relative to the C=O group). The receptor is flat and the urea hydrogen is in *syn-anti* orientation. Computational study shows the *anti-anti* isomer is most stable conformation over *syn-syn* or *syn-anti* conformer[9] and which is observed in case of the free receptor.

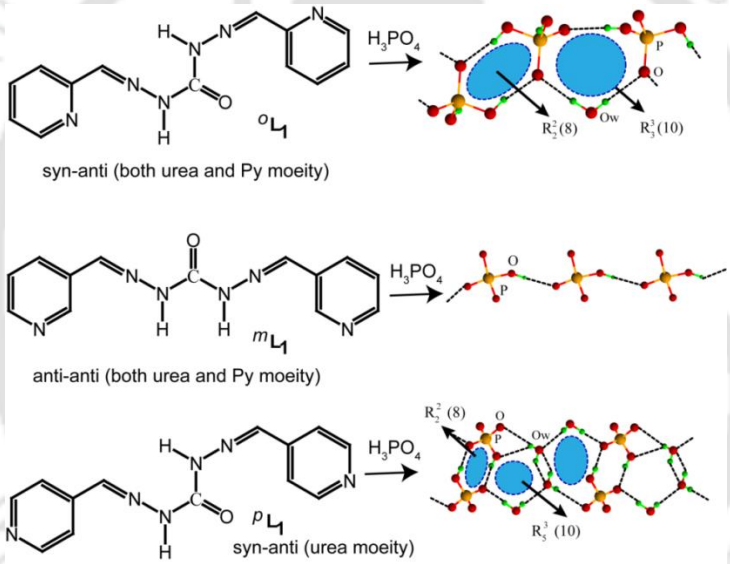

Scheme 3.1 The conformation of each isomer in protonated state and pyridine N-atom directed diverse anion-water assemblies.

Self-association between urea groups in this case was inevitably cancelled due to presence of water molecule. The water is H-bonded with urea hydrogen N3···O3w = 3.027(2) Å, and N4···O2w = 2.998(2) Å. The crystallized water molecules form a water trimer. Two trimer meet an inversion centre at O2w and O4w forming a discrete water hexamer $[H_2O]_6$ containing square like water tetrameric core and two pendent water molecules O3w, are finally intercalated in the crystal host as explained in Figure 3.1a. The square is made of O2w and O4w, forming a structural motif R_4^4 (8). The water hexamer is tightly held by O2w···O4w = 2.873(2) Å, O4w···O3w = 2.888(3) Å and O4w···O2w = 2.834(3) Å H-bonding interactions. The structural analysis of tetramer shows the four oxygen and the

four hydrogen atoms involved in the cyclic array of hydrogen bonds are almost coplanar and the ∠O2w–O4w–O2w and ∠O4w– O2w–O4w bond angle is 89.7° and 90.3°, indicate perfect square array of water molecules. In the tetrameric cluster the H-atoms pertain less stable *uudd* geometry. The small water clusters such as tetramer[12] and hexamers,[13] provide information for understanding the behaviour of bulk water. The Ow···Ow found in this water cluster is very similar to those observed in liquid water (2.854 Å) and little longer than in the case of ice (I_c 2.750 Å and I_h 2.759 Å).[13] The hexamer is surrounded by six receptor and additionally interacts with N–H···Ow, and C–H···Ow (Figure 3.1b). The packing diagram along *a*-axis shows the confinement of water hexameric cluster $[H_2O]_6$ in the channel of the receptor. The presence of water cluster is well verified with presence of a broad peak centred at 3407 cm^{-1}. The bulk phase purity of the crystals is examined by coherence of experimental simulated PXRD pattern (Figure A3.4).

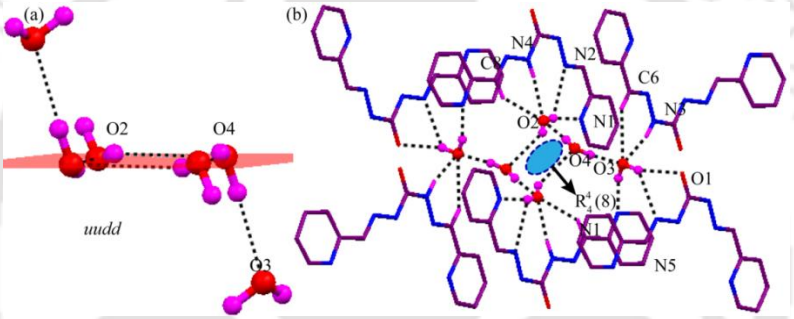

Figure 3.1 (a) Discrete water hexameric cluster $[H_2O]_6$ containing square shaped water tetramer with *uudd* geometry in free receptor **1**. (b) Interaction of the cluster $[H_2O]_6$ with the receptor.

3.3.1 Structural description of [^{o}L$_1$H$_2$·2I·3H$_2$O](2)

The reaction of ^{O}**L$_1$** with hydriodic acid formed the dark red complex **2** which crystallizes in *P-1* space group. The receptor is doubly protonated as expected form 1:2 complex with iodide ion and asymmetric unit contains one $^{O}\mathbf{L_1H_2}^{2+}$, two iodide ion and three water of crystallization. It is noticed conformational change of the receptor in protonated state and here it is the *syn-anti* conformation whereas urea H-atom remains same (Scheme 3.1). Crystallographic analysis shows two iodide ions are tetra coordinated and partially hydrated at least containing two water molecules. Three water molecules and two iodide ions are H-bonded, two such ensemble are assembled transforming into a discrete H-bonded iodide-water cluster $[I_4\text{-}(H_2O)_6]^{4-}$ (Figure 3.2a). The hybrid cluster contains a cyclic core of iodine-water tetramer $[I_2\text{-}(H_2O)_2]^{2-}$ composed of O2w···I1 = 3.480(3)/3.780(3) Å H-bonds and two pendent water-iodide trimer $[I\text{-}(H_2O)_2]^{1-}$ having contacts O3w···I2 = 3.500(2) Å and O4w···I2 = 3.530(2) Å. Though I1–O2w–I1–O2w possess a planar geometry, the bond angle ∠I1–O2w–I1 = 132.8(9)° and ∠O2w–I1–O2w =

47.2(7)° clearly defy the square geometry of the tetramer. The hybrid iodide-water tetramer can be classified as R_4^2 (6) motif. It is observed total four types I···O distances, among them three are less or equal to 3.50 Å. The I···O distances in this report are shorter than the averaged theoretical value of 3.67 Å for the lowest-energy conformer.[14] The shorter I···O distances show stronger interactions between the I^- and water molecules through H-bonds in this complex indicate highly stable iodide-water cluster in crystal host. With the best of our knowledge, discrete iodide-water cluster $[I_4\text{-}(H_2O)_6]^{4-}$ found in the simple system like this have not been reported previously except one report of $[I\text{-}(H_2O)_6]^-$.[14] As the solid state report of iodide-water cluster is very rare and may be help full to the structural and solution chemist. So our report is new and can be fruitful in the realm of anion-water clusters. The iodine anion water cluster is of particular interest because it has large polarizability and a large ionic radius.[15] On the other hand, it is big debate in the current study of halogen hydration, whether the halide is inside the clusters or on their surface and how many water molecules are required for its complete solvation.[16] At this stage, our the finding is very important to structural chemist and may

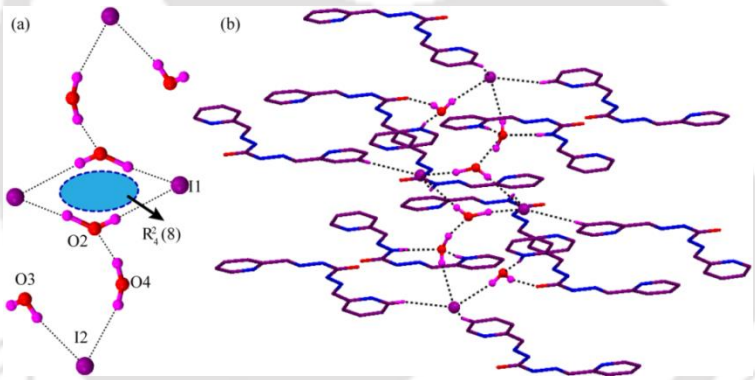

Figure 3.2 (a) The perspective diagram of the discrete anion-water cluster $[I_4\text{-}(H_2O)_6]^{4-}$ containing a cyclic tetramer in complex **2**. (b) Extensive H-bonded networks showing the interactions of the $[I_4\text{-}(H_2O)_6]^{4-}$ cluster with the protonate receptor.

be help full resolve many issues regarding iodide-water hydration. The anion-water cluster $[I_4\text{-}(H_2O)_6]^{4-}$ occupy the empty space in the crystal void of complex **2** and extensively interact through multiple Ow/N–H···Ow, N/C–H···I^- H-bond with the cationic receptor. The active participation of aromatic CH, urea NH and PyH^+ stabilize the iodide-water cluster with H-bonding distances and angles C1···I2 = 3.870(2) Å and ∠C1–H1···I2 = 156.0(1)°, C2···I2 = 3.890(2) Å and ∠C2–H2···I2 = 143.0(1)°, $N1^+$···Ow3 = 2.700(3) Å and ∠$N1^+$–H1N···Ow3 = 163.0(1)°, Ow3···O1 = 2.870(3) Å and ∠Ow3–H3OA···O1 = 155.0(22)°, N4···I1 = 3.650(2) Å and ∠N4–H4N···I1 = 139.0(1) Å, C11···I1 = 3.870(2) Å and ∠C11–H11···I1 = 136.0(1)° as depicted in Figure 3.2b. The crystal packing along *b*-

axis shows layered array of the protonated receptor with the inclusion of iodide-water cluster to its void. The presence of water cluster is well verified with presence of a broad peak centred at 3407 cm^{-1}. The bulk phase purity of the crystals is examined by coherence of experimental simulated PXRD pattern.

3.3.2 Structural description of [^{o}**L**$_1$**H**$_2$·**SO**$_4$·3**H**$_2$**O**](3)

The reaction of ^{o}**L**$_1$ with sulfuric acid (H_2SO_4) gave the colorless complex **3**. X-ray structural elucidation of the complex shows that it crystallizes in triclinic system with space group $P\bar{1}$. The asymmetric unit contains one doubly protonated $^{o}\mathbf{L_1H_2}^{2+}$, sulfate anion and three crystalline water molecules. The receptor forms 1:1 complex with trihydrated sulfate anion. The protonated receptor is planar and similar conformation like complex **2**. It forms strong H-bonding interactions with the sulfate anion and water molecules. The detailed coordination environment of SO_4^{2-} suggests that, it is stabilized

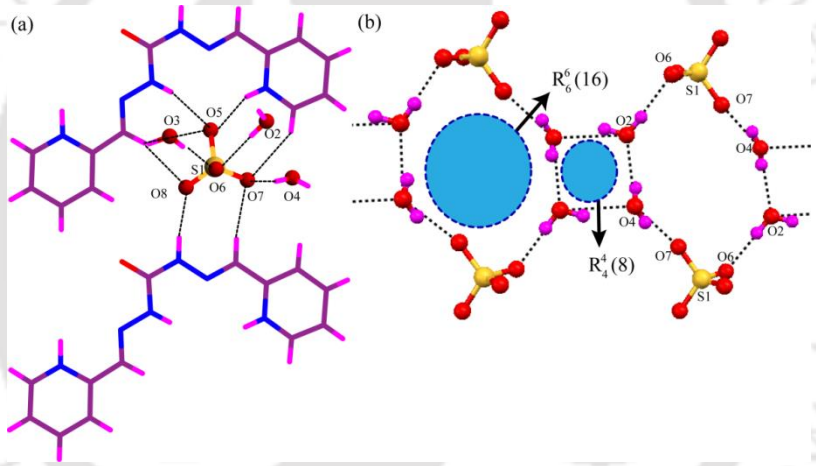

Figure 3.3 (a) Coordination mode of sulfate anion in complex **3.** (b) Depicting infinite chain of fused sulfate-water hexamer $[(SO_4)_2–(H_2O)_4]_\infty^{4-}$ and water tetramer. (c) Space-filling representation of two fused rings.

via ten H-bonding interactions with two receptor cations and three water molecules, comprised of three N–H···O (two urea NH and one PyH^+), three O···H_2O (lattice water) and four C–H···O strong bonds (three imine and one aromatic). The detailed H-bonding interactions (distance and angle) are as follows: N1···O5 = 2.733(3) Å and ∠N1–H1N···O5 = 161.0(3)°, N4···O5 = 2.970(2) Å and ∠N4–H4N···O5 = 163.5(1)°, N3···O8 = 2.866(2) Å and ∠N3–H3N···O8 = 169.0(1)°, O2w···O6 = 2.781(3) Å and ∠O2w–H2B···O6 = 175.6(2)°, O3w···O6 = 2.762(3) Å and ∠O3w–H3A···O6 = 173.0(3)°, O4w···O7 = 2.689(3) Å and ∠O4w–H4A···O7 = 162.4(2)°, C5···O7 = 3.311(3) Å and ∠C5–H5···O7 = 143.2(2)°, C6···O7 = 3.385(2) Å and ∠C6–H6···O7 = 156.6(2)°, C8···O8 = 3.283(3) Å and ∠C8–H7···O8 = 160.1(2) °, C8···O5 = 3.396(3) Å and ∠C8–

H7···O5 = 141.2(2)°. Two oxygen atoms of sulfate ion O6 and O8 behave as bifurcated H-bond acceptor while O5 and O7 behave as trifurcated H-bond acceptor resulting in ten H-bonds within acceptable donor-to-acceptor distances (Figure 3.3a). Interestingly, in complex **3** two hydrated sulfate anions met each other in opposite direction *via* two H-bonding interactions between O2w and O4w water molecules, which eventually led the formation of an unusual sulfate-water hexameric ring $[(SO_4)_2–(H_2O)_4]$. There are very rare reports of hydrated sulfate anion, though recently structural properties of sulfate-water cluster and their importance have been emphasized by theoretical[17] and experimental[18] studies. So this structural report is relatively new The cyclic hexameric sulfate-water cluster was formed *via* six H-bonding interactions among two sulfate anions and four water molecules, and only two oxygen atoms of each sulfate anion are involved in H-bonding interactions in this cluster (Figure 3.3b). The solid-state arrangement of water molecules and sulfate anions probably helps the formation of H-bonded sulfate-water network. It is noted that the hexameric ring is not planar and form classical chair conformation where four water molecules lies in the plane and two sulfate anions are present above and below of the plane. The hexameric sulfate-water ring is mainly stabilized by strong H-bonding interactions with urea NH and PyH^+ functions of the protonated receptors. The H-bonding interactions involved in cyclic sulfate-water cluster are O2w—H2B···O6 (O2w···O6 = 2.781(3) Å, ∠O2w—H2B···O6 = 175.6(2)°), O4w—H4A···O7 (O4w···O7 = 2.689(3) Å, ∠O4w—H4A···O7 = 162.4(2)°) that gave $R_6^6(16)$ motif. Further, it also interact with the water molecules of neighbor clusters through H-bonding which subsequently led the formation of 1D polymeric aggregates of sulfate-water clusters in the hydrophobic pocket of the receptors along crystallographic *b* axis (Figure A3.6). The infinite polymeric aggregates were made by repeating two fused rings (Figure 3.3b), of which one is sulfate-water hexamer and other one is water tetramer. Close inspections of the distance and angle of this water tetramer confirmed it to be nearly square array. In addition crystal packing viewed along *a* axis generate hydrophilic sulfate-water channel surrounded by hydrophobic receptor. The presence of H-bonded hydrated sulfate anion in complex **3** has also been confirmed by solid-state FT-IR analysis. The presence of a moderate signal at 3435 cm^{-1} and a strong signal ~1100 cm^{-1} in complex **3** attributed to the stretching frequencies of the water and sulfate anion respectively which are absent in free receptor. Additionally, the bulk purity of the sulfate complex **3** was also established by nearly similar experimental and simulated PXRD pattern (Figure A3.7a).

3.3.3 Structural description of [2 ^{o}L$_1$H·2H$_2$PO$_4$·3H$_2$O](4)

On protonation with phosphoric acid, ^{O}**L$_1$** yielded complex **4**. Single crystal X-ray analysis of dihydrogen phosphate complex **4** reveals that it is in monoprotonated state, form 1:1 colorless complex with $H_2PO_4^-$ anion. The asymmetric unit of complex **4** contains two symmetry independent mono protonated ^{O}**L$_1$H$_2^+$**, two different symmetric $H_2PO_4^-$ ions and three lattice water molecules. Similar to complex **2,** both the receptors are coplanar and present same conformation. It forms H-bonding interactions with $H_2PO_4^-$ anions and water molecules. The coordination environments of two crystallographically non-equivalent $H_2PO_4^-$ anions are different. Interestingly, extended the H-bonding contacts on $H_2PO_4^-$ anions in complex **2** shows that one water molecule (O1w) acts as a bridging H-bond donor between two symmetry independent $H_2PO_4^-$

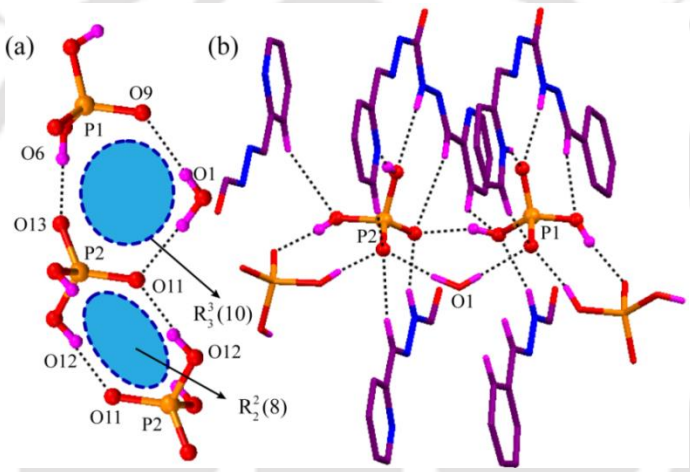

Figure 3.4 (a) Showing alternative arrangement of cyclic trimeric and dimeric rings of hydrated $H_2PO_4^-$ anions in complex **4**. (b) Space-filling model of two inter connected cyclic ring motifs of $H_2PO_4^-$ anions. (c) Coordination mode and stabilization of the infinite chain of hydrated $H_2PO_4^-$ anions *via* H-bonding interactions with cationic receptor.

anion and form unusual water bridge cyclic trimer $[H_2PO_4\text{-}H_2O\text{-}H_2PO_4]^{2-}$, while two same symmetric $H_2PO_4^-$ anions form cyclic dimer $[H_2PO_4\text{-}H_2PO_4]^{2-}$ *via* complementary strong H-bonding interactions and resulted structural motif $R_3^3(10)$ and $R_2^2(8)$ respectively (Figure 3.4a). The detailed H-bonding parameters involved in cyclic trimer and dimer are as follows: O1w···O9 = 2.829(7) Å and ∠O1w–H1B···O9 = 177.0(9)°, O1w···O12 = 2.777(6) Å and ∠O1w–H1A···O12 = 174.0(7)°, O6···O13 = 2.580(5) Å and ∠O6–H6O···O13 = 158.0(2)°, O7···O9 = 2.531(4) Å and ∠O7–H7O···O9 = 170.0(2)°, O11··O12 = 2.571(5) Å, and ∠O11–H11O···O12 = 168.7(2)°. Full H-bonding details are given in supporting information. These two cyclic ring motifs are arranged in alternative fashion and ultimately led the formation of an interesting polymeric assembly of hydrated $H_2PO_4^-$ anions in the hydrophobic environment of complex **4** along the *a* axis. These

cyclic anionic rings are mainly stabilized by strong H-bonding interactions with urea NH and PyH^+ functions of the protonated receptor(s). Probably the geometry of the mono protonated receptor and the unique H-bonding dual (donor and acceptor) nature of the $H_2PO_4^-$ anion play crucial role in the formation of polymeric assembly of hydrated $H_2PO_4^-$ anions in complex **4**. Moreover, the detailed coordination environments of $H_2PO_4^-$ anions show that the $H_2P(1)O_4^-$ is stabilized *via* ten H-bonds while $H_2(2)PO_4^-$ is stabilized *via* eleven H-bonds (Figure 4.3b). In case of $H_2(1)PO_4^-$ oxygen atoms O7 and O8 form two H-bonds each in bifurcated fashion, while O6 and O9 form three H-bonds each in trifurcated fashion. Whereas for $H_2(2)PO_4^-$ O10 and O11 form two H-bonds each in bifurcated fashion, while trifurcated and tetrafurcated mode of H-bonding interactions are observed for O13 and O12 respectively. Structural study in-depth shows among three crystalized water molecules only one directly involved in H-bonding with $H_2PO_4^-$ anions, but other two water molecules (O2w and O3w) interacts with C=O (carbonyl) and pyridine moiety shown in Figure S23. But in case of sulfate complex **3** all three water molecules interacts with sulfate anion. The packing diagram along *c* axis shows dihydrogen phosphate-water and water molecules lies in two different hydrophobic pockets forming anion-water and water channel respectively. The vibrational stretching frequency of complex **4** indicates a broad band centered around 3440 cm^{-1} and sharp peak ranging from 1120-1157 cm^{-1} that can be attributed to O-H and P-O bond suggesting presence of water molecule and $H_2PO_4^-$ anion. The bulk phase purity of the complex was also confirmed by PXRD study where simulated and experimental pattern closely matches each other.

3.3.5 Structural description of $[^{O}L_1H_2{\cdot}ClO_4{\cdot}2H_2O]$(5)

The complex **5** crystalizes in $P\bar{1}$ space group and X-ray structure reveals that the doubly protonated receptor forms 1:2 (receptor: anion) light yellow complex. The asymmetric unit contains one doubly protonated $^{O}\mathbf{L_1H_2}^{2+}$, two perchlorate anions and two lattice water molecules. The complex **5** exhibit same orientation of Py and urea moiety like complex **2.** ClO_4^- anion form cyclic anion-water ring transforming into infinite $[(ClO_4)_2\text{-}H_2O]_\infty^{2-}$ chain *via* H-bonding and few unusual interactions as depicted in Figure 3.5a. The hydrogen atom of O2w are shared between two neighbored ClO_4^- ions. The water molecule O2w donate hydrogen to two ClO_4^- ion by O2w···O5 = 3.016(5) Å, O2w···O8= 2.766(6) Å and acts as H-bond acceptor from urea NH (N3···O2w = 2.816(4) Å). Very interestingly it is observed anion-anion $ClO_4^-\cdots ClO_4^-$ and anion-water (lone pair) $ClO_4^-\cdots$O2w contacts with distances O5···O10 = 2.994(4) Å and O9···O2w = 2.929(5) Å in the perchlorate-water chain and play important role in stabilization of the infinite chain. The anion-anion interaction is

exploited very recently by solid state structural evidences.[19] Study shows the majority of structures containing the O···O separation ranges between 2.85 and 3.05 Å.[20] Hence O···O

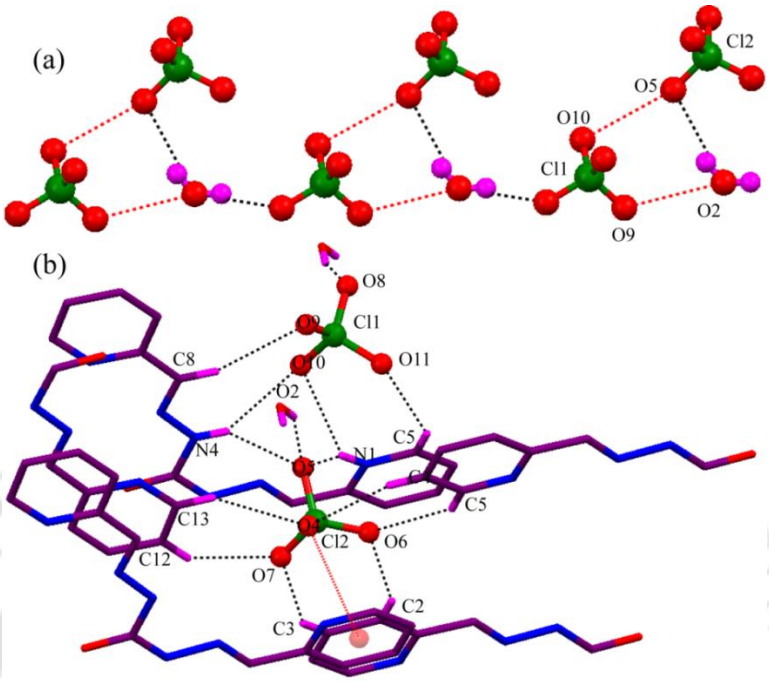

Figure 3.5 (a) View showing infinite perchlorate-water chain $[(ClO_4)_2\text{-}H_2O]_\infty^{2-}$ and $ClO_4^-\cdots Ow$ and $ClO_4^-\cdots ClO_4^-$ interactions (red lines) in complex **5**. (b) Pictorial diagram explaining coordination environment of two perchlorates ion and very interesting $ClO_4^-\cdots\pi^+$ interactions.

distance found in this anion-water assembly is further validated as it fall in that range. Structural analysis shows while one water molecule (O2w) interacts with ClO_4^- ion, other water molecule (O3w) connects the two planar protonated receptors through H-bonding interactions with C=O and PyH^+, form square like geometry resulting an H-bonding $R_2^2(6)$ motif Figure A3.7b. The bonding parameters in square motif are O3w···O1 = 2.840(4) Å, ∠O3w—H3A···O1 = 150.0(6)° and O3w···O1 = 3.009(4) Å, ∠O3w–H3B···O1 = 134.0(5)°. The coordination environments of two ClO_4^- anions are different. The $Cl(1)O_4^-$ is six and $Cl(2)O_4^-$ is ten coordinated *via* several N–H···O (urea and PyH^+),O···H_2O and C–H···O interactions (Figure 3.5b). Notably, for $Cl(2)O_4^-$ two oxygen atom O4 and O6 lies perfectly perpendicular to pyridinium moiety of receptor and form very important anion···π^+ interactions with distance of 3.212 Å and 3.733 Å (Figure 3.5b). This separation is little larger than previously reported similar types interactions.[21] The protonated receptor in complex **5** form hydrophobic layers and perchlorate-water are entrapped between the layers forming hydrophilic chain. The broad band centered around 3444 cm^{-1} and 1083-1138 cm^{-1} in the FT-IR spectrum of complex **5** can be attributed to the O-H and

Cl-O stretching frequency. Nearly similar experimental and simulated PXRD pattern of complex **5** confirmed the bulk phase purity of the complex.

3.4.1 Structural description of [$^{m}L_1H_2{\cdot}HPO_4{\cdot}H_2O$](6)

Reaction of *meta* isomer $^{m}\mathbf{L_1}$ with H_3PO_4 lead to the formation of the complex **6.** The structural analysis shows that it is the 1:1 complex and phosphate is di-anionic. The complex crystallizes in orthorhombic system with space group *Pna2₁* and asymmetric unit contains one $^{m}\mathbf{L_1H_2}^{2+}$, one HPO_4^{2-} and one water of crystallization. In this case the receptor in protonated state displays *anti-anti* (both urea and Py moiety with respect to C=O). The receptor is flat and makes a linear wire which is further confirmed by comparable torsion angle ∠O1-C14-N4-N5 and ∠O1-C14-N3-N2 ~ 2.7° [N–NH–(C=O)–NH–N]. This kind conformation was not observed for *ortho* isomer $^{o}\mathbf{L_1}$ which resulted new type of solid state interactions (will be discussed latter). The only HPO_4^{2-} ion is H-bonded each other by a single contact point O6···O4 = 2.552(5) Å [angle 160.7(2)°] and assembled into a 1-D infinite chain $[HPO_4^{2-}]_\infty$ with graph sheet notation C(3) as shown in Figure 3.6a. The only water molecule does not interact with HPO_4^{2-} ion, indeed donate its two hydrogen to two C=O groups having distances O2w···O1 = 2.878(6) Å and 2.923(6) Å [angles 143(6)° and 163(5)°] and helps to assemble the receptors. The linear orientation of the receptor makes possible simultaneous participation of urea moiety for binding of HPO_4^{2-} anion. The details inspection of HPO_4^{2-} binding shows that the HPO_4^{2-} is bounded

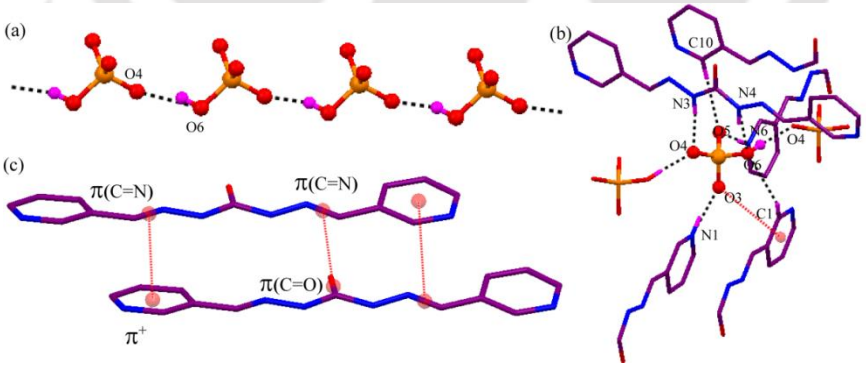

Figure 3.6 (a) Depiction of 1-D infinite chain $[HPO_4^{2-}]_\infty$ by single point intermolecular H-bond among HPO_4^{2-} in complex **6**. (b) View showing the H-bonding and $HPO_4^{2-}\cdots\pi^+$ (red line) interactions around HPO_4^{2-} anion. (c) The stacking interaction comprised of various types π···π and $\pi^+\cdots\pi$ contacts.

strongly *via* four N–H···O, two C–H···O, two O–H···O H-bonds and one interesting anion···π^+ interaction giving nine coordinated HPO_4^{2-} anion as explained in Figure 3.6b. Thus O3 of HPO_4^{2-} is involved in two point contacts with the hydrogen atoms of PyH^+ and

$HPO_4^{2-}\cdots\pi^+$ where as H4N and H6OA make contacts with O4. Further, O5 form bifurcated H-bond with H10 and H6N. O8 of HPO_4^{2-} form trifurcated H-bond by accepting hydrogen from N3 and C1, and donating hydrogen to another HPO_4^{2-} anion. The details H-bonding parameters in the coordination sphere of HPO_4^{2-} are as follows, N1···O3 = 2.544(5) Å and ∠N1–H1N···O3 = 167.7(3)°; HPO_4^{2-}(O3)···π^+ = 3.609 Å; N4···O4 = 2.791(5) and ∠N4–H4N···O4 = 168.2(3)°; C10···O5 = 3.381(5) Å and ∠C10–H10···O5 = 150.3(3)°; N3···O6 = 2.954(5) Å and ∠N3–H3N···O6 = 165.7(2)°; C1···O6 = 3.356(6) Å and ∠C1–H1···O6 = 131.0(3)°. By virtue of the perfect linearity of the receptor various types π···π stacking observed in the stair case molecular packing. The receptor slips little from one layer to another and π electron cloud of the PyH^+, C=N and C=O interacted in various fashion as explained in Figure 3.6c. The intermolecular stacking from various π^+ and π electron are $\pi^+\cdots\pi$ = 3.405/3.428 Å (PyH^+ and C=N) and π···π = 3.458 Å (C=N and C=O). The crystal packing diagram along *a*-axis shows the existence of infinite chain $[HPO_4^{2-}]_\infty$ and water molecule between the stacked layers of the receptor. The presence of water and HPO_4^{2-} anion was also confirmed by FT-IR spectrum where band centered at about 1129 and 1157 cm^{-1}. The bulk phase purity of the complex was checked by superimposable simulated and experimental PXRD pattern.

3.5.1 Structural description of [2^{p}L$_1$H·SiF$_6$·4H$_2$O](7)

The reaction of *para* isomer with $^p\mathbf{L_1}$ HF acid in glass vial yielded 2:1 (receptor:anion) complex **7** which crystallizes in the monoclinic space group *P2/c*, with asymmetric units consisting of one mono-protonated $^p\mathbf{L_1H^+}$, one half SiF_6^{2-} anion and two water of crystallization. In this case it is observed *syn-anti* orientation of urea moiety with respect to C=O group like complex **2**. The receptor is coplanar like complex **2** and non-linear unlike *meta* isomer in complex **6** which is further reflected in large difference torsion angle values ∠O1-C7-N4-N5 ~ 172.9° and ∠O1-C14-N3-N2 ~ 2.2° [N–NH–(C=O)–NH–N]. Though the conformation of $^p\mathbf{L_1H^+}$ and $^o\mathbf{L_1H_2^{2+}}$ is similar, but significant difference in crystal packing of the receptor is noticed (will be explained latter). The interesting structural features obtained from aggregation of water and SiF_6^{2-} anion. The water molecule O2w acts as a bridge between two SiF_6^{2-} anion by donating hydrogen to F2 and F3 atom forming tetrameric $[(SiF_6^{2-})_2\text{-}(H_2O)_2]^{4-}$ cluster as shown in Figure 3.7a. Extension of the structures reveals infinite chain of $[(SiF_6^{2-})_2\text{-}(H_2O)_2]^{4-}$ with the structural motif $R_4^4(12)$ is running through the receptor host. The short contacts involved in making the infinite chain are O2w···F2 = 2.944(5) Å and angle ∠O2w–H2OA···F2 = 163.0(7)°; O2w···F3 = 2.761(5) Å and angle ∠O2w–H2OB···F2 = 159.0(5)°. Our solid state report of

tetrameric $[(SiF_6^{2-})_2\text{-}(H_2O)_2]^{4-}$ cluster and Ow···F distances is quiet similar to the previous report[22a] and cluster is quite different from our report during SiF_6^{2-} anion recognition where anion is coordinated only with water molecules rather forming any cyclic motif.[22b]

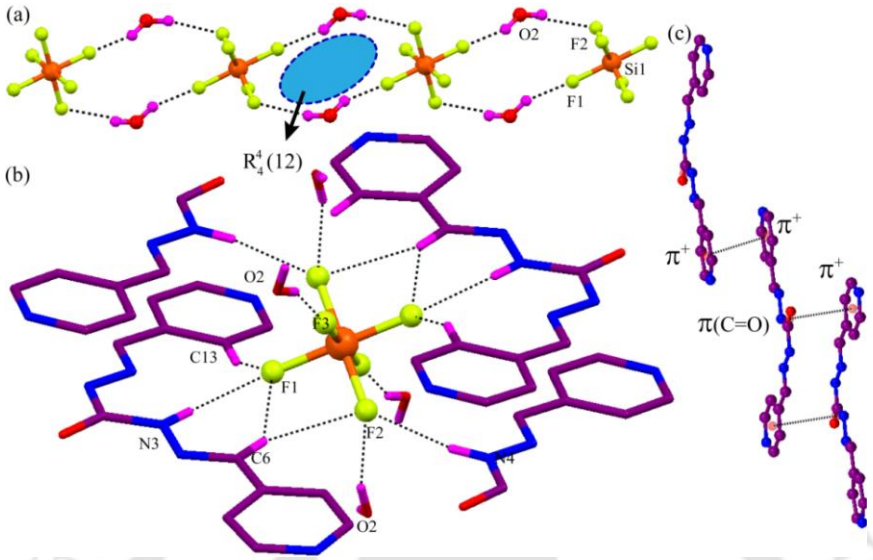

Figure 3.7 (a) Infinite chain of 1-D tetrameric cluster of $[(SiF_6^{2-})_2\text{-}(H_2O)_2]_\infty^{4-}$ in complex **7**. (b) Magnified view of fourteen coordinated SiF_6^{2-} anion. (c) Various $\pi^+\cdots\pi$ and $\pi^+\cdots\pi^+$ interaction in staircase aggregation of mono protonated $^{P}\mathbf{L_1H^+}$.

The coordination environment about the SiF_6^{2-} is satisfied by N–H···F, Ow–H···F and C–H···F H-bonding as depicted in Figure 3.7b. Details structural view shows it is fourteen coordinated, among them two symmetry equivalent F3 only coordinated with water molecule and other two sets of equivalent F2, F1 are tri-coordinated. The bond distances in SiF_6^{2-} fall in the of 2.742(5) Å to 3.435(4) Å. Higher degree of coordination for SiF_6^{2-} is reported, shows it may even greater as eghiteen.[22b] contact between the receptor shows only this case PyH^+ and Py is H-bonded each other *via* strong N6···N1 = 2.742(5) Å H-bond and form 1-D aggregation of the receptor in zigzag fashion (Figure A3.8a). The zigzag layers are interconnected with the next layer *via* water molecule O3w which formed H-bond with the acceptor C=O group with contacts O3w···O1 = 2.876(8)/2.918(7) Å. As a result distinguishable crystal packing in complex **7** was observed where infinite chain $[(SiF_6^{2-})_2\text{-}(H_2O)_2]^{4-}$ and O3w occupy different void. In the assembly of the protonated receptors, here it is also observed $\pi^+\cdots\pi$ ($PyH^+\cdots C{=}O$) $\pi^+\cdots\pi^+$ ($PyH^+\cdots PyH^+$) play crucial role as explained in Figure 3.7c. Very strong and broad features at approximately 3416 cm^{-1} in the FT-IR spectra of complex **7** arise from O-H stretching frequencies of the waters of crystallization. The bulk phase purity of the complex was confirmed from the PXRD data. The diffraction patterns of complex **7** matched closely with simulated PXRD patterns obtained from their single crystal X-ray structures.

3.5.2 Structural description of [^{p}L$_1$H$_2$·2NO$_3$·3H$_2$O](8)

The reaction of ^{p}**L$_1$** with HNO_3 produced 1:2 the complex **8** and crystallizes in triclinic space group $P\bar{1}$. The asymmetric unit contains one $^{p}\mathbf{L_1H_2}^{2+}$, two nitrate anion and three crystallized water molecules. While refining, after several effort to fit H-atom on water molecules O6w and O7w in logical manner on Fourier map was failed. In solid state the conformation of the receptor in this complex is similar like complex **7.** Inspection in the crystal structure shows all three crystallized water molecules and one nitrate ion are involved in anion-water aggregation leading to infinite 1-D anion-water chain containing cyclic nitrate-water cluster $[(NO_3)_2\text{-}(H_2O)_6]_\infty^{2-}$ (Figure 3.8a). The centrosymmetric nitrate-water cluster is composed of various Ow–H···Ow and Ow–H···ONO_2^- H-bonding interactions. Three water molecules (O5w, O6w and O7w) and one NO_3^- ion form acyclic tetramer (NO_3^--O6w-O5w-O7w) having distances, O6w···O10 = 2.790(3) Å, O6w···O5w = 2.762(8) Å and O5w···O7 = 2.750(1) Å. Two such tetramers are interlinked through O9 of NO_3^- ion at O7w end of the tetramer (O7w···O9 = 2.580(3) Å) forming the inversion symmetry related nitrate-water cluster $[(NO_3)_2\text{-}(H_2O)_6]^{2-}$. Each cyclic octamer are connected with other at the point of O7w and O10 forming an infinite 1-D chain of the cluster $[(NO_3)_2\text{-}(H_2O)_6]_\infty^{2-}$ containing fused tetrameric ring. There are few reports on nitrate-water cluster like $[(NO_3)_4\text{-}(H_2O)_6]^{4-}$ [23] and $[(NO_3)_6\text{-}(H_2O)_6]^{6-}$ [24] embedded into metal-organic frame work and calix[4]arene based purely organic system respectively. Existence of the nitrate-water cluster in such a simple system is a worth to pay attention. Our report is very similar with the cyclic core of the cluster $[(NO_3)_6\text{-}(H_2O)_6]^{6-}$. It is noted that the O···O distance within the anionic nitrate–water cluster ranges from 2.58 to 2.78 Å. The bond distance found in this case is shorter than those observed in the nitrate–water clusters.[23, 24] Especially the distance 2.58 Å is just little longer than 2.50 Å (low barrier H-bond) is very strong. Hence it can be sounded our finding of anion-water cluster is highly stable and tightly included in the inter-space of the receptor. Details study in coordination site shows two nitrate ion is stabilized by N–H···O, Ow–H···O, C–H···O and anion···π^+ interactions. The $N(7)O_3^-$ is tetra-coordinated whereas $N(10)O_3^-$ is eight coordinated as explained in Figure 3.8b. The striking difference in the molecular crystal packing of the complex **8** compared to complex **2** (though their conformation is very similar) that receptor moieties are oriented in the opposite direction with a strong dimeric association. In this case it is observed, the *syn*-oriented urea NH and C=O, a complementary donor-acceptor pair form stable dimer of the receptor with the contact N4···O1 = 2.882(7) Å

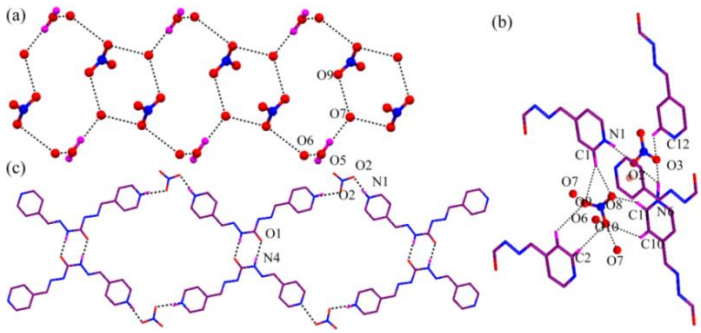

Figure 3.8 (a) View of the H-bonded assembly of infinite nitrate-water cluster $[(NO_3)_2\text{-}(H_2O)_6]_\infty^{2-}$ containing two fused rings in complex **8**. (b) Representation of nitrate ion stabilization by various interactions including $NO_3^-\cdots\pi^+$ (red line). (c) Nitrate ion induced 1-D aggregation of N–H···O=C H-bonded dimer of the receptor.

(Figure 3.8c). This is the only case in series of anion complexes studied here, where anion recognition and ligand association occurred simultaneously. As the both N-atom is protonated, no chance to form any $N^+–H_{Py}\cdots N_{Py}$ unlike the complex **7**. In this case NO_3^- come into play of forming $N^+–H\cdots$ moiety. Due to presence of planar nitrate ion the receptor oriented in such way that only $\pi^+\cdots\pi^+$ is possible (Figure A3.9b) unlike other complexes. The dimer is finally extending into a 1-D layered arrangement of receptor along the *a*-axis through NO_3^- (N7) which interacts with N-atom of PyH^+ having bonding parameters, N1···O2 = 2.764(7) Å and angle ∠N1–H1N···O2 = 165.0 (10)°; N6···O3 = 2.729(7) Å and angle ∠N6–H6N ···O3 = 154.0(8)°. The packing diagram viewed down along the *a*-axis shows that nitrate-water occupy void between the adjacent layers. The presence of the water molecules and nitrates were also confirmed by FT-IR spectroscopy where a broad peak for O-H at 3414 cm^{-1} and shape peak for N-O at 1018 and 1101 cm^{-1} are fairly prominent. The powder XRD pattern of complex **8** is identical to the simulated one which implied that the presence crystals in mass scale.

3.5.3 Structural description of $[^{p}\mathbf{L_1H_2}\cdot\mathbf{HPO_4}\cdot\mathbf{3H_2O}]$(9)

Acidification of $^{4}\mathbf{L_1}$ with H_3PO_4 acid generates 1:1 complex **9** and crystallographic analysis revealed that the receptor in its double protonated form. It crystallizes in the triclinic space group $P\bar{1}$ and asymmetric unit contains one $^{p}\mathbf{L_1H_2}^{2+}$, one HPO_4^{2-} and three water of crystallization. Our best effort to add hydrogen atom on water molecule O4w was unsuccessful. Orientation of urea hydrogen is similar to that of other complexes in this series. The phosphate anion in this case is mono protonated like *meta* isomer in complex **6**. Unlikely in complex **6**, it is seen 1-D assembly of HPO_4^{2-} anion and water molecule did not participate at all. But in this case all three molecules facilitate the anion-water cluster assembly through H-bond formation. Crystal structure analysis shows that HPO_4^{2-} ion undergoes self-dimerization $[HPO_4^{2-}]_2$ with graph sheet notation $R_2^2(8)$ and forms H-

bond through donor-acceptor combination between O7 and O5 with very strong contact 2.562(3) Å (angle ∠O7–H7O···O5 = 166.4(2) °). The other oxygen atom of the dimer like O5, O6 and O7 are available as H-bond acceptor with the water molecules O2w and O3w. The water molecules act as a bridging agent between two hydrogen phosphate dimers. Indeed a single H-bonded water dimer of O2w and O3w is extended from O5 oxygen of the $[HPO_4^{2-}]_2$ dimer where both H-atom of O2w is shared with O3w and O5 having separations O2w···O5 = 2.826(3) Å and angle ∠O2w–H2OA···O5 = 179.0(7)°; O2w···O3w = 2.960(8) Å and angle ∠ O2w–H2OB···O3w = 165.0(5)° which formed anion-cluster $[(HPO_4^{2-})_2\text{-}(H_2O)_2]^{4-}$ asexplained in Figure 3.9a. Very interestingly the $[HPO_4^{2-}]_2$ dimer with two dangling water molecules (O2w and O3w) interlinked each other through the formation of double H-bonded water dimer (O3w···O3w = 2.880(1) Å) in order to build fused pentameric rings. Hence the infinite phosphate-water chain is consisting of several rings like fused hydrogen phosphate-water pentamer, hydrogen phosphate dimer and water dimer (Figure 3.9a). Infinite 1-D assembly of phosphate-water with minimum repeating unit $[(HPO_4^{2-})_2\text{-}(H_2O)_2]$ expressed into the cationic channel of the receptor. Our structural finding of di basic phosphate-water assembly is relatively unique and can be verified by recent scientific reports. It is well known that dihydrogen phosphate owing to proton donors and acceptors, it tends to aggregate into oligomeric and polymeric structures in the solid state. Pure anionic clusters of $H_2PO_4^-$ in organic crystals containing polymeric to discrete structural motif have been reported previously.[25] In comparison the hydrogen

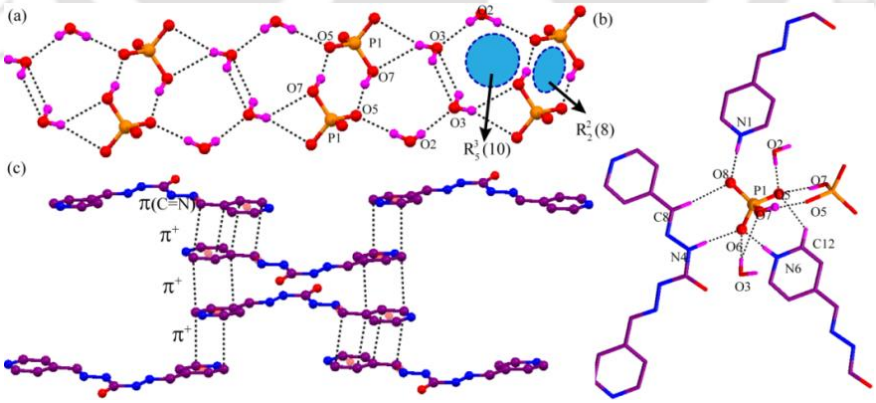

Figure 3.9 (a) Representation of the infinite hydrogen phosphate-water chain containing water and HPO_4^{2-} dimer and fused pentamer in complex **9**. (b) View showing the coordination environment around HPO_4^{2-} dianion. (c) Snapshot of stacking interaction performed by $\pi^+\cdots\pi^+$ and $\pi^+\cdots\pi$ interaction.

phosphate-water assembly is almost unexplored. Therefore from this perspective these structural elucidation phosphate-water clusters is interesting to structural chemists. Solid state binding of the hydrogen phosphate anion shows it is ten coordinated and fulfilled by

several N–H···O, Ow–H···O, O–H···O and C–H···O H-bonding interactions as highlighted in Figure 3.9b. O6 and O8 oxygen atom of HPO_4^{2-} accepts two pyridinium NH and one urea NH with bonding parameters N1···O8 = 2.616(4) Å and angle ∠N1–H1N···O8 = 174.1(2)°, N6···O6 = 2.631(4) Å and angle ∠N6–H6N···O8 = 175.0(4)°, N4···O6 = 2.841(3) Å and angle ∠N4–H4N···O6 = 165.0(2)°. The contacts details of other imine and aromatic carbon C8 and C12 are C8···O8 = 3.209(4) and angle ∠C8–H8···O8 = 156.2(2)°, C12···O5 = 3.299(4) Å and angle ∠C12–H12···O5 = 131.8(2)°. Details inspection in molecular structure indicates various $\pi^+\cdots\pi^+$ and $\pi^+\cdots\pi$ interactions arising from pi cloud of PyH^+ and C=N helps to grow stacked structure of the receptor (Figure 3.9c). The close packing plot reveals infinite anion-water chain runs along with stacking direction of the receptor. Furthermore, the presence of water and phosphate anion in the complex **9** was identified by FT-IR spectra. The complex showed a broad band at around 3420 cm^{-1} and 1120-1162 cm^{-1} that can be assigned to the O−H and P−O stretching vibration of water and phosphate ion present in the complex. The almost identical simulated and experimental PXRD pattern indicate the bulk phase purity of the crystals.

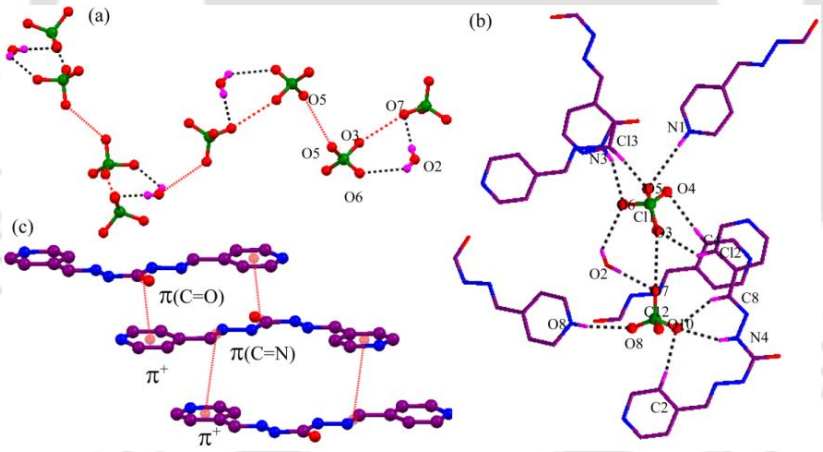

Figure 3.10 (a) Close up view of the 1-D infinite zigzag perchlorate-water cluster containing the repeating unit $[(ClO_4)_2\text{-}H_2O]_\infty^{2-}$, red contacts indicates the $ClO_4^-\cdots ClO_4^-$ interactions. (b) Magnified view showing coordination of ClO_4^- ion with urea NH, pyridinium NH^+, water OH and aromatic CH H-bonds. (c) Layer structure of cationic moieties through $\pi^+\cdots\pi$ stacking interactions.

3.5.4 Structural description of [^{p}L$_1$H$_2$·ClO$_4$·H$_2$O](10)

Crystals of complex **10** were obtained from reaction of ^{p}**L$_1$** and $HClO_4$ acid. X-ray study shows it is doubly protonated and crystallizes in monoclinic space group $P2_1/c$, with asymmetric unit containing one $^p\mathbf{L_1H_2}^{2+}$, two ClO_4^- and one water of crystallization. The conformation of the receptor in this salt is similar to others in this series. The anion-water assembly is also almost identical to that of complex **5**. Structural analysis shows the only water molecule is H-bonded between two perchlorate ion forming a $[(ClO_4^-)_2\text{-}H_2O]^{2-}$

cluster with contacts O2w···O7 = 3.008(6) Å and angle ∠O2w–H2OA···O7 = 176.0(24)°; O2w···O6 = 3.150(1) Å and angle ∠O2w–H2OB···O7 = 132.0(24)°. It is noted that the anion-water cluster is further connected with each other through ClO_4^-···ClO_4^- and ClO_4^-···O2w interactions transforming into 1-D infinite chain as explained in Figure 3.10a. Despite the same number of water and perchlorate ion present in the anion-cluster in both complexes (**5** and **10**), it is observed perchlorate-anion progress in a zigzag fashion containing two additional ClO_4^-···ClO_4^- interactions which is not observed in complex **5**. Two perchlorate ions is hepta and octa-coordinated, the coordination mode and stabilization of $[(ClO_4)_2\text{-}H_2O]_\infty^{2-}$ is highlighted in Figure 3.10b. The H-bond arising from urea NH, pyridinium NH, water OH and aromatic CH, all play fundamental role in coordinating with perchlorate ions. Close inspection shows the π electron cloud of C=O, C=N and pyridinium moiety interacts among them and furnishes various π^+···π contacts as shown in Figure 3.10c. The broad band centered around 3370 cm^{-1} and 1092-1142 cm^{-1} in the FT-IR spectrum of complex **10** can be attributed to the O-H and Cl-O stretching frequency. Nearly similar experimental and simulated PXRD pattern of complex **10** confirmed the bulk phase purity of the complex.

3.6 Thermogravimetric analysis

Thermo gravimetric analysis (TGA) to examine the thermal stability of all the complexes and henceforth stability of anion-water clusters was performed. TG curve of free receptor $^{o}\mathbf{L_1}$ shows release of three water molecules with a significant weight loss 17.52 % (calcd 16.61%) from 60-100 °C. This change is also appeared in DSC plot from endothermic peak at 100 °C shown in Figure A3.5a. TGA of complex **2** shows a weight loss 8.73% (calcd. 9.34%) 100-122 °C for three crystallized water molecules which is also appeared in DSC plot by giving a endothermic peak. The weight loss 7.8% (calcd 8.5%) in complex **3** corresponding to two water molecules removed at 116 °C while one water molecule is retained up to 145 °C and released along with the decomposition of the complex, which suggest the water molecules involved in cyclic sulfate-water cluster released first and then the removal of strongly bounded water molecule (by PyH^+ moiety and sulfate anion) took place. Unfortunately there was not observed any curve in these temperature regions even after several repeat, though endothermic peak at 220 °C corresponding to decomposition of the complex is appeared on the DSC plot (Figure A3.5b). In case of complex **4**, although the coordination environments of three water molecules are different but did not observe any gradual loss of water, rather TGA study exhibited a facile weight loss of

6.70% (calcd 6.86%) at 120 °C indicating the removal of all three water molecules simultaneously. The endothermic and exothermic peaks at 118 °C and 210 °C are seen which indicates the loss of water and decomposition of the complex respectively. The complex **5** holds the water molecules weakly as observed from TG study where weight loss 6.85 % (calcd 7.12%) related to two water molecules released early at 92 °C. The exhibition of endothermic peak at 90 °C and endothermic peak at 260 °C in its DSC plot suggest the water loss and decomposition of the complex. The complex **6** lost its only one water molecule (Exp. 3.95%, calcd 4.68%) at around 110 °C showing a endothermic peak at that region is little less compared to complex **4** due to coordination environment. two water molecules from complex **7** is removed at 125 °C giving a weight loss 4.01% (calcd 4.8%) which is further confimed from a endothermic peak at 123 °C in DSC plot. The complex **8** shows a weight loss 11.26% (calcd 12.15%) at 130 °C for three water molecules and for what a endothermic peak is appeared in DSC plot. the complex **9** shows a weight loss 12.04% (calcd. 12.91%) for two water molecules at 125 °C compared to complex **4** for a endothermic peak is appeared.

3.7 Species distribution curve and determination of anion binding constant

The protonation constant of $^{o}\mathbf{L_1}$ and binding constant of $^{o}\mathbf{L_1H_2}^{2+}$ with tetrahedral anions were determined by potentiometric method in water/methanol (9:1) medium (Figure 3.11). The distribution curve showed $^{o}\mathbf{L_1H_2}^{2+}$ predominate at pH lower than 3.8. Upon addition of base it starts to lose the proton and the monoprotonated species exist up to pH 4.5. The further increase in pH shows the abundance of neutral receptor $^{o}\mathbf{L_1}$ which predominates after pH 6.5. The binding affinity of $^{o}\mathbf{L_1H_2}^{2+}$ towards several tetrahedral oxyanion showed that the log K value for SO_4^{2-}, $H_2PO_4^-$ and ClO_4^- are 0.49, 0.35 and 0.08 respectively. These values suggest receptor interacts with SO_4^{2-} and $H_2PO_4^-$ ion strongly compared to perchlorate ion (Table 3.2a and 3.2b).

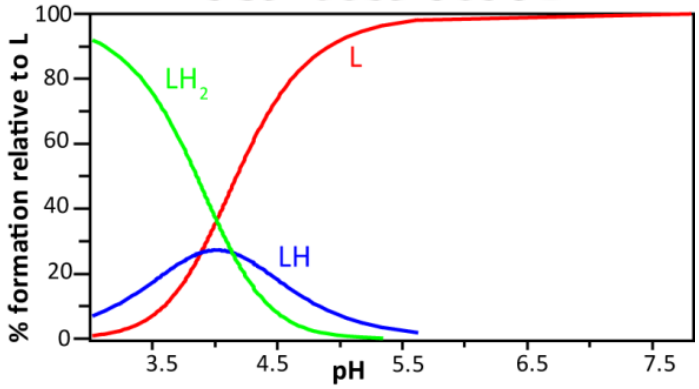

Figure 3.11 Species distribution curve for protonation of $^{o}\mathbf{L_1}$.

Conclusion

Solid state recognition of anions in their various hydrated states by H-bond rich isomeric pyridine-urea receptor has been systematically investigated. The formation of stable discrete water hexamer and hybrid iodide-water cluster $[I_4\text{-}(H_2O)_6]^{4-}$ containing a tetrameric core of either water or iodide water respectively, infinite sulfate-water chain containing chair like sulfate-water hexamer $[(SO_4)_2\text{-}(H_2O)_4]_\infty^{4-}$, infinite chain of dihydrogen phosphate–water trimer $[(H_2PO_4)_2\text{–}H_2O]_\infty^{2-}$ and a simple perchlorate-water chain has been presented by *ortho* isomer of pyridine-urea functionalized hydrophobic system. Whereas *meta* isomer gave simple 1-D infinite $[HPO_4]_\infty^{2-}$ chain. The *para* isomer stabilizes infinite chain of 1-D tertameric cluster $[(SiF_6^{2-})_2\text{-}(H_2O)_2]_\infty^{4-}$, nitrate-water cluster $[(NO_3)_2\text{-}(H_2O)_6]_\infty^{2-}$ containing two fused rings, assembly of phosphate-water with minimum repeating unit $[(HPO_4^{2-})_2\text{–}(H_2O)_3]$ and perchlorate-water cluster. Very interestingly C–N (C=O and NH) can rotate freely, showing considerable flexibility for the receptor which leads to different configurations in its acid adducts. The *ortho* and *para* isomer is 'V' structured whereas *meta* isomer form a wire like linear structure. In all cases the anions are stabilized by N–H···O (urea NH and PyH^+), O···H_2O (lattice water), C–H···O and anion···π^+ interactions. Moreover other supramolecular interactions like anion···anion/anion–π^+ and π^+···π/ π^+···π^+ also play an important role in complexation and packing of molecules in the solid state. It is observed that versatile anion-binding units have a decreased tendency to self-associate by urea···urea hydrogen bonding through coordination with anions. Thermal stability of anion-water cluster was established by TGA and binding constant of the receptor with anions was determined by potentiometric titration in aqueous medium. Our study of hydration of anions in hydrophobic environment studied in protic solvent are relevant to highly hydrophobic biological systems which may open the opportunity of study of complex behavior of anions in aqueous phase.

References

1. (a) Lee, A.; Dawson, P. A.; Markovich, D. *Int. J. Biochem. Cell Biol.* **2008**, *37*, 1350. (b) Marcus, Y.; *Ion Solvation*, Wiley, Chichester, **1986**. (c) Richens, D. T.; *The Chemistry of Aqua Ions*, Wiley, Chichester, **1997**.
2. (a) Cametti, M.; Rissanen, K. *Chem. Commun*. **2009**, 2809. (b) Hudnall, T. W.; Chiu, C.-W.; Gabbai, F. P. *Acc. Chem. Res*. **2009**, *42*, 388.
3. Ma, B.-Q.; Sun, H.-L.; Gao, S. *Chem. Commun*. **2004**, 2220.
4. (a) Sleigh, S. H J. L. *Nature*. **1998**, *393*, 671. (b) Peters, J.; Baumeister, W.; Lupas, A. *J. Mol. Biol*. **1996**, *257*, 1031. (c) Li, Y.; Jiang, L.; Feng, T.-B.; Lu, X.-L. *Cryst. Growth Des*. **2008**, *8*, 368. (d) Tame, J. R. H.; Dodson, E. J.; Wilkinson, A. J. *Biochemistry*. **1997**, *36*, 9747.
5. (a) Cametti, M.; Rissanen, K. *Chem. Soc. Rev*. **2013**, *42*, 2016. (b) Bakhoda, A.; Khavasi, H. R.; Safari, N. *Cryst. Growth Des*. **2011**, *11*, 933. (c) MacGillivray, L. R.; Atwood, J. L.; *J. Am. Chem. Soc*. **1997**, *119*, 2592. (d) Wang, Q.-Q.; Day, V. W.; Bowman-James, K. *Angew. Chem., Int. Ed*. **2012**, *51*, 2119. (e) Chakraborty, S.; Dutta, R.; Arunachalam, M.; Ghosh, P. *Dalton Trans*. **2014**, *43*, 2061.
6. Sessler, J. L.; Gale, P. A.; Cho, W. S. Anion Receptor Chemistry; Royal Society of Chemistry: Cambridge, U.K., **2006**.
7. Chang, Y. L.; West, M. A.; Fowler, F. W.; Lauher, J. W. *J. Am.Chem. Soc*. **1993**, *115*, 5991.
8. (a) Schauer, C. L.; Matwey, E.; Fowler, F. W.; Lauher, J. W. *J. Am. Chem. Soc*. **1997**, *119*, 10245. (b) Plater, M. J.; de Silva, B. M.; Skakle, J. M. S.; Howie, R. A.; Riffat, A.; Gelbrich, T.; Hursthouse, M. B. *Inorg. Chim. Acta*. **2001**, *325*, 141.
9. Custelcean, R.; Moyer, B. A.; Bryantsev, V. S.; Hay, B. P. *Cryst. Growth Des*. **2006**, *6*, 555.
10. Chang, Y. L.; West, M. A.; Fowler, F. W.; Lauher, J. W. *J. Am. Chem. Soc*. **1993**, *115*, 5991.
11. Barragán, F. J.; Rosa, d. l.; J. L. Ariza, Gómez.; Pino, F. *Mikrochim. Acta*, **1984**, *82*, 171.
12. (a) Supriya, S.; Das, S. K. *New J. Chem*. **2003**, *27*, 1568. (b) Long, L.-S.; Wu, Y.-R.; Huang, R.-B. Zheng, L.-S. *Inorg. Chem*. **2004**, *43*, 3798. (c) Tao, J.; Ma, Z.-J.; Huang, R.-B.; Zheng, L.-S. *Inorg. Chem*. **2004**, *43*, 6133. (d) Zuhayra, M.; Kampen, W. U.; Henze, E.; Soti, Z.; Zsolnai, L.; Huttner, G.; Oberdorfer, F. *J. Am. Chem. Soc*. **2006**, *128*, 424.
13. (a) Ye, B.-H.; B.-B. Ding.; Weng, Y.-Q.; Chen, X.-M. *Inorg. Chem*. **2004**, *43*, 6866. (b) Y.-C. Liao, Y.-C. Jiang and S.-L. Wang, *J. Am. Chem. Soc*. **2005**, *127*, 12794.
14. Dong, W.; Ou-Yang, Y.; Song, H.-B.; Liao, D.-Z.; Jiang, Z.-H.; Yan S.-P.; Cheng, P.; *Inorg. Chem*. **2006**, *45*, 1168.
15. Lee, H. M.; Kim, D.; Kim, K. S. *J. Phys. Chem*. **2001**, *114*, 4461.
16. Lee, H. M.; Kim, D.; Kim, K. S. *J. Phys. Chem*. **2002**, *116*, 5509.
17. (a) Asmis, K. R.; Neumark, D. M. *Acc. Chem. Res*. **2012**, *45*, 43. (b) Yu, J.-J.; Zhang, Y.-H.; Li, Z.-S. *J. Phys. Chem. B* **2012**, *116*, 12597. (c) Zhou, J.; Santambrogio, G.; Brummer, M.; Moore, D. T. *J. Chem. Phys.* **2006**, *125*, 111102.
18. (a) Jose, D. A.; Kumar, D. K.; Ganguly, B.; Das, A. *Inorg. Chem*. **2007**, *46*, 5817. (b) Xia, Y.; Wu, B.; Liu, Y.; Yang, Z.; Huang, X.; He, L.; Yang, X.-J. *CrystEngComm*. **2009**, *11*, 1849.
19. Fedyanin, I. V.; Lyssenko, K. A. *CrystEngComm* **2013**, *15*, 10086.
20. Manna, P.; Seth, S. K.; Mitra, M.; Choudhury, S. R.; Bauzá, A.; Frontera, A.; Mukhopadhyay, S. *Cryst. Growth Des.* **2014**, *14*, 5812.
21. Lee, E. C.; Kim, D.; Jurecka, P.; Tarakeshwar, P.; Hobza, P.; Kim, K. S. *J. Phys. Chem. A* **2007**, *111*, 3446.
22. (a) Ratajczak-Sitarz, M.; Katrusiak, A.; Dega-Szafran, Z.; Stefański, G. *Cryst. Growth Des*. **2013**, *13*, 4378. (b) Basu, A.; Chutia, R.; Das, G. *CrystEngComm*, **2014**, *16*, 4886.
23. Liu, D.; Li, H.-X.; Ren, Z.-G.; Chen, Y.; Zhang, Y.; Lang, J.-P. *Cryst. Growth Des.*, **2009**, *9*, 4562.
24. Liu, L.-L.; Ren, Z.-G.; Wan, L.-M.; Ding, H.-Y.; Lang, J.-P. *CrystEngComm*, **2011**, *13*, 5718.
25. (a) Rajbanshi, A.; Wan, S.; Custelcean, R. *Cryst. Growth Des.* **2013**, *13*, 2233. (b) Hossain, M. A.; Işıklan, M.; Pramanik, A.; Saeed, M. A.; Fronczek, F. R. *Cryst. Growth Des.* **2012**, *12*, 567.

Annexure

Table 3.1a Crystallographic parameters and refinement details.

code name	**1**	**2**	**3**	**4**	**5**
empirical formula	$C_{13}H_{18}N_6O_4$	$C_{13}H_{20}I_2N_6O_4$	$C_{13}H_{20}N_6O_8S$	$C_{26}H_{36}N_{12}O_{13}P_2$	$C_{13}H_{18}Cl_2N_6O_{11}$
formula weight	322.33	578.15	420.42	786.61	505.23
cryst syst	triclinic	triclinic	Triclinic	Triclinic	Triclinic
a (Å)	7.7817(16)	9.6708(3)	8.0541(8)	9.009(2)	7.5545(4)
b (Å)	10.369(2)	10.4499(4)	8.3073(8)	14.1152(17)	8.7273(4)
c (Å)	10.554(2)	10.7216(4)	14.7666(13)	15.276(4)	16.7176(9)
α (degree)	82.674(7)	83.939(2)	85.767(7)	116.185(17)	79.566(3)
β (degree)	76.685(6)	74.072(2)	87.441(8)	97.676(19)	80.063(3)
γ (degree)	76.070(6)	75.792(2)	66.606(9)	93.033(14)	70.872(3)
V ($Å^3$)	802.0(3)	1009.19(6)	904.18(16)	713.9(6)	1016.49(9)
space group	*P-1*	*P-1*	*P-1*	*P-1*	*P-1*
Z value	2	2	2	2	2
ρ(cal)(g/cm^3)	1.335	1.903	1.544	1.524	1.651
μ(Mo Kα) (mm^{-1})	0.102	3.145	0.237	0.210	0.392
T(K)	298(2)	298(2)	298(2)	298(2)	298(2)
R1; wR2 (I> 2 σ(I))	0.0524; 0.1231	0.0330; 0.0460	0.0482, 0.1108	0.0825, 0.2470	0.0623, 0.1987
R1; wR2(all)	0.0765; 0.1349	0.0753; 0.0801	0.0706, 0.1290	0.1316, 0.3407	0.0800, 0.2118
Residual electron density(e/Å)	0.305	0.818	0.249/-0.353	0.904, -1.225	0.670/-0.365
good-of-fit	0.903	1.089	1.033	1.068	1.033
reflection collected	3922	4479	7190	13692	9861
Independent reflection	2466	2991	4045	8787	4163
CCDC No.	927368	1033866	927368	943362	927369

Table 3.1b Crystallographic parameters and refinement details.

code name	**6**	**7**	**8**	**9**	**10**
empirical formula	$C_{13}H_{17}N_6O_6P$	$C_{26}H_{34}F_6N_{12}O_6Si$	$C_{13}H_{20}N_8O_{10}$	$C_{13}H_{21}N_6O_8P$	$C_1H_{16}Cl_2N_6O_{10}$
formula weight	384.30	752.71	448.34	420.31	487.22
cryst syst	orthorhombic	monoclinic	triclinic	triclinic	monoclinic
a (Å)	13.5324(7)	12.5555(16)	7.3126(14)	9.5603(6)	10.6249(15)
b (Å)	25.6228(19)	9.1067(11)	9.151(2)	9.9263(7)	13.6369(15)
c (Å)	4.7665(2)	14.3436(19)	14.894(3)	10.9125(8)	14.473(2)
α (degree)	90.00	90.00	87.016(7)	111.305(7)	90.00
β (degree)	90.00	97.277(13)	83.964(8)	95.367(5)	110.155(17)
γ (degree)	90.00	90.00	84.026(8)	97.899(6)	90.00
V ($Å^3$)	1652.73(17)	1626.8(4)	984.9(3)	944.04(11)	1968.6(5)
space group	*P n a* 2_1	*P 2/c*	*P -1*	*P -1*	*P* $2_1/c$
Z value	4	2	2	2	4
ρ(cal)(g/cm^3)	1.544	1.528	1.498	1.472	1.644
μ(Mo Kα) (mm^{-1})	0.214	0.168	0.130	0.201	0.398
T(K)	298(2)	298(2)	298(2)	298(2)	298(2)
R1; wR2 (I> 2 σ(I))	0.0583; 0.1451	0.0806; 0.2432	0.0982; 0.2652	0.0656; 0.1801	0.0926; 0.2667
R1; wR2(all)	0.0774; 0.1615	0.1221; 0.3145	0.1978; 0.3352	0.0802;0.1968	0.1266; 0.3073
Residual electron density(e/Å)	-0.368/0.063	-0.633/0.077	-0.529/ 0.073	-1.125/0.117	-0.700/0.100
good-of-fit	1.112	0.975	0.981	1.041	1.044
reflection collected	4239	4198	4714	4837	5110
Independent reflection	2527	3065	3787	3333	2953
CCDC No.	1050472	1050474	1050473	1050475	1050476

Table 3.2a Overall (log $ß_i^H$) and Stepwise Protonation (log k_i^H) Constants of L in H_2O/MeOH (9:1 v/v).

equilibrium reaction	log $ß_i^H$	equilibrium reaction	log k_i^H
$L + H^+ = LH^+$	4.14	$L + H^+ = LH^+$	4.14
$L + 2H^+ = LH_2^{2+}$	8.23	$LH^+ + H^+ = LH_2^{2+}$	4.09

T= 298.2 ± 0.1 K and I = 0.10 ± 0.01 M in $NaNO_3$

Table 3.2b Overall (log $ß_i^H$) and Stepwise (log k_i^H) Association Constant of the indicated in H_2O/MeOH (9:1 v/v).

equilibrium	SO_4^{2-}	$H_2PO_4^-$	ClO_4^-	NO_3^-
$L + 2H^+ + A = LH_2A$ (overall)	8.72	8.58	8.31	–
$LH_2^{2+} + A = LH_2A$ (Stepwise)	0.49	0.35	0.08	–

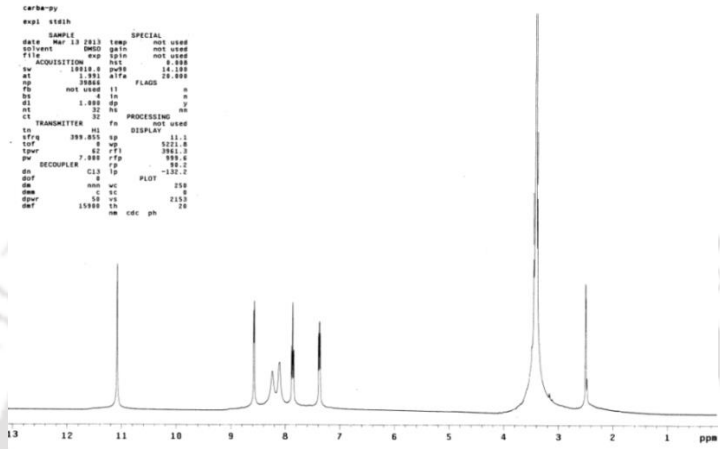

Figure A3.1. ^{1}H NMR spectrum of receptor $^o\mathbf{L_1}$ in DMSO-d_6 at 298 K.

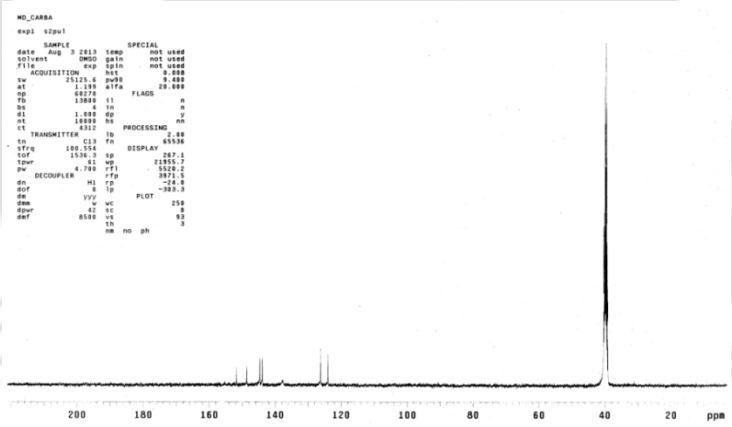

Figure A3.2. ^{13}C NMR spectrum of receptor $^o\mathbf{L_1}$ in DMSO-d_6 at 298 K.

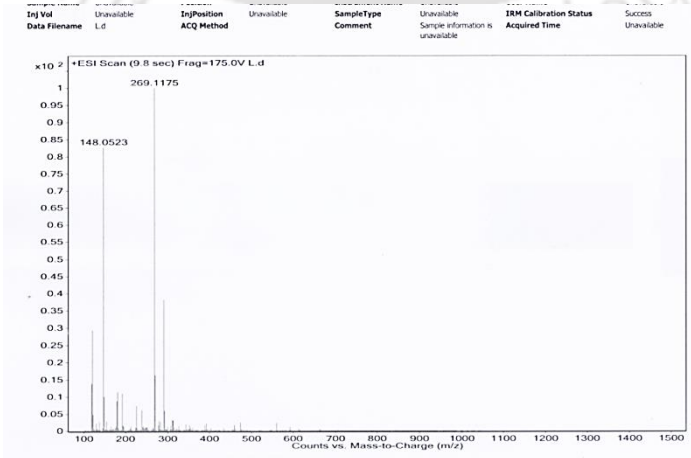

Figure A3.3. ESI-Mass spectrum of receptor $^o\mathbf{L_1}$.

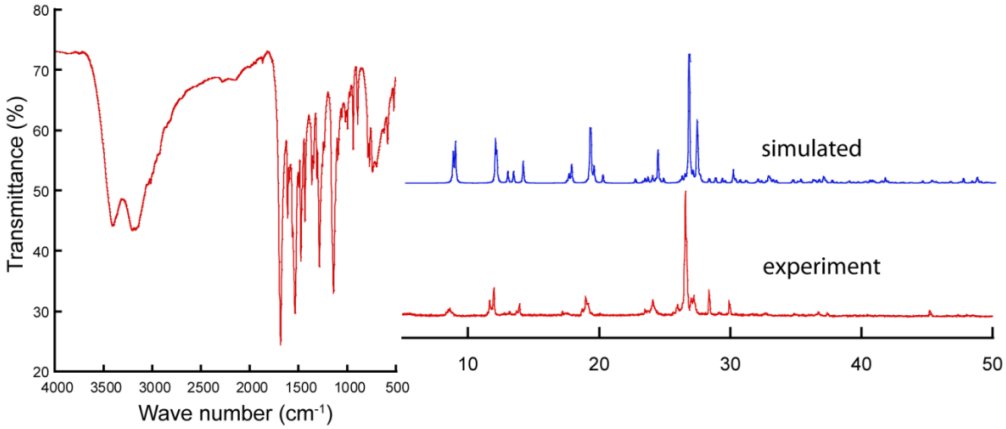

Figure A3.4. FT-IR spectrum of receptor **$^{o}L_1.3H_2O$** and powder X-ray diffraction: simulated pattern from the single crystal X-ray of **$^{o}L_1.3H_2O$** (blue), experimental pattern from the crystalline solid (red).

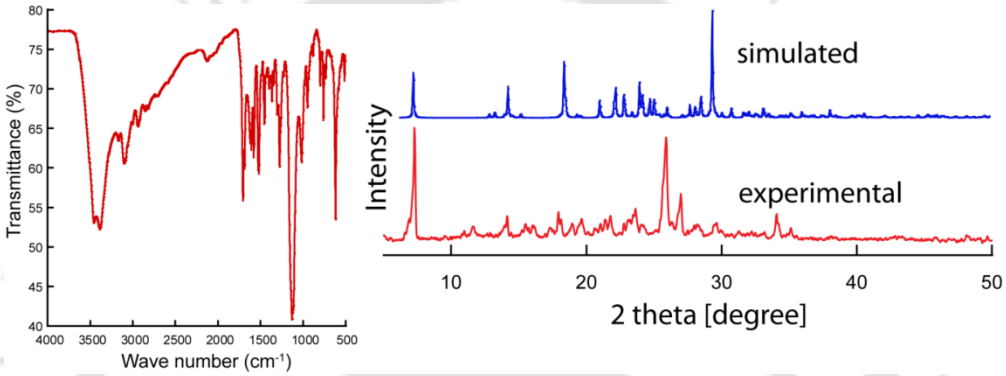

Figure A3.5. FT-IR spectrum of receptor **[$^{o}L_1H_2{\cdot}SO_4{\cdot}3H_2O$](3)** and powder X-ray diffraction: simulated pattern from the single crystal X-ray of complex **[$^{o}L_1H_2{\cdot}SO_4{\cdot}3H_2O$](3)** (blue), experimental pattern from the crystalline solid of complex (red).

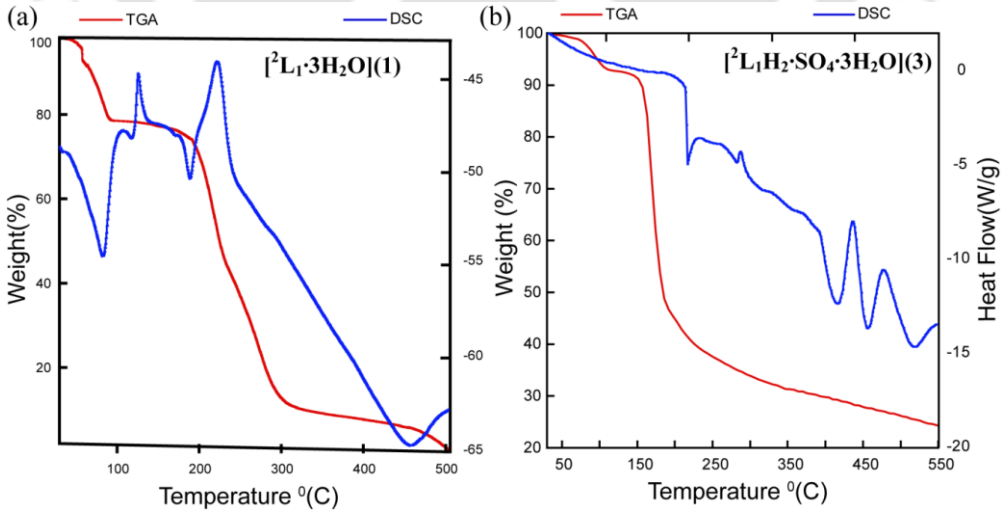

Figure A3.6. Thermogravimetric analysis (TGA) and differential scanning calorimetry curve of **$^{o}L_1.3H_2O$** and **[$^{o}L_1H_2{\cdot}SO_4{\cdot}3H_2O$](3)** at a heating rate of 5 °C per min.

Chapter 4

Aliphatic and Aromatic Capped Tripodal Receptors for Hydrated Anion Recognition: Effect of Ligand Flexibility

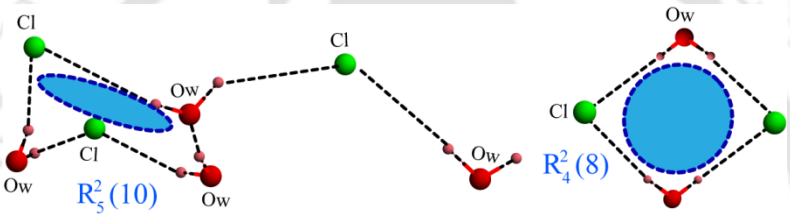

4.1 Back ground and focus on this chapter

The upsurge of the recent publication of theoritical[1] and experimental[2] aspect in the realm of world best important and essential for all living organism, water molecule has taken a serious attention of scientist to look after its structure and characteristics as it could give us nature of water-water interaction in atmosphere, earth, ocean, and biological system.[3] The detailed understanding of water the anomalous behavior of water molecule in stabilization and functioning of bio-molecules.[4] The *in-vitro* study of water cluster help to understand the biological implication of water cluster as folding, function, activity of protein[5] through hydrogen bonding and hydrophobic interaction.[6] At the molecular level there are several type water cluster emanated starting from dimers,[7] trimers,[8] teramers,[9] pentamers,[10] hexamers,[11] heptamers,[12] octamers,[13] nonamers,[14] decamers,[15] undecamers,[16] dodecamers[17] or even greater[18] in various organic environment[19] and metal mediated host owing to coordination tendency of water to metal. Therefore elucidation of H-bonding pattern in several surroundings is important. But minuscule number known containing cyclic water cluster having inorganic ion such as $[(NO_3)_6(H_2O)_6]^{6-}$,[20] $[(NO_3)_4(H_2O)_6]^{4-}$,[21] $[F_2(H_2O)_6]^{2-}$,[22] $[Cl(H_2O)_4]^-$,[23] $[Cl(H_2O)_3]^-$,[24] $[Cl_2(H_2O)_6]^{2-}$,[25] $[Br_2(H_2O)_6]^{2-}$,[26] $[NH_2(H_2O)_4]^-$ [27] and up to date chloride–water cluster in purely organic environment is very rare.[28,16a] But immense imploration of inorganic ion as in chemical and natural process have been accepted unanimously.[29] Interaction between water cluster and surrounding ions or host molecule play a vital role in nucleation and growth of molecular crystal. Keeping in mind the immense significance of water molecules, a lesser extent, aggregation of anion and water as solvated anions have also been focused recently owing to various imperative role of water/anion in ion translocation in water membrane interface,[30] diffusion of ion across bilayer membrane,[31] electrical phenomena in troposphere and ionosphere[32] and mobility of ions in ion channel[33]. Hence characterization of various topology of anion-water cluster in restricted environment is also important that in many cases could reflect complex H-bonding network around hydrated anion and as well as in ion channels. Among the inorganic anions, halide ions particularly is special interest due to unique shape as well as high natural occurrence and key role in several biological processes.[34] In this stage we are still in search to gather more knowledge about control factors of formation of ion cluster in such channels Curiously, compared to water assemblies hybrid anion-water assemblies are not adequately known for unveiling their structural relations, anion-water H-bonding patterns, even though recent structural reports on anion-water clusters [35] has opened the window to increase the knowledge bearing these phenomena.

The apical N-atom based (**L_2**) and benzene capped (**L_3**) tripodal receptor functionalized with mercaptobenzimidazole moiety offers anion complexation owing to protonation site. The tripodal platform inevitably generates ample interaction sites and produce multiple anions within a molecular system. The tripodals are enriched with various types of interacting sites giving NH···O/X, CH···O/S/π and π···π non-covalent interactions upon protonation. The most startling feature of this report is that a dichotomy in anion-water cluster is resulted from two closely related tripodal receptors.

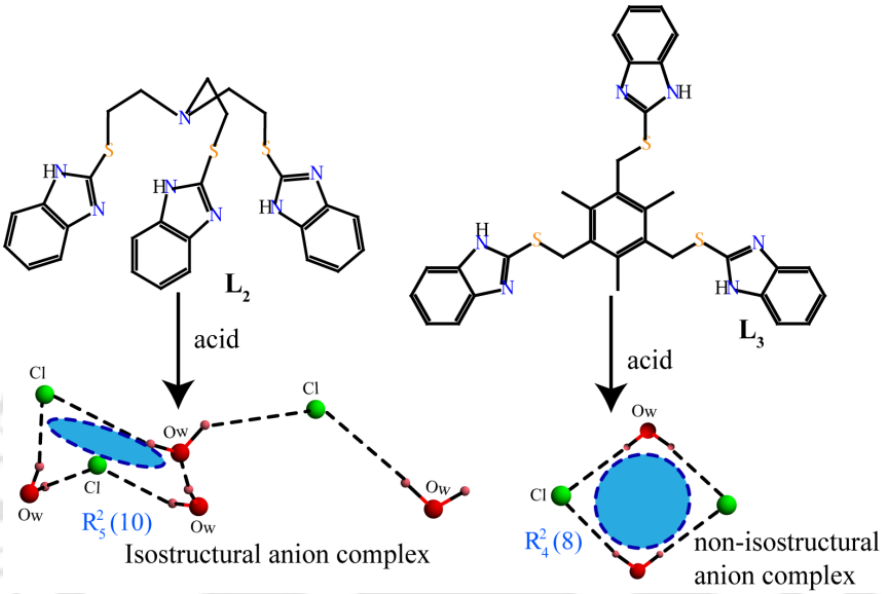

Scheme 4.1 Apical N-atom and benzene capped tripodal directed diverse chloride-water assembles.

4.2 Structural aspect of anion binding with L_2

The apical N-atom based tripodal **L_2** on treatment with HCl or HBr acids generate corresponding isostructural salts from slow evaporation of MeOH:H_2O mixture. All three benzimidazole moiety became protonated and anion interacts with crystallized water molecules giving unique hydrated anion structures. The formation and stability of the anion-water clusters were established by X-ray diffraction, PXRD, TGA, DSC, NMR titration.

4.3.1 Structural description of $[L_2H_3{\cdot}Cl_3{\cdot}4H_2O]$(2a)

Single crystal X-ray diffraction analysis showed that the complex crystallizes in monoclinic space group $P2_1/c$ with Z=4 giving asymmetric unit of the structure containing one triprotonated $\mathbf{L_2H_3^{3+}}$, three chloride ions and four water of crystallization. Bowl shaped tripodal receptor having hydrogen bond donor benzimidazole group exposed to

outside to form strong hydrogen bond complex with anion or solvent molecules. After addition of acid, benzimidazole nitrogen became protonated and made two nitrogen equivalents that offers important binding site for these anion/water. Flexible cationic tripodal receptor provides the required platform to host chloride-water cluster. The chloride-water cluster along with atom labeling scheme is shown in Figure 4.1a. Each pentameric cluster consisting two chloride and three water molecules are connected to the next pentamer unit by the tail having one chloride and one water molecule. The tail is a linker between two puckered heteroatomic chloride-water clusters (Figure 4.1b). Pentameric cluster consisting of two chloride ion and three water molecules formed

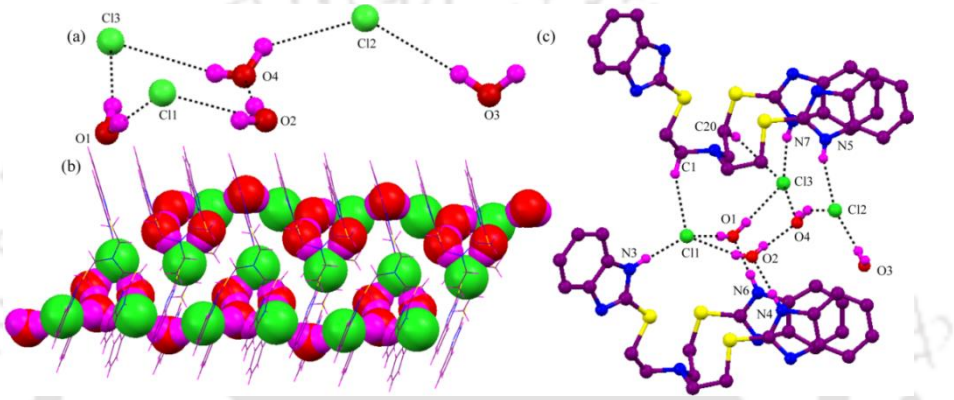

Figure 4.1 (a) Depicting Chloride-Water pentamer $[Cl_3\text{-}(H_2O)_4]^{3-}$ in **2a** having half chair conformation with a tail of chloride and water. (b) Crystal packing exhibiting chloride-water channels propagating through hydrophobic channel created by the organic host. (c) Extensive H-bonded networks showing the interactions of the chloride-water pentamer $[Cl_3\text{-}(H_2O)_4]^{3-}$ cluster with the protonate receptor $\mathbf{L_2H_3}^{3+}$.

cyclopentane like half chair structure. Any three atom in the pentamer lies in the same plane, while other two above the plane. The chloride-water cluster is packed between two hydrophobic layers in a zigzag fashion. These clusters in the adjacent layers are in *anti*-fashion (Figure 4.1b). Three different chloride anions are strongly held in the lattice through several O–H···Cl and N–H···Cl hydrogen bonds. As depicted in Figure 4.1c, two hydrogen bonds held between Cl1 nearby water molecules [O1···Cl1 = 3.183(5) Å and O2···Cl1 = 3.150(6) Å] and one with imidazole N—H of tripodal ligand [N3···Cl1 = 3.098(7) Å]. Similar hydrogen bonding observed for Cl2 also [O3···Cl2 = 3.275(6) Å, O4···Cl2 = 3.070(1) Å and N5···Cl2 = 3.120(6) Å]. However Cl3 is connected to four such strong hydrogen bonds [O1···Cl3 = 3.210(6) Å, O3···Cl3 = 3.212(6) Å, O4···Cl3 = 3.190(1) Å and N7···Cl3 = 3.164(6) Å]. The suitable bond angle distribution among different atoms in cyclic pentamer makes any three atoms e.g. O1-Cl1-O2 are in the same plane like half chair conformation of cyclopentane with exception of remaining two atoms are out of the plane. In this hybrid chloride water cluster one oxygen atom of pentameric

unit (O4) does not interacts with any imidazole N−H of tripodal and offers O2···O4 strong interaction in the chloride water cluster of bond length 2.680(1) Å and bond angle ∠O2···H4O−O4 = 168.1(5)°. The O···O separation is 2.68 Å is stronger than previously reported $Cl(H_2O)_4$[23], $(H_2O)_5$[10]. All the water molecules form strong hydrogen bonds with imidazole N−H and chloride anions [N6···O1 = 2.716(7) Å, N4···O2 = 2.712 Å and N2···O3 = 2.768(8) Å]. The bond distance between N···O is comparable with known amide water pentamer[27]. There are three aromatic moieties in which one unit offered three different π···π interaction one is intra-molecular interaction with a distance of 3.739 Å and another two π···π interactions are inter-molecular type between adjacent moieties with a distance of 3.902 Å and 3.859 Å. The vibrational stretching frequency of the O−H bond pertaining a broad peak at 3425 cm^{-1} corresponding to chloride-water cluster has been characterized by FT-IR spectroscopy. The simulated PXRD pattern of chloride-water cluster essentially matches with the experimental PXRD pattern. This suggests the chloride-water cluster present in massive amount (Figure A4.9).

4.3.2 Structural description of $[L_2H_3{\cdot}Br_3{\cdot}4H_2O]$(2b)

The bromide complex **2b** crystallizes in monoclinic space group $P2_1/c$. The asymmetric unit contains one $\mathbf{L_2H_3^{3+}}$, three bromide ions and four water molecules of crystallization. The bromide is isostructural to the chloride complex **2a**. A detailed view in the interaction pattern shows a bromide-water cluster $[Br_3\text{-}(H_2O)_4]^{3-}$ containing a cyclic half chair like pentamer $[Br_2\text{-}(H_2O)_3]$ and tail of $[Br\text{-}(H_2O)]$ like complex **2a** is generated and connected by various H-bonding interactions (Figure 4.2). The bromide-water cluster is stabilized by N−H···Br, N−H···Ow, Ow−H···Br and Ow−H···Ow H-bonding interaction, fall in range of 2.690(1) Å to 3.339(5) Å. In the solid state we observed the appended tail $[Br\text{-}(H_2O)]$ helps to build extended polymeric bromide-water aggregates which run through the

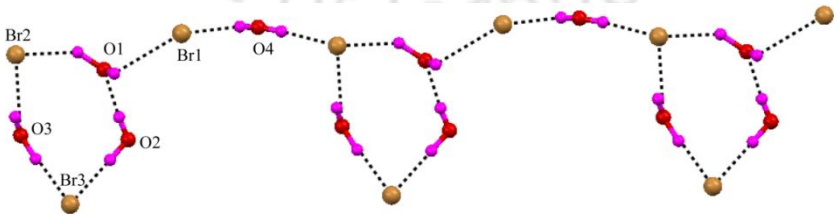

Figure 4.2 Infinite chain of bromide-water pentamer $[Br_2\text{-}(H_2O)_3]$ observed in isostructural complex **2b**.

cationic $\mathbf{L_2H_3^{3+}}$. In FT-IR spectroscopy a broad band appeared at 3405 cm-1 corresponding to N−H bond. The simulated PXRD pattern is essentially similar to the experimental PXRD pattern. This suggests the complex **2b** present in mass scale.

4.4 Structural aspect of anion binding with L_3

The benzene capped tripodal **L_3** crystallizes as hydrate or anion complexes on acidification in MeOH-H_2O mixture. The tripodal arms on the planar platform are flexible and crystal structure of the receptor shows all three benzimidazole moiety takes *uuu* conformation. We have also explored various classic and non-classic interactions leading to supramolecular aggregation of host-guest ensemble. All structures were well examined by different techniques such as NMR, IR, TGA, DSC, PXRD and XRD.

4.5 Structural description of $[L_3 \cdot 2H_2O]$(3)

Crystallographic analysis shows that compound **L_3** crystallizes in orthorhombic space group P$c2_1/n$ with an asymmetric unit containing the benzene capped planar tripodal (**L_3**) and two water of crystallization. Three arms of the receptor are flexible, can show various conformation likely up-up-up (*uuu*), down-up-up. Among them most stable conformation is down-up-up as it has less steric hindrance. Though crystal structure reveals that it is the up-up-up conformation interestingly among three, one arm is placed on the parallel plane defined by benzene cap whereas other two arms are situated orthogonally with respect to plane of the benzene. In crystal lattice, the free tripodal receptor interacts with water molecule through its benzimidazole N-atom where each moiety acts as donor and acceptor

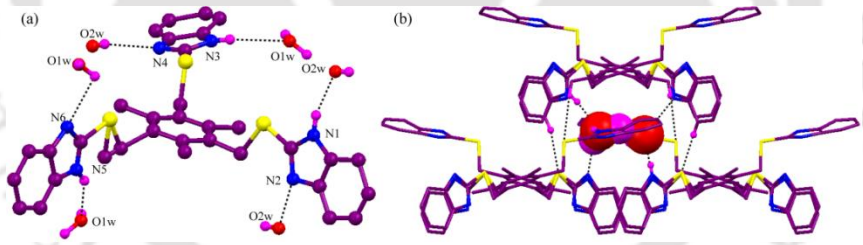

Figure 4.3 (a) Depicting conformation of **L_3** and H-bonding interaction with water molecules in compound **3**. (b) Top view showing trapping of discrete water dimer inside the cavity created by six **L_3**.

towards two symmetry independent water molecules, giving total six water molecules surrounding to one receptor as shown in Figure 4.3a. Two perpendicular arms are H-bonded with two symmetric water molecules having N1···O2w = 2.910(1) Å, O2w···N2 = 2.970(1) Å and N5···O1w = 3.070(3) Å, O1w···N6 = 2.780(3) Å contacts. On the other hand, the planar arm interacts with both symmetry independent water molecules (O1w and O2w) with H-bonding distances N3···O1w = 3.330(2) Å and O2w···N4= 2.910(1) Å. Very interestingly two water molecules are surrounded by total six tripodal receptor, and hence trapped into the hydrophobic cavity decorated by tripodal arms as illustrated in Figure

4.3b. Both water molecules are tetra-coordinated arrangement, and O1w accept two hydrogen from N3, N5 and donate two hydrogen to N6 and O2w and show a distorted tetrahedral geometry and lie 0.645 Å above the plane. The close distance between two water molecule is O1w···O2w = 3.100(3) Å, which resulted a discrete water dimer having ($D_1^1(3)$) motif. Likewise O2w acts as two H-bond acceptor and donor towards O1w, N1 and N2, N4 that would make a tetrahedral geometry around O2w and lie 0.578 above the plane. As a result the supramolecular structure with suitable H-bonding functionality stabilize the discrete hydrophilic water dimer into its hydrophobic pocket. The molecular packing diagram along *a*-axis shows supramolecular assembly of the tripodal receptor creating hydrophobic void by tripodal arms and each voids are occupied by water dimer. Each three sulfur atoms are efficiently H-bonded to two aromatic C−H and one aliphatic C−H of neighboring receptor with separation C3···S1 = 3.560(1) Å, C17···S3 = 3.590(1) Å and C34···S2 = 3.800(3) Å. The benzene cap also formed π···π (Cg···Cg = 3.765 Å) interaction with the arm parallel to its cap. The vibrational stretching frequency of the crystalline material **3** indicate a broad band around 3205 cm^{-1} that can be attributed to O−H bond suggesting the presence of water molecule which peak is absent in powder form of $\mathbf{L_3}$ only. The bulk phase purity of the crystalline compound **3** has also been confirmed by PXRD study where simulated and experimental pattern coincide each other.

4.5.1 Structural description of $[L_3H_2{\cdot}2F{\cdot}H_2O]$(3a)

Single crystal X-ray study reveals that complex **3a** crystallizes in monoclinic system belonging to the *C2* space group. There are one double protonated $\mathbf{L_3}$, two fluoride ions and one lattice water molecule (two half occupied water molecules) in an asymmetric unit of complex **3a**. The benzene capped tripodal receptor in protonated state retain same conformation as in compound **3**. Crystallographic analysis shows all three arms of $\mathbf{L_3H_2^{2+}}$ interact with only fluoride ions (Figure 4.3a), the parallel arm is strongly H-bonded with two fluoride ions having N1···F2 = 2.798(8) Å and N2···F1 = 2.750(1) Å contacts. The other two perpendicular arms donate NH hydrogen towards fluoride ions with strong H-bond distances fall in the donor-acceptor range of N3···F1 = 2.720(9) Å, N4···F1 = 2.760(8) Å and N5···F2 = 2.806(9) Å, N6···F2 = 2.704(9) Å. The most striking feature of complex **3a** is the identification of discrete fluoride-water trimer $[F_2\text{-}(H_2O)_{0.5}]^{2-}$ notified as ($D_2^2(5)$) motif in the receptor as shown in Figure 4.4b. It is clear from the solid state structure that from each benzimidazole N-atom fluoride-water trimer is extended. As illustrated in Figure 4.4b fluoride-water trimer is surrounded by six $\mathbf{L_3H_2^{2+}}$ and one arm

from each receptor is H-bonded with fluoride ions (F1 and F2) to engulf small cluster inside the cationic channel. The geometry of trimer $[F_2\text{-}(H_2O)_{0.5}]^{2-}$ shows all three atoms lie on the same plane and formed 'V' shaped structure. The trimer is mainly stabilized by six N−H···F, two Ow−H···F and two C−H···Ow H-bonding interactions. The average H-bonding in $[F_2\text{-}(H_2O)_{0.5}]^{2-}$ is observed 2.740 Å ranging from 2.720 Å to 2.806 Å. Both fluoride ions (F1 and F2) are tetra-coordinated and lie on a plane of three donors N-atom from benzimidazole moiety, and oxygen atom lies on the perpendicular to the plane. Hence F^- ion shows trigonal pyramidal geometry. But the water molecule (O1w) form flatter tetrahedral geometry (0.493 Å above the donor-acceptor plane of two F2 and one C31). In the aggregation of the $\mathbf{L_3H_2}^{2+}$ S-atom play an important role while interacting with the neighbour receptor by forming two aromatic C13···S2 = 3.610(1) Å and C20···S3 = 3.620(1) Å) and one aliphatic C29···S1 = 3.713(9) Å H-bonds. The benzene cap also form π···π stacking (Cg···Cg = 3.681 Å) with parallel arm (Figure A4.14a). The molecular packing along *bc* plane shows the existence of fluoride-water trimer in cationic channel created by $\mathbf{L_3H_2}^{2+}$. The presence of crystalline water was also assured by the broad band centered around 3202 cm^{-1} in complex **3a** in FT-IR spectra can be assigned to the O−H stretching frequency. The bulk phase purity of the complex **3a** is supported by similar experimental and simulated PXRD pattern.

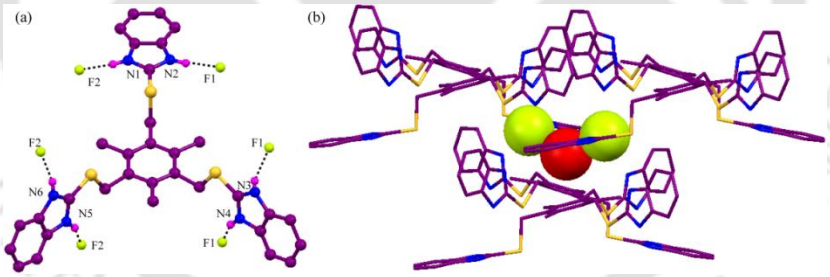

Figure 4.4 (a) Depicting conformation of $\mathbf{L_3H_2}^{2+}$ in complex **3a** and H-bonding interactions with fluoride ions. (b) Top view showing the discrete fluoride-water cluster $[F_2\text{-}(H_2O)_{0.5}]^{2-}$ is engulfed by six $\mathbf{L_3H_2}^{2+}$.

4.5.2 Structural description of $[\mathbf{L_3H_2}\cdot 2Cl\cdot 2H_2O]$ (3b)

Single crystal X-ray diffraction study confirmed that complex **3b** crystallizes in orthorhombic space group *Pnma*. The asymmetric unit contains one half of the $\mathbf{L_3H_2}^{2+}$, one chloride ion and one water of crystallization. The $\mathbf{L_3H_2}^{2+}$ is highly symmetric and symmetry plane bisect at right half of the complex. Solid state structure indicate the similar conformation like complex **3a**, posing all three arms are in the same direction, among three arms, one arm is perfectly parallel to the plane of the benzene cap, while other two are perpendicular but little tilted towards the plane of benzene cap which is not

observed in other cases (hence resulted a different packing diagram, will be discussed latter) as shown in Figure 4.5a. The coordination environment of the receptor is shown in Figure A4.13, in which six NH acts as donor for acceptor Cl^- ions and Ow molecules. The parallel arm is symmetrically surrounded by two chloride ions having distance N3···Cl1 = 3.055(4) Å. While each two perpendicular arms binds to one water and one chloride ion

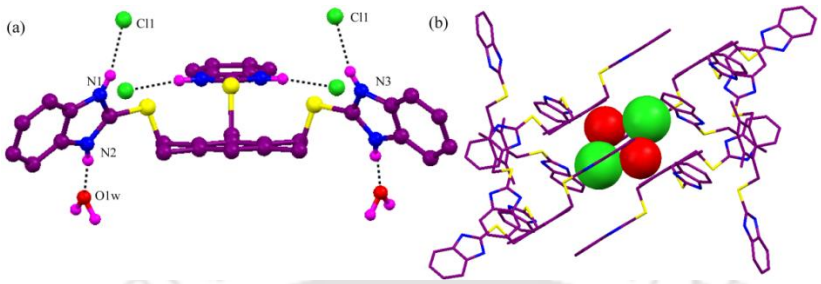

Figure 4.5 (a) Depicting conformation of $\mathbf{L_3H_2}^{2+}$ in complex **3b** and H-bonding interactions of the receptor with chloride ions and water molecules. (b)

having N1···Cl1 = 2.988(4) Å and N2···O1w = 2.712(5) Å contacts. A very interesting aspect of crystal structure of the complex **3b** is that we have isolated a H-bonded discrete cyclic chloride-water tetramer motif $[Cl_2\text{-}(H_2O)_2]^{2-}$ with structural notation ($R_4^2(8)$), which is exploited into the void created by the receptor as explained in Figure 4.5b by highlighting the tetramer as a spacefill model. As a result discrete tetramer motif is stabilized into such a cationic channel by contribution H-bonding made of six $\mathbf{L_3H_2}^{2+}$ as illustrated in Figure 4.5b. A detailed study of the tetramer shows all four atoms in the cluster lie on a plane. In the tetramer, water molecule act as two H-bond donor towards chloride ions having Cl1···O1 = 3.065(4) Å and Cl1`···O1` = 2.924(5) Å distances which are shorter than previously reported values in chloride-water tetramer motif[36] suggesting highly stable cluster in the cationic channel. In addition to that total four N−H···Cl, four Ow−H···Cl, two N−H···Ow and two C−H···Ow contacts are involved in stabilization of discrete tetramer. Water molecules and Chloride ions are tetra coordinated. A detailed view in coordination structure shows that Cl^- ion lie 0.822 Å from the plane of O1w, O1w` and N1, forming a distorted tetrahedral geometry, whereas water molecule is ideally placed on a plane of Cl1, Cl1` and N2 adopting trigonal pyramidal structure. The packing diagram of the complex **3b** is interestingly different to that of **3** and **3a,** here we observed square arrangement $\mathbf{L_3H_2}^{2+}$ with square distribution of chloride-water tetramer in cationic channel along *bc* plane**.** The surprising contrary in insight of crystal packing of chloride complex **3b** compared to others is that one receptor is orthogonally arranged with respect other giving C—H_{alp}···π = 3.631 Å (C—H_{alp} of –CH_3 group and π cloud of another

benzene cap) and this kind of arrangement is absent in other complexes. Hence receptor in this case organizes in such orientation (Figure A4.14b) that unlike other cases, here we did not observe any π···π stacking between benzimidazole moiety. Though a π···π interaction between benzene cap and benzimidazole moiety, only aliphatic C15···S1 = 2.949(1) Å and C12···S2 = 2.932(1) Å H-bonding (but no C—H_{ar}···S) play key in supramolecular assembly of the receptor. We confirmed the presence water molecule in crystal lattice complex **3b** by FT-IR spectra and broad vibration frequency appears at 3205 cm^{-1} corresponding to O−H stretching vibration. The bulk phase purity of the complex is also confirmed by PXRD study where simulated and experimental pattern coincide each other (Figure A4.11).

4.6.1 Thermogravimetric analysis of complexes of L_2

Thermal stability of the complexes **2a** and **2b** was studied by thermogravimetric analysis (TGA) and differential scanning calorimetry (DSC) (Figure Figure A4.6). TGA curve of the chloride complex **2a** shows two consecutive weight losses. First weight loss of 8.9% (calcd 9.9%) at ~160 °C suggests the loss of four water molecules from the lattice. This temperature is well above 100 °C, indicates the strong hydrogen bonding between water cluster and the host molecules in the crystal lattice. After losing crystalline water molecule, the dehydrated complex appears to be stable up to ~ 230 °C and decomposition stars after this temperature. The complete decomposition of the dehydrated complex happened at ~400 °C. Both DSC and cyclic DSC curve shows the exothermic peak at ~ 130 °C corresponding to loss of water molecule and endothermic peak at around 160°C defines the melting of the dehydrated complex. Very interestingly cyclic DSC plot shows while losing temperature the melting liquid complex returned to its solid form and reconfirmed that the dehydrated complex stable 230 °C. The bromide complex **2b** started to loose water molecule after 100 °C and all four water is lost at 144 °C accompanied a weight loss of 8.52% (calcd. 8.36%). The dehydrated salt is stable upto 245 °C and decomposed after this temperature. An appearance of exothermic and endothermic peak at 145 °C and 210 °C corresponding to weight loss and melting of the complex.

4.6.2 Thermogravimetric analysis of complexes of L_3

Thermal stability of the compound **3** and complexes **3a** and **3b** was studied by thermogravimetric analysis (TGA) and differential scanning calorimetry (DSC) (Figure A4.12.). The results obtained from thermal analysis are well agreed with crystallographic

findings. The water molecule from fluoride complex **3a** was expelled at higher temperature compared to free receptor due to ionic environment around water molecule as expected. The weight loss 3.42 % for one water molecule is consistent with calculated 2.71% at 150 °C on TGA plot of **3a**. The dehydrated salt is stable upto 300 °C and melted after this temperature. In the DSC plot appearance of endothermic and exothermic peak at 155 °C and 366 °C corresponding to water loss and melting of the solid respectively. There was a weight loss of 6.21% (calcd. 5.02%) for two water molecules in chloride complex **3b** at 145 °C in TGA plot which is little less than fluoride complex as expected duo relatively weak H-bond in chloride-water cluster. The dehydrated complex starts to decompose at 330 °C. These thermal changes were also confirmed from DSC plot of the chloride complex which produced endothermic and exothermic peak.

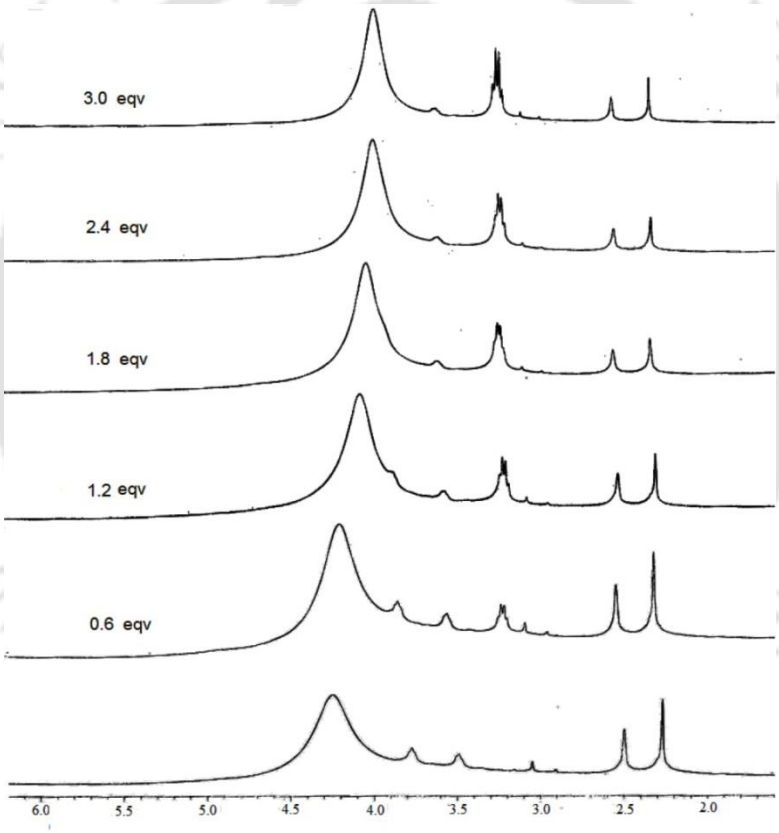

Figure 4.6 ^{1}H-NMR spectra of tosylated salt of $\mathbf{L_2}$ (2mM) with increasing amount of TEACl (10mM) in d_6-DMSO showing significant change of water peak.

4.6.3 Monitoring of chloride-water cluster formation in complex 2a by NMR spectroscopy

In ^{1}H-NMR spectroscopy, the ligand $\mathbf{L_2}$ shows chemical shift of −NH appears at 12.522 ppm, where as in chloride cluster there is no peak at that region, rather it appears at 5.076 ppm along with water peak. In order to investigate the formation chloride-water cluster in

solution state, we have demonstrated ^{1}H-NMR titration in d_6-DMSO at 298 K which has been carried out by tetraethyl ammonium chloride (TEACl) with tosylate salt of **L_2** (Figure 4.5). Here we choose the tosylate anion because of its very weakly binding affinity towards cation, so it can be replaced by chloride anion very easily. Upon addition of TEACl up-field chemical shift of water peak occurs and its continued upto three equivalent of chloride. This attributes to the strong H-bonding of water with chloride and formation of chloride-water cluster in solution state which has already been confirmed in solid state.

4.7 Conclusions

In the summery, we have crystallographically characterized the novel discreet isostructural halide-water cluster ($[X_3(H_2O)_4]^{3-}$, X= Cl^-, Br^-) having half chair like pentameric unit [$X_2(H_2O)_3$] by **L_2** in complex **2a** and **2b**. These anion-water clusters has been trapped by benzimidazole based tripodal hydrophobic host. The conformationally flexible apical N-atom based tripodal receptor that arranged (pre-organized) in a particular way and made bowl shape which subsequently formed the anion-water cluster channel in the solid state. The formation of a chloride-water cluster in solution was also confirmed by ^{1}H NMR titration experiments. We have also developed a benzene capped bowl shaped tripodal **L_3** decorated with benzimidazole moiety which stabilizes various infinite or discrete water and hybrid anion-water clusters. Our study successfully describes infinite 1D water chain $[H_2O]_\infty$ in compound **3** and fluoride-water trimer $[F_2\text{-}(H_2O)_{0.5}]^{2-}$ in **3a** or cyclic chloride water tetramer $[Cl_2\text{-}(H_2O)_2]^{2-}$ in **3b** stabilized by the receptor **L_3**. Anion-water assembles are governed by multiple non-covalent (N−H···X^- and C−H···X^- H-bond, CH···π and π···π) and electrostatic interactions. Association of such structurally diverse hydrophilic water/anion-water ensemble into the organic channels may be helpful to analyse transportation of water in water-membrane interface and ion-channel in biomimetic manner. Most interestingly our observations underscore the conformationally flexible tripodals depending upon platform structure resulted a dichotomy in anion-water cluster formation. The benzene cap and apical N-atom based receptor furnishes nonisostructural and isostructural anion-water clusters respectively which allows tenability of anion-water clusters providing interesting anion-water structural relationship. From thermal analysis we have established stability of the complexes as well as anion-water/water cluster which shows the H-bonding that builds anion-water clusters are strongly incorporated inside

crystal lattice of the receptors. However this study would provide new insight in the heteroatomic water cluster chemistry and effect of ligand structure on its formation.

References

1. (a) Siu, C. K.; Balai, O. P.; Bondybey, V. E.; Beyer, M. K. *J. Am. Chem. Soc*. **2007**, *129*, 3238. (b) Hontama, N.; Inokuchi, Y.; Ebata, T.; Dedonder-Lardeux.; Jouvet, C.; Xantheas, S. S. *J. Phys. Chem. A* **2010**, *114*, 2967. (c) Li, J. G.; Yu, J. H.; Xu, R. R. *Phys. Chem. Chem. Phys.* **2009**, *11*, 1291;
2. (a) Singh, N. J.; Park, M.; Min, S. K.; Suh, S. B.; Kim, K. S. *Angew. Chem., Int. Ed*., **2006**, *45*, 3795. (b) Dai, F. N.; He, H. Y.; Sun, D. F. *J. Am. Chem. Soc*. **2008**, *130*, 14064. (c) Wang, X.; In, H. L.; Mu, B.; Tian, A.; Liu, G. *Dalton Trans*. **2010**, *39*, 6187. (d) Massera, C.; Melegari, M.; Ugozzoli, F.; Dalcanale, E. *Chem. Commun*. **2010**, *46*, 88.
3. Rasaiah, J. C.; Garde, S.; Hummer, G. *Annu. Rev. Phys. Chem*. **2008**, *59*, 713.
4. (a) Ludwig, R. *Angew. Chem., Int. Ed*. **2001**, *40*, 1808. (b) Yu, L., Adv. *Drug Del. Rev*. **2001**, *48*, 27. (c) Reutzel, S. M.; Kleemann, E. L.; Lewellen, P. L.; Borghese, A. L.; Antione, L. J. *J. Pharm. Sci*. **2003**, *92*, 1196.
5. (a) Sleigh, S. H.; Tame, J. R. H.; Dodson, E. J.; Wilkinsion, A. J. *Biochemistry*. **1997**, *36*, 9747. (b) Oh, B.-H.; Ames, G. F.-L.; Kim, S.-H. *J. Biol. Chem.* **1994**, *269*, 26330. (c) Tame, J. R. H.; Sleigh, S. H.; Wilkinson, A. J.; Ladbury, J. E. *Nat. Struct. Biol*. **1996**, *3*, 998.
6. (a) Peters, J.; Baumeister, W.; Lupas, A. *J. Mol. Biol*. **1996**, *257*, 1031. (b) Yin, H.; Hummer, G.; Rasaiah, C. J. *J. Am. Chem. Soc*. **2007**, *129*, 7369. (c) Ernst, J. A.; Clubb, R. T.; Zhou, H.-X.; Gronenborn, A. M.; Clore, G. M. *Science*. **1995**, *267*, 1813.
7. Chand, D. K.; Bharadwaj, P. K. *Inorg. Chem*. **1998**, *7*, 5050.
8. MacGillivary, L. R.; Atowod, J. L. *J. Am. Chem. Soc*. **1997**, *119*, 2592.
9. Luo, G.-G.; Xiong, H.-B.; Sun, D.; Wu, D.-L; Huang, R.-B.; Dai, J.-C. *Cryst. Growth. Des*. **2011**, *11*, 1948.
10. Ma, B.-Q.; Sun, H.-L.; Gao, S. *Chem. Commun*. **2004**, 2220.
11. Doedens, R. J.; Yohannes, E.; Khan, M. I. *Chem. Commun*. **2002**, 62.
12. Wang, F.-Q.; Zheng, X.-J.; Wan, Y.-H.; Sun, C.-Y.; Wang, Z.-M. *Inorg. Chem*. **2007**, *46*. 2956.
13. Rodríguez-Cuamatzi, P.; Vargas-Díaz, G.; Höpfl, H. *Angew. Chem., Int. Ed*. **2004**, *43*, 3041.
14. Pradeep, C. P.; Supriya, S.; Zacharias, P. S.; Das, S. K. *Polyhedron*. **2006**, *25*, 3588.
15. Hu, N.-H.; Li, Z.-G.; Xu, J.-W.; Jia, H.-Q.; Niu, J.-J. *Cryst. Growth. Des*. **2007**, *7*, 15.
16. Ma, B.-Q.; Sun, H.-L.; Gao, S. *Angew. Chem., Int. Ed*. **2004**, *43*, 1374.
17. Liu, Q.-Y.; Xu, L. *CrystEngComm*. **2005**, *7*, 87.
18. Luan, X.; Chu, Y.; Wang, Y.; Li, D.; Liu, P.; Shi, Q. *Cryst. Growth. Des*. **2006**, *6*, 812.
19. (a) Oxtoby, N. S.; Blake, A. L.; Champness, N. R.; Wilson, C. *Chem.-Eur. J*. **2005**, *11*, 4643. (b) Xu, W.-Z.; Sun, J.; Huang, Z.-T.; Zheng, Q.-Y. *Chem. Commun*. **2009**, 171.
20. Liu, L.-L.; Ren, Z.-G.; Wan, L.-M.; Dinga H.-Y.; Lang, J.-P. *CrystEngComm*. **2011**, *13*, 5718.
21. Liu, D.; Li, H.-X.; Ren, Z.-G.; Chen, Y.; Zhang, Y.; Lang, J.-P. *Cryst. Growth. Des*. **2009**, *9*, 4562.
22. Arunachalam, M.; Ghosh, P. *Chem. Commun*. **2009**, 5389.
23. Custelcean, R.; Gorbunova, M. G. *J. Am. Chem. Soc*. **2005**, *127*, 16362.
24. Saha, R.; Biswas, S.; Steele, I. M.; Dey, K.; Mostafa, G. *Dalton Trans*. **2011**, *40*, 3166.
25. (a) Butchard, J. R.; Curnow, O. J.; Garett, D. J.; Maclagan, R. G. A. R.; *Angew. Chem., Int. Ed.* **2006**, *45*, 7550. (b) Mascal, M.; Infantes, L.; Chisholm, *J. Angew. Chem., Int. Ed*., **2006**, *45*, 32.
26. Bakhoda, A.; Khavasi, H. R.; Safari, N. *Cryst. Growth. Des*. **2011**, *11*, 933.
27. Saeed, M. A.; Wong, B. M.; Fronczek, F. R.; Venkatraman, R.; Hossain, M. A. *Cryst. Growth. Des*. **2010**, *10*, 1486.
28. (a) Lakshminarayanan, P. S.; Kumar, D. K.; Ghosh, P. *Inorg.Chem*. **2005**, *44*, 7540. (b) Das, M. C.; Ghosh, S. K.; Sen, S.; Bharadwaj, P. K. *CrystEngComm*. **2010**, *12*, 2967.
29. (a) Koch, M. C.; Steinmeyer, K.; Lorenz, C.; Ricker, K.; Wolf, F.; Otto, M.; Zoll, B.; Lehmann-Horn, F.; Grzeschik, K. H.; Jentsch, T. J. *Science*. **1992**, *257*, 797. (b) Spicer, C. W.; Chapman, E. G.; Finlayson-Pitts, B. J.; Plastridge, R. A.; Hubbe, J. M.; Fast, J. D. Berkowitz, C. M. *Nature*, **1998**, *394*, 353. (c) Chakrabatri, S.; Parker, M. F. L.; Morgan, C. W.; Schafmeister, C. E.; Waldeck, D. H. *J. Am. Chem. Soc*. **2009**, *131*, 2044.
30. (a) Matile, S. *Chem. Soc. Rev.* 2001, *30*, 158. (b) Ohtaki, H.; Radnai, T. *Chem. Rev*. **1993**, *93*, 1157.
31. (a) Zhou, H.-X.; *J. Phys. Chem. Lett.* **2010**, *1*, 1973. (b) Andersson, Martin.; Keizer, H. M.; Zhu, C.; Fine, D.; Dodabalapur, A.; Duran, R. S. *Langmuir*. **2007**, *23*, 2924.
32. (a) Arshadi, M.; Yamdagni, R.; Kebarle, P. *J. Phys. Chem.*, **1970**, *74*, 1475. (b) Crutzen, P. J.; Arnold, F. *Nature*. **1986**, *324*, 651.
33. (a) Akabas, M. H. *Chloride Channels*. *In Encyclopaedia of life sciences*, Macmillan Reference Ltd.: London, **2001**. (b) Richens, D. T. *The chemistry of Aqua Ions*, Wiley, Chichester, **1987**.

34. (a) Custelcean, R.; Gorbunova, M. G. *J. Am. Chem. Soc*. **2005**, *127*, 16362. (b) Kopylovich, M. N.; Tronova, E. A.; Haukka, M.; Kirillov, A. M.; Kukushkin, V. Y.; Fraústo da Silva, J. J. R.; Pombeiro, A.J.L. *Eur. J. Inorg. Chem.* **2007**, 4621. (c) Mascal, M.; Infantes, L.; Chisholm, *J. Angew. Chem., Int. Ed*., **2006**, *45*, 32.
35. (a) Barboiu, M.; Dumitrescu, D.; van der Lee, A. *Cryst*. *Growth Des*. **2014**, *14*, 3062. (b) Eggers, P. K.; Fyles, T. M.; Mitchell, K. D. D.; Sutherland, T. *J. Org. Chem*. **2003**, *68*, 1050. (c) Bisht, K. K.; Kathalikkattil, A. C.; Suresh, E. *Cryst. Growth Des*. **2012**, *12*, 556. (d) Cao, M.-L.; Wu, J.-J.; Mo, H.-J.; Ye, B.-H. *J. Am. Chem. Soc*. **2009**, *131*, 3458.
36. (a) Chakraborty, S.; Dutta, R.; Arunachalam, M.; Ghosh, P. *Dalton Trans.* **2014**, *43*, 2061. (b) Basu, A.; Das, G. *Chem. Commun*. **2013**, *49*, 3997.

Annexure IV

Table 4.1 Crystallographic parameters and refinement details.

code name	**2a**	**2b**	**3**	**3a**	**3b**
empirical formula	$C_{27}H_{38}Cl_3N_7O_4S_3$	$C_{27}H_{38}Br_3N_7O_4S_3$	$C_{33}H_{34}N_6O_2S_3$	$C_{33}H_{34}F_2N_6OS_3$	$C_{33}H_{36}Cl_2N_6O_2S_3$
formula weight	727.20	860.55	640.86	663.86	716.80
cryst syst	Monoclic	monoclinic	orthorhombic	monoclinic	orthorhombic
a (Å)	9.9647(2)	10.2349(7)	12.3286(8)	12.355(10)	8.7092(4)
b (Å)	11.1184(3)	11.3045(7)	13.8630(6)	13.750(3)	20.3226(10)
c (Å)	31.7620(8)	31.991(2)	19.0679(9)	19.305(4)	19.5314(8)
α (degree)	90.00	90.00	90.00	90.00	90.00
β (degree)	103.5680(10)	104.319(4)	90.00	88.53(4)	90.00
γ (degree)	90.00	90.00	90.00	90.00	90.00
V ($Å^3$)	3420.75(14)	3586.4(4)	3258.9(3)	3278(3)	3456.9(3)
space group	$P\ 2_{1/c}$	$P\ 2_1/c$	$Pc2_1/n$	$C2$	$Pnma$
Z value	4	4	4	4	4
ρ(cal)(g/cm^3)	1.412	3.591	1.306	1.345	1.377
μ(Mo Kα) (mm^{-1})	0.71073	1.579	0.267	0.274	0.409
T(K)	298(2)	298(2)	298(2)	298(2)	298(2)
R1; wR2 (I> 2 σ(I))	0.0339; 0.0497	0.0457;0.0782	0.1481;0.4045	0.0800; 0.2163	0.0822;0.2691
R1; wR2(all)	0.0452; 0.0508	0.0907;0.1737	0.1759; 0.4363	0.0951; 0.2432	0.1165;0.3106
Residual electron density ($e\ Å^{-3}$)	0.402/ -0.354	0.577/-0.647	0.642/-0.789	0.317/-0.294	0.459/-0.931
good-of-fit	0.921	0.893	1.347	1.052	1.089
Reflection measured	5848	9289	5388	4412	4484
Unique reflns	4763	8190	3708	2921	2672
Reflection parameters	420	429	415	414	230
CCDC No.	836926	993149	993145	993146	993147

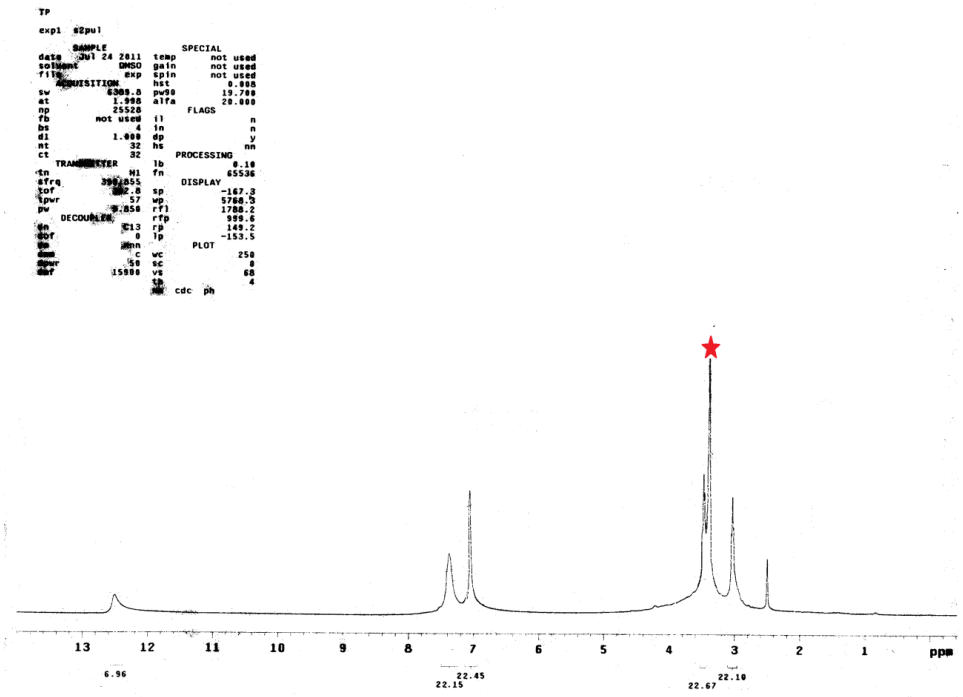

Figure A4.1. ^{1}H-NMR(400 MHz) spectra of $\mathbf{L_2}$ in d_6-DMSO at 298 K. Indicated peak represent the solvent.

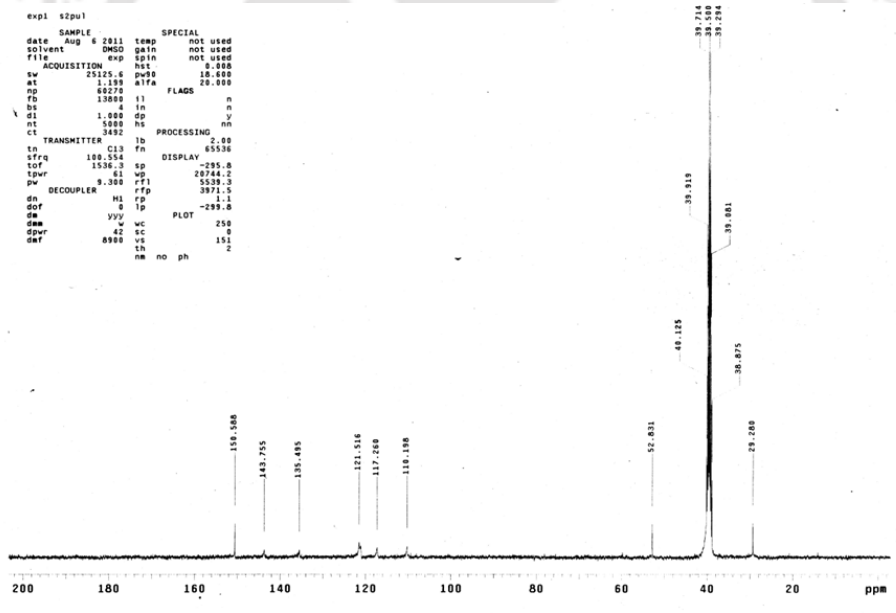

Figure A4.2. ^{13}C NMR spectrum of receptor $\mathbf{L_2}$ in DMSO-d_6 at 298 K.

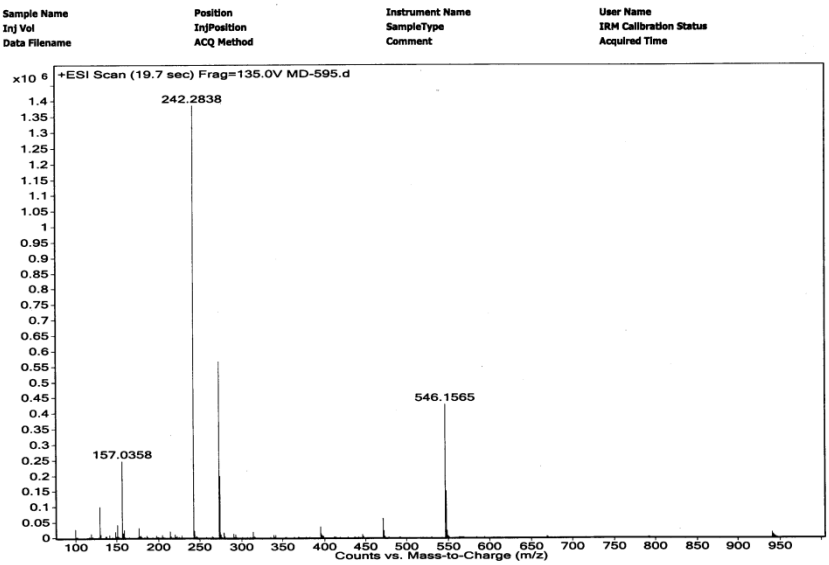

Figure A4.3. ESI-Mass spectrum of receptor $\mathbf{L}_2$ in methanol.

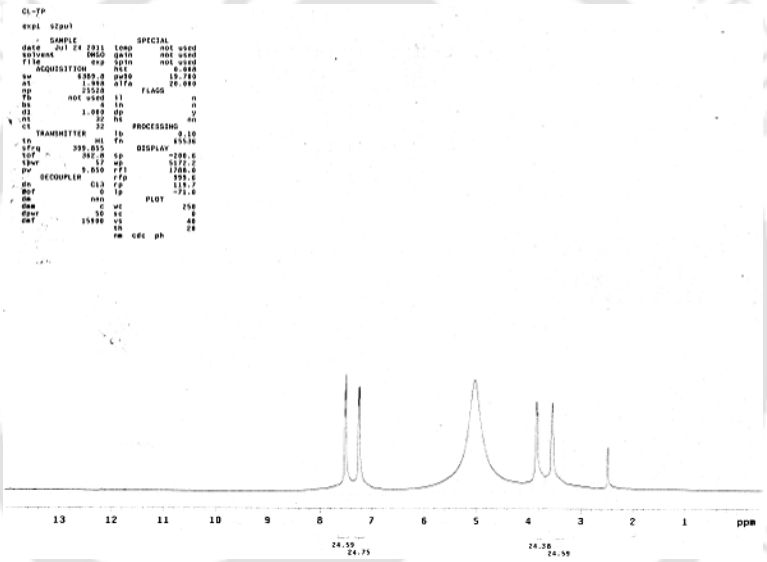

Figure A4.4. ^{1}H NMR(400 MHz) spectra of **2a** in d_6-DMSO at 298K.

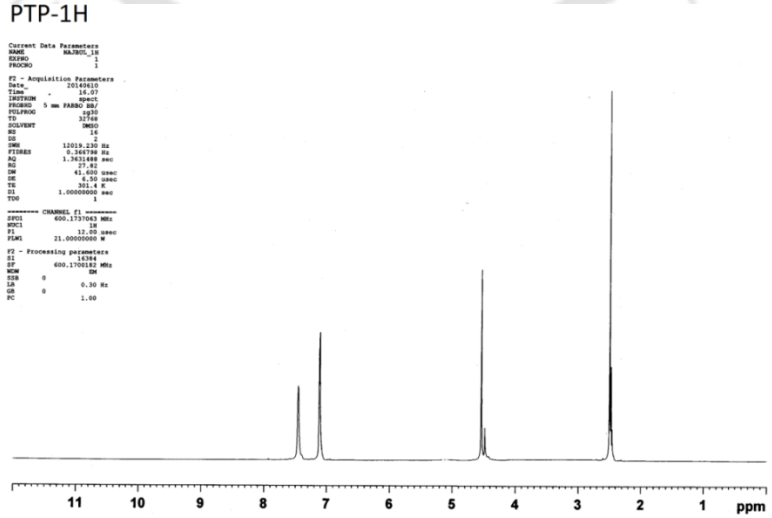

Figure A4.5. ^{1}H-NMR spectrum of receptor $\mathbf{L}_3$ in d_6-DMSO at 298 K.

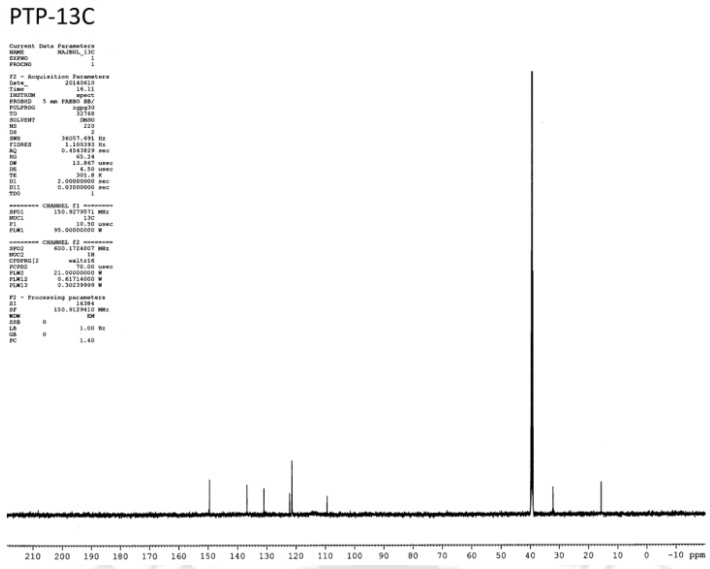

Figure A4.6. ^{13}C-NMR spectrum of receptor **L_3** in d_6-DMSO at 298 K.

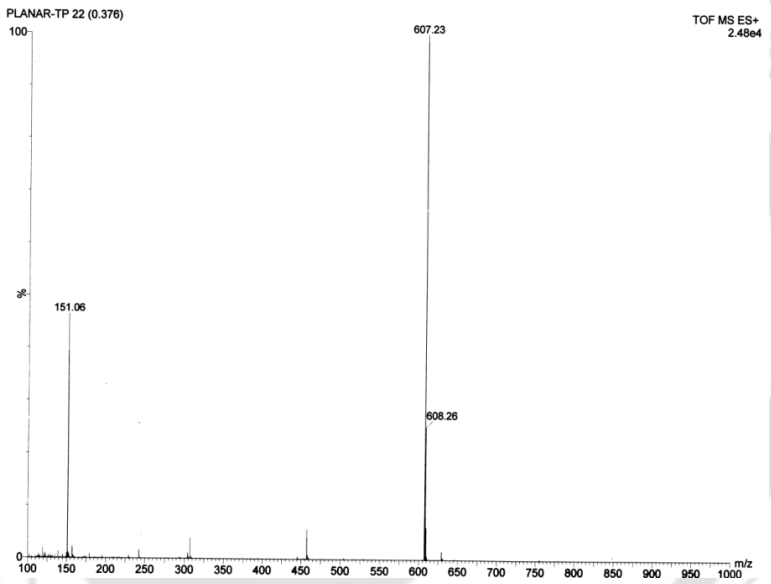

Figure A4.7. ESI-Mass spectrum of receptor **L_3** in methanol.

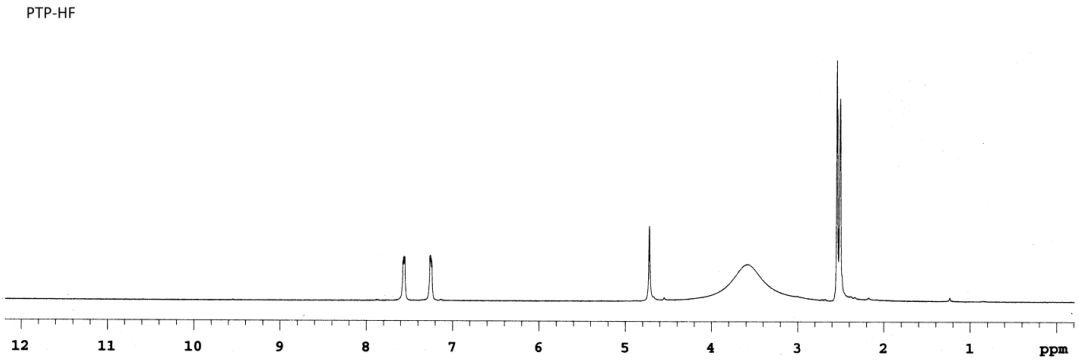

Figure A4.8. ^{1}H-NMR spectrum of complex **[L_3H_2·2F·H_2O](3a)** in d_6-DMSO at 298 K.

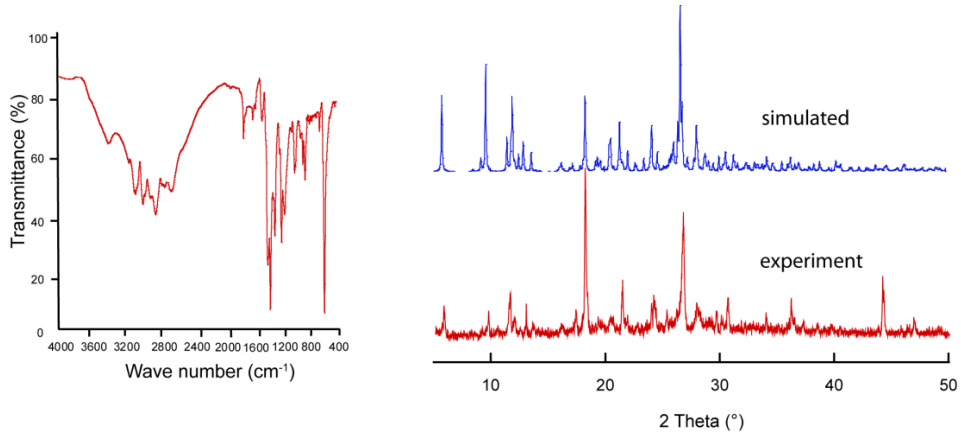

Figure A4.9. FT-IR spectrum of receptor **[$L_2H_3{\cdot}Cl_3{\cdot}4H_2O$](2a)** and powder X-ray diffraction: simulated pattern from the single crystal X-ray of **[$L_2H_3{\cdot}Cl_3{\cdot}4H_2O$](2a)** (blue), experimental pattern from the crystalline solid (red).

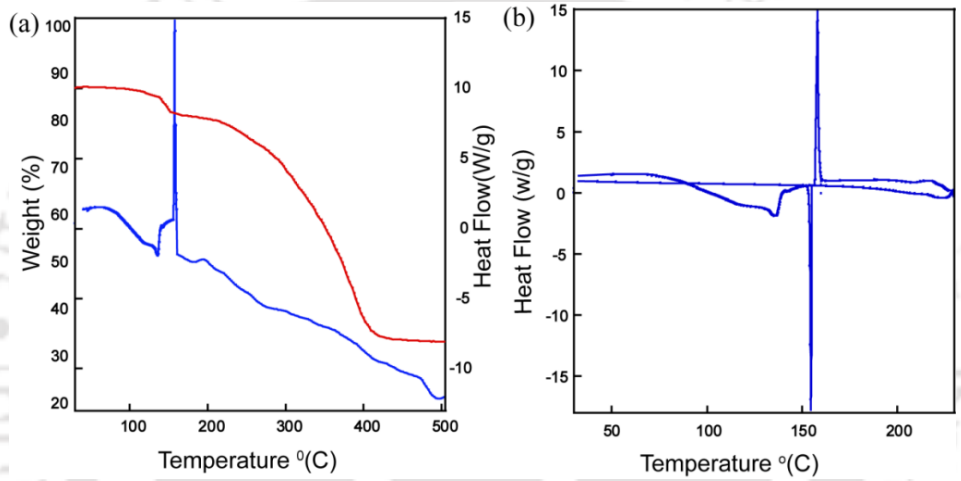

Figure A4.10. (a) Thermogravimetric analysis (TGA, red line) differential scanning calorimetry (DSC, blue line) curve (b) Cyclic DSC curve of **[$L_2H_3{\cdot}Cl_3{\cdot}4H_2O$](2a)** at a heating rate of 5 °C per min.

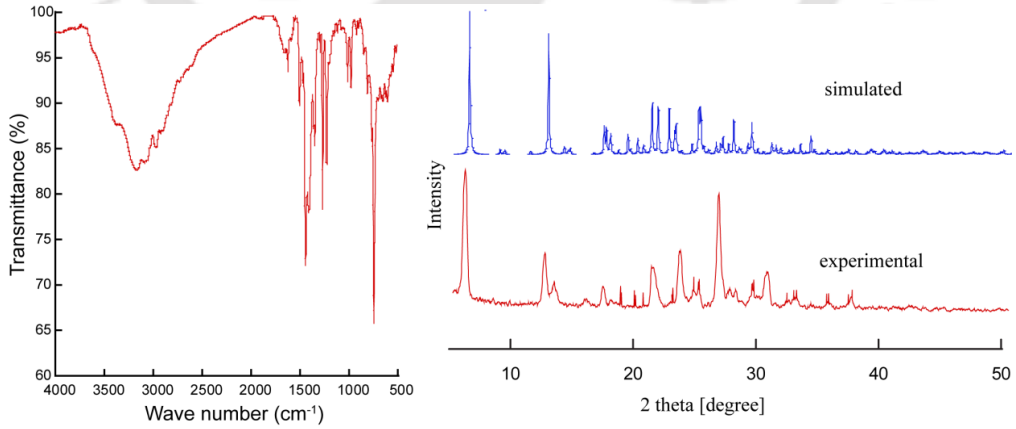

Figure A4.11. FT-IR spectrum of receptor **[$L_3H_2{\cdot}2Cl{\cdot}2H_2O$] (3b)** and powder X-ray diffraction: simulated pattern from the single crystal X-ray of **[$L_3H_2{\cdot}2Cl{\cdot}2H_2O$] (3b)** (blue), experimental pattern from the crystalline solid (red).

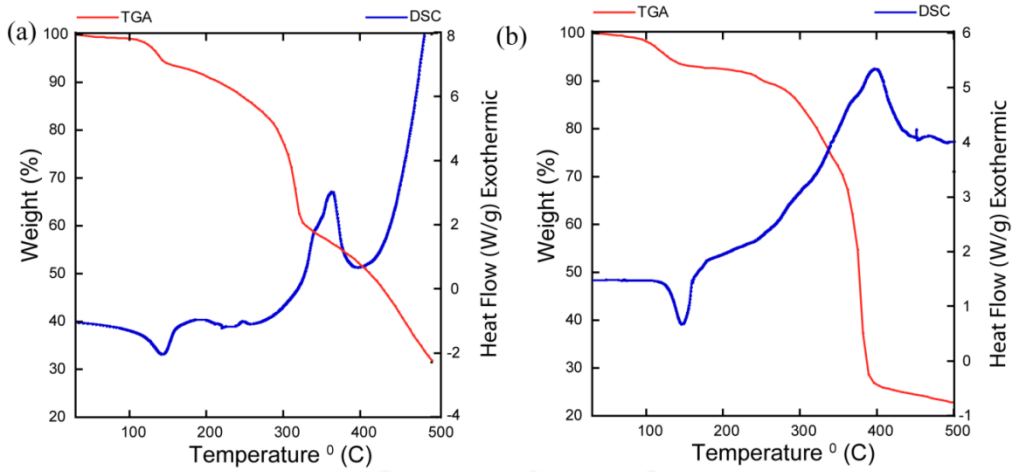

Figure A4.12. Thermogravimetric analysis (TGA) and differential scanning calorimetry (DSC) curve of **$L_3.2H_2O$(3)** and **[L_3H_2·2Cl·2H_2O] (3b)**at a heating rate of 5 °C per min.

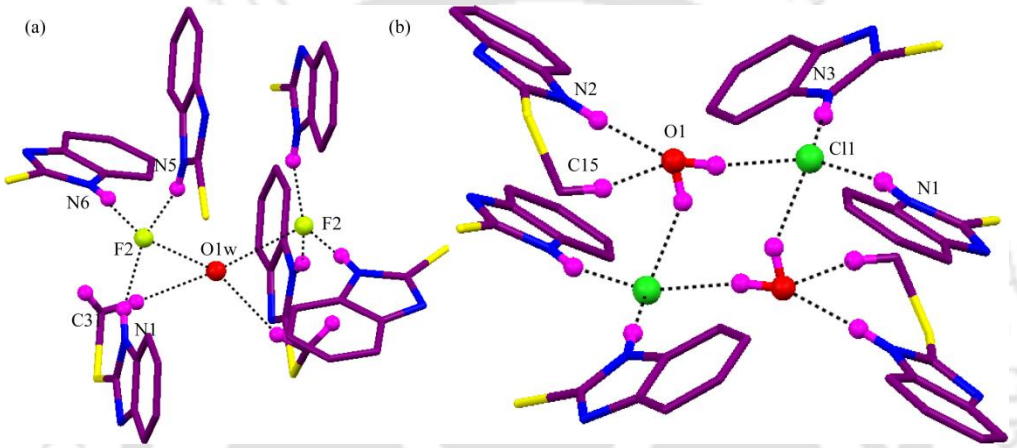

Figure A4.13. (a) Perspective view explaining interaction of trimer $[F_2\text{-}(H_2O)_{0\cdot5}]^{2-}$ in complex **3a**. (b) View explaining interactions and stabilization the $[Cl_2\text{-}(H_2O)_2]^{2-}$ cluster in complex **3b**.

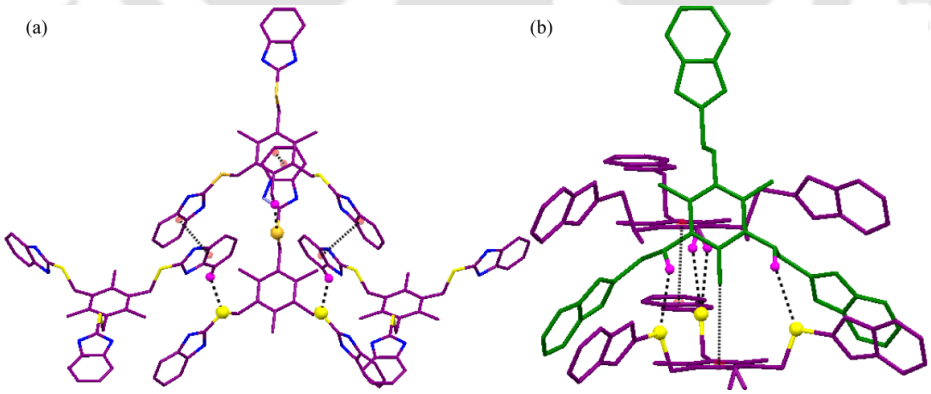

Figure A4.14. (a) Explaining H-bonding interaction between C—H $_{alp,ar}$ and S-atom, between benzene cap and benzimidazole and π···π stacking between benzimidazole moiety in complex **3a**. (b) Explaining H-bonding interaction between C—H $_{alp,ar}$ and S-atom and π···π stacking between benzimidazole and benzene cap in complex **3b.** Interestingly one receptor lie perpendicularly through benzene cap by C12—H···π interaction. In this case we did not observe any π···π interaction between benzimidazole.

Chapter 5

Hydrated Anion Glued Capsular and Non-capsular Assembly of a Tripodal Receptor

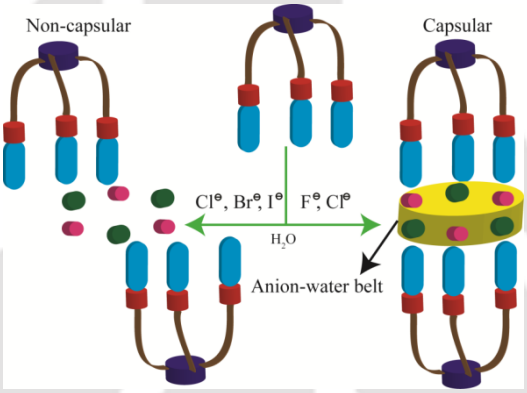

5.1 Back ground and focus on this chapter

Halide ions are ubiquitous and plays diverse role in nature and physiology.[1] Fluoride ion remains in strongly hydrated form due to its high hydration enthalpy. So consumption of fluoride containing drinking water is a concerning matter as its high level causes skeletal and dental fluorosis.[2] An important aspect of chloride ion in CIC (Charcot Leyden crystal) channels in transportation of chloride ion across cellular membrane is well established.[3] Another halide ion iodide remains dissolved in sea water and believed to be main source of iodide ions in atmosphere which increases ozone level in upper atmosphere.[4]

Oxyanions are unique due to their various shape, charge density and diverse reactivity in aqueous medium.[5] It is a big challenge to account complex hydration nature of polyatomic anionic species such as oxyanions. Particularly strong H-bonding ability of oxyanions (owing to high charge density) with the synthetic receptors opened the hope of their structural study. In the list of oxyanions, perchlorate anion is known to jeopardize human life by malfunctioning thyroid as it competes with iodide ion. sulfate anion occupy end of the Hofmeister series due to strong ability to decrease the protein solubility.[6] Nitrate anion is the most abundant species in troposphere and contaminate atmosphere as well as ground water as nitric acid.[7]

It is worth to mention that anion-water cluster mediated assembly has been less extensively studied with few exceptions of halide-water cluster mediated supramolecular capsules.[8-11] So in this direction anion-water induced assembly process is particularly a new window and can provide much more information about the behavior of hydrated anions in various supramolecular systems. In our continuing study on anion-water clusters and their role in formation of supramolecular architectures.[10,12]

For a receptor to be suitable for anion complexation must have several H-bonding sites capable of stabilizing anions in solid state by satisfying their coordination number. In this chapter our receptor (**L_4**) design is backed up by introducing three $-NH_2$ groups in a tripodal scaffold. The big advantages of polyammonium based anion receptors are high degree of protonation that enhance the possibility of binding of multiple anions. The solubility of such protonated receptors in protic solvent open the scope for the study of solvation properties of anions and anion-water interactions in highly polar medium in confined systems which is very relevant to realistic phenomenon. We have designed very important and new receptor considering these features having apical nitrogen atom and three amine groups forming a N_4 unit. Another famous N_4 unit (tren based receptor) has

widely been studied where apical nitrogen atom does not get protonated.[13] But in our case proper decoration by placing of ethereal function in the tripodal amine helps for the protonation of the apical nitrogen and allow the binding of multiple anions in protic solvent. The interesting outcome of this report is that we are able to isolate anion or anion-water assisted capsular and non-capsular supramolecular assembly and most significantly anion-water clusters by tripodal receptor in aqueous medium.

5.2 Structural aspect of anion binding with the polyammonium based tripodal receptor (L_4)

The tripodal **L_4** was prepared by reduction of nitro functionalized tripodal.[10] The change of functional group from $–NO_2$ to $–NH_2$ have resulted few great structural features while complexing with anions. The receptor has gained more H-bonding sites and presence of basic nitrogen allows proronation, as a result anions are stabilized by both supramolecular and electrostatic interactions. Most interestingly, the crystallization of anion complexes in aqueous medium shows surprising presence of crystallized water molecule, which interacts with water molecule giving various anion-water structural connection. Moreover the receptor form C_{3v} symmetric orientation of three arms eventually leads anion/hydrated anion assisted capsular and non-capsular assembly.

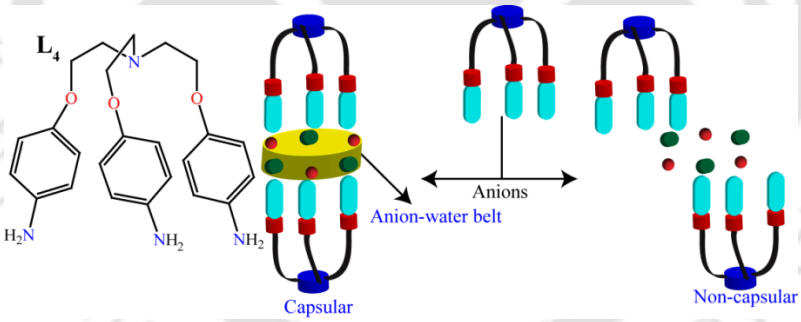

Scheme 5.1 Schematic diagram of the receptor and hydrated anion mediated capsular and non-capsular assembly

5.3 Structural description of L_4(4)

The free receptor **L_4** was crystallized during evaporation of the ethanolic solution within 24 hrs. Structural study obtained from single crystal X-ray shows that **L_4** crystallizes in highly symmetric hexagonal *R3c* space group. Solid state structure indicates the asymmetric unit contains only the receptor and a C_{3v} axis passes through the apical N-atom. The average bond distance between apical nitrogen and adjacent carbon in free receptor (N−C) is 1.477 Å. The ethereal separation (O···O = 4.798 Å) of three identical

oxygen atom and torsion angle value (N_{apical}–C–C–O_{ether} = 81.1°) suggest that receptor adopted an orientation in between folded and open conformation[10] as depicted in Figure 5.1. Interaction pattern shows all three ethereal oxygen form highly directed C_{ar}—H···O (C5···O1 = 3.536(2) Å) H-bond. All three $-NH_2$ groups are involved in H-bonding with aliphatic CH_2, phenyl ring with distances N2···C2 = 3.611(3) Å and C8···N2 = 3.593(2) Å respectively. The receptor is stabilized by all these weak interactions in solid state.Close inspection in the crystal packing indicates that each tripodal unit is surrounded by six neighbored tripodal units that form a cyclohexane like highly symmetric hexagonal structure. There are three aliphatic C−H···π interactions (C2···Cg = 3.811 Å) between two tripodal unit that generate sheet structure of the tripodal. IR spectra of free receptor **L_4** showed two sharp bands at 3430 cm^{-1} and 3350 cm^{-1} for N−H stretching frequency (Figure A5.4). Experimental and simulated PXRD pattern of free receptor **L_4** confirmed the bulk phase purity (Figure A5.4).

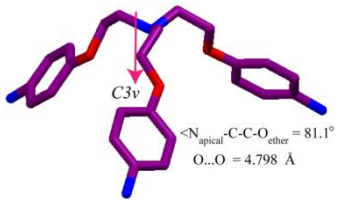

Figure 5.1 Crystal structure of L_4 showing an orientation neither in a folded nor in an open conformation and a C_{3v} axis of symmetry passing through apical N-atom.

5.3.1 Structural description of [L_4H_4·4F·5H_2O](4a)

Single crystal X-ray study of the complex **4a** shows it crystallizes in monoclinic system with centrosymmetric space group *C2/c*. The asymmetric unit contains one protonated receptor $[\mathbf{L_4}H_4]^{4+}$, four fluoride ions and five water of crystallization. The protonated receptor contains a C_{3v} axis passing through apical N-atom and fluoride ion (F1). Crystal structure shows that all four nitrogen atoms of the tripodal receptor are protonated and produced tetra fluorinated highly ionic environment. Protonation on apical N-atom in fluoride complex **4a** is further confirmed by the bond distance between apical N-atom and adjacent carbon (N−C) increased to 1.507 Å as observed in literature for apical nitrogen protonated receptors.[14] The hydrogen on apical nitrogen is directed towards the cavity and interacts with three ethereal oxygen atom in trifurcated fashion (average N1···O = 2.744 Å) that instigate the locks up conformation by decreasing the size of the cavity compared to free receptor **L_4** (Figure A5.7a). With the formation of trifurcated H-bond, the concomitant decrease in ethereal bond distance (average O···O = 3.529 Å) and torsion angle (average N_{apical}–C–C–O_{ether} = 60°) also support the organization of three arms in the same direction and formation of bowl shaped cavity. In protonated form three phenyl rings are orthogonal each other and as a consequence we observed three intramolecular C−H_{ar}···π interactions

among three tripodal arms. Three ammonium groups, the main H-bonding part of the receptor acts as a donor toward water and fluoride ion, interacts with total four water molecules and five fluoride ions. Very interestingly complex **4a** in the solid state form bimolecular capsule by association of two $[\mathbf{L_4}H_4]^{4+}$ unit *via* these H-bonding interactions and stitched by fluoride-water cluster depicted in Figure 5.2a. A top view shown in Figure 5.2a describes the formation of fluoride-water belt in the bimolecular capsule. One fluoride ion (F1) perfectly buried at the center of the bimolecular capsule and interacts with two neighbouring water molecules (O5w). The capsule is built mainly from H-bonding interactions of $[NH_3]^+$ groups with fluoride ions and water molecules. The

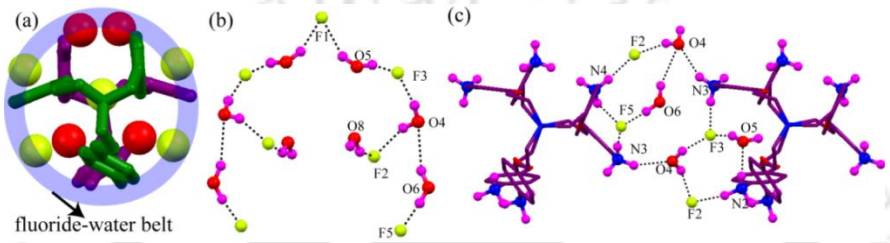

Figure 5.2 (a) Top view explaining the bimolecular molecular capsule stitched by fluoride-water belt and encapsulation of one fluoride ion. (b) Picture depicting the longest fluoride-water chain $[F_7\text{-}(H_2O)_8]^{7-}$ observed in complex **4a**. (c) View showing interaction between two capsules mediated by fluoride-water.

distance between two apical N-atoms in the bimolecular capsular is 17.157 Å. It is evident from the Figure 5.2c that each bimolecular capsule interacts with the neighbour capsule which is accompanied by several strong and weak H-bonding interactions arising from fluoride ions and water molecules. This would actually lead the formation of supramolecular structure made of the protonated tripodal receptor. Close inspection shows two capsules are assembled by fluoride-water cluster and with the help of $[NH_3]^+$ group it actually resulted the structural motif consisting of $[F^-\text{-}H_2O\text{-}NH_3^+]$ backbone. A backbone of $[F^-\text{-}H_2O\text{-}NH_3^+]$ motif having fused hexameric (one) and pentameric ring (two) gave $[F_4\text{-}(H_2O)_4\text{-}(NH_3)_4]$ twelve membered cyclic motif existing between two capsules. The startling feature in the crystal structure of complex **4a** is the formation of a long fluoride-water chain $[F_7\text{-}(H_2O)_8]^{7-}$ which is highlighted in Figure 5.2b. The chain is mainly stabilized by strong O···F, N···O and N···F H-bonding interactions. The chain contains a mirror plane passing through F1. Further aromatic hydrogen $C{-}H_{ar}\cdots F$ and aliphatic hydrogen $C{-}H_{alp}\cdots F$, $C{-}H_{alp}\cdots O$ also takes part in weak interactions and plays a crucial role to grow supramolecular assembly. Crystal packing along *b*-axis shows $[L_4H_4]^{4+}$ unit form cationic bilayer and surrounded by fluoride-water hydrophilic channel. IR spectra of complex **4a** exhibit a peak at 3435 cm^{-1} expected for water molecule in crystal lattice

(**Figure A5.5**). The comparable simulated and experimental PXRD pattern suggested to the bulk phase purity of the crystalline complex (**Figure A5.5**).

5.3.2 Structural description of [L_4H_4·4Cl](4b)

The solid state structure of the chloride complex **4b** displayed by X-ray analysis shows it crystallizes in highly symmetric hexagonal system of space group *R-3c* with crystallographically independent one third of the tetra-protonated receptor $[\mathbf{L_4}H_4]^{4+}$ and three chloride ions as asymmetric unit. In this case the complex does not contain any water of crystallization. conformation of the protonated receptor is similar to complex **4a**. Similarly, three arms are posed each other vertically and form C_{ar}–H···π interactions that also stabilized bowl shaped conformation. Here, two $[\mathbf{L_4}H_4]^{4+}$ units meet face to face and bimolecular capsule is built which is explained by top view in Figure 5.3a. In this case total six chloride ions are involved in capsule and holds two $[\mathbf{L_4}H_4]^{4+}$ unit firmly through formation of chloride ion belt enriched with Cl···H–N H-bonding interactions with $[NH_3]^+$ groups. The distance between two vertical N-atoms in this capsule is dropped to 16.706 Å as compared to **4a** presumably due to absence of water molecules in the capsular assembly. Each capsule attached with the adjacent capsule through the formation cyclic [Cl^--NH_3^+] motif highlighted in Figure 5.3b. Crystal packing viewed along *c*-axis results star like assembly of the molecular capsules. The extended packing diagram along *a*-axis produced anionic channel surrounded by cationic bilayers. The IR spectrum of the dehydrated complex does not contain any peak in the region of 3400-3200 cm^{-1} indicating absence of water molecule as expected. The complex remains in pure phase even in larger quantity as observed from similar simulated and experimental PXRD pattern.

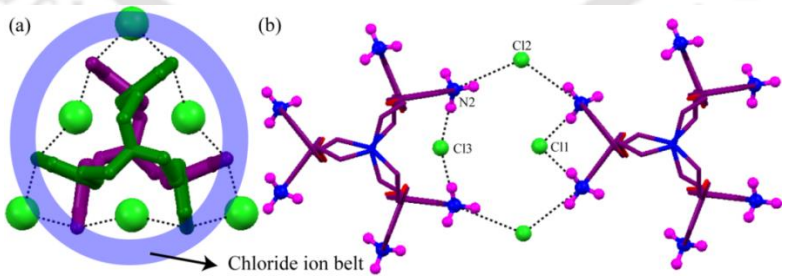

Figure 5.3 (a) Top view showing bimolecular capsule stitched by chloride ion belt in complex **4b**. (b) View depicting the interaction between two molecular capsules mediated by [Cl^--NH_3^+]

5.3.3 Structural description of [$2L_4H_4$·8Cl·$5H_2O$](4c)

Crystallographic analysis reveals that complex **4c** crystallizes in triclinic *P-1* space group with an asymmetric unit containing one independent tetra-protonated receptor $[\mathbf{L_4}H_4]^{4+}$,

four chloride ions and three water molecules. In solid state structure we observed, half part (green) is related to other half by forming an inversion center through the water molecule (O6w) giving molecular structure [2**L**H_4·8Cl·5H_2O] showed in Figure 5.4a. In complex **4c** the protonated receptor [$\mathbf{L_4}H_4$]$^{4+}$ slips from the face to a distant position and does not form any capsular assembly unlike the complex **4a** which is illustrated in Figure 5.4b**.** Each tripodal receptor interacts with the adjacent tripodal by several H-bonding interactions arising from N−H···Cl, N−H···Ow and Ow−H···Cl that generates the supramolecular structure. Close inspection in crystal structure shows three $[NH_3]^+$ groups of one [$\mathbf{L_4}H_4$]$^{4+}$ unit interacts with other two [$\mathbf{L_4}H_4$]$^{4+}$ unit *via* chloride-water bridge and such way they form non-capsular structure. The [$\mathbf{L_4}H_4$]$^{4+}$ units are linked each other by chloride-water [Cl_2-H_2O 'V' shaped] bridge, with the help of $[NH_3]^+$ groups form several fused cyclic rings (octamer, hexamer, pentamer and tetramer). The packing diagram of complex **4c** along *c*-axis shows that the hydrophilic layer of chloride-water channel propagate through cationic bilayer generated by protonated receptor. The weak interactions mainly comprising of aromatic C−H_{ar}···Cl and aliphatic C−H_{alp}···Cl are also involved in supramolecular assembly. The presence of H-bonded water molecule has also been confirmed by solid-state FT-IR analysis. The presence of a moderate broad signal at 3440 cm^{-1} in complex **4c** is attributed to the stretching frequency of the water molecule which is absent in free receptor. Additionally, the bulk phase purity of the complex **4c** has been established by PXRD experiment.

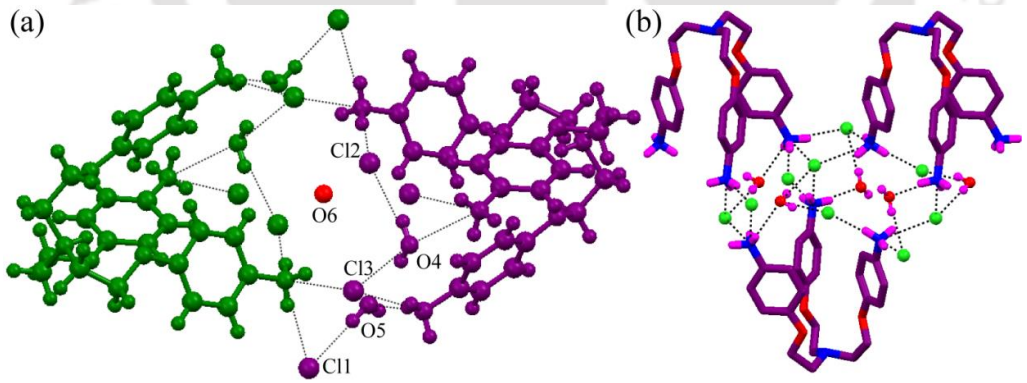

Figure 5.4 (a) Color scheme showing the cetrosymmetric molecular structure having an inversion center with respect to O6w in complex **4c**. (b) Depicting non-capsular assembly and interaction of [$\mathbf{L_4}H_4$]$^{4+}$ with adjacent receptor mediated by chloride-water.

5.3.4 Structural description of [L_4H_4·4Br·5H_2O](4d)

Single crystal X-ray shows the complex **4d** crystallizes in commonly available monoclinic system of space group $P2_1/c$ with an asymmetric unit that contains one tetra-protonated

$[\mathbf{L_4}H_4]^{4+}$, four bromide ions and five lattice water molecules. One bromide ion (Br3) lies on the C_{3v} symmetric apical N-atom. Bowl shaped cavity of hydrated bromide complex **4d** like other complexes. Crystal structure study shows the $[\mathbf{L_4}H_4]^{4+}$ units displaced from the face to a distant position in such a manner that they form non-capsular assembly like hydrated chloride complex **4c.** Each units are connected each other by [Br^--H_2O] linker enriched with several H-bonding. The noteworthy feature of complex **4d** is that we observed an unique anion-water cluster $[Br_5\text{-}(H_2O)_6]^{5-}$ having cyclic six membered ring $[Br_2\text{-}(H_2O)_4]^{2-}$ and tail $[Br\text{-}(H_2O)_2]^-$ which is illustrated in Figure. 5.5a. A careful analysis reveals that centrosymmetric cyclic hexamer composed of one bromide ions (Br2), two water molecules (O7w, O5w) and their centrosymmetric equivalents and resulted the formation of cyclohexane chair like conformation. The hybrid cyclic hexamer is quite similar to purely water hexamers found in several hydrated crystal systems[15] where bromide ion replaces the water molecule and persist the similar conformation (chair like). In the chair conformation four water molecules lies on the basal plane, two bromide are on above and below of the plane. In the hexamer two hydrogen of O5w is accepted by Br2 and O7w, whereas one hydrogen of O7w is accepted by Br2 giving a H-bonded motif $R_4^4(12)$. The H-bonding involved in cyclic hexamer are as follows; Br2···O5w = 3.362(6) Å, Br2···O7w = 3.267(7) Å and O5w···O7w = 2.805(9) Å. The Br···O and O···O separation in this hybrid water cluster is comparable to reported value observed in bromide-water clusters[16,17] and water hexamers.[18] Two type of bond angles found in cyclic hexamer *viz* ∠O5–Br2–O7 = 67.0(2)° and ∠O7–O5–Br2 = 110.4(2)° are ideal for tetrahedral water molecule which is frequently observed in hexagonal ice.[19] Other bond angles like ∠O–O–O, ∠O–O–Br, ∠Br–O–Br and ∠Br–Br–O existing outside of the hexameric ring span the range of 64.0(1)-131.5(1)°. Detail structural scrutiny of hybrid bromide-water hexamer shows that it is bi-substituted at O7w and mono-substituted at Br2. O7w contains bromide ion (Br4) in axial and water molecule (O6w) in equatorial position, Br2 contains one water molecule (O4w) in axial position from where a tail of $[O4w\text{-}Br3\text{-}O6w]^-$ is extended. The tail along with hexamer meet each other at O7w of the next hexamer in a centrosymmetric fashion with perfect inversion center leading to the formation of fused decameric ring (with hexamer) and as a result extended polymeric chain of hybrid bromide-water cluster is obtained in the crystal lattice as shown in Figure 5.5c. The decameric ring is also substituted at Br3 by $[O8w\text{-}Br1]^-$. The strong and medium H-bonds involved in decamer are Br2···O4w = 3.267(7) Å, Br3···O4w = 3.316(6) Å and Br3···O6w = 3.356(5) Å. The coordination environment of bromide-water cluster $[Br_5\text{-}(H_2O)_6]^{5-}$ is depicted in Figure

5.5b which clearly shows that several tripodal arms are involved in stabilization of the cluster through its [NH_3^+] end that form H-bonds with bromide ions and water molecules. Crystal packing along *b*-axis shows the propagation of hydrophilic bromide-water channel surrounded by cationic bilayer of the protonated receptor. In addition few other weak interactions like C9−H_{al}···Br1, C4−H_{ar}···Br4, C2−H···O7w and C10···Cg also helps for aggregation of the protonated receptor. We confirmed the presence water molecule in crystal lattice of hydrated bromide complex **4d** by IR spectra and broad vibration frequency appears at 3435 cm^{-1} corresponding to O−H stretching vibration. The bulk phase purity of the complex is also confirmed by PXRD study where simulated and experimental pattern coincide each other.

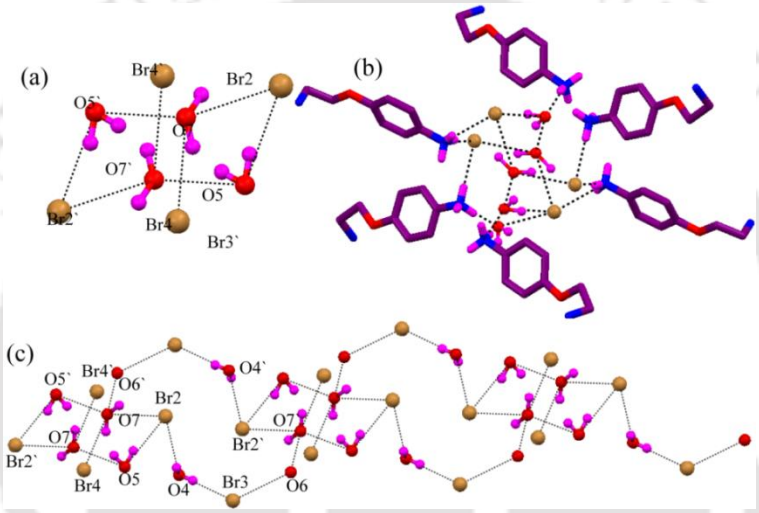

Figure 5.5 (a) View depicting minimum repeating fragment of bromide-water cluster $[Br_5\text{-}(H_2O)_6]^{5-}$ containing hexameric chair $[Br_2\text{-}(H_2O)_4]^{2-}$ in **4d**. (b) Infinite array of bromide-water cluster in which two $[Br_5\text{-}(H_2O)_6]^{5-}$ met in an inversion center and formed fused decameric ring. (c) Partial structure depicting interaction of bromide-water hexamer with [$\mathbf{L_4}H_4^+$].

5.3.5 Structural description of [$4\mathbf{L_4}H_4{\cdot}16I{\cdot}7H_2O$](4e)

The complex **4e** crystallizes in triclinic system with a *P-1* space group. The asymmetric unit contains two crystallographic independent tetra-protonated receptor [$\mathbf{L_4}H_4$]$^{4+}$ (N1 and N5 unit; naming according to the numbering of apical N-atom), eight iodide ions and four water of crystallization. Each protonated tripodal receptor in the asymmetric unit possesses a C_{3v} symmetry passing through apical N-atom containing iodide ion (I1) in N1 unit. Structural analysis shows one arm stay away from the other two arms by a small margin and not able to form any C−H···π interaction with other two arms, hence we observed only one orthogonal C−H···π interaction in N5 unit, whereas in N1 unit we observed three C−H···π interactions falling in acceptable distances. In iodide complex each

tripodal unit displaced from the face and connected through iodide-water interactions to form non-capsular assembly like complex **4a** and **4b (**Figure A5.7c). Solid state structure shows two symmetry independent tripodal receptors form two types of non-capsular aggregations with the help of H-bonding substances like iodide ions, water molecules and $[NH_3]^+$ groups. It is noteworthy to mention that we observed a well-defined discrete iodide-water cluster in non-capsular assembly formed by N5 unit. The iodide ion (I4) and two water molecules (O7w and O10w) formed 'V' shaped structure *via* I4···O10w = 3.630(3) Å and O7w···O10w = 2.830(4) Å H-bonding interactions. Such two 'V' shaped structures met each other through two oxygen end *via* O7w···O10w = 2.920(4) Å contact and led to the formation of iodide-water cluster $[I_2\text{-}(H_2O)_4]^{2-}$ containing cyclic water tetramer shown in Figure 5.6a. The water tetramer in iodide-water cluster contains a perfect inversion center at the center of the square. The four water molecule lies on a plane and two iodide ions occupy above and below of the plane forming chair like conformation. To the best possible placement of H-atoms in this cluster we noticed O7w donate its two

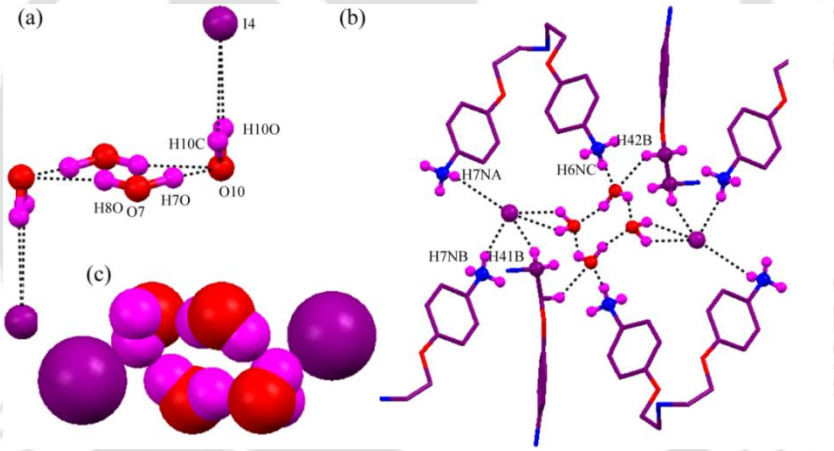

Figure 5.6 (a) (c) Image showing iodide-water cluster $[I_2\text{-}(H_2O)_4]^{2-}$ having square arrangement of water tetramer in complex **4e**. (d) Space fill model of $[I_2\text{-}(H_2O)_4]^{2-}$ cluster. (e) View describing interaction and stabilization $[I_2\text{-}(H_2O)_4]^{2-}$ cluster by cationic tripodal receptor.

hydrogen atoms towards two symmetric O10w and O10w presumably donates its two hydrogen to I4 ion. From the contribution of donor-acceptor properties of water molecules a cyclic water tetramer is formed with a H-bonding motif $R_4^2(8)$**.** The discreet iodide-water cluster is surrounded by cationic tripodal and stabilized by several strong and weak H-bonding interactions shown pictorially in Figure 5.6b. The water molecule O7w of tetramer accept two hydrogen from N6 and C42 of the tripodal receptor forming N6···O7w =2.780(3) Å and C42···O7w = 3.270(2) Å H-bonding. On the other hand, iodide ion (I4) interacts with its neighbored tripodal receptor *via* N7···I4 = 3.600(2) Å, N7···I4 = 3.650(1)

Å and C41···I4 = 3.850(1) Å contacts. With the best of our knowledge structural study of iodide-water cluster is very less,[20] our report of iodide-water cluster $[I_2\text{-}(H_2O)_4]^{2-}$ in organic system has not been reported previously. So iodide-water cluster $[I_2\text{-}(H_2O)_4]^{2-}$ observed in organic receptor is unprecedented. Crystal packing motif of complex **4e** as viewed down along *a*-axis showing the cationic bilayer assembly formation of cationic ligand moieties with the iodide-water channel being entrapped between the adjacent bilayers. The IR spectra of complex **4e** indicate a broad band centered around 3420 cm^{-1} and that can be attributed to O-H stretching frequency suggesting presence of water molecule. The bulk phase purity of the complex has also been confirmed by PXRD study where simulated and experimental pattern coincide each other.

5.3.5 Structural description of $[L_4H_4{\cdot}4H_2PO_4{\cdot}H_2O]$(4f)

The Complex **4f** crystallizes in the triclinic system in $P\bar{1}$ space group and asymmetric unit contains one tetra protonated receptor $[\mathbf{L_4}H_4]^{4+}$, four $H_2PO_4^-$ anions and one water of crystallization. A C_{3v} symmetry axis passes through apical N-atom. All H-atoms of each $[NH_3]^+$ groups are involved in strong H-bonding with $H_2PO_4^-$ ions and water molecule in monofurcated fashion. Structural study shows that the protonated receptor $[\mathbf{L_4}H_4]^{4+}$ slips from the face and form non-capsular assembly and interconnected by $H_2PO_4^-$ ion. All four $H_2PO_4^-$ ions interacts with $[NH_3]^+$ groups, aliphatic, aromatic hydrogen and water molecule with various coordination number like eight (P1), nine (P2), six (P3) and eight (P4) (Figure A5.8a). The binding pattern of $H_2PO_4^-$ ion is often compared with water molecule owing to its H-bond donor-acceptor ability, hence it could be suitable anion to generate anion clusters like water cluster. As a result, in most of the cases $H_2PO_4^-$ ion undergoes self-polymerization to form extended polymeric structure containing various cyclic rings. Although recent study shows few examples of large cyclic anionic clusters of $H_2PO_4^-$ ion.[21] In this case we are able to establish self-associated big anion cluster consisting of ten anions from the contribution of complementary donor-acceptor H-bonding interactions as depicted in Figure 5.7a. Details structural insight into the cyclic cluster shows it contains several fused cyclic rings namely hexamer, tetramer and trimer. The cyclic hexamer is connected by single O-H···O H-bond giving a structural motif $R_6^6(24)$. In this cluster the $H_2P(1)O_4^-$ ion acts as double H-bond acceptor and connects two $H_2P(2)O_4^-$ and $H_2P(3)O_4^-$ ion to form a linear trimeric chain. Two equivalent linear trimers met each other in anti-fashion and interlinked *via* single O11–H···O13 H-bond which led to the formation of cyclic hexameric $H_2PO_4^-$ ion cluster with perfect inversion

center inside the ring. In trimeric cluster $H_2P(4)O_4^-$ ion acts as two H-bond donor towards $H_2P(2)O_4^-$ and $H_2P(3)O_4^-$ ion and play as bridging anion *via* strong O16–H···O14 and O19–H···O10 H-bond. Two $H_2P(2)O_4^-$ and $H_2P(3)O_4^-$ ion also interacted *via* single H-bond O15–H···O10 completing the cyclic trimer and resulted a structural motif $R_3^2(10)$. Interestingly two $H_2P(2)O_4^-$ and $H_2P(3)O_4^-$ ion of cyclic trimers are interlinked *via* single O11–H···O13 H-bond generating a tetrameric ring with $R_4^4(16)$ motif. Thus we observed a unique structural topology of self-polymerized anion cluster containing ten $H_2PO_4^-$ ion having hexameric cluster linked to tetrameric and trimeric clusters.[22] The hexameric ring is very close to cyclohexane like structure where four $H_2PO_4^-$ ions (all P1 and P2) in

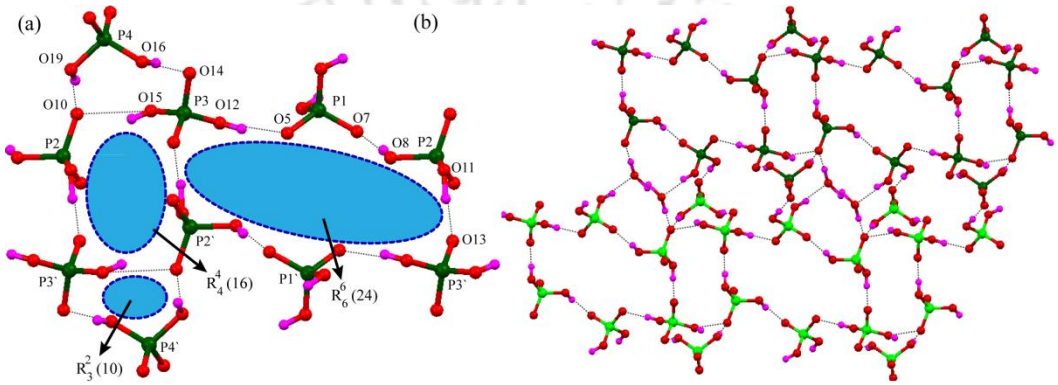

Figure 5.7 (a) Showing dihydrogen phosphate anion cluster of ten anions consisting hexameric (longest closed loop) cluster linked to a trimeric and a tetrameric clusters in complex **4f**. (b) Grow structure depicting infinite 2D assembly of anion cluster

hexamer lies in same plane and two $H_2PO_4^-$ ions (P3) lies above and below of the plane. The O···O separations in this anionic cluster fall in the range of 2.434(3) Å to 2.670 Å which is comparable with reported value found in dihydrogen phosphate clusters.[21] These H-bonds can be considered as low barrier H-bond as donor-acceptor distance is less than 2.80 Å.[23] Moreover very small contacts 2.434(3) Å, 2.490(5) Å and 2.510(3) Å suggest highly stable H-bonded anion cluster. The extended crystal packing along *c*-axis profoundly produced H-bond directed 2D anion cluster assembly which is highlighted in Figure 5.7b. Furthermore, crystal packing along *a*-axis generate hydrophilic $H_2PO_4^-$-H_2O channel that entrapped between the bilayers of the protonated receptor (Figure S21). The vibrational stretching frequency of complex **4f** indicate a broad band centered around 3444 cm^{-1} and sharp peak at 1102-1129 cm^{-1} that can be attributed to O–H and P–O bond suggesting presence of water and $H_2PO_4^-$ ion. The bulk phase purity of the complex is confirmed by PXRD study where simulated and experimental pattern coincide each other.

.

5.3.6 Structural description of $[2LH_4{\cdot}9ClO_4{\cdot}Na{\cdot}6H_2O]$(4g)

Complex **4g** crystallizes in the highly symmetric hexagonal *P-3* space group with an asymmetric unit containing symmetry independent one third of tetra-protonated receptor [$\mathbf{L_4}H_4^+$], one half of perchlorate ion, one sixth of another perchlorate ion, one sixth of $[Na(ClO_4)_6]^{5-}$ and one water of crystallization. The conformation of protonated receptor is similar to complex **4a**. Noticeably one perchlorate ion $Cl(1)O_4^-$ lies exactly on the C_{3v} symmetric apical N-atom. All three $[NH_3^+]$ group are symmetrically coordinated by three ClO_4^- ions and one water molecule. The coordination environment of two perchlorate ions

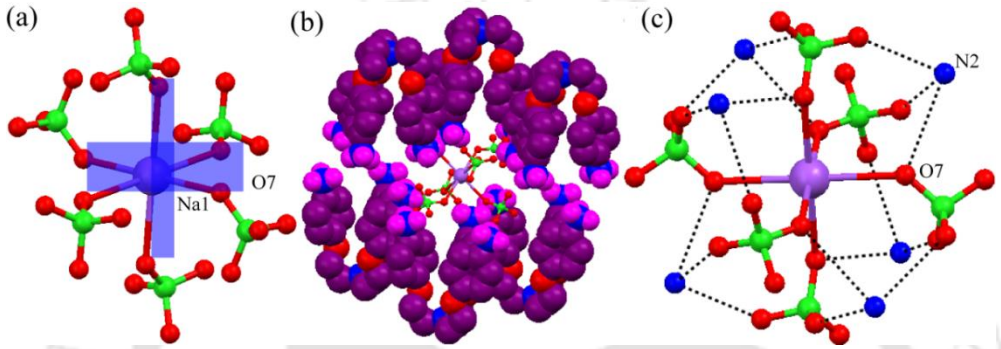

Figure 5.8 (a) Close view of the perfect octahedral geometry of anion cluster $[Na(ClO_4)_6]^{5-}$. (c) Trapping of $[Na(ClO_4)_6]^{5-}$ cluster by six tripodal receptors in **4g**. (d) A close view showing six tripodal coordinated with the $[Na(ClO_4)_6]^{5-}$ (N-atom of tripodal arm share the octahedral face).

(where $Cl(1)O_4^-$ and $Cl(2)O_4^-$ nine and five coordinated respectively) and presence of water dimer is observed. Most interestingly, we found a discrete anionic cluster $[Na(ClO_4)_6]^{5-}$ in the tripodal receptor which is highlighted in Figure 5.8a. The anionic cluster is constructed from six perchlorate ion and all six anions are located perfectly on octahedral environment of the sodium ion. In this cluster one oxygen of $Cl(2)O_4^-$ ions is coordinated with sodium ion having bond distance Na1···O7 = 2.700(1) Å. This observation is quite similar to the reported $[Na(ClO_4)_6]^{5-}$ anionic cluster which is encapsulated in tren based macrocycle.[24] Each face of the encapsulated $[Na(ClO_4)_6]^{5-}$ anionic cluster interacts with six nitrogen atom of the tripodal. This type of interaction can be seen in our cluster as well with the exception that at a time only one arm of a single tripodal unit interacts giving total six protonated receptor surrounding to $[Na(ClO_4)_6]^{5-}$ anionic cluster in non-capsular fashion. Such a way, the anionic cluster is stabilized into the protonated tripodal receptor. Close view in Figure 5.8b explained that the six tripodal receptor surrounded anionic cluster $[Na(ClO_4)_6]^{5-}$. Crystal structure of complex **4g** showed $[Na(ClO_4)_6]^{5-}$ anionic cluster mediated supramolecular aggregation of the tripodal receptor in non-capsular fashion like complex **4c**. As Crystal packing structure viewed along *b*-axis

clearly reveals that the formation of cationic bilayer chain and hydrophilic ($[Na(ClO_4)_6]^{5-}$-ClO_4^--H_2O) channel trapped between the bilayer of the protonated receptor. The broad band centered around 3430 cm^{-1} and 1083-1138 cm^{-1} of complex **4g** in FT-IR spectra can be assigned to the O–H and Cl–O stretching frequency. The bulk phase purity of the complex **4g** is supported by similar experimental and simulated PXRD pattern.

5.3.7 Structural description of $[L_4H_4{\cdot}2HSO_4{\cdot}SO_4]$(4h)

Complex **4h** crystallizes in $P\bar{1}$ space group and the asymmetric unit has one tetra-protonated $[\mathbf{L_4}H_4]^{4+}$ receptor, two hydrogen sulfate ions and one sulfate ion. The conformation of the protonated receptor is similar to other complexes. The details structural analysis shows that two tripodal units are held together face to face by efficient involvement of H-bonding and electrostatic interaction that led to the formation of bimolecular capsule (Figure 5.9a). The capsular complex contains two HSO_4^- ions and two

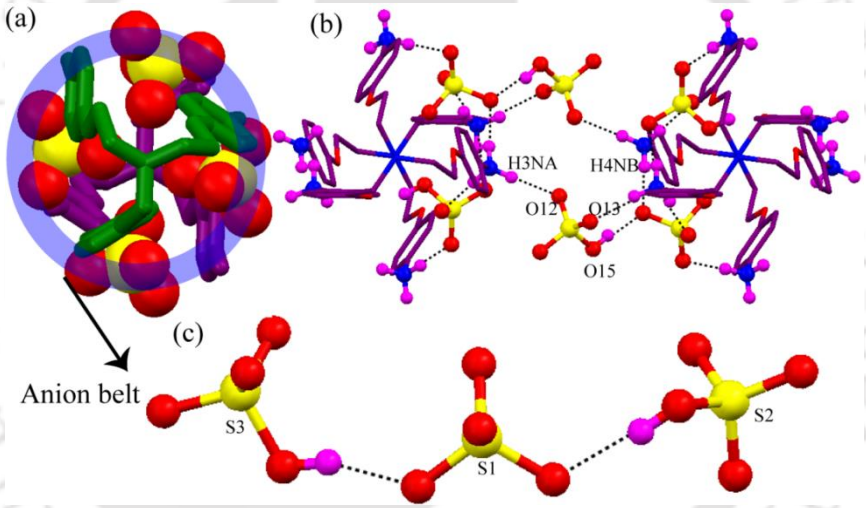

Figure 5.9 (a) Top view showing the anion belt formation in bimolecular capsule in complex **4h**. (b) Close contacts between two bimolecular capsules mediated by hydrogen sulfate ion. (c) Close view showing the discrete sulfate-hydrogen sulfate anion trimer $[SO_4\text{-}(HSO_4)_2]^{4-}$.

SO_4^{2-} ions that actually led to the formation of anion belt as depicted in Figure 5.9a. The anion belt strongly hold the bimolecular capsule by H-bonding and electrostatic interaction. The details interactions involved in anion belt arising from H-bonding among sulfate ions, hydrogen sulfate ions and ammonium groups is illustrated by partial structure.Indeed, the anion belt in this capsular assembly generated a structural motif comprising of $[(SO_4)_2\text{-}(HSO_4)_2\text{-}(NH_3)_6]$. The distance between two apical N-atom in capsular complex is 18.922(5) Å. The $HS(3)O_4^-$ ion connects two bimolecular capsular assembly and hold firmly through $[HS(3)O_4^-\text{-}NH_3^+]$ interaction (Figure 5.9b). It is

interesting to note that three symmetry independent sulfate anions interact each other and form a discrete linear trimeric $[(HSO_4)_2\text{-}SO_4]^{4-}$ anionic chain (Figure 5.9c). In this chain $S(1)O_4^{2-}$ ion acts as a bridge and accept two hydrogen (through O4 and O6) from neighboring $HS(2)O_4^-$ and $HS(3)O_4^-$ ion. As observed anions shows variety of coordination like nine, five and six for $S(1)O_4^{2-}$, $HS(2)O_4^-$ and $HS(3)O_4^-$ ion respectively. The crystal packing along *c*-axis shows the formation of anion adducts $HSO_4^-\text{-}SO_4^{2-}$ surrounded by cationic bilayer. In FT-IR spectroscopy band appeared in the range of 1175-1205 cm^{-1} corresponding to S–O bond suggesting the presence of sulfate ion in complex **4h**.

5.3.8 Structural description of $[LH_4{\cdot}2SO_4{\cdot}H_2O]$(4i)

Asymmetric unit in complex **4i** contains one $[\mathbf{L_4}H_4]^{4+}$, two SO_4^{2-} ions and one water of crystallization. The conformation of protonated receptor is similar to other complexes. In complex **4i** like complex **4a**, two $[\mathbf{L_4}H_4]^{4+}$ moiety utilizes H-bonding and electrostatic interaction with water molecule and SO_4^{2-} ion, and met face-to-face to form sulfate-water induced bimolecular capsule (Figure 5.10a). The bimolecular capsule contains total four SO_4^{2-} ions, two water molecules and strongly stitched by sulfate-water belt. It is clear that SO_4^{2-} ion accepts H-bond from $[NH_3]^+$, water molecule and formed well defined cyclic motif in the capsular complex. Bimolecular capsule is formed from active participation of donor $[NH_3]^+$ and water molecule, and acceptor SO_4^{2-} ion with several fused pentamer and

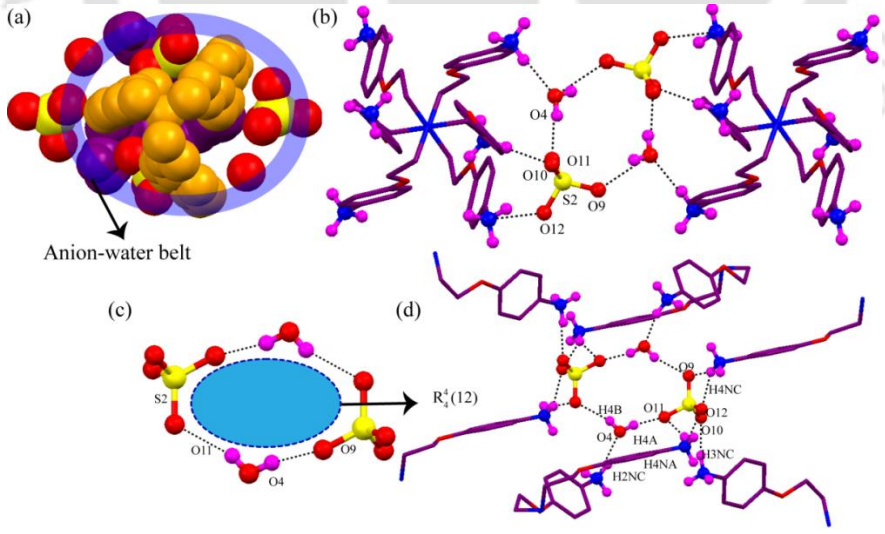

Figure 5.10 (a) Top view of the capsule explaining the sulfate-water belt in complex **4i**. (b) Illustration of interaction between two capsules mediated by $SO_4^{2-}\text{-}H_2O$. (c) Illustrating sulfate-water tetramer $[(SO_4)_2\text{-}(H_2O)_2]^{4-}$ with structural motif $R_4^4(12)$. (d) Stabilization of discrete $[(SO_4)_2\text{-}(H_2O)_2]^{4-}$ by tripodal receptor.

tetramer rings. The distance between two apical N-atom in capsular assembly is 17.728 (2) Å. Two capsular complex is mainly held by sulfate-water tetramer $[(SO_4)_2\text{-}(H_2O)_2]^{4-}$ and play crucial role to build supramolecular capsular assembly of the cationic tripodal receptor (Figure 5.10b). Molecular interaction shows two crystallographic independent SO_4^{2-} ions are stabilized by $[NH_3]^+$ groups and water molecules with the formation of eleven (S1) and ten (S2) coordinated H-bonds along with some C–H···O contacts as shown in Figure A5.8. The most appealing feature in complex **4i** is two equivalent sulfate ions $S(2)O_4^{2-}$ accepts two hydrogen atoms from two symmetry independent water molecule (O4w) through two oxygen (O9, O11) and form discrete sulfate-water tetramer $[(SO_4)_2\text{-}(H_2O)_2]^{4-}$ (Figure 5.10c). In this cluster water molecule (O4w) acts as a bridging H-bond donor between two sulfate ions and form strong H-bond. From the donor-acceptor combination it results a well-defined cyclic motif $R_4^4(12)$. The sulfate-water tetramer is surrounded by eight arms of the cationic tripodal through $[NH_3]^+$ end and stabilized by H-bonding interaction (Figure 5.10d). The literature survey on solid state structure of hydrated sulfate anions shows there are only few examples of defined sulfate-water cluters.[25] The previously reported sulfate-water tetramer[25a] where only one oxygen of sulfate ion simultaneously accept two hydrogen from two water molecules and subsequent decrease in ring size ($R_4^2(8)$ motif) was observed compared to our report. In our report $[(SO_4)_2\text{-}(H_2O)_2]^{4-}$ tetramer water and sulfate ion reside in the same plane. The packing diagram along *c*-axis generates hydrophilic sulfate-water channel surrounded cationic bilayers of the tripodal. We confirmed the presence water molecule in crystal lattice complex **4i** by FT-IR spectra and broad vibration frequency appears at 3425 cm^{-1} and 1120-1195 cm^{-1} corresponding to O–H and S–O stretching vibration. The bulk phase purity of the complex is also confirmed by PXRD study where simulated and experimental pattern coincide each other.

5.4 Thermogravimetric analysis

Binding strength of water molecule in the highly ionic environment of the tripodal receptor, number of water molecule present in the system and thermal stability of the different complexes was investigated by thermogravimetric analysis (TGA) and differential scanning calorimetry (DSC) experiment. The thermal stability of the water molecule in the solid can be correlated to the formation of H-bonded network in the crystal lattice. The capsular and non-capsular assembled supramolecular structures are a consequence of anion-water and anion-water-receptor interactions. The fluoride complex

4a, exhibited continuous weight loss (for water molecule) up to ~194 °C, there is a weight loss of 5.75% at ~104 °C, which matches very well with calculated value 6.07% corresponding to two water molecules. Partially dehydrated complex is stable up to ~135 °C and after this remaining three water molecules (found 8.45%; calcd. 9.01%) are lost and continue to ~194 °C along with the melting of the complex. In DSC clear endothermic peak is observed at ~97 °C and at ~188 °C corresponding to these weight losses (Figure A5.6). On other hand the anhydrous chloride complex **4b** did not show any weight loss in the range of ~30-256 °C as expected from its crystal structure (absence of lattice water molecule) and is stable up to ~256 °C before it melts. This result is also achieved by the appearance of a sharp endothermic peak at ~256 °C in its DSC plot. For the chloride complex **4c**, removal of all water molecules (five crystalline water molecules) are observed in a single step, with the weight loss of 6.26% (calcd. 7.34%) at ~88 °C. The indication of this weight loss is also noticed from endothermic peak at ~84 °C in its DSC curve. The dehydrated complex is stable up to ~240 °C and started to melt after ~240 °C. The bromide complex **4d** started to degrade lattice water molecules early stages at ~76 °C, a weight loss 10.15% (calcd. 10.78%) relative to five water molecules. This is further confirmed by an endothermic peak at ~76 °C in its DSC curve. The dehydrated complex is stable up to ~285 °C and then started to melt with an appearance of a endothermic peak at ~280 °C. Removal of water molecules from the iodide complex **4e** occurred in single step. A one step weight loss of 3.70% (calcd. 3.26%) at ~105 °C for seven water molecules is observed and confirmed an endothermic peak at ~105 °C in DSC curve. The dehydrated salt is stable up to ~288 °C. After this temperature complex started to melt and for which an endothermic peak is appeared at ~275 °C in DSC curve. The hydrogen phosphate complex **4f** exhibited a weight loss 2.34% (calcd. 2.16%) at the temperature range 130-182 °C for only one crystallized water molecule. The high stability of water molecule is attributed due to strong H-bonding interaction by $H_2PO_4^-$ ion, [NH_3^+] groups and water molecules (dimer, O···O = 2.764 Å). The dehydrated complex is stable upto 220 °C. A clear appearance of endothermic peak at 140 °C and 235 °C in DSC plot are the evidences for the loss of water and melting of the complex. In perchlorate complex **4g** weight loss of 5.40% (calcd. 5.65%) corresponding to the loss of six water molecules as early as 90 °C and the dehydrated complex is stable upto 275 °C and decomposed after this temperature. The water molecule is loosely bounded by comparably weak H-bond in ClO_4^--H_2O and dimer (O···O = 3.070 Å) in comparison to the previous one and thus lost before 100 °C. The removal of water molecule and decomposition of complex is supported by a small

endothermic and big exothermic peak at 85 °C and 275 °C in DSC plot respectively. The hydrogen sulfate complex **4h** did not show any weight loss at the region of 30-230 °C in its TGA and DSC plot which also corresponds to its X-ray structure. The complex **4h** is stable upto 258 °C and produced an endothermic peak at 258 °C. One water molecule in sulfate complex **4i** is retained upto 220 °C and a weight loss 2.45% (calcd. 2.82%) corresponding to this water molecule is observed in TGA plot. Strong H-bonding by two sulfate ions and one [NH_3^+] group is responsible for the observed high dehydration temperature of the complex. This result corroborates the result of crystal structure analysis. The removal of water molecule is established from DSC plot with a small endothermic peak at 210 °C. The dehydrated complex started to decompose after its melting temperature 260 °C by generating an endothermic peak at 260 °C.

Conclusion

In summary, we have shown the capsular and non-capsular assembly of the cationic tripodal receptor by hydrophilic anion-water cluster. We established fluoride-water cluster belt, chloride ion belt, sulfate-hydrogen sulfate and sulfate-water belt mediated supramolecular assembly in bimolecular capsular fashion. On the other hand formation of non-capsular supramolecular association of the receptor is observed by chloride-water, bromide-water, iodide-water, phosphate-water and perchlorate-water. Moreover our observations underscore extended polymeric bromide-water cluster $[Br_5\text{-}(H_2O)_6]^{5-}$ having defined cyclohexane like chair conformation and discrete iodide-water cluster $[I_2\text{-}(H_2O)_4]^{2-}$ containing water tetramer in solid state. We have showed extended polymeric structure of $H_2PO_4^-$ anion which is built mainly from contribution of self-complementary H-bonding between various fused rings namely hexamer, tetramer and trimer. CSD data base showed only few examples of larger oligomers of $H_2PO_4^-$ anion (higher than dimer) is reported.[21] Hence structural report of this type higher oligomeric cluster is important to anion cluster chemistry. In addition we described octahedrally arranged discrete anionic cluster $[Na(ClO_4)_6]^{5-}$ which is rarely seen in literature.[24] Moreover we isolated discrete sulfate-hydrogen sulfate trimer $[SO_4\text{-}(HSO_4)_2]^{4-}$ and sulfate-water tetramer $[(SO_4)_2\text{-}(H_2O)_2]^{4-}$ in solid state. Existence of hydrophilic anion-water channels surrounded by cationic bilayers of tripodal receptor can elucidate the behavior of hydrated anionic species in confined environment. Indeed a systematic survey of anion complexation in this type system, having various shape, size and charge density would surely add much more information to the anion coordination chemistry. Our structural demonstration on anion

and anion-water clusters would give us the idea about solid state interactions, self-aggregations and structural relationship of anions with synthetic receptor

References

1. (a) Hoffmann, E. K. *Biochem. Biophys. Acta*., 1986, **864**, 1. (b) Sessler, J. L.; Gale, P. A.; Cho, W. S. *In Anion Receptor Chemistry* (Monographs in Supramolecular Chemistry); Ed.; RSC: Cambridge, 2006; pp 1-413; (c) Zhou, P.; Tian, F.; Zou, J.; Ren, Y.; Liu, X.; Shang, Z. *J. Phys. Chem., B* **2010**, *114*, 15673
2. Ayoob, S.; Gupta, A. K. *Crit. Rev. Environ. Sci. Technol*., **2006**, *36*, 433.
3. (a) Dutzler, R.; Campbell, E. B.; Cadene, M.; Chait B. T.; MacKinnon, R. *Nature*., **2002**, *415*, 287. (b) Miller, C. *Nature*., **2006**, *440*, 484.
4. (a) Rädlinger, G.; Heumann, K. G. *Environ. Sci. Technol*., **2000**, *34*, 3932. (b) Saunders, R. W.; Kumar, R.; MacDonald, S. M.; Plane, J. M. C. *Environ. Sci. Technol*., **2012**, *46*, 11854. (c) Saiz-Lopez, A.; Plane, J. M. C. A.; Baker, R.; Carpenter, L. J.; von Glasow, R.; Gómez Martin, J. C.; McFiggans, G. Saunders, R. W. *Chem. Rev*., **2012**, *112*, 1773. (d) Guzman, M. I.; Athalye, R. R. Rodriguez, J. M.; *J. Phys. Chem.*, A **2012**, *116***,** 5428.
5. (a) Wang, X. B.; Yang, X.; Wang, L.; *Int. Rev. Phys. Chem*. **2002**, *21*, 473. (b) Wang, X. B.; Wang, L. S. *Annu. Rev. Phys. Chem*. **2009**, *60*, 105. (c) Robertson, W. H.; Johnson M. A. *Annu. Rev. Phys. Chem*. **2003**, *54*, 173. (d) Yang, X.; Wang, X. B.; Wang, L. S. *J. Phys. Chem. A* **2002**, *106*, 7607.
6. (a) Hofmeister, F. *Arch. Exp. Pathol. Pharmacol*. **1888**, *24*, 247. (b) O'Brien, J. T.; Prell, J.; Bush, M.; Williams, E. R. *J. Am. Chem. Soc*. **2010**, *132*, 8248.
7. (a) Fnlayson-Pitts, B. J. *Chem. Rev*. **2003**, *103*, 4801. (b) *Science and Technology for Disposal of Radioactive Tank Wastes*; Schultz, W. W.; Lombardo, N. J., Eds.; Plenum: New York **1998**. (c) Keeneya, D. R.; Hatfieldb, J. L. *In Nitrogen in the Environment*: *Sources, Problems, and Management*; Hatfield, J. L., Follett, R. F., Eds. Elsevier: Oxford, U.K., **2008**; pp 453.
8. Arunachalam, M.; Ghosh, P. *Chem. Commun*., **2009**, 5389.
9. Arunachalam M.; Ghosh, P. *Chem. Commun*., **2011**, *47*, 6269.
10. Basu, A.; Das, G. *Chem. Commun*., **2013**, *49*, 3997.
11. Chakraborty, S.; Dutta, R.; Arunachalam, M.; Ghosh, P. *Dalton Trans*., **2014**, *43*, 2061.
12. Hoque, M. N.; Basu, A.; Das, G. *Cryst. Growth Des*., **2012**, *12*, 2153.
13. Bose, P.; Ravikumar, I. Ghosh, P. *Inorg. Chem*., **2011**, *50*, 10693.
14. Dey, S. K.; Ojha, B.; Das, G. *CrystEngComm*., **2011**, *13*, 269.
15. (a) Hu, T.; Zhao, X.; Hu, X.; Xu, Y.; Sun, D.; Sun, D. *RSC Adv*., **2011**, *1*, 1682. (b) Khullar, S.; Mandal, S. K. *CrystEngComm*., **2013**, *15*, 6652; (c) Ghosh, S. K.; Bharadwaj, P. K. *Inorg. Chem*., **2004**, *43*, 5180. (d) Ghosh, S. K.; Bharadwaj, P. K. *Inorg. Chem*., **2003**, *42*, 8250.
16. Bakhoda, A.; Khavasi, H. R.; Safari, N. *Cryst. Growth Des*., **2011**, *11*, 933.
17. Manna, P.; Seth, S. K.; Bauzá, A.; Mitra, M.; Choudhury, S. R.; Frontera, A.; Mukhopadhyay, S. *Cryst. Growth Des*., **2014**, *14*, 747.
18. (a) Hu, T.; Zhao, X.; Hu, X.; Xu, Y.; Sun, D.; Sun, D.. *RSC Adv*., **2011**, *1*, 1682. (b) Ghosh, S. K. Bharadwaj, P. K. *Inorg. Chem*., **2004**, *43*, 5180;
19. D. Eisenberg and W. Kauzmann, *The Structure and Properties of Water*, Oxford University Press: Oxford, UK, 1969.
20. W. Dong, Y. Ou-Yang, H.-B. Song, D.-Z. Liao, Z.-H. Jiang, S.-P. Yan and P. Cheng, *Inorg. Chem.*, 2006, **45**, 1168.
21. Hossain, M. A.; Isiklan, M.; Pramanik, A.; Saeed, M. A.; Fronczek, F. R. *Cryst. Growth Des.* **2012**, 12, 567.
22. Rajbanshi, A.; Wan, S.; Custelcean, R.; *Cryst. Growth Des*. **2013**, *13*, 2233.
23. (a) Garcia-Viloca, M.; GonzálezLafont. A.; Lluch, J. M. *J. Am. Chem. Soc*. **1997**, *119*, 1081. (b) Engelhart, A. E.; Mortonb, T. H.; Hud, N. V. *Chem. Commun*. **2009**, 647.
24. Mateus, P.; Delgado, R.; Brandão, P.; Félix, V. *J. Org. Chem*. **2009**, *74*, 8638
25. (a) Xia, Y.; Wu, B.; Liu, Y.; Yang, Z.; Huang, X.; He, L.; Yang, X.-J. *CrystEngComm*. **2009**, *11*, 1849. (b) Jose, D. A.; Kumar, D. K.; Ganguly, B.; Das, A. *Inorg. Chem*. **2007**, *46*, 5817.

Annexure V

Table 5.1a Crystallographic parameters and refinement details.

Code name	**L_4**	**4a**	**4b**	**4c**	**4d**
Empirical formula	$C_{24}H_{30}N_4O_3$	$C_{24}H_{44}F_4N_4O_8$	$C_{24}H_{34}Cl_4N_4O_3$	$C_{48}H_{78}Cl_8N_8O_{11}$	$C_{24}H_{44}Br_4N_4O_8$
Formula weight	422.52	592.63	568.35	1224.77	836.22
Crystal system	Hexagonal	Monoclinic	Hexagonal	Triclinic	Monoclinic
a (Å)	19.2271(4)	23.2013(12)	12.7399(8)	11.4963(6)	12.6464(4)
b (Å)	19.2271(4)	11.1503(4)	12.7399(8)	12.2339(6)	11.5355(4)
c (Å)	10.2751(2)	24.7773(10)	62.0390(5)	13.0811(8)	24.2735(8)
α (degree)	90.00	90.00	90.00	111.373(5)	90.00
β (degree)	90.00	114.561(6)	90.00	113.194(5)	104.935(2)
γ (degree)	120.00	90.00	120.00	94.457(4)	90.00
V ($Å^3$)	3289.61(12)	5830.00(5)	8720.20(10)	1521.28(14)	3421.50(2)
space group	*R3c*	*C2/c*	*R-3c*	*P-1*	$P2_1/c$
Z value	6	8	12	1	4
ρ(cal)(g/cm^3)	1.280	1.350	1.229	1.337	1.621
μ(Mo Kα) (mm^{-1})	0.086	0.116	0.438	0.430	4.751
T(K)	298(2)	298(2)	298(2)	298(2)	298(2)
R1; wR2 (I> 2 σ(I))	0.0349; 0.1059	0.0780; 0.2311	0.0478; 0.1313	0.0492; 0.1656	0.0353; 0.1029
R1; wR2(all)	0.0379; 0.1095	0.1039; 0.2563	0.0715; 0.1497	0.0682; 0.2006	0.0545; 0.1205
Residual electron density	0.122/-0.170	0.783/-0.364	0.548/-0.172	0.604/-0.537	0.451/-0.638
good-of-fit	0.906	0.980	1.004	0.690	0.910
Reflection measured	16238	13715	12681	11469	30309
Unique reflns	1799	4624	2527	5194	6895
Reflection parameters	94	391	110	365	404
CCDC No.	961078	961079	961080	961081	961082

Table 5.1b Crystallographic parameters and refinement details.

code name	**4e**	**4f**	**4g**	**4h**	**4i**
empirical formula	$C_{96}H_{150}I_{16}N_{16}O_{19}$	$C_{24}H_{44}N_4O_{20}P_4$	$C_{48}H_{80}Cl_9N_8NaO_{48}$	$C_{24}H_{36}N_4O_{15}S_3$	$C_{24}H_{36}N_4O_{12}S_2$
Formula weight	3862.67	832.51	1911.24	716.78	636.71
cryst syst	Triclinic	Triclinic	Hexagonal	Triclinic	Triclinic
a (Å)	12.6814(6)	12.8225(8)	12.8725(14)	12.365(3)	10.5903(3)
b (Å)	13.0383(6)	13.3153(7)	12.8725(14)	12.677(2)	12.1999(4)
c (Å)	20.9938(10)	13.7615(9))	13.6616(19)	12.679(2)	12.6930(4)
α (degree)	75.377(2)	65.496(6)	90.00	72.785(16)	92.034(2)
β (degree)	87.245(2)	64.074(7)	90.00	62.375(19)	107.203(2)
γ (degree)	88.453(2)	61.250(6)	120.00	65.503(19)	110.886(2)
V ($Å^3$)	3354.50(3)	1789.24(19)	1960.5(4)	1589.0(5)	1445.28(8)
space group	*P -1*	*P -1*	*P-3*	*P -1*	*P -1*
Z value	1	2	1	2	2
ρ(cal)(g/cm^3)	1.909	1.545	1.619	1.498	1.463
μ(Mo Kα) (mm^{-1})	3.750	0.299	0.439	0.310	0.253
T(K)	298(2)	298(2)	298(2)	298(2)	298(2)

R1; wR2 (I> 2 σ(I))	0.0677; 0.1751	0.0545, 0.1604	0.1043, 0.3177	0.0562; 0.1712	0.0667, 0.1885
R1; wR2(all)	0.0965; 0.1946	0.0705, 0.1864	0.1434, 0.3762	0.0809; 0.2060	0.0750, 0.1983
Residual electron density	3.107/-3.423	1.026/ -0.538	0.645/-0.879	0.869/-0.590	0.960/ -1.095
good-of-fit	1.112	0.787	1.207	0.762	1.042
Reflection measured	14556	14383	5448	11525	21536
Unique reflns	8849	9098	3315	7998	7154
Reflection parameters	694	517	189	420	394
CCDC No.	978948	961084	961087	961085	961086

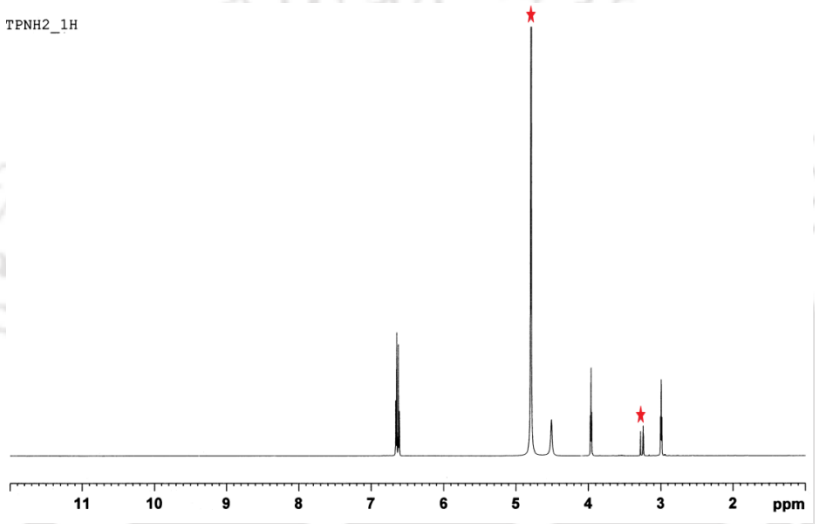

Figure A5.1. ^{1}H-NMR spectrum of receptor **L_4** in CD_3OD at 298 K. Indicated peaks represent the solvent.

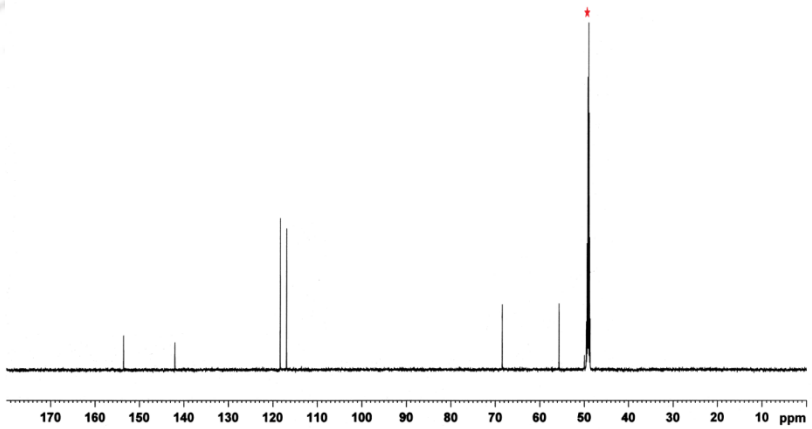

Figure A5.2. ^{13}C-NMR spectrum of receptor **L_4** in CD_3OD at 298 K. Indicated peak represent the solvent.

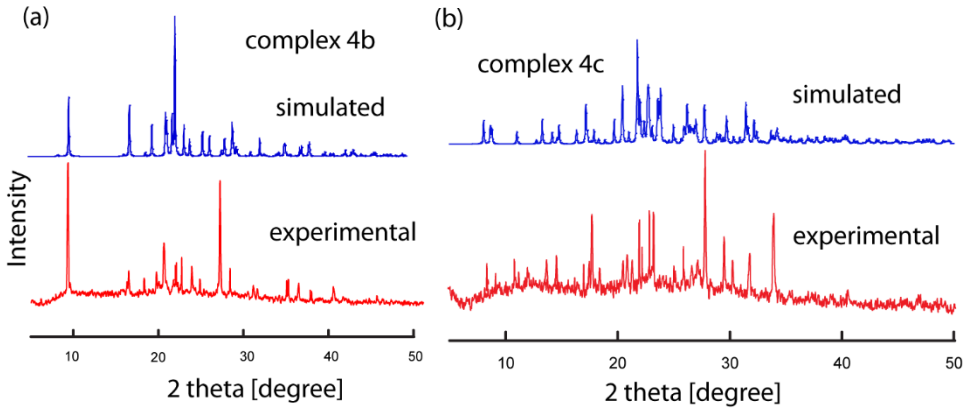

Figure A5.3. (a) Powder X-ray diffraction: simulated pattern from the single crystal X-ray of complex [$\mathbf{L_4}H_4$·4Cl](**4b**) (blue), experimental pattern from the crystalline solid of complex [$\mathbf{L_4}H_4$·4Cl](**4b**) (red). (b) the same for complex **[2$\mathbf{L_4}H_4$·8Cl·5H_2O](4c)**

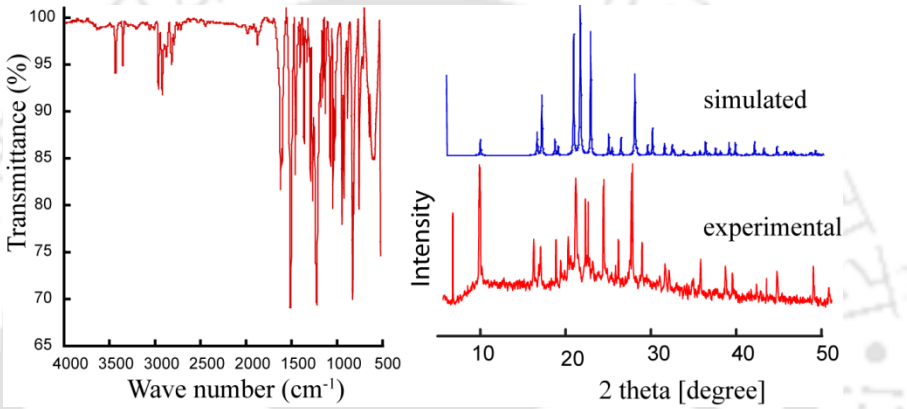

Figure A5.4. FT-IR spectrum of receptor $\mathbf{L_4}$ and powder X-ray diffraction: simulated pattern from the single crystal X-ray of $\mathbf{L_4}$ (blue), experimental pattern from the crystalline solid (red).

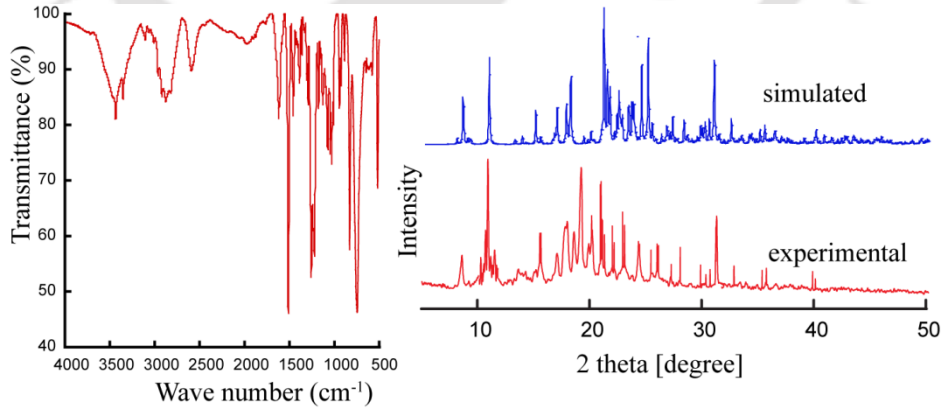

Figure A5.5. FT-IR spectrum of receptor **[$\mathbf{L_4}H_4$·4F·5H_2O](4a)** and powder X-ray diffraction: simulated pattern from the single crystal X-ray of complex **[$\mathbf{L_4}H_4$·4F·5H_2O](4a)** (blue), experimental pattern from the crystalline solid of complex (red).

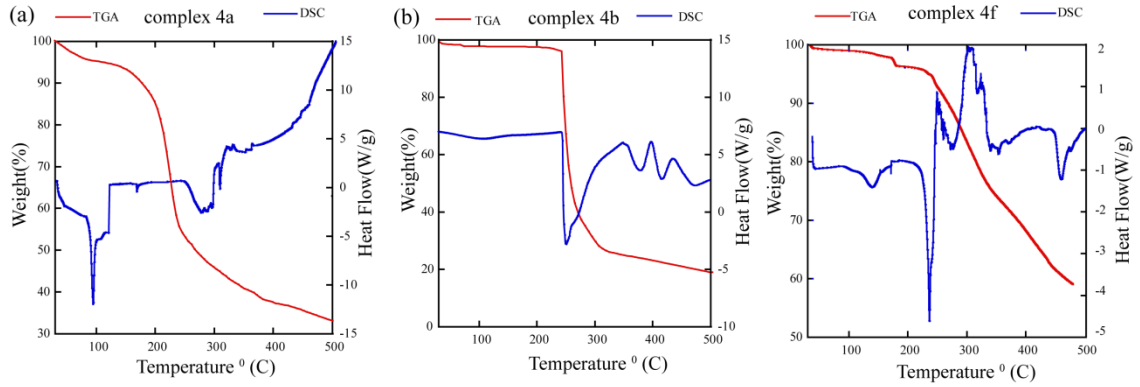

Figure A5.6. Thermogravimetric analysis (TGA) and differential scanning calorimetry curve of (a) **[L_4H_4·4F·5H_2O](4a)**, (b) **[L_4H_4·4Cl](4b)** and (c) **[L_4H_4·4H_2PO_4·H_2O](4f)** at a heating rate of 5 °C per min.

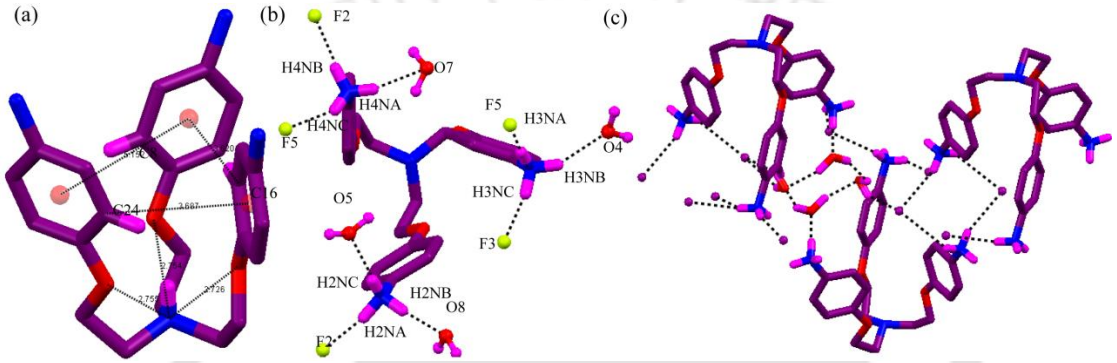

Figure A5.7. (a) (a) Showing N−H···O and C−H···π interactions that stabilized the bowl shaped conformation of the tripodal receptor in protonated receptor. (b) Depicting H-bonding interactions of [NH_3^+] groups with fluoride ions and water molecules in **[L_4H_4·4F·5H_2O](4a)**. (c) Non-capsular assembly of two symmetry independent N1 and N5 unit mediated by several iodide-water H-bonding interactions in complex **[4L_4H_4·16I·7H_2O](4e)**.

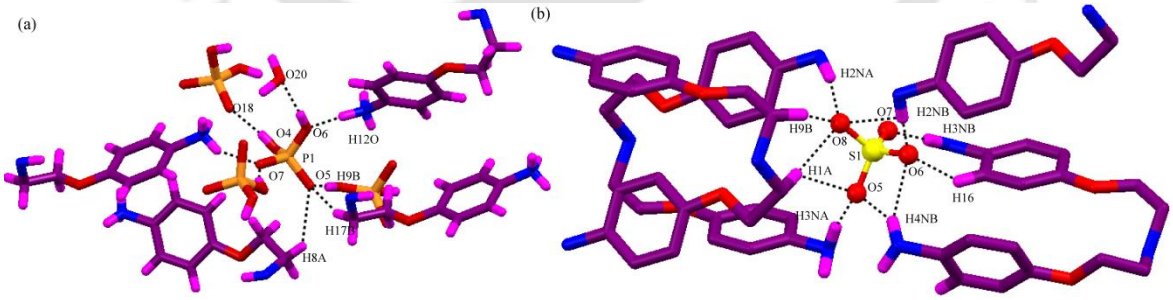

Figure A5.8. (a) Close-up view of the H-bonding interactions of $H_2PO_4^-$ anion with [$L_4H_4^+$] units and water molecule in complex **[L_4H_4·4H_2PO_4·H_2O](4f)**. (b) Close-up view of the H-bonding interactions of SO_4^{2-} anion with [$L_4H_4^+$] units and water molecule in complex **[LH_4·2SO_4·H_2O](4i)**.

Chapter 6

Anion Complexation with Cyanobenzoyl Substituted Tripodal Amide Receptors: A Comparative Study between First and Second Generation Receptor

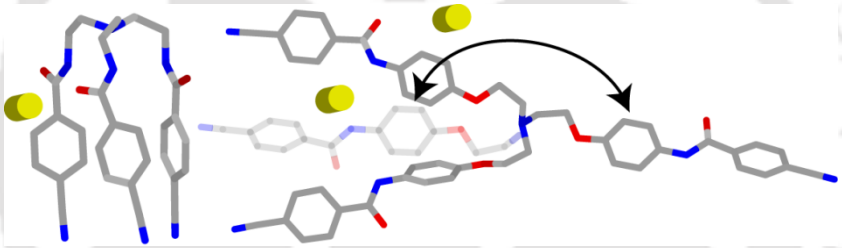

6.1 Back ground and focus on this chapter

Anions are vital species and have widespread use in environmental, biological processes and molecular recognition studies.[1-6] Various artificial systems have been reported to achieve selective molecular recognition and sensing of anions and these system provides a fascinating control in formation of supramolecular assemblies.[7-9] Recognition of anionic species is often accomplished by electrostatic and H-bonding interactions.[10-14] Since beginning of supramolecular chemistry, tris(2-aminoethyl)-amine (tren) is effectively used as a primary building block along with amine, amide and urea functions for variety of anion recognition with high level of satisfaction.[15] Nature often recognizes anion, functionalized with amide as H-bond donors. Therefore, a variety of molecular receptors have been developed containing amide platform that perform recognition of anionic targets by establishing a complementary H-bonds.[16-18] Few amide base receptors containing tren as building block recognize anions through side cleft or capsular binding.[19] Anion complexation and anion induced supramolecular assembly is more challenging as H-bonds formed by anions are weaker that are strongly influenced by external stimuli like pH, nature of guest and solvent.[20] When anions are an inevitable part of supramolecular aggregates, by proper tuning the assembly and disassembly processes can be explored nicely. So it was anticipated that if the anion is changed with other anions it might collapse or re-orient the assembly. Therefore, by varying the geometry of the anions involved in a self-assembly process, it should in principle be possible to re-orient or rupture the self-assembled architectures to form a completely new assembled system. A very promising result reported by P. Ghosh *et.al* shows orientation of all six arms of a benzene capped hexaamide in presence of fluoride forming a dimeric capsular complex. The most astonishing fact is that in presence of acetate ion the conformation of the receptor changed completely and result non-capsular assembly.[21] Most recently we have shown conformational changes in cresol-based tripodal molecules based on anion.[22]

6.2 Structural aspect of anion binding with first (L_5) and second (L_6) generation cyanophenyl substituted tripodal amides

I have synthesized cyanobenzoyl substituted flexible tripodal amides which includes two types receptor, (i) First generation receptor (**L_5**) where tren is used as a simple building block (ii) elongated second generation tripodal (**L_6**) where tri amine (**L_4**, Chapter 5) of a tripodal is used as a building block (**L_6**). Two receptors elegantly exploited for anion complexation and a comparative study of anion binding was carried out in solid and

solution state binding. I also examined the dimensionality and nature of the anions play a crucial role in making various molecular interactions possible in complexation of various anions in both receptors. Most importantly I have noticed that the self-alignment and orientation of the flexible second generation tripodal is greatly influenced by the very specific shape of the anion. The amide functionality have been sent to a distant position which would result bigger cavity and subsequently intimidate the N−H···O=C intramolecular H-bond unlike in **L_5**. In spite of that I am lucky enough to draw fine comparison of recognition anionic guests of different shapes and geometry and solid state organization of the two kind of receptor by just varying the length of the arm. Very especially the reorientation of the receptor **L_6** was observed during recognition of octahedral SiF_6^{2-} anion.

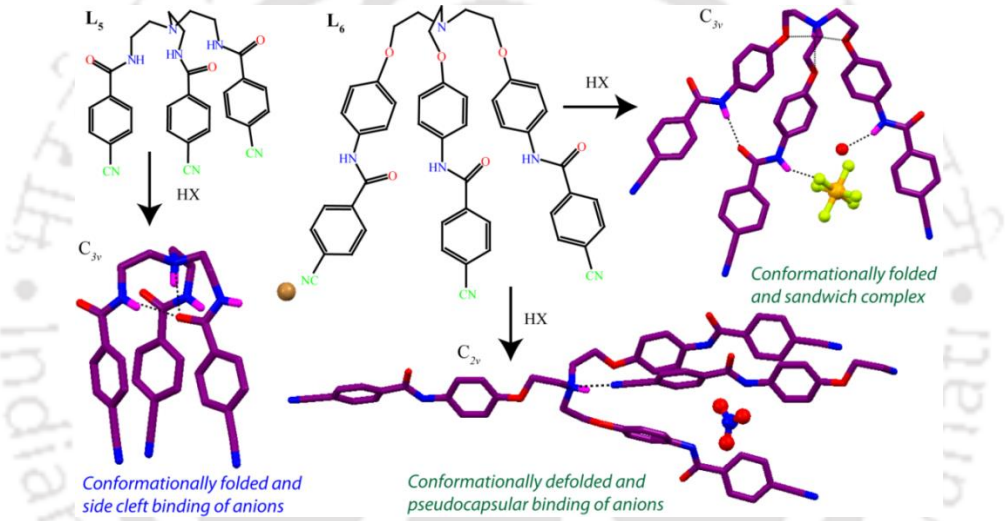

Scheme 6.1 Schematic representation of the receptors and comparison of anion binding.

6.3 Structural description of L_5(5)

The receptor **L_5** crystallizes in monoclinic space group C2/*c*. The receptor contains C_{3v} symmetry and carbonyl group has tendency to stay outwards from the cavity. Among three amide oxygen, O3 of one arm acts as an acceptor and is involved in strong intramolecular H-bond interaction with the donor amide hydrogen H2N which possibly holds the arms together. As a result the receptor is conformationally locked and makes the amide hydrogen unavailable. The amide oxygen O1 is H-bond with amide hydrogen H3N and ortho aromatic hydrogen H15 in cooperative fashions which lead to the centrosymmetric dimer shows in Figure. 6.1a. The oxygen O2 interacts in H4N of the next receptor which finally resulted 1-D assembly of the receptor where they are arranged in up and down fashion showed Figure. 6.1a. These H-bonds including C−H···π firmly held the 1-D

assembly of the receptor. Hence all three amide oxygens form bifurcated H-bonds either with NH or aromatic CH. The average N−H···O and C−H···O distances are 2.976 Å and 3.367 Å which are fairly comparable to previously reported values.[19] Very interestingly two −CN groups (N5 and N7) involved in N···H−C_{ar} H-bond with aromatic hydrogen as well as π···H−C_{ar} by virtue of π-cloud of the −CN group (Figure. 6.1a).

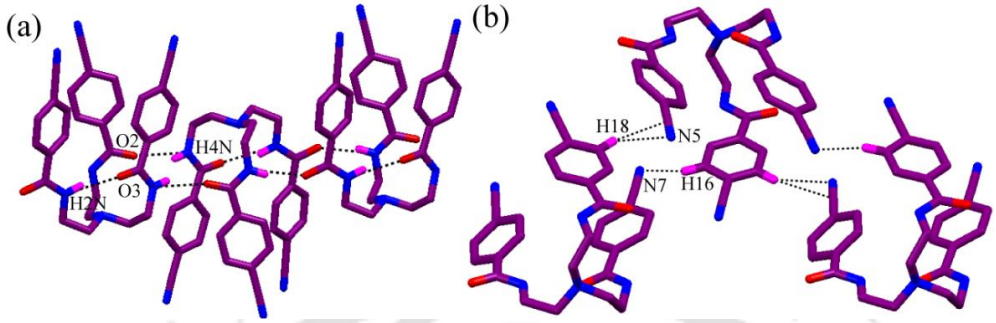

Figure 6.1 (a) Intra and intermolecular N···H−O H-bonded 1-D assembly in receptor $\mathbf{L_5}$. (b) C−H···N and C−H···π interaction of electron rich −CN group.

6.4.1 Structural description of [L_5H·Br](5a)

The tripodal receptor is enriched with H-bond functionalities and anion coordination could be studied. I have extensively studied the coordination of a newly designed substituted tren-based triamide $\mathbf{L_5}$, having cyano functionality with anionic guests of different size and geometry. I treated the receptor in acidic condition and apical nitrogen get protonated to produce anion complexes which will be discussed here. The spherical anion like halide coordination was achieved for what the bromide salt of the ligand was prepared from the reaction of $\mathbf{L_5}$ with HBr in DMF and crystallizes as **5a** in the triclinic space group $P\bar{1}$.

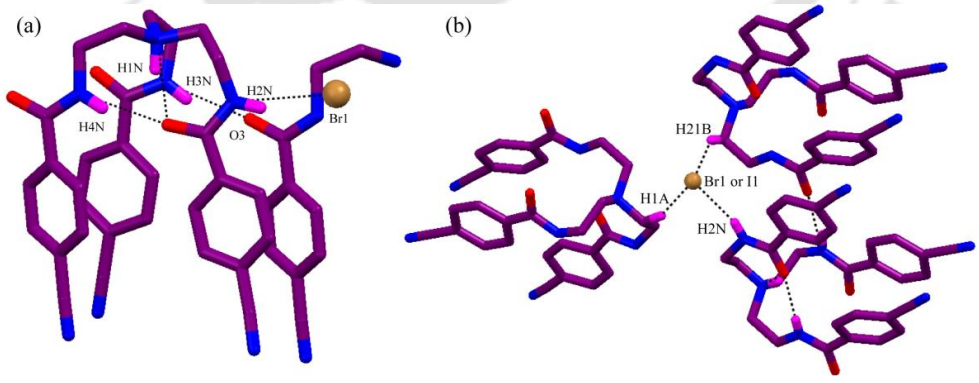

Figure 6.2 (a) (a) Mercury structure depicting the conformation of the protonated receptor and intra and intermolecular H-bonding of amide hydrogen in complex **5a.** (b) Close-up view of three H-bonding interactions with bromide /iodide ion in complex **5a** and **5b**

As expected the apical N-atom is protonated and pointed towards the C_{3v} cavity of the receptor. One of the three amide C=O is directed within cavity is strongly H-bonded with

protonated N-atom (N1···O1 = 2.750(3) Å) which is the main driving force for the generation of anionic complex in acid medium showed in Figure 6.2a. Additionally another intramolecular H-bonding is also observed between the *endo* oriented the carbonyl O1 and amide hydrogen H4N with distance of N4···O1 = 2.878(3) Å. Other two *exo*-oriented O2 and O3 interact with phenyl hydrogen H17 and H15, H3N of next receptors. Though two amide hydrogen are pointed towards C_{3v} symmetric cavity, Br^- ion could not be encapsulated due to the strong intramoleular H-bonds which did not allow the receptor to open to well come bromide ion. As a result, the Br^- ion remains outside the cavity, and is surrounded by three $\mathbf{L_5H^+}$ receptors containing three H-bonding contacts as explained in Figure 6.2b. These are one N–H···Br^- interactions of the amide hydrogen H2N and two contacts *via* C–H···Br^- interactions from methlyene hydrogen H1Aand H21B of the tren moiety. Hence bromide ion in this case is tricoordinated and lie outside of the hydrogen bond donor plane. The packing diagram of the complex **5a** showing various intermolecular H-bonding interactions as viewed down the *b*-axis. Where each layers are well connected through –CN and aromatic CH.–Several short contacts around −CN shows, it interact mainly aromatic ortho CH and methylene CH hydrogen. The presence of Br^- ion inevitably disrupts the formation dimeric interaction between receptors as observed in case of free receptor.

6.4.2 Structural description of $[L_5H{\cdot}I]$(5b)

As a course of anion-receptor interaction, I have also isolated isostructural iodide complex **$[L_5H{\cdot}I]$(3)** of the receptor. The crystal structure analysis shows that inter and intra molecular interaction patter are exactly similar to that of complex **5b**. The conformation of the protonated receptor and coordination environment around I^- ion is similar to complex **5b** (Figure 6.2b). The tricoordinated geometry of halide ion is in good agreement by a reported tripodal triamide.[11] Therefore we have not performed any structural analysis of the complex **5b**.

6.4.3 Structural description of $[(L_5H)_2{\cdot}2NO_3{\cdot}H_2O]$(5c)

Complex **5c** crystallizes in triclinic system and the asymmetric unit contains NO_3^-, one water in complex **5c** along with one protonated receptor $\mathbf{L_5H^+}$. The conformation of the receptor in these case is similar and interaction pattern of amide NH and C=O is also retained here like the other complexes. In complex **5c** NO_3^- is surrounded by two cationic receptors and water molecules providing total seven H-bonds from the contribution of one

N···H–O, two Ow···H–O and four C···H–O contacts as explained in Figure 6.3a. Details inspection reveals that O4 and O6 accept two and one methylene hydrogen H21A, H22B and H11B respectively. O5 of NO_3^- ion is making four contacts *via* one amide hydrogen H4N, one ortho H29 and water O7w molecules. Notably, the crystalline water molecule act as bridging H-bond donors between two NO_3^- ions thus forming a discrete nitrate-water cluster $[(NO_3^-)_2\text{-}(H_2O)]^{4-}$. Two planes containing two water and two nitrate ion bisect each other. The anion-water contacts in the cluster are O7w···O5 = 2.770(2) and 2.880(2) Å. The cluster is surrounded by six $\mathbf{L_5H^+}$ and completely encapsulated in the cavity made of the receptors. Two receptors cover the tetramer cluster from the top and bottom, and four others interact from both sides. It is clear that water O7w is tetracoordinated and H-bonded to H19 and H28 including two NO_3^- ion. The other short contacts coming from –CN group is appeared to be like other complexes.

6.4.3 Structural description of $[L_5H{\cdot}ClO_4]$(5d)

The structural aspects of the perchlorate complex **5d** is strikingly similar to those of the other complexes. In this case, ClO_4^- ion is surrounded by total five cationic tripodal receptors and is coordinated by ten intermolecular H- bonds as highlighted in Figure 6.3b. ClO_4^- ion forms one amide N···H–O, three aromatic C···H–O and six methylene C···H–O contacts reaching a total of ten H-bonds. The oxygen O4 behaves as trifurcated H-bond acceptor from H4N amide NH (N4) and two methylene H21A and H22A. O5 atoms are involved in H-bonding to one aromatic H26 and two methylene hydrogen H11B and H22b. The oxygen O6 offer trifurcated H-bonds and oxygen is connected with one aromatic H16 and two methylene H1A and H11A. O7 is single point H-bonded to aromatic H25.

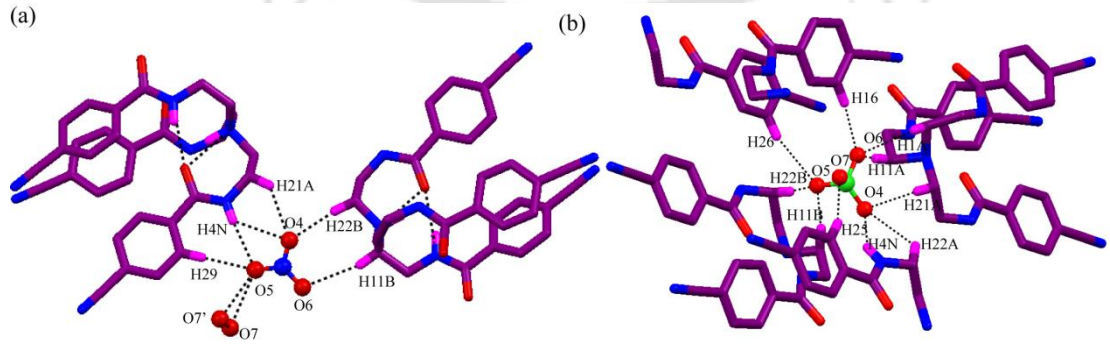

Figure 6.3 (a) Simplified sketch of the seven coordinated NO_3^- ion in complex **5c**. (b) Illustration of the H-bonding around ClO_4^- anion in complex **5d**.

6.5 Structural aspect of anion binding with L_6

The first generation tripodal amide could not encapsulate the anions inside its C_{3v} symmetric cavity, possibly the intramolecular H-bond tightly hold the arms which resists the opening of the arm to encapsulate anions. Hence the intramolecular H-bond kept busy few amide hydrogen and not available for binding of anions at a time. Concomitantly the conformation became very rigid and not suitable for guest encapsulation. Therefore the binding pocket have been moved (amide hydrogen) to make suitable cavity. Keeping mind these possible drawbacks which were great setback in case of first generation, we have decided to enlarge the length of the arm by which the anion binding site shifted to a distant position surely ruled out the close contact between amide NH and CO (hence intramolecular H-bonds) and clearly generate big space. Therefore the bigger cavity may suitably accommodate anionic guests. Crystallization of the receptor **L_6** in neutral medium was unsuccessful like **L_5**, so acidification was carried out which resulted very impressive receptor-anion interaction with of various dimensionality like spherical, planar and tetrahedral.

6.5.1 Structural description of $[4LH{\cdot}4HF_2{\cdot}3H_2O]$(6a)

The fluoride complex **6a** obtained from reaction of **L_6** with HF in plastic vial. The asymmetric unit contains one mono-protonated **L_6H^+**, one HF_2^- ion and two water molecules as crystallization solvent. Crystal structure shows significant change in conformation of the receptor in contrast to first generation tripodal, where one arm of the protonated tripodal receptor is directed opposite to the other two arms. As the receptor is very flexible and can project its arm in various orientations. As expected the anion coordination and other solid state interaction pattern changed dramatically. The apical N-atom is H-bonded with the ethereal oxygen atom (O2 and O3) of two closely connected arms. Very interestingly the arm which is directed opposite to the other two arms is strongly H-bonded with apical NH^+ *via* nitrogen of −CN group forming a pseudo C_{3v} symmetric cavity (Figure. 6.4a). Details structural analysis shows that F1 ion resides around pseudo cavity, is strongly H-bonded by one amide hydrogen H2N, one water O7w and three aromatic hydrogen H5, H11 and H29 as depicted in Figure. 6.4a. Very interestingly we have observed the formation of HF_2^- species on treatment with HF acid. Details structural analysis shows that HF_2^- resides around pseudo cavity, F1 ion is strongly H-bonded to one amide hydrogen H2 and three aromatic hydrogen H5, H11 and H29 as depicted in Figure. 6.4a. There is no more intramolecular H-bond between amide

hydrogen and carbonyl as per our assumption and between two closely connected arms enough space was there that few water molecules had to come and fill up the pseudo cavity through various interactions. The other F2 of HF_2^- also encapsulated in the pseudo cavity and H-bonded with amide hydrogen H7A and two aromatic hydrogen H11 and H46. Stabilization of such kind bifluoride in amide based macrocyclic receptor is also reported by Bowman-James and coworkers.[23] Moreover, a close inspection of the H-bond interaction between carbonyl and CH resulted a dimeric like structure of the receptor where O4 acts as acceptor from H34A and H36. There is no more intramolecular H-bond between amide hydrogen and carbonyl as per our assumption and between two closely connected arms enough space was there that few water molecules had to come and fill up the pseudo cavity through various interactions. Among two crystallized water molecule one half occupied water molecule O7w stays in pseudo cavity and other water molecule O8w remain outside, they show four and six point H-bond with amide and aromatic hydrogen. Moreover, a close inspection of the H-bond interaction between carbonyl and CH resulted a dimeric like structure of the receptor where O4 acts as acceptor from H34A and H36. The progress 1D dimeric assembly with help of cyano group through formation of C−H···N and C−H···π contacts.

6.5.2 Structural description of [L_6H·Br](6b)

The attempt to make other halide complexes also results corresponding anion complexes. The complex **6b** was obtained from the reaction of HBr with $\mathbf{L_6}$. Due to very poor crystal data chloride and iodide complex can't be reported. Though roughly we could see from these structure, conformation of the receptor remains same as in fluoride complex **6b**, only difference is that they contains solvent water or DMF molecules as crystallizing solvent. Very interestingly we noticed that chloride, bromide and iodide complexes are isostructural though fluoride complex **6b** does not belong to this category. A sharp difference in orientation one amide hydrogen H3N of two closely connected arms was observed compared to complex **6b** and remains outside of the pseudo cavity, whereas in complex **6b** such hydrogen pointed towards the cavity. As a consequence, solid states interactions changed noticeably. In case of bromide complex we could not assign the solvent molecules, hence PLATON/SQUEEZE was performed to refine the receptor along with the bromide ion (1.5 Br ion) by excluding the disordered solvent electron densities. These calculations amount to 554 electrons per unit cell or 98 electrons per molecule and may be attributed to two water and two DMF molecules. Proton NMR study and

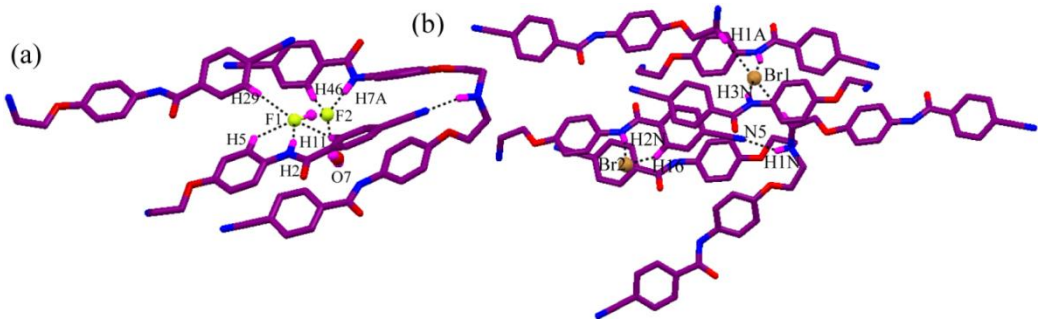

Figure 6.4 (a) Crystal structure of complex **6a** depicting the interaction of amide hydrogen with fluoride and water molecule and formation of pseudo capsular cavity. (b) Illustration of various H-bonding interactions around bromide in complex **6b**. interactions changed noticeably.

thermogravimetric analysis (TGA) (Figure A6.10.a) of the crystals further supports the crystallographic assignment. Solid state structure indicates the distant arm is H-bonded with protonated N-atom through cyano group forming a pseudo cavity similar to fluoride complex **6a**. Interaction of Br1 in Figure 6.4b shows it is tetra coordinated and all four donor atoms lie on a perfect square geometry. Br1 accept hydrogen from two symmetric amide H3N and methylene H1A. The other half occupied Br2 ion is H-bonded with amide hydrogen H2N and ortho aromatic hydrogen H16. The contacts around bromide ion fall in the range of 3.471(2)-3.808(2) Å. Close contact between receptors through cyano N7 and methylene hydrogen H33A which connects two layer of pseudo capsular assembly.

6.5.3 Structural description of $[L_6H{\cdot}NO_3{\cdot}H_2O]$(6c)

Now we have investigated receptor-anion interaction by taking planar NO_3^- ion. Treatment of $\mathbf{L_6}$ with HNO_3 resulted the complex **6c** where one mono protonated $\mathbf{L_6H^+}$, one NO_3^- and two water crystallization is present in an asymmetric unit. The conformation of the receptor is similar to fluoride complex **6a**. Single-crystal X-ray analysis of complex **6c** revealed that the distant arm is H-bond with apical N-atom through cyano group making a pseudo capsular cavity like others and amide hydrogen of two closely connected arms are pointed towards the cavity unlike bromide complex **6b**. As we see in Figure 6.5a cationic tripodal. In this case NO_3^- is eleven coordinated arising from two amide N–H···O, four aromatic C–H···O one water Ow–H···O and one anion···π (π cloud of –CN). The nitrate oxygen O6 is involved in strong H-bond with H4N and O9w, and moderate C–H···O interaction with the aromatic hydrogen H27 and H43 whereas O8 is in interaction with the amide H3N and aromatic H30, H37 and H43 suggesting that each O6 and O8 behaves as tetrafurcated H-bond acceptors in the anion complex. In addition to the above eight interactions, nitrate oxygen O7 is engaged in H-bonding interaction with amide H4N

and the aromatic hydrogen H30 including interesting anion···π interaction coming from π enriched –CN group (N5). The bond distances around NO_3^- ion fall in the range of 2.587(3)- 3.630(4) Å. The water molecule O9w is H-bonded with another NO_3^- ion forming a nitrate-water cluster $[(NO_3^-)_2\text{-}H_2O]^{2-}$. As we see in Figure 6.5a the NO_3^- is situated in the pseudo cavity and surrounded by total four arms of three cationic tripodal.

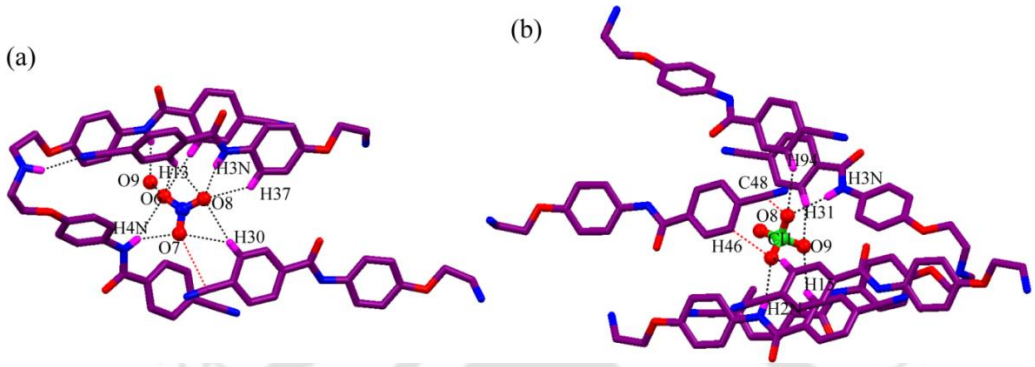

Figure 6.5 (a) Illustration of various H-bonding interactions around NO_3^- in complex **6c**. (b) Partial view of the eight coordinated ClO_4^- ion in complex **6d**. The red contact implies Anion···π interaction (π electron of −CN).

The nitrate-water cluster is completely confined within the void created by the receptors and passed through two pseudo capsular cavity. The water O9w accepts two amide hydrogen H2N giving tetracoordinated nearly planar geometry. The other water molecule O10w show similar geometry by interacting with methylene hydrogen H2B and carbonyl oxygen O3. One carbonyl oxygen O3 of the folded tripodal arm is H-bonded with aromatic and methylene hydrogen H4 and H2A form a dimeric interaction between two receptors like fluoride complex **6a**. The dimer is self-organized *via* C–H···O/N (carbonyl and cyano) H-bonds between different aromatic and methylene hydrogen atoms.

6.5.4 Structural description of $[L_6H{\cdot}ClO_4]$(6d)

The anion complex of the receptor with tetrahedral oxyanion like perchlorate was crystalizes with disordered DMF-water molecules. These electron densities were moved during refinement and the count of electron removed in total was 226 per two symmetry independent molecules which account for five DMF and three water molecules and further verified by TGA experiment of the crystal of complex **6d**. Similar mode of conformational adaptability has been obtained in complex **6d** (Figure A6.10.b). The perchlorate anion occupies the pseudocavity generated by three arms of two receptors. The symmetrically non-equivalent ClO_4^- ions involving chlorine atoms Cl(1) and Cl(2) are H-bonded with six

arms of five tripodal receptors and four arms of three tripodal receptors respectively (Figure 6.5b). $Cl(1)O_4^-$ and $Cl(2)O_4^-$ ion shows eight and seven coordination respectively. Perchlorate oxygen O8 acts as bifurcated H-bond acceptor with amide and aromatic hydrogen H3N and H94 including one interesting anion···π interaction between $Cl(1)O_4^-$ and π cloud of electron rich –CN group, whereas O9 behaves as bifurcated H-bond acceptor by interacting with two aromatic protons H31 and H15. O10 behaves as trifurcated H-bond by accepting amide and aromatic hydrogen H2N and H12, H15 finally satisfying eight coordination. The details contacts parameters are given in Table 1. The overall non-covalent interactions result in the formation assembly of receptors stitching the adjacent arrays by C–H···O/N (carbonyl and –CN group) H-bonds.

6.5.5 Structural description of $[(L_6H)_2{\cdot}SIF_6{\cdot}4H_2O{\cdot}2DMF]$(6e)

Anion specific conformational adaptability of the second generation tripodal amide

The elongated tripodal receptor **L_6** shows a dramatic conformational change in presence of only octahedral SiF_6^{2-} anion. Conformation of the receptor with anion is very similar for spherical, trigonal planar and tetrahedral anions. When the receptor is treated with HF in glass vial, it gave the hexafluoro silicate complex **$[(L_6H)_2{\cdot}SIF_6{\cdot}4H_2O{\cdot}2DMF]$(6e)**. The X-ray structure indicates the asymmetric contains one mono protonated **L_6H^+**, one-half hexafluoro silicate anion, two water and one DMF molecule as crystallizing solvent. The intramolecular H-bonding interactions are different than those observed in other complexes of the **L_6** receptor. In this case, the *endo* orientaed hydrogen is internally bonded with three ethereal oxygen atoms with average N···O = 2.7 Å distance. These H-bonding interactions actually organize the three flexible arms in one direction showing dramatic change in conformation of the receptor from scattered orientation as shown in Figure 6.6a. This structure is very similar to our previously reported nitro-phenyl appended second generation tripodal amide.[27] Where we had showed solvent induced binding discrepancy of SiF_6^{2-} anion. In other communication we had structurally authenticated for the conformational changes in cresol-based tripodal receptor, based onanion specificity.[22] Here we have shown the elongated flexible tripodal amide in presence of only SiF_6^{2-} anion completely folded and stabilize the anion through formation of a sandwitch type complex in side cleft binding mode as depicted in Figure 6.6b. Though all three arms are in same direction, the protonated receptor is not able to create a suitable cavity to encapsulate the anion. Only two arms from each receptor interaction with SiF_6^{2-},

the third arm forms H-bonds with the oxygen atom of a carbonyl group of the next side arm of the same receptor. The binding of SiF_6^{2-} clearly demonstrates that the anion in complex **6e** is located outside the tripodal cavity and stabilized by mainly N–H···F and

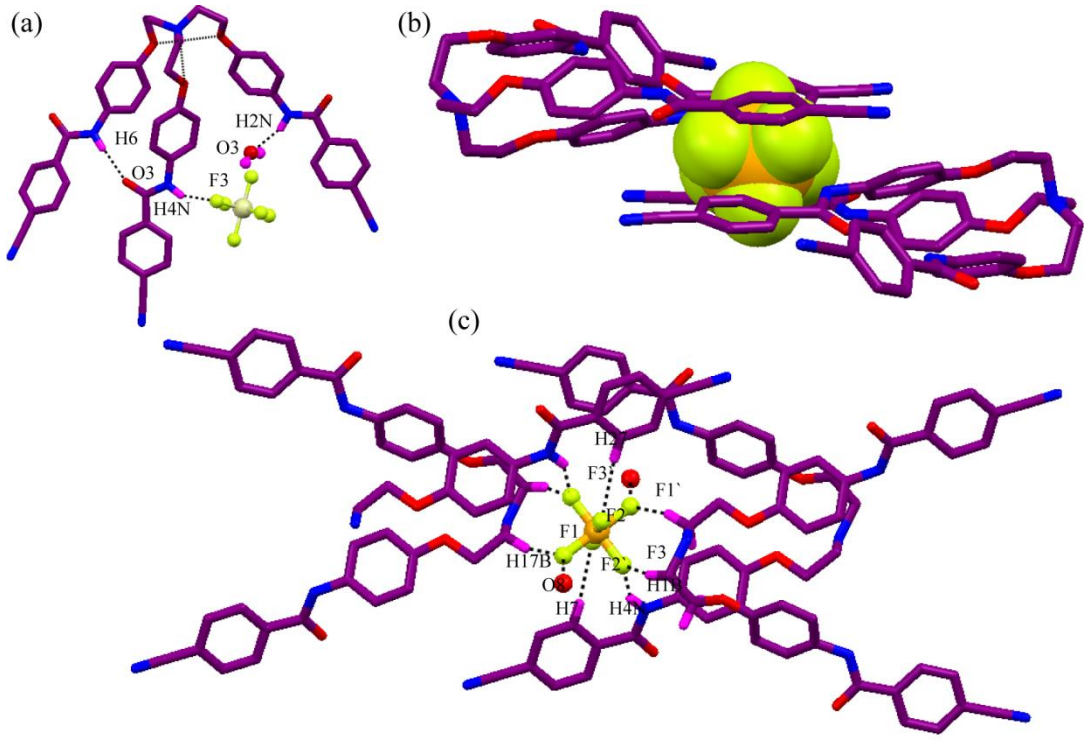

Figure 6.6 (a) C_{3v} symmetric folded conformation of $\mathbf{L_6}$ induced by SiF_6^{2-} anion in complex **6e**. (b) Sandwich type complex formation in solid state. (c) Coordination environment of SiF_6^{2-} anion.

C–H···F H-bonds from the four receptors with addition Ow–H···F from two water molecules as depicted in Figure 6.6c. The complete coordination environment of SiF_6^{2-} suggests that it is stabilized *via* ten H-bonding. The fluorine atom F1 is H-bonded one water molecule O8w and methylene hydrogen H17B, whereas fluorine atoms F2 is making single point contact aromatic hydrogen H27, F3 is in interaction with amide hydrogen H4N and methylene hydrogen H1B. The other three fluorine atoms are symmetry equivalent, having similar contact point resulting overall in ten H-bonding contacts on SiF_6^{2-} anion. Therefore number of H-bonds around SiF_6^{2-} is low compared to our tripodal amide receptor, though twelve coordinated SiF_6^{2-} anion by tripodal urea and amine receptor is reported.[24, 25] The short contacts around –CN group is quite different than that observed in the other complexes of $\mathbf{L_6}$. π electron cloud of the –CN group does not participate any contacts unlike the other complex. Only one –CN (N7) group participate in H-bonding with aromatic hydrogen H12, while two are reluctant to form any contacts.

6.6 Anion binding studies in solution by ^{1}H NMR spectroscopy

The interesting solid state chemistry of the acidic amide protons also insists us to investigate its solution phase interaction with various guest anions. For this, the respective solution of anions was added sequentially to the DMSO solution of the receptors (DMSO is chosen for the solubility purpose) and the changes in the protons frequencies are recorded at room temperature. The maximum shift is observed for the fluoride among the halides (Cl^-, Br^- and I^-) while it is the dihydrogen phosphate which dominates among the oxyanions like NO_3^- and ClO_4^-. Again between the two amide based receptors, **L_6** interacts in an effective way than **L_5** as greater shift of NH hydrogen is observed in **L_6** (**Figure A6.11.** and **A6.12.**) which is probably due to the presence of more acidic amide NH in this receptor.

The amide NH of **L_5** is shifted downfield upon addition of fluoride solution while aromatic CHs are splited and moved into opposite directions (**Figure A6.13.**). This could be explained on the basis of two different effects of the hydrogen bonding interactions between the guest anions and the receptor on the aromatic CH: first, the increases in electron density on the aromatic ring through-bond propagation induces a shielding effect; secondly, the increase of polarization of the C–H bonds through space which creates a positive charge on the aromatic hydrogen caused deshielding.[42] Thus, it must be the ortho-CH (CHa), next to the NH which experiences a through space polarization effect and moved to downfield region and as the CH(b) is far away from the amide hydrogen, it experiences a upfield shift due to the through bond charge propagation associated with the hydrogen bonded complex. The strong involvement of the amide NH is reflected in the ppm *vs* equv plot which recorded a huge downfield shift of 3.014 ppm after 8 equv. of fluoride solution. At this stage, CHa is shifted to 0.43 downfield and CHb to 0.117 upfield. Another basic anion $H_2PO_4^-$, however interacts weakly with the receptor **L_5** and after 3 equv. of the aforesaid anion, the NHa is shifted 0.183 ppm downfield. Again, the changes with the anions such as Cl^-, Br^-, NO_3^- etc are negligible.

Deprotonation of NH protons is also observed for **L_6** in presence of fluoride anion. However as shown in **Figure A6.14.**, all other aromatic CHs are also on moved with the escalating the concentration of the aforesaid anion solution. The H_b and H_c are shifted downfield (Δ ppm Hb = 0.028, Δ ppm Hc = 0.126) while H_a and H_d (Δ ppm Ha = 0.073, Δ ppm Hd = 0.08) which are far away from the amide NH are shifted upfield. Thus the first set of protons which are pointed in the same direction of the amide NH are definitely

polarized through space interaction by the guest fluoride anion and that is why they are shifted to downfield. And due to the formation of the same negatively charged species the second set of protons are upfield shifted. first set of protons which are pointed in the same direction of the amide NH are definitely polarized through space interaction However, after excess addition of fluoride we also did not observe the characteristic HF_2^- peak at downfield region. This is probably due to the lower stability of the HF_2^- species in the solution.[43] Again with $H_2PO_4^-$ anion, the NH_a is shifted to 0.276 ppm downfield and the aromatic CHs interacts in the same fashion (Δ ppm H_a = -0.034, Δ ppm H_b = 0.026, Δ ppm H_c = 0.039 and Δ ppm H_d = -0.027). Again, the changes with the anions such as Cl^-, Br^-, NO_3^- etc are negligible.

Conclusions

In summary, we have synthesized cyanobenzoyl substituted two tripodal amide receptors of having different length and successfully exploited their high potential towards anion recognition of various dimensionalities. The C_{3v} symmetric first generation tripodal **L_5** remains as locked conformation in free and protonated states through intramolecular N−H···O H-bond. This incur encapsulation of anions irrespective of size, shape and charge, therefore anion recognition take place through side cleft binding fashion only. Then we have applied a synthesis stagey to cancel intramolecular H-bond, where cyanobenzoyl was appended from a bigger platform like triphenyl amine to give second generation tripodal **L_6**. Such modification resulted three major advantages like (i) the possibility of making C_{3v} symmetric cavity for anion encapsulation as the H-bonding between apical N-atom and ethereal O-atom could be able to hold three arms tightly, (ii) ruled out the intramolecular N−H···O H-bond which make amide hydrogen ready for anions and (iii) produced larger space for anion recognition. Though the crystal structure of the anion complexes shows close vicinity of two arms, while the other projected in the opposite direction. In the protonated state one arm is H-bonded with apical N-atom through –CN group forming pseudo capsular cavity. The anions remain in the pseudo cavity and H-bonded with one or more amide hydrogen. The most appealing feature of the **L_6** is that selective anion induced reorganization resulted change in conformation from open C_{2v} symmetry to folded C_{3v} in presence of only SiF_6^{2-} anion and forms a sandwich type complex. Two neutral receptors interact with fluoride ion strongly among the halide ions as very large chemical shift of amide hydrogen observed. Though the receptors are reluctant to bind with oxyanion strongly except relatively better amide hydrogen shift by

$H_2PO_4^-$ in both receptors. It is also clear form solution studies that anion interacts with **L_6** to a greater extent than **L_5**. This phenomena is further validated by its solid state anion binding as the number of H-bond around anions in **L_6** is apparently higher than in **L_5**.

References

1. Ayoob. S.; Gupta, A. K. *Crit. Rev. Environ. Sci. Technol*. **2006**, *36*, 433.
2. USEPA, *Perchlorate environmental contamination: Toxicological review and risk characterization*. External review draft. NCEA-1-0503, Washington, DC, **2002**.
3. Sessler, J. L.; Gale, P. A.; Cho, W.-S. *Anion Receptor Chemistry*, Cambridge, **2006**.
4. Gale, P. A.; García-Garrido, S. E.; Garric, J. *Chem. Soc. Rev*. **2008**, *37*, 151.
5. Götz, R. J.; Robertazzi, A.; Mutikainen, I.; Turpeinen, U.; Gamez P.; Reedijk, J. *Chem. Commun*. **2008**, 3384.
6. Bowman-James, K. *Acc. Chem. Res*. **2005**, *38*, 671.
7. Santos-Figueroa' L. E.; Moragues, M. E.; Climent, E.; Agostini, A. Martínez-Máñez, R.; Sancenón, F. *Chem. Soc. Rev*. **2013**, *42*, 3489.
8. Rais, D.; Yau, J.; Mingos, D. M. P.; Vilar, R.; White, A. J. P.; Williams, D. J. *Angew. Chem., Int. Ed*. **2001**, *40*, 3464.
9. Gimeno, N.; Vilar, R. *Coord. Chem. Rev*. **2006**, *250*, 3161.
10. Hossain, M. A.; Liljegren, J. A.; Powell, D.; Bowman-James, K. *Inorg. Chem.* **2004**, *43*, 3751.
11. Lakshminarayanan, P. S.; Suresh, E.; Ghosh, P. *Inorg. Chem.* **2004**, *45*, 4372.
12. Kang, S. O.; Hossain, M. A.; Powell, D.; Bowman-James, K. *Chem. Commun*. **2005**, 328.
13. Saeed, M. A.; Thompson, J. J.; Fronczek, F. R.; Hossain, M. A. *CrystEngComm*., **2010**, *12*, 674.
14. Dey, S. K.; Ojha, B.; Das, G. *CrystEngComm*. **2011**, *13*, 269.
15. Dutta, R.; Ghosh, P. *Chem. Commun*. **2014**, *50*, 10538.
16. Llinares, J. M.; Powell, D.; Bowman-James, K. *Coord. Chem. Rev*. **2014**, *240*, 57.
17. Schottel, B. L.; Chifotides, H. T.; Dunbar, K. R. *Chem. Soc. Rev*. **2008**, *37*, 68.
18. Garcia-Espana, E.; Díaz, P.; Llinares J. M.; Bianchi, A. *Coord. Chem. Rev*. **2006**, *250*, 2952.
19. Ravikumar, I.; Lakshminarayanan, P. S.; Ghosh, P. *Inorganica Chimica Acta*. **2010**, *363*, 2886.
20. Lehn, J. M. *Supramolecular Chemistry Concepts and Perspectives*, VCH, Weinheim, **1995**.
21. Arunachalam, M. Ghosh, P. *Chem. Commun*. **2011**, *47*, 6269.
22. Dey, S. K.; Pramanik, A.; Das, G. *CrystEngComm*. **2011**, *13*, 1664.
23. Kang, S. O.; Powell, D. R.; Day, V. W.; Bowman-James, K. *Angew. Chem. Int. Ed.*, **2006**, *45*, 1921.
24. Van der Sluis, P.; Spek, A. L. *Acta Crystallogr., Sect. A*: *Found. Crystallogr*. **1990**, *46*, 194.
25. Ward, Jr. K. *J. Am. Chem. Soc*. **1935**, *57*, 914.

Annexure VI

Table 6.1a Crystallographic parameters and refinement details.

code name	L_5(5)	[L_5H·Br] (5a)	[L_5H·I] 5b)	[L_5H·NO_3·H_2O] (5c)	[L_5H·ClO_4] (5d)
empirical formula	$C_{30}H_{27}N_7O_3$	$C_{30}H_{28}N_7O_3Br$	$C_{30}H_{28}N_7O_3I$	$C_{30}H_{30}N_8O_7$	$C_{30}H_{28}$ N_7O_7Cl
formula weight	533.59	614.49	661.49	614.60	634.04
cryst syst	monoclinic	triclinic	triclinic	triclinic	triclinic
a (Å)	19.7331(5)	7.6711(5)	7.7036(7)	7.7878(5)	7.7883(13)
b (Å)	14.8638(5)	11.9923(9)	12.0659(11)	11.9857(8)	12.119(2)
c (Å)	19.2351(6)	16.3251(11)	16.4604(14)	16.6759(12)	16.814(3)
α (degree)	90.00	71.874(5)	72.706(5)	71.155(4)	73.176(10)
β (degree)	100.017(2)	85.255(5)	84.786(5)	84.920(4)	84.484(9)
γ (degree)	90.00	87.127(5)	86.852(5)	88.018(4)	86.573(11)
V ($Å^3$)	5555.8(3)	1421.92(17)	1454.2(2)	1467.31(17)	1511.2(5)
space group	*C 2/c*	*P -1*	*P -1*	*P -1*	P -1
Z value	8	2	2	2	2
ρ(cal)(g/cm^3)	1.276	1.435	1.511	1.387	1.393
μ(Mo Kα) (mm^{-1})	0.086	1.490	1.145	0.102	0.186
T(K)	298(2)	298(2)	298(2)	298(2)	298(2)
R1; wR2 (I> 2 σ(I))	0.0531, 0.1301	0.0421, 0.0766	0.0583, 0.1199	0.0759, 0.2365	
R1; wR2(all)	0.1086, 0.1557	0.0821, 0.0875	0.1314, 0.1429	0.1114, 0.2697	0.0832, 0.2649
Residual electron density(e/Å)	0.164/-0.245	0.312/-0.395	1.149/-1.186	0.548/-0.504	0.1324, 0.3068
good-of-fit	1.015	0.990	0.908	1.087	1.096
reflection collected	3510	3629	3466	3199	4410
Independent reflection	6812	5801	6798	5627	7453

Table 6.1b Crystallographic parameters and refinement details.

code name	4LH·4HF_2·3H_2O(6a)	L_6H·Br (6b)	L_6H·NO_3·H_2O (6c)	L_6H·ClO_4 (6d)	($L_6H)_2$·SiF_6·4$H_2$0·2 DMF (6e)
empirical formula	$C_{192}H_{172}F_8N_{28}O_{27}$	$C_{48}H_{40}$ N_7O_6Br	$C_{48}H_{42}N_8O_{10}$	$C_{48}H_{40}$ $N_7O_{10}Cl$	$C_{102}H_{94}F_6N_{16}O_{18}Si$
formula weight	3455.58	890.77	890.88	910.32	1974.02
cryst syst	monoclinic	triclinic	monoclinic	monoclinic	triclinic
a (Å)	28.7467(16)	9.4588(5)	16.7671(5)	15.9320(10)	13.0320(8)
b (Å)	18.6826(16)	13.6915(7)	18.6175(5)	18.5172(6)	13.7659(9)
c (Å)	16.7739(11)	20.4866(10)	28.0023(10)	36.597(2)	15.5660(11)
α (°)	90.00	91.493(3)	90.00	90.00	99.496(5)
β (°)	111.627(4)	94.733(2)	102.197(3)	98.905(6)	108.367(5)
γ (°)	90.00	103.295(2)	90.00	90.00	101.296(5)
V ($Å^3$)	8374.5(10)	2570.4(2)	8543.9(5)	10666.6(10)	2520.6(3)
space group	C 2/c	*P -1*	*I 2/c*	*P 21/a*	*P -1*
Z value	2	2	8	8	1
ρ(cal)(g/cm^3)	1.370	1.151	1.382	1.134	1.301
μ(Mo Kα) (mm^{-1})	0.099	0.849	0.099	0.129	0.109
T(K)	298(2)	298(2)	298(2)	298(2)	298(2)
R1; wR2 (I> 2 σ(I))	0.0519, 0.1892	0.0573, 0.1704	0.0710, 0.2730	0.0977, 0.2061	
R1; wR2(all)	0.0859	0.0874, 0.1852	0.1101, 0.3148	0.2438, 0.2866	0.0744, 0.1883
Residual electron density(e/Å)	0.31/ -0.27	1.435/-0.322	0.373/-0.383	0.436/-0.220	0.1969, 0.2404
good-of-fit	1.158	1.031	1.093	0.987	1.040
reflection collected	4867	7346	5935	15793	6677
Independent reflection	8756	13138	10907	27403	10949
CCDC No.	1041361	1041362	1041363	1041364	1041365

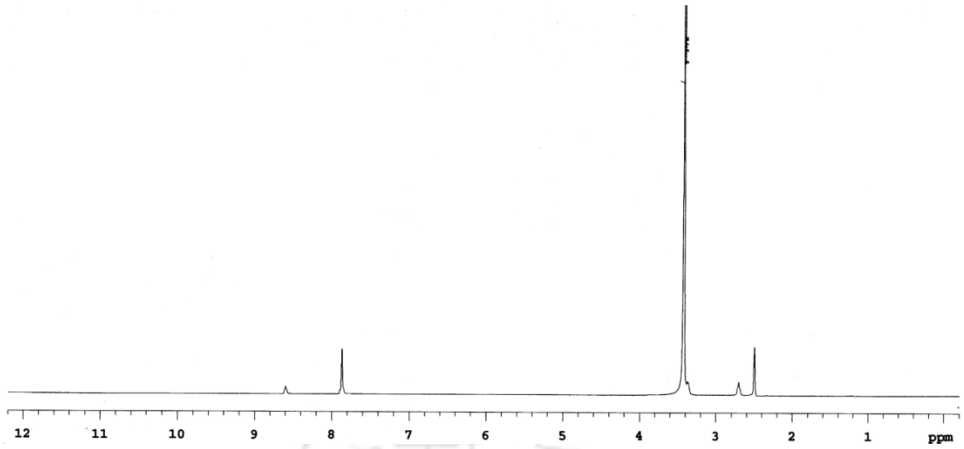

Figure A6.1. ^{1}H NMR spectrum of receptor $\mathbf{L_5}$ in DMSO-d_6 at 298 K.

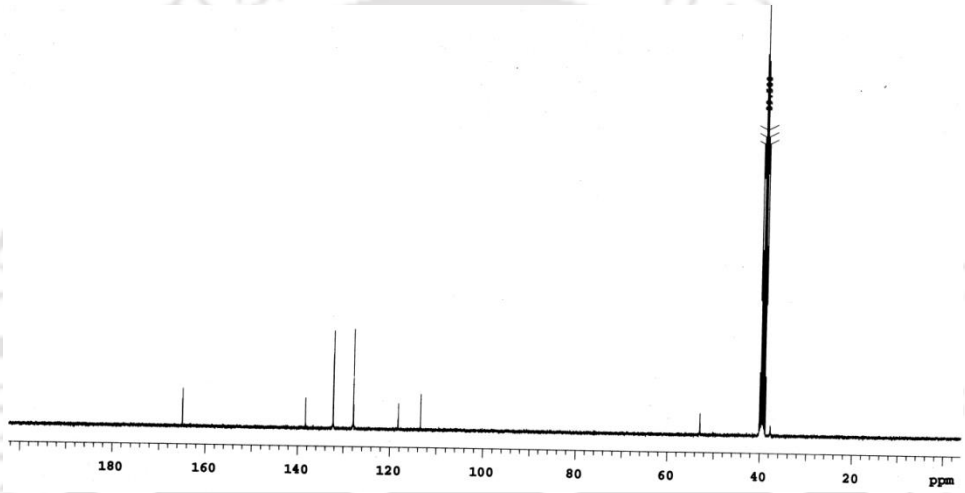

Figure A6.2. ^{13}C NMR spectrum of receptor $\mathbf{L_5}$ in DMSO-d_6 at 298 K.

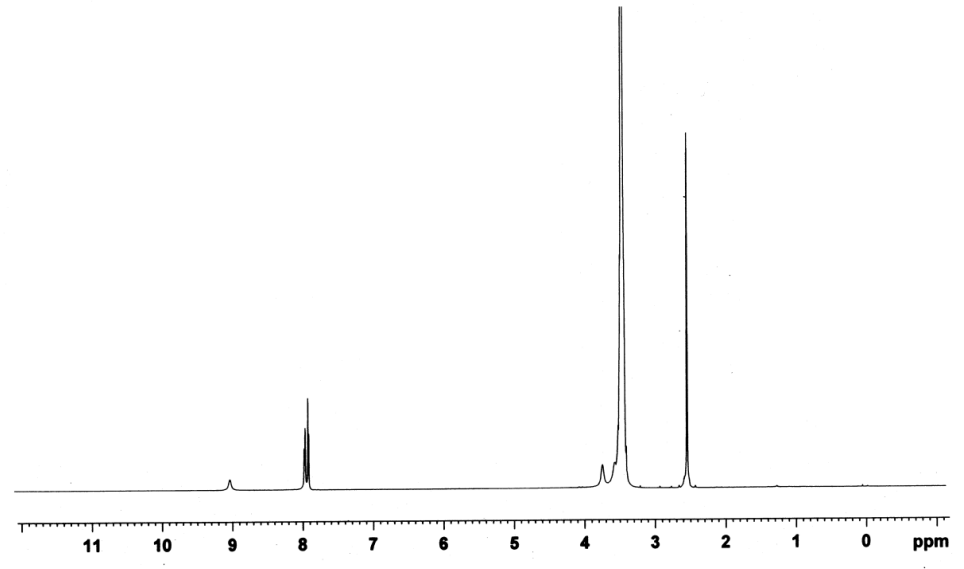

Figure A6.3 ^{1}H NMR spectrum of receptor **[$\mathbf{L_1H}$·Br](2)** in DMSO-d_6 at 298 K.

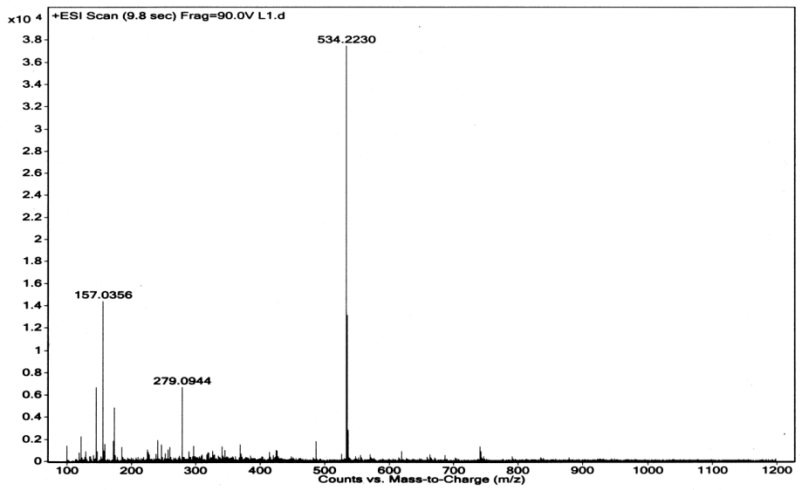

Figure A6.4. ESI mass spectra of $\mathbf{L_5}$.

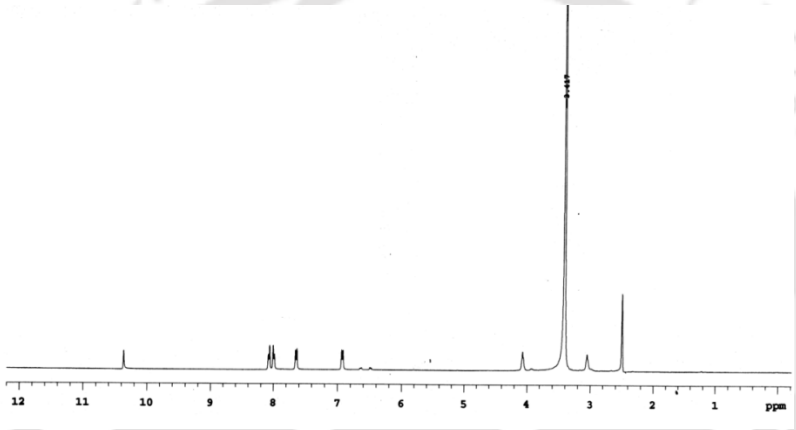

Figure A6.5. ^{1}H NMR spectrum of receptor $\mathbf{L_6}$ in DMSO-d_6 at 298 K.

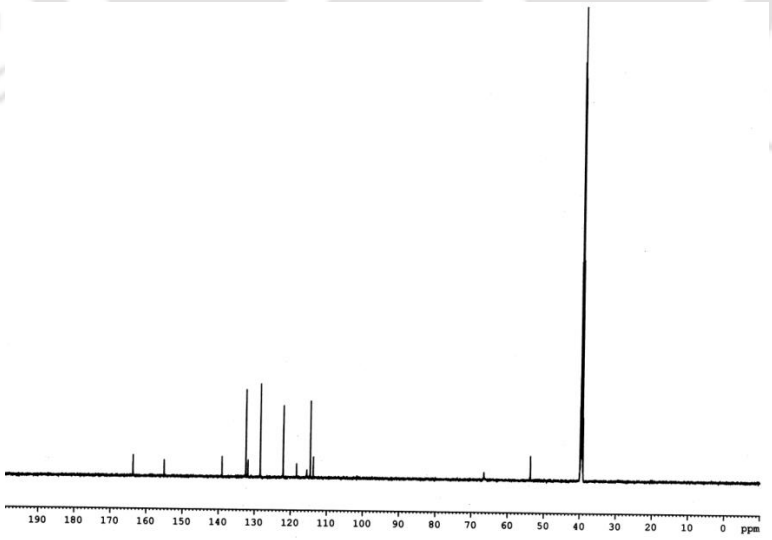

Figure A6.6. ^{13}C NMR spectrum of receptor $\mathbf{L_6}$ in DMSO-d_6 at 298 K.

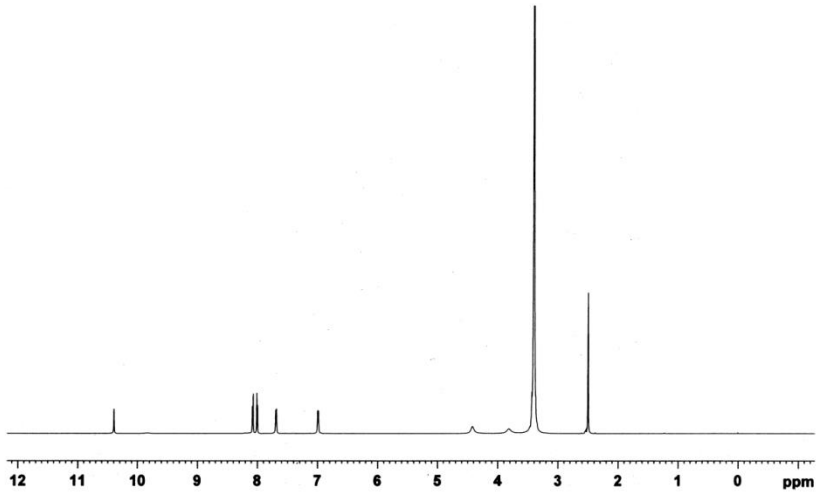

Figure A6.7. ^{1}H NMR spectrum of receptor **[L_2H·F·2$H_2$0](6)** in DMSO-d_6 at 298 K.

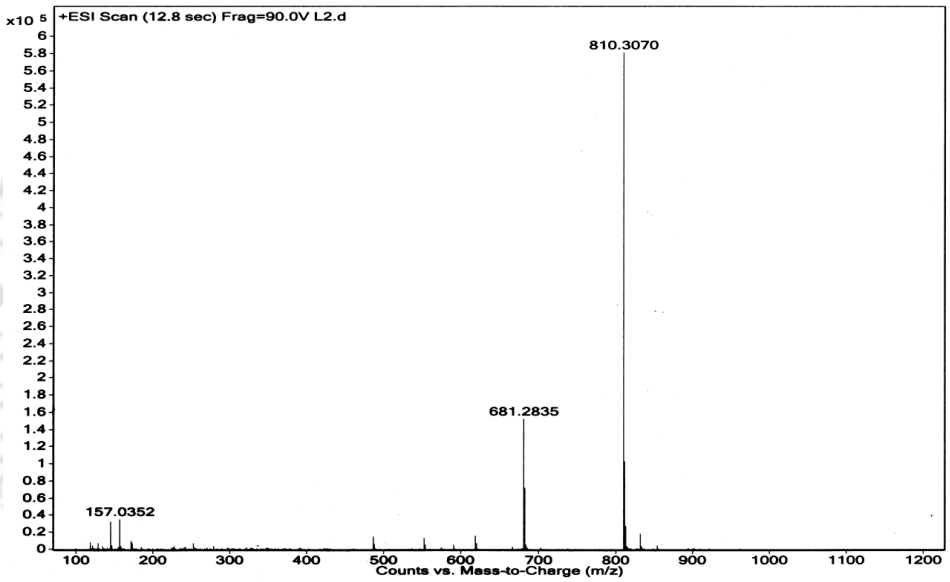

Figure A6.8. ESI mass spectra of receptor $\mathbf{L_6}$.

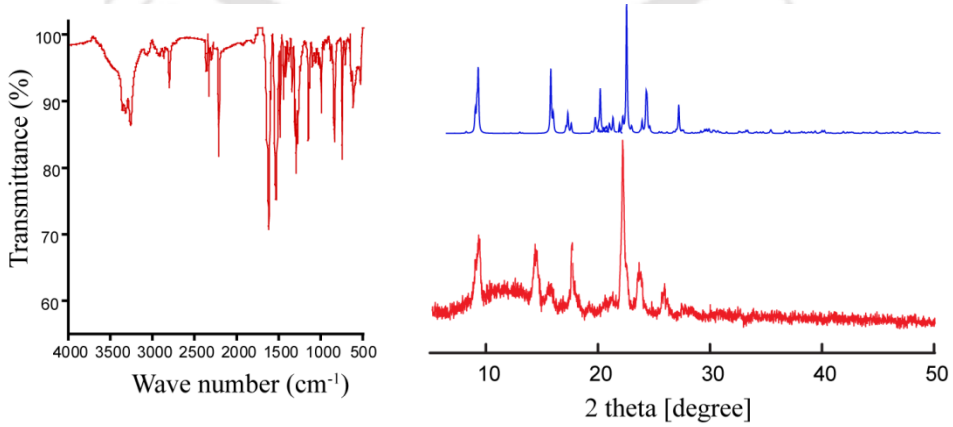

Figure A6.9. FT-IR spectrum of receptor $\mathbf{L_5}$ and powder X-ray diffraction: simulated pattern from the single crystal X-ray of $\mathbf{L_5}$ (blue), experimental pattern from the crystalline solid (red).

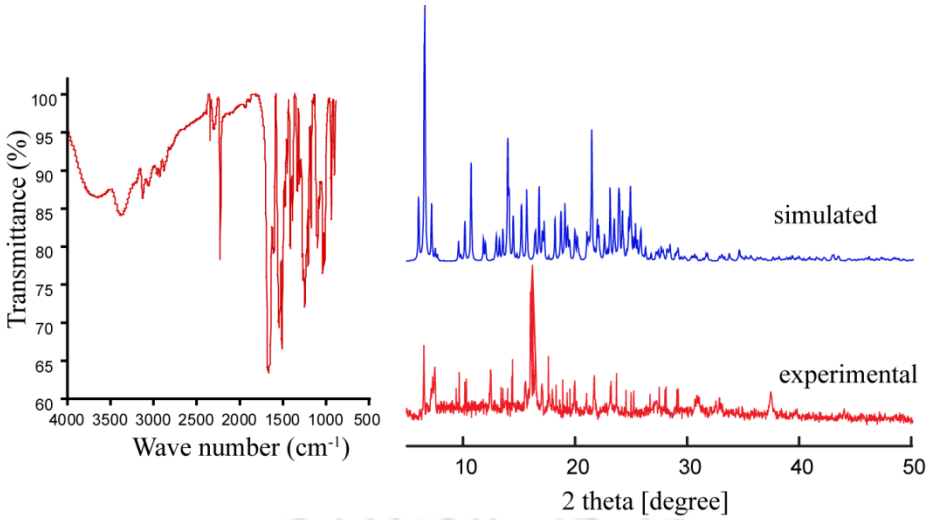

Figure A6.10. FT-IR spectrum of receptor **[$(L_6H)_2$·SIF_6·$4H_2O$·2DMF](6e)** and powder X-ray diffraction: simulated pattern from the single crystal X-ray of **[$(L_6H)_2$·SIF_6·$4H_2O$·2DMF](6e)** (blue), experimental pattern from the crystalline solid (red).

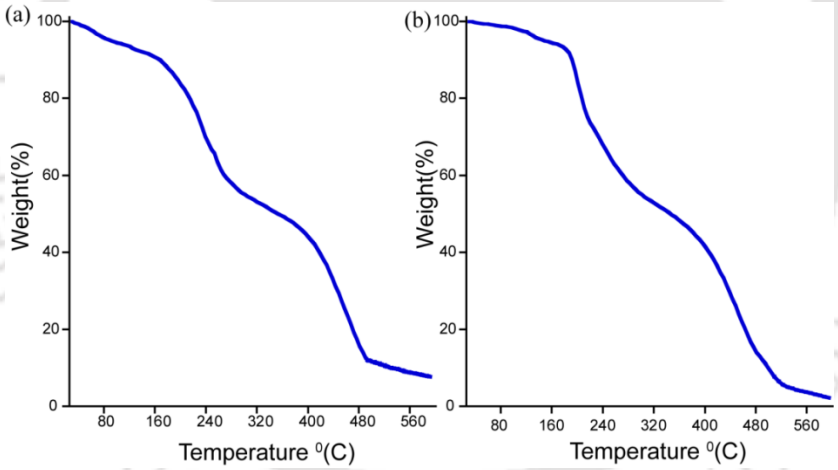

Figure A6.10. (a) Thermogravimetric analysis (TGA) curve of **[L_6H·Br](6b)** at a heating rate of 5 °C per min. Platon/Squeeze was carried out to exclude undefined electrons and to justify the crystallographic findings the TGA experiment was done. Thermal Analysis performed on dried crystals of bromide complex **7**; indicate the loss of two water and two DMF molecules with a weight 15.36 % (Calcd. 16.23 %) as multi-step process from 85 ºC and 185 ºC. (b) Thermogravimetric analysis (TGA) curve of **[L_6H·ClO_4](6d)** at a heating rate of 5 °C per min. Platon/Squeeze was carried out to exclude undefined electrons and to justify the crystallographic findings the TGA experiment was done. Thermal Analysis performed on dried crystals of perchlorate complex **9**; indicate the loss of three water and five DMF molecules with a weight 3.01 % (Calcd. 2.5 %) as multi-step process from 80 ºC and 170 ºC.

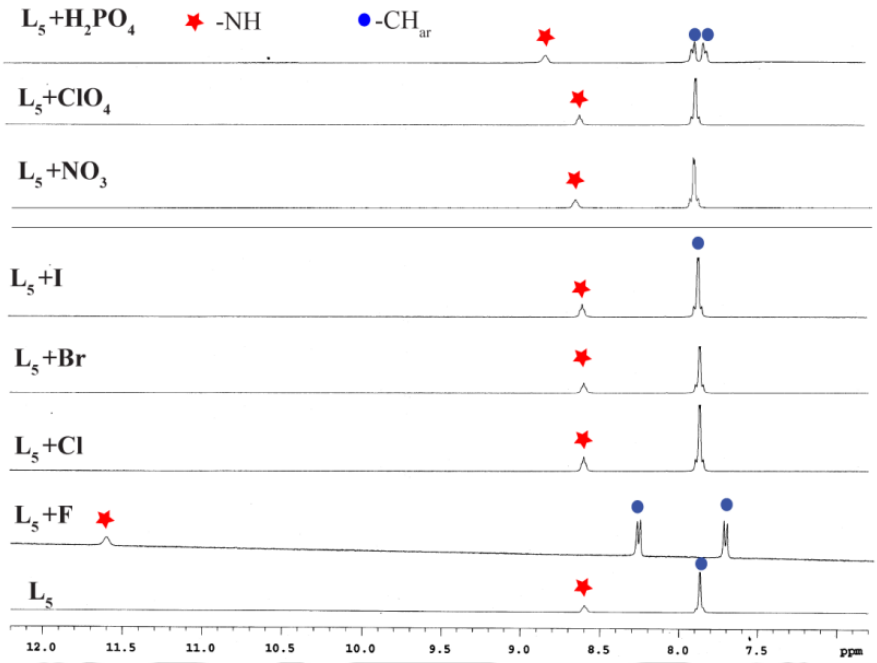

Figure A6.11. Partial ^{1}H NMR spectra in d_6-DMSO showing the maximum observable shifts of amide –NH peak upon the addition of excess (5 equiv.) anions in **L**$_5$.

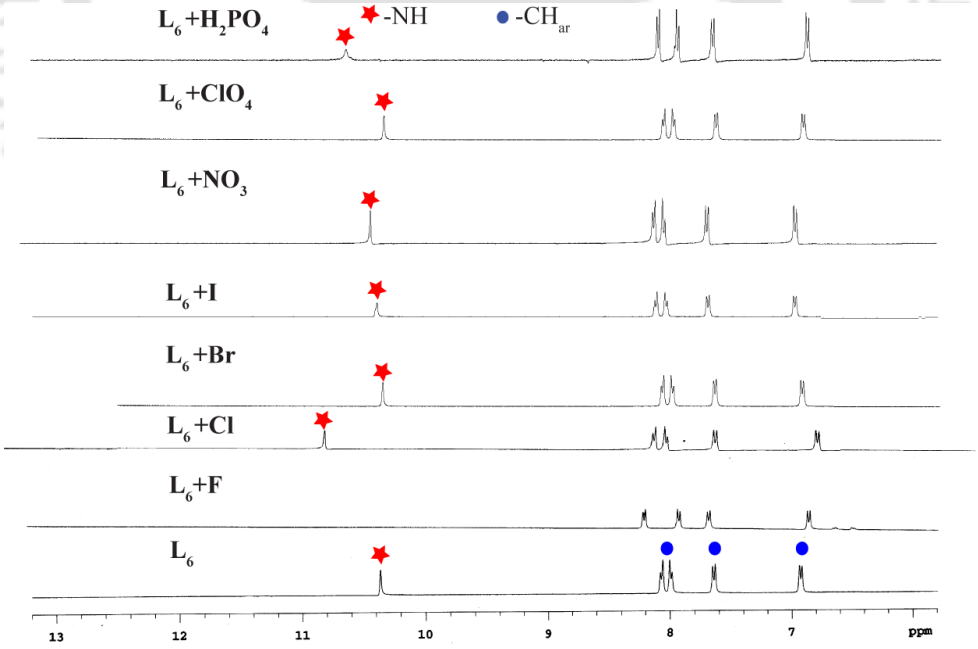

Figure A6.12. Partial ^{1}H NMR spectra in d_6-DMSO showing the maximum observable shifts of amide –NH peak upon the addition of excess (5 equiv.) anions in **L**$_6$.

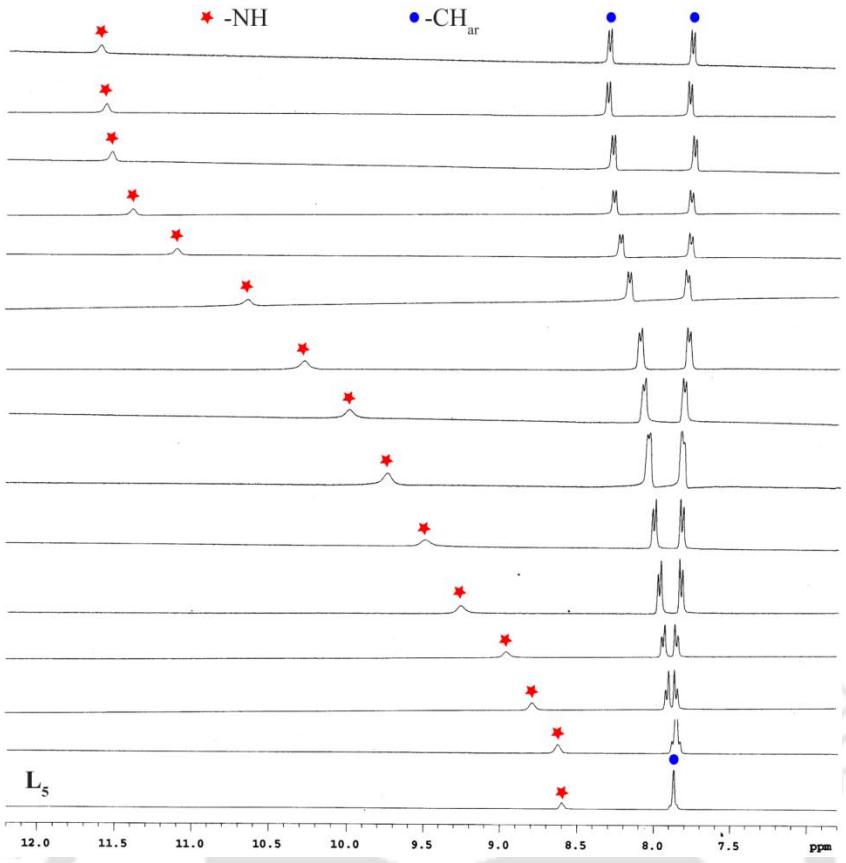

Figure A6.13. Stacking plot showing shift of amide –NH and –CH hydrogen with gradual addition of TBAF solution to **L**$_5$ in DMSO-d_6.

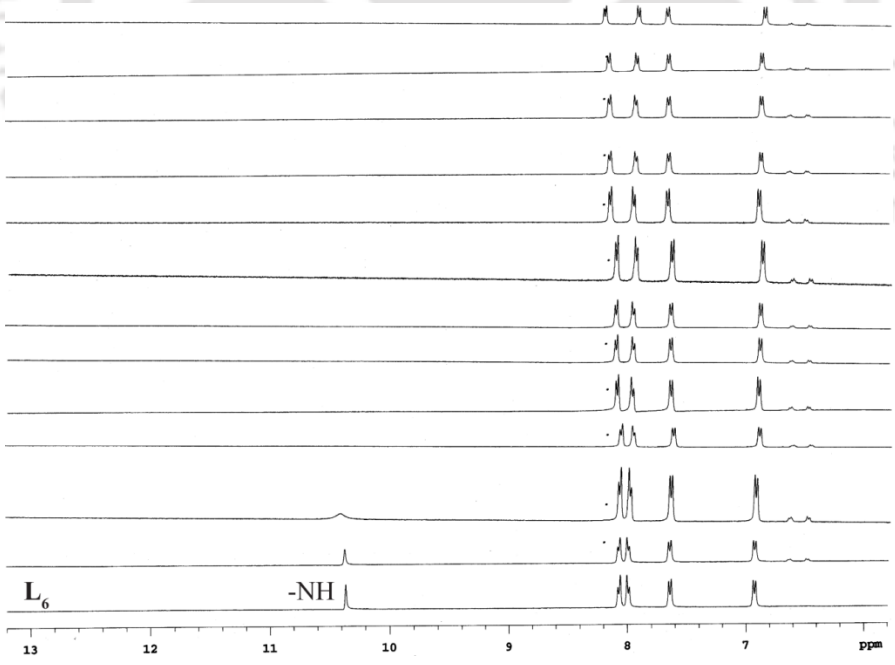

Figure A6.14. Stacking plot showing shift of amide –NH and –CH hydrogen with gradual addition of TBAF solution to **L**$_6$ in DMSO-d_6.

Chapter 7

Hybrid Anion-Water Cluster Mediated Self-Assembly of Tripodal Polyammonium Receptor: Effect of Length of the Receptor

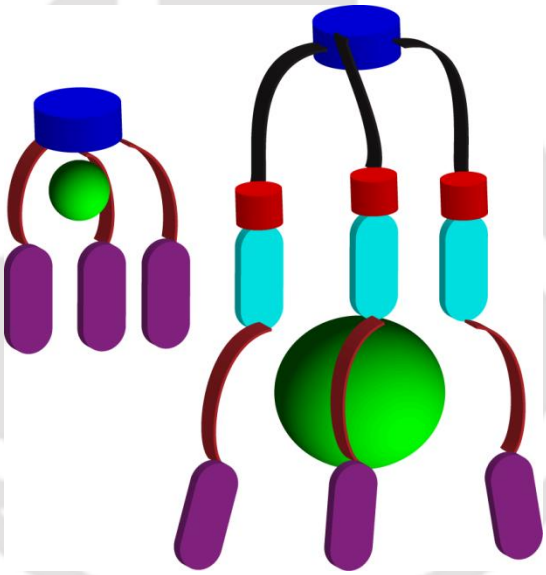

7.1 Back ground and focus on this chapter

Anion complexation by synthetic organic receptors is an admirable field to the researchers.[1] In the past decade intensive research for anions have been elevated due to its imperative role in biological system,[2a,b,c,d] catalysis of reaction,[2e] environmental issue[2f] and atmospheric chemistry.[2g,h,i] Particularly very potential sulfate anion is prevalent in health, energy and industrial environment. Therefore an endeavor study is in progress in haunting of their many structural and physical behaviors. For example the single crystal structure of the sulfate binding proteins (SBP) present in Salmonella typhimurium shows it is seven coordinated and surrounded by neutral environment of five peptide NH groups, one serine –OH group and the indole –NH of the tryptophan side chain, and buried into the hydrophobic cavity of protein.[3] Sulfate anion is troublesome species in nuclear waste and in radioactive waste, also hampers vitrification process hence demands remedy of these pollutant through easily accessible manner.[4] Separation of sulfate anion from aqueous phase is quite challenging as it remains strongly hydrated form owing to high hydration energy of sulfate ion.[5] On the other hand, sulfate is known to cause hardness of water intimidating health issue.[6] An increased understanding of the binding of sulfate anion based on structural data can ultimately aid in addressing the problem of sulfate in the environment. So appropriate modulation of organic hosts for anion complexation would actually help to address these issues. In the deep of design principle, it is considered that anions may be stabilized by electrostatic interaction and H-bonding or both simultaneously. Recently emerging techniques for anion complexation involved mainly ammonium, amide, urea and thio-urea as a binding sites.[7] As an example, it is already proven that sulfate ion shows maximum twelve coordination for what plethora reports are available on urea or thio-urea containing receptors including our effort.[8] But the special design of receptor which ensure electrostatic interaction along with H-bonding might be playing important impact on reducing the demand of maximum number H-bonding sites.

7.2 Structural aspect of anion binding with first (L_7) and second (L_8) generation chlorophenyl substituted tripodal amines

Two tripodal receptors were synthesized by reacting *p*-chlorobenzaldehyde with two tripodal amine platform different in arm length by a simple Schiff base reaction in methanol followed by $NaBH_4$ reduction which resulted first and second generation tripodals **L_7** and **L_8** respectively. The X-ray mountable single crystals were grown from slow evaporation of MeOH or DCM-MeOH mixture over 2-3 weeks at low temperature.

Two receptors are different only in the length of tripodal arms which subsequently generates two cavities of having varied size. Both the receptors form C_{3v} arrangement of arms and very sweetable for anion encapsulation. Receptors are enriched with polyammonium groups as H-bonding sites and positive charge also strong enough to stabilize anion within the cavity. The first generation tripodal **L_7** on treatment with hydrofluoric acid form unimolecular capsule of fluoride ion. Whereas the extended second generation tripodal **L_8** on treatment with sulfuric acid due to lager cavity size form unimolecular capsule of hydrogen sulfate dimer. Moreover the receptor **L_8** stabilize a hydrogen bonded discrete hydrogen sulfate-water cluster $[(HSO_4)\text{-}(H_2O)]_4^{4-}$. In all cases anions are stabilized by N−H···anion and C−H···anion interactions. Therefore at end we have drawn a fair comparison of cavity induced anion encapsulation by two tripodal receptors.

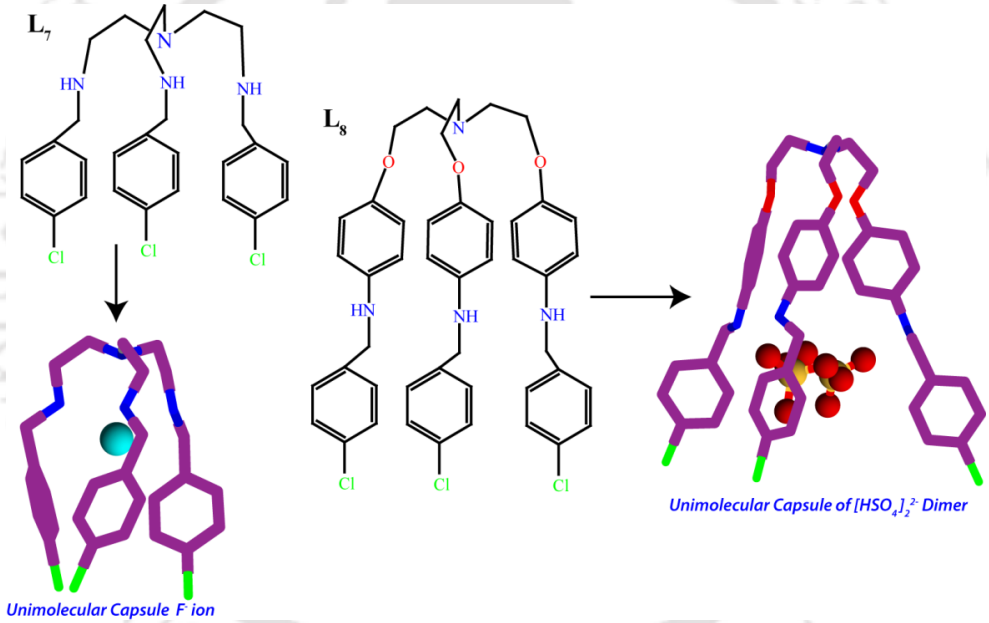

Scheme 7.1 Schematic representation of two receptors and cavity induced unimolecular capsular complex.

7.3.1 Structural description of $[L_7H_3{\cdot}F_3]$(7a)

The fluoride complex **7a** of first generation tripodal crystallizes in a monoclinic crystal system with a *R3* space group. The asymmetric unit of complex **7a** contains one third of $\mathbf{L_7H_3^{3+}}$ and three fluoride ions. All basal three N-atom is tri-protonated and tripodal contains a C_{3v} symmetry passing through apical N-atom. Among six ammonium hydrogen (NH_2^+) three are pointed towards the cavity and remaining three left outside of the cavity. The average bond distance between the bridgehead N-atom and the adjacent carbon atom is 1.470 Å which is very close to the average N−C bridgehead bond distance observed in free receptor (1.478 Å).[9] It is also evident from the literature that when the bridgehead

nitrogen in tren based systems is in the unprotonated state the average N−C distance ranges from 1.46 to1.48 Å.[9] This clearly indicates that the bridgehead nitrogen in **7a** is in the unprotonated state and all the three secondary N-atoms are in protonated form to satisfy the overall trinegative charge, though potentially four protonating sites are available in the receptor. Among three one fluoride ion is perfectly situated within the

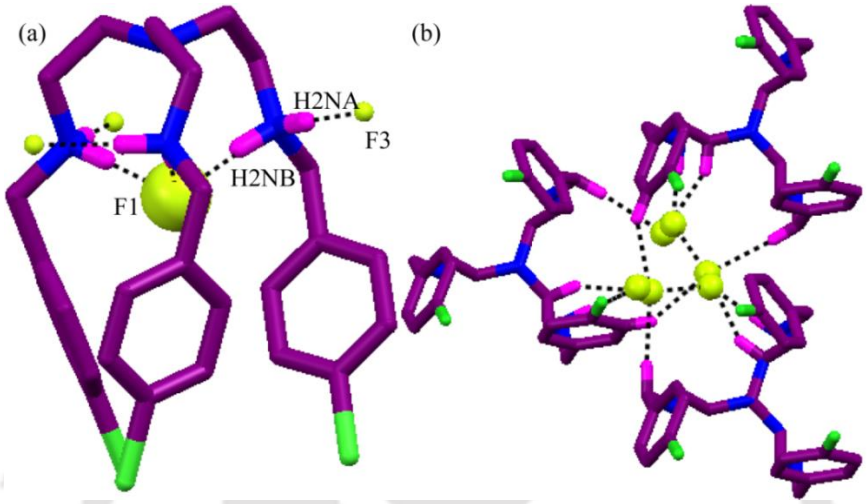

Figure 7.1 (a) Unimolecular capsule of fluoride ion (spacedfill) and H-bonding interaction of *exo* and *endo*-oriented ammonium hydrogen ($-NH_2^+$) with fluoride ions in complex **7a**. (b) Fluoride chain is H-bonded aliphatic, aromatic and ammonium hydrogens.

cavity and stabilized by three N−H···F^- H-bonding as shown in Figure 7.1a. The contact between basal nitrogen and encapsulated fluoride atom N2···F1 is 2.613(3) Å. The another fluoride ion F3 is H-bonded with *exo*-oriented ammonium hydrogen N2···F3 = 2.682(5) Å. F3 ion is tricoordinated as other two contacts comes from fluoride halogen bond F2···F3 = 2.512(3) Å. The third fluoride ion F2 is pentacoordinated from the contribution of two F···F and three C−H···F contacts.[10] A coiled like halogen bonded fluoride chain is expressed through the cationic tripodal as explained in Figure 7.1b. The packing diagram of viewed down *a* axis is depicted in Figure A7.9 shows exterior fluoride ions are surrounded by fluoride encapsulated cationic tripodal.

7.3.2 Structural description of $[L_8H_4{\cdot}4HSO_4{\cdot}2H_2O]$(8a)

Complex **8a** crystallizes in the triclinic space group $P\bar{1}$. Single crystal X-ray analysis revealed that the asymmetric unit contains one C_{3v} symmetric tetraprotonated $\mathbf{L_8}$, four hydrogen sulfate ions and two crystallized water molecules. The apical N-atom is protonated and stabilized by hydrogen bonding with ethereal oxygen (the average $N_{apical}\cdots C_{alp}$ = 1.507 Å> 1.478 Å also support apical N-atom protonation).[9] This type of polyamine system shows general tendency to form both HSO_4^- and SO_4^{2-} species,[11]

though in this particular case we observed all are HSO_4^- ions (total four anions for one tetra-positive cationic receptor). Interestingly, two HSO_4^- ion resides inside the cavity, whereas two others lie outside of the cavity interacts with water molecules. Intramolecular $C-H_{ar}\cdots\pi$ interactions present in first generation part (phenyl ring next to ethereal oxygen), whereas there is no such interactions in second generation part (phenyl ring next to ammonium function) as the arms are well separated away to create enough cavity for anions. It is evident from crystal structure that the $HS(4)O_4^-$ and $HS(2)O_4^-$ are H-bonded each other through O20 in bifurcated manner with O11 and O12 of $HS(2)O_4^-$ (O20···O11 = 2.680(1) Å and O20···O12 = 2.970(1) Å) forming $(HSO_4^-)_2$ dimer which is trapped inside the cavity of the protonated receptor as explained in Figure 7.2a. One sulfate ion $HS(4)O_4^-$ of the dimer exactly lie on the C_{3v} symmetric apical N-atom. H-atom of the protonated secondary N-atom are equally distributed inside (three H-atom) and outside of the cavity (remaining three). The dimer of such big tetrahedral anions is favored inside the cleft due to N–H···O, C–H···O H-bond and electrostatic interactions. These interactions

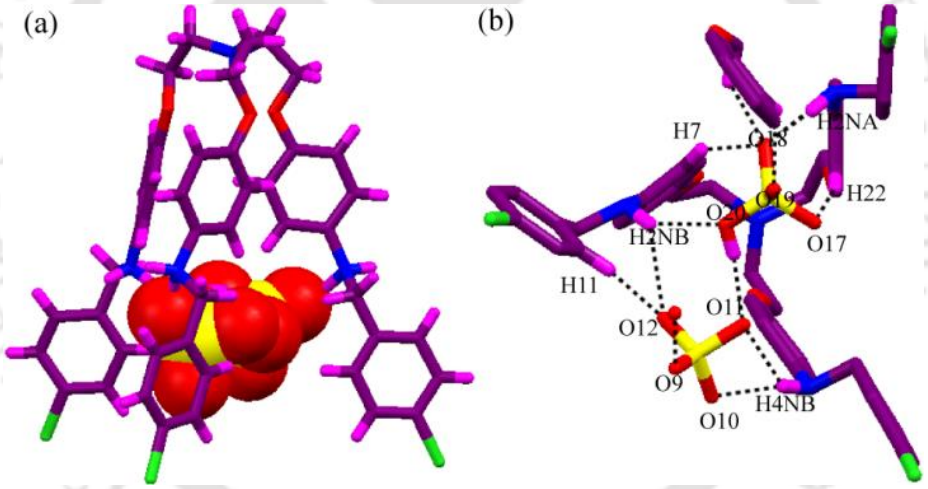

Figure 7.2 (a) Unimolecular capsule of hydrogen sulfate dimer $[HSO_4^-]_2$ by protonated second generation L_8 in complex **8a**. (b) Top view showing H-bonding interactions around encapsulated dimer.

commensurate the anion-anion repulsion between two closely bound anions (e.i HSO_4^- dimer) and stabilized it inside the cavity. The dimer could not utilize all six available NH_2^+ hydrogen as three of them pointed out side and interacts with additional HSO_4^- ion and crystalized water molecule. Therefore coordination of sulfate ion is maximized with the help aliphatic and aromatic hydrogen. Examining coordination environment of the $HS(2)O_4^-$ ion in dimer indicates that it is octacoordinated and served by three N–H···O (N···O =), one Ow–H···O, two O–H···O, one C_{ar}–H···O and one C_{alp}–H···O H-bonding. The $HS(4)O_4^-$ is also octacoordinated. The $HS(4)O_4^-$ is surrounded by two N–H···O, two

O−H···O, three C_{ar}–H···O and one C_{alp}–H···O contacts as shown in Figure 7.2b. So at a glance encapsulated HSO_4^- dimer is backed up by several H-bonding coming from five NH···O (2.75 Å to 3.31 Å), six CH···O and four OH···O H-bond. It is noteworthy to mention that HSO_4^- ions in this are octacoordinated or less (two other exterior $HS(1)O_4^-$ and $HS3)O_4^-$ is eight and penta coordinated will be discussed) and remains as a unsaturated coordination. Whereas highest coordination number of sulfate ion is known to have twelve and achieved by MOF functionalized with urea receptor in solid state[12] and organic urea based receptor.[13] So it is the electrostatic interaction between positively

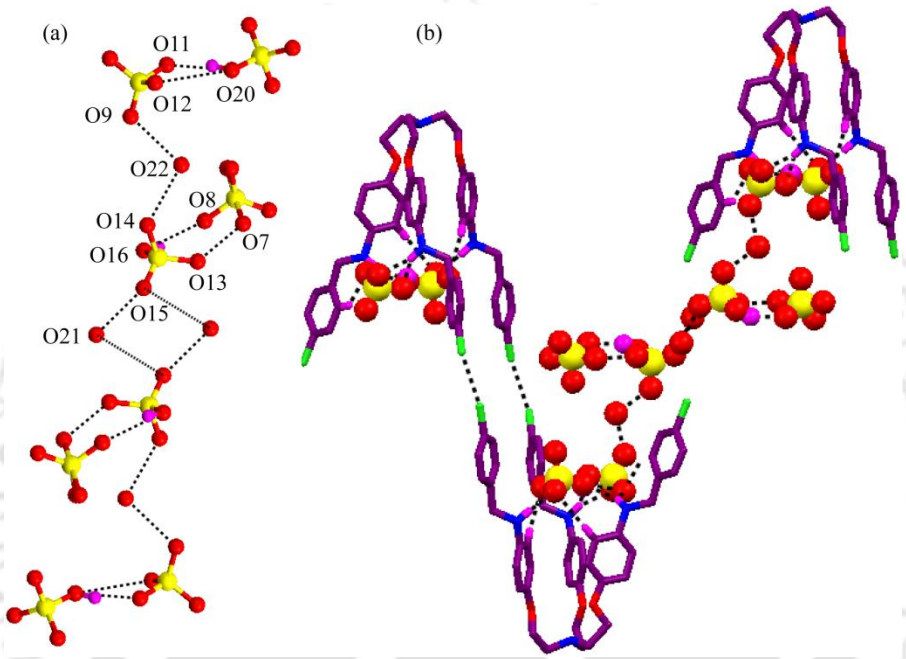

Figure 7.3 (a) Showing big discrete anion-water cluster $[(HSO_4)_8\text{-}(H_2O)_4]^{8-}$ where several hydrogen sulfate dimers are connected by water molecules. (b) Hydrogen sulfate-water and Cl···Cl halogen bonded supramolecular assembly of unimolecular capsule.

charged secondary amine and negatively charged hydrogen sulfate as well as H-bonding stimulate to encapsulate such big dimer of tetrahedral anion inside cavity in spite of being unsaturated in H-bonding. Although solid recognition of hydrogen sulfate by tripodal urea have been reported by A. Hossain and stabilized by seven H-bond but does not form any capsular assembly rather it interacts with urea functionality of side of the ring.[14] The encapsulation of a single sulfate ion is perfectly described by tetrahedral metal-organic cage.[15] There are few fascinating design for encapsulation of sulfate by macrocyclic receptors which provides enough cavity for sulfate anion in acidic and neutral medium.[7a] In all cases a single sulfate ion is trapped and stabilized by only H-bonding or both H-bonding and electrostatic interaction. With the best of our knowledge till date no report on

encapsulation hydrogen sulfate dimer by synthetic receptor.[16] So from the report of solid state recognition of tetrahedral oxyanion, we can conclude that encapsulation of hydrogen sulfate dimer by the extended second general tripodal is not known previously. The versatility of big cavity formation by elongated second generation tripodal is well utilized by encapsulation of halide-water tetramer followed by another report urea based receptor for encapsulation of hydrogen phosphate and carbonate anion.[17]

By knowing the importance of hydrogen sulfate and its hydrated adduct in the atmospheric aerosol formation, we have got prime opportunity to explore a hybrid cluster formation from hydrogen sulfate and water. As we already mentioned, apart from encapsulated dimer $(HSO_4^-)_2$, two exterior HSO_4^- take part in giving interesting out come from the crystal. An inspection in crysllographic analysis shows that water molecules and two exterior HSO_4^- are associated *via* typical H-bonding, give rise to big anion-water cluster $[(HSO_4)\text{-}(H_2O)]_4^{4-}$ as highlighted in Figure 7.3a. The sulfate ions $HS(1)O_4^-$ and $HS(3)O_4^-$ outside of the cavity are octa and penta coordinated, the coordination sphere are filed up by N−H···O, O−H···O, Ow−H···O and $C_{ar/alp}$−H···O H-bond. Detailed study indicates the water molecule O22w acts bridging between two $HS(2)O_4^-$ and $HS(3)O_4^-$ ion in which one is encapsulated, other $HS(3)O_4^-$ form a cyclic dimer motif $[HS(1)O_4^-\text{-}HS(3)O_4^-]$. The interaction in dimer between two HSO_4^- ion is favored by O7···O13 = 2.340(2) Å, O16···O8 = 2.890(2) Å. This dimer is different from encapsulated one, where two HSO_4^- ion is connected by single OH···O H-bond. Hence structural motif is observed in the dimer can be denoted as $R_2^2(8)$. Though we could not add H-atom on water molecules, this notation might help to understand donor acceptor nature of atoms present in the ring. An equivalent of the dimer $[HS(1)O_4^-\text{-}HS(3)O_4^-]$ motif is inversely related with another one. Two sets of sulfate dimer (encapsulated dimer and exterior dimer) is bridged by water molecule O22w and form pentamer. Two such sulfate-water pentamer finally connected by another water molecule Ow21 forming a big discrete anion-water $[(HSO_4)_8\text{-}(H_2O)_4]^{8-}$. It is very fascinating that the $[(HSO_4)_4\text{-}(H_2O)_2]^{4-}$ cluster is connected with the unimolecular capsule through water molecule O21w from its both ends and help to build capsular assemblies of the protonated tripodal receptor. Very interestingly, self-assembly of the unimolecular capsule is also favored by two Cl···Cl halogen bonds having contact 3.385(5) Å. Hence self-assembly process is processed along *c* axis in two fashion, the unimolecular capsule is connected by Cl···Cl halogen bond and $[(HSO_4)\text{-}(H_2O)]_4^{4-}$ cluster in as explained Figure 7.3b.

7.4 Thermogravimetric analysis

Binding strength of water molecule in the highly ionic environment of the tripodal receptor, number of water molecule present in the system and thermal stability of the different complexes was investigated by thermogravimetric analysis (Figure A7.8) and differential scanning calorimetry (DSC) experiment (Figure A7.). The fluoride complex **7a** as expected did not show any weight loss at the region of 100-150 °C, except decomposition of the salt at 240 °C. The hydrogen sulfate complex **8a**, exhibited continuous weight loss (for five water molecules) up to ~180 °C, there is a weight loss of 7.80% which matches very well with calculated value 7.04% corresponding to five water molecules. These characteristic peaks were also appeared in the respective DSC plot.

Conclusions

In summary, this chapter sounds profoundly the art in receptor design for encapsulating of anion of different shape and size. Our structural demonstration emanates few eye catching features in context of supramolecular chemistry. A comparative solid state anion binding shows the first generation tripodal $\mathbf{L_7}$ owing to have smaller cavity encapsulate small anion like fluoride, whereas second generation tripodal $\mathbf{L_8}$ able to trap bigger anion like sulfate. We have transformed first to second generation tripodal for creating ample space for anions eventually bigger anions. Choosing of polyammonium functionality allows presence of multiple anions, and offers electrostatic and H-boning interaction. Indeed, as per our assumption, among four anions two hydrogen sulfate anion is well seated as a dimer giving a unimolecular capsular complex $(HSO_4)_2\subset{}^{2}$**L-Cl**. whereas $\mathbf{L_7}$ forms unimolecular complex of one single fluoride ion $F\subset{}^{1}$**L-Cl**. two exterior anions give us anion-water structural relationship through solid state recognition of big discrete anion-water cluster$[(HSO_4)_8\text{-}(H_2O)_4]^{8-}$. The cluster also plays an important of supramolecular aggregation of the unimolecule capsule along with Cl···Cl halogen bond. The trapping of environmentally hazard sulfate ion by synthetic receptor and hydration of sulfate anions might be helpful to understand many environmental and biological causes.

References

1. (a) Gale, P. A. *Chem. Soc. Rev.* **2010**, *39*, 3746. (b) Sessler, J. L.; Gale, P. A.; Cho, W. S. *Anion Receptor Chemistry; Royal Society of Chemistry*: *Cambridge*, **2006**. (c) Gale, P.A.; Busschaert, N.; Haynes, C. J. E.; Karagiannidis, L. E.; Kirby, I. L. *Chem. Soc. Rev*., **2014**, *43*, 205. (d) Dutta, R.; Ghosh, P. *Chem. Commun.* **2014**, *50*, 10538. (e) Gale, P. A.; Busschaert, N.; Haynes, C. J. E.; Karagiannidis, L. E.; Kirby, I. L. *Chem. Soc. Rev.* **2014**, *43*, 205. (f) Hay, B. P. *Chem. Soc. Rev*. **2010**, *39*, 3700. (g) Custelcean, R. *Chem. Soc. Rev*. **2010**, *39*, 3675.
2. (a) Davis, J. T.; Okunola, O.; Quesada, R. *Chem. Soc. Rev.* **2010**, *39*, 3843. (b) Busschaert, N.; Wenzel, M.; Light, M. E.; Hernández, P. I.; Tomás, R. P.; Gale, P. A. *J. Am. Chem. Soc*. **2011**, *133*, 14136. (b) Cametti, M.; Rissanen, K. *Chem. Commun.* **2009**, 2809. (c) Krik, K. L. *Biochemistry of Halogens and Inorganic Halides, Plenum Press, New York*, **1991**. (d) Kleerekoper, M. *Endocrinol. Metab. Clin. North Am.* **1998**, *27*, 441. (e) Siddiqui, Z. N.; Khan, K. *ACS Sustainable Chem. Eng*. **2014**, *2*, 1187. (f) Eller, R.; Stepien´, M.; Fowler, C. J.; Lee, J. T.; Sessler, J. L.; Moyer, B. A. *J. Am. Chem. Soc.* **2007**, *129*, 11020. (g) Yu, F. Q.; Turco, R. P. *Molecular Clusters to Nanoparticles: Role of Ambient Ionization in Tropospheric Aerosol Formation.* (h) Yu, F.; Turco, R. P. *J. Geophys. Res. Atmos.* **2001**, *106*, 4797. (i) Lee, S. H.; Reeves, J. M.; Wilson, J. C.; Hunton, D. E.; Viggiano, A. A.; Miller, T. M.; Ballenthin, J. O.; Lait, L. R. *Science*. **2003**, *301*, 1886.
3. Pflugrath, J. W.; Quiocho, F. A. *Nature.* **1985**, *314*, 257.
4. (a) Research Needs for High-Level Waste Stored in Tanks and Bins at U.S. Department of Energy Sites, National Research Council, National Academy Press, **2001**, p. 55 B. (b) Moyer, B. A.; Custelcean, R.; Hay, B. P.; Sessler, J. L.; Bowman-James, K.; Day, V. W.; Kang, S. O. *Inorg. Chem.* **2013**, *52*, 2473. (c) Rajbanshi, A.; Moyer, B. A.; Custelcean, R. *Cryst. Growth Des*. **2011**, *11*, 2702.
5. (a) Weinga¨rtner, H.; Franck, E. U.; Wiegand, G.; Dahmen, N.; Schwedt, G.; Frimmel, F. H.; Gordalla, B. C.; Johannsen, K.; Summers, R. S.; Ho¨ll, W.; Jekel, M.; Gimbel, R.; Rautenbach, R.; Glaze, W. H. *Ullman's Encyclopedia of Industrial Chemistry*, Wiley-VCH Verlag GmbH & Co., **2000**.
6. Heizer, W. D.; Sandler, R. S.; Seal, E.; Murrai, S. C.; Busby, M. G.; Schliebe, B. G.; Pusek, S. N. *Dig. Dis. Sci*. **1997**, *42*, 1055.
7. (a) Kang, S. O.; Hossain, M. A.; Powell, D.; Bowman-James, K. *Chem. Commun*., **2005**, 328. (b) Jose, D. A.; Kumar, D. K.; Ganguly, B.; Das, A. *Inorg. Chem.* **2007**, *46*, 5817.
8. Basu, A.; Das, G. *Dalton Trans.* **2012**, *41*, 10792.
9. Bose, P.; Ravikumar, I.; Ghosh, P. *Inorg. Chem*. **2011**, *50*, 10693.
10. Barcelo-Oliver, M.; Estarellas, C.; Garcia-Raso, A.; Terron, A.; Frontera, A.; Quinonero, D.; Mata, I.; Molins, E.; Deya, P. M. *CrystEngComm*. **2010**, *12*, 3758.
11. Hoque, M. N.; Basu, A.; Das, G. *Cryst. Growth Des*. **2012**, *12*, 2153.
12. Custelcean, R.; Moyer, B. A.; Hay, B. P. *Chem. Commun.* **2005**, *48*, 5971.
13. (a) Custelcean, R.; Remy, P.; Bonnesen, P. V.; Jiang, D.; Moyer, B. A. *Angew. Chem. Int. Ed*. **2008**, *47*, 1866. (b) Custelcean, R.; Bock, A.; Moyer, B. A. *J. Am. Chem. Soc.* **2010**, *132*, 7177.
14. Pramanik, A.; Thompson, B.; Hayes, T.; Tucker, K.; Powell, D. R.; Bonnesen, P. V.; Ellis, E. D.; Lee, K. S.; Yu, H.; Hossain, M. A. *Org. Biomol. Chem.*, **2011**, *9*, 4444.
15. (a) Yi, S.; Brega, V.; Captaina, B.; Kaifer, A. E. *Chem. Commun*., **2012**, *48*, 10295. (b) Custelcean, R.; Bonnesen, P. V.; Duncan, N. C.; Zhang, X.; Watson, L. A.; Berkel, G. V.; Parson, W. B.; Hay, P. B. *J. Am. Chem. Soc.* **2012**, *134*, 8525.
16. (a) Mendy, J. S.; Pilate, M. L.; Horne, T.; Day, V. W.; Hossain, M. A. *Chem. Commun*. **2010**, *46*, 6084. (b) Kang, S. O.; Day, V. W.; Bowman-James, K. *Org. Lett.* **2009**, *11*, 16.
17. (a) Basu, A.; Das, G. *Chem. Commun*., **2013**, *49*, 3997. (b) Basu, A.; Das, G. *J. Org. Chem.*, **2014**, *79*, 2647.

Annexure VII

Table 7.1 Crystallographic parameters and refinement details.

code name	**7a**	**8a**
empirical formula	$C_{27}H_{39}Cl_3N_4F_3$	$C_{13}H_{20}I_2N_6O_4$
formula weight	579.96	1224.56
cryst syst	rhomohedral	triclinic
a (Å)	15.1048(4)	12.0514(14)
b (Å)	15.1048(4)	12.9761(15)
c (Å)	12.2144(6)	19.1248(18)
α (degree)	90.00	83.526(8)
β (degree)	90.00	88.508(8)
γ (degree)	120.00	75.854(10)
V ($Å^3$)	2413.42(15)	2881.6(5)
space group	*R 3*	*P-1*
Z value	3	2
ρ(cal)(g/cm^3)	1.354	1.406
μ(Mo Kα) (mm^{-1})	0.349	0.380
T(K)	298(2)	298(2)
R1; wR2 (I> 2 σ(I))	0.349; 0.0788	0.1149; 0.2834
R1; wR2(all)	0.0489; 0.0852	0.2354; 0.3284
Residual electron density(e/Å)	0.305	0.086
good-of-fit	1.060	0.970
reflection collected	1946	14972
Independent reflection	1438	8695
CCDC No.	1061889	1061890

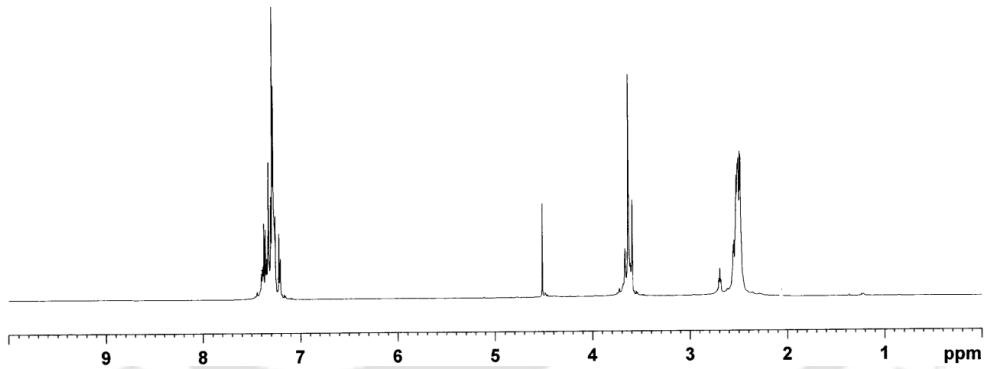

Figure A7.1. ^{1}H NMR spectrum of receptor **L_7** in DMSO-d_6 at 298 K.

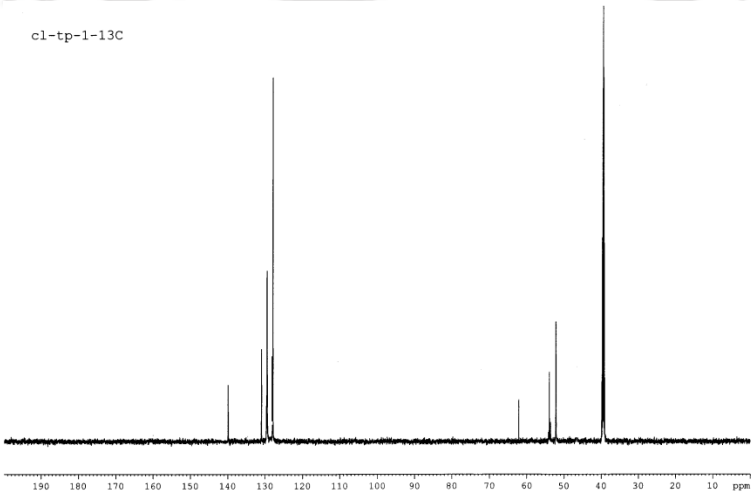

Figure A7.2. ^{13}C NMR spectrum of receptor **L_7** in DMSO-d_6 at 298 K.

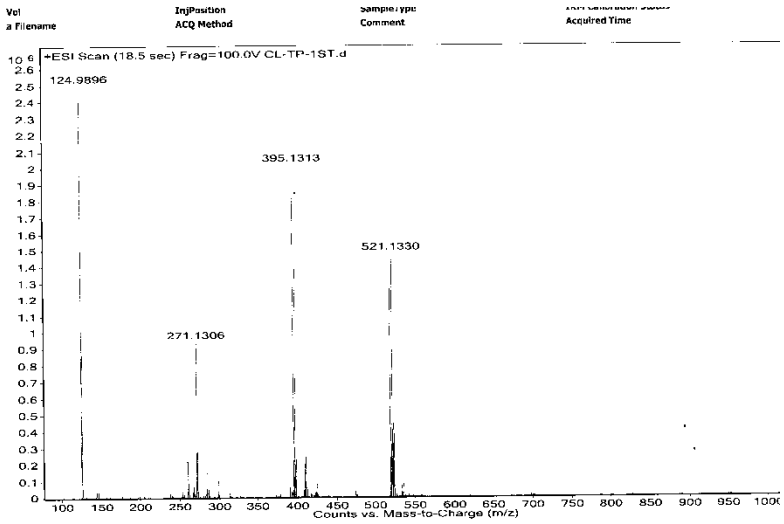

Figure A7.3. ESI mass spectra of $\mathbf{L_5}$.

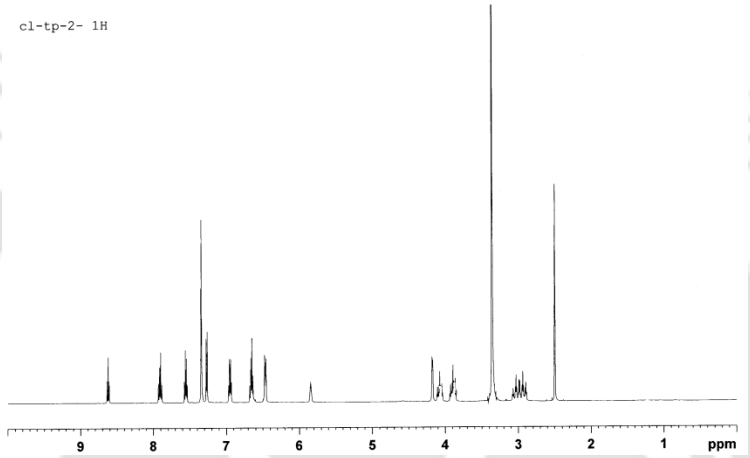

Figure A7.4. ^{1}H NMR spectrum of receptor $\mathbf{L_8}$ in DMSO-d_6 at 298 K.

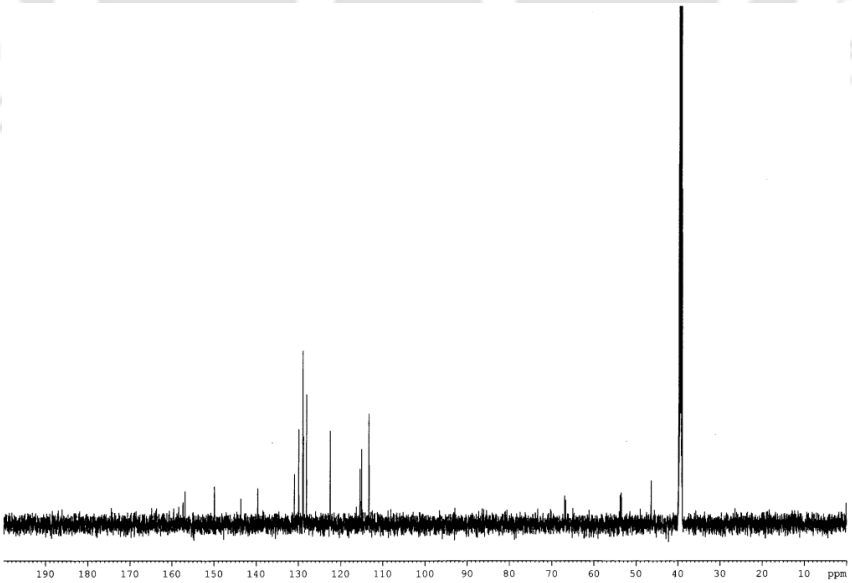

Figure A7.5. ^{13}C NMR spectrum of receptor $\mathbf{L_7}$ in DMSO-d_6 at 298 K.

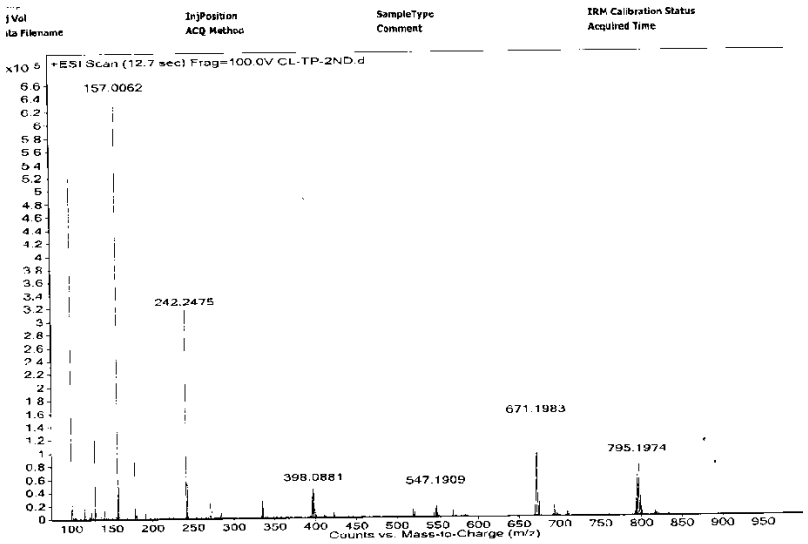

Figure A7.6. ESI mass spectra of $\mathbf{L_8}$.

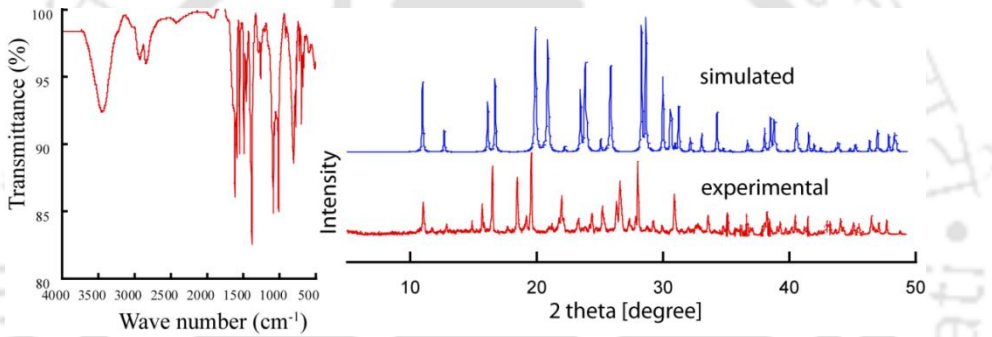

Figure A7.6. FT-IR spectrum of receptor $\mathbf{L_7}$ and powder X-ray diffraction: simulated pattern from the single crystal X-ray of $\mathbf{L_7}$ (blue), experimental pattern from the crystalline solid (red).

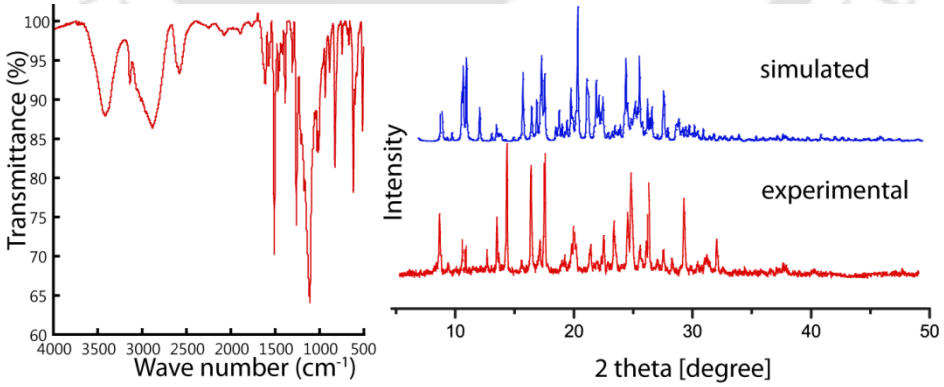

Figure A7.7. FT-IR spectrum of receptor $\mathbf{L_8}$ and powder X-ray diffraction: simulated pattern from the single crystal X-ray of $\mathbf{L_8}$ (blue), experimental pattern from the crystalline solid (red).

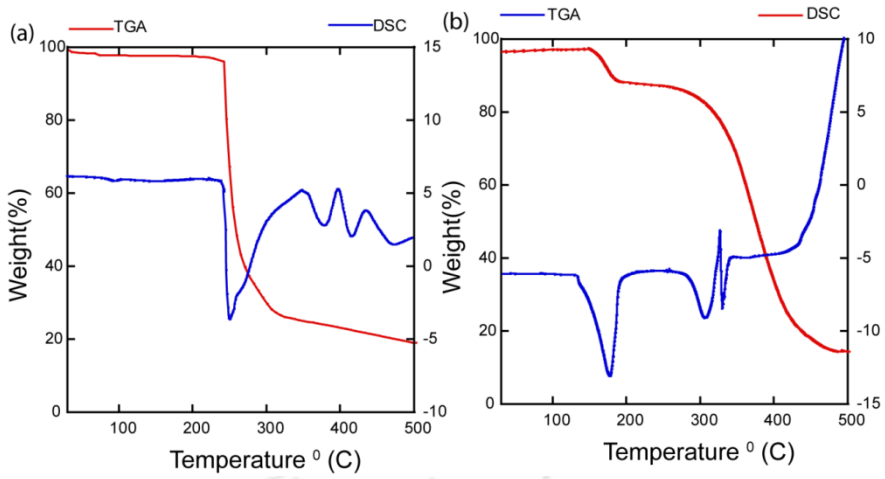

Figure A7.8. Thermogravimetric analysis (TGA) and differential scanning calorimetry curve of (a) **[$L_7H_3 \cdot F_3$](7a)**, (b) **[$L_8H_4 \cdot 4HSO_4 \cdot 2H_2O$](8a)** at a heating rate of 5 °C per min.

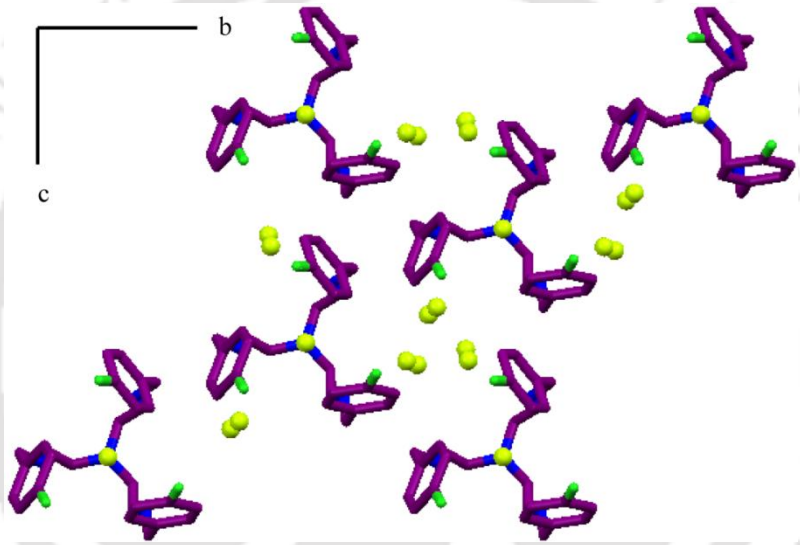

Figure A7.9. Packing diagram in fluoride complex **[$L_7H_3 \cdot F_3$](7a)**.

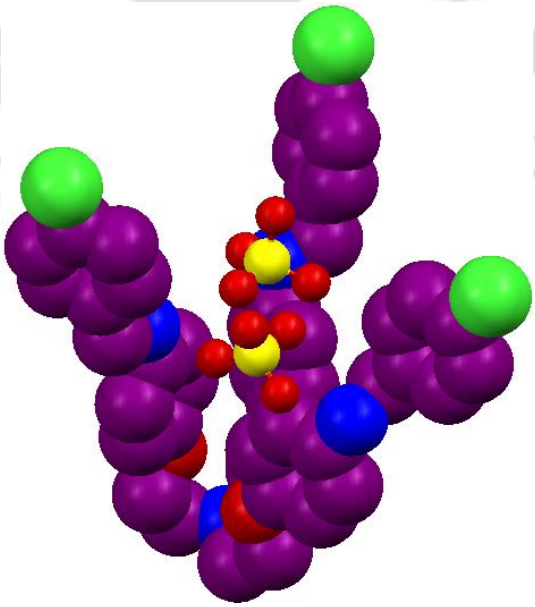

Figure A7.10. Encapsulation of hydrogen sulfate dimer within the enlarged cavity of second generation tripodal **L_8** in complex **[$L_8H_4 \cdot 4HSO_4 \cdot 2H_2O$](8a)**.

Conclusion and Future Directions

In this thesis, artificial receptors for anions and hydrated anions have been investigated extensively based on N–H fragments, mostly from urea derivatives; ring substituted (benzimidazole), polyamine ($-NH_2$), and amides. The newly synthesized acyclic receptors (**L_1-L_8**) containing these fundamental anion binding sites were explored very well for identification of anion-water structural relationship. In addition the present findings also establish anion-water cluster induced formation of capsular, pseudo-capsular and polymeric assembly of the studied receptor molecules. The effectiveness of the design approach has been established in several cases to function as efficient hosts for anions or hydrated anions.

Pyridine-urea based three isomeric receptors ($^{O}\mathbf{L_1}$, $^{m}\mathbf{L_1}$, and $^{p}\mathbf{L_1}$) shows pyridine directed diverse anion and anion-water clusters formation of spherical, planar, tetrahedral and octahedral anions. Various orientation of urea hydrogen is observed in three isomers. The success of the urea subunit as a receptor may depend upon the fact that it possesses two close N–H fragments, which can chelate a spherical ion or establish two parallel H-bonds with two oxygen atoms of an inorganic oxyanion. Anion complexes of these receptors crystallize with water molecule and generates cyclic anion-water motif or anions (hydrogen phosphate) self-aggregated formed anionic cluster.

An interesting design of benzimidazole appended apical N-atom (**L_2**) and benzene cap (**L_3**) bowl shape tripodal receptors generate wide variety anion-water assemblies just on the basis of basal structure. Both the receptors have multiple protonation sites and able to create highly ionic environment. The apical N-atom based tripodal generated isostructural halide-water clusters. Whereas when the basal structure changed to planar cap the solid state crystal structure shows it forms non-isostructural halide complexes. In this case benzimidazole NH plays active role in stabilization of anion-water adducts.

The newly synthesized C_{3v} symmetric polyamine tripodal receptor **L_4** has been devoted to employing the anion/anion-water induced capsular and non-capsular assembly. The cationic tripodal generates multiple anions and with some crystalized water molecules produce various anion-water structural motif which could very helpful in predicting hydration nature of anions. Very interesting the receptor is capable of forming new types cluster assembly of anions like $H_2PO_4^-$ and ClO_4^- anions. Anion-water belt induced

stitching of two cationic receptors in capsular/non-capsular fashion is the interesting outcome.

The extension of the receptor **L_4** to a second generation tripodal **L_6** and another synthesis of first generation tripodal amides **L_5** establishes the cavity induced anion recognition. The **L_5** in protonated state forms C_{3v} symmetric cavity, but intramolecular H-bonding between amide NH and –CO group makes it unavailable for anion binding. Therefore it shows side cleft anion binding. Whereas **L_6** such intramolecular is absent as the primary anion binding is moved to distant position. Hence a pseudo-capsular binding of anion is observed by C_{2v} symmetric tripodal. Interestingly, **L_6** in presence SiF_6^{2-} anion folded conformation giving C_{3v} symmetric cavity. This observation accounts the anion induced conformation of the receptor **L_6** in protonated state which confirms the adaptability of flexible **L_6** as an anion receptor.

Very impressive synthesis of two closely related tripodal polyamine receptors **L_7** and **L_8** of having various sizes of cavities have successfully exploited for size selective anion encapsulation. The first generation tripodal **L_7** due to having smaller cavity, it forms unimolecular capsule of small anion like F^-. Whereas in second tripodal **L_8** anion binding site is shifted to position in such a way that forms larger cavity which generates unimolecular capsule of big anion like hydrogen sulfate dimer. Additionally, solid state recognition of big discrete anion-water cluster $[(HSO_4)_8\text{-}(H_2O)_4]^{8-}$ is worth of mentioning.

Thus, the thesis demonstrates some many advances in the area of supramolecular chemistry of anionic species and related subjects. The recognition of anions and hydrated anions with in molecular assembly/molecular cavity in solid state is definitely a field which can expand considerably in real-world applications, such as sensing, catalysis and the medicinal use of transmembrane anion transport. Thus recognition of different anion-water clusters by capsular assemblies would be useful to develop new generation receptors for anions in their hydrated form. A crucial task for going towards technological applications is the construction of receptors for the recognition of hydrated anions rather than naked anions which could be of better approach to target anions in natural environment. The overall study could inspire the rational design of future receptors for the recognition of anion–water clusters which will be effective from fundamental and an applicative viewpoint.

Najbul Hoque

Academic Summary

2010 - Present	PhD student at Indian Institute of Technology Guwahati, India.
Thesis title:	"An Endeavor in Receptor Design for Solid State Recognition of Anions/Hydrated Anions"
2008-2010:	Masters in Chemistry (Indian Institute of Technology Delhi, New Delhi, 110016, India.
2005-2008:	Graduation (Chemistry), Krishnath College, Kalyani University, West Bengal, India.
2003-2005:	12th (Science), WBCHSE, West Bengal, India, 74.00%.
2003	10th , WBBSE, West Bengal, India, 81%.

Research Interest

Crystal engineering, Supramolecular aspects of the molecular assemblies, Molecular Organization and Recognition of anions/hydrated anions, Aggregation of anion/anion-water cluster, Molecular Capsules, Non-covalent (H-bond, halogen bond, Anion—pi and pi—pi etc) interactions in stabilities of supramolecular complexes, Design of novel crystalline solids for anions.

Research Experience

PhD Research (January 2010 - Present)

Brief Research Topic:

- Synthesis and characterization of novel functionalized organic receptor molecules for anions ranging from spherical to tetrahedral.
- Isomeric linear molecules enriched with H-bond and their typical to anion-water cluster formation.
- N-atom bridge head and benzene cap tripodal (polyammonium) recognizes halide-water cluster and shows influence of ligand structure towards their formation.
- Anion/hydrated anion-water glued capsular and non-capsular assembly of a polyammonium based tripodal and formation pure anion cluster.
- A fine comparison of anion binding by 1st and 2nd generation tripodal amide.
- A fair comparison of cavity induced capsular assembly of polyammonium based 1st and 2nd generation tripodal and recognition of anion-water cluster.

Expertise:

Single crystal X-ray Structure determination, Spectroscopic techniques (UV-Vis, Fluorescence, FT-IR), NMR spectroscopy, mass spectrometry, Thermo gravimetric (TG) and differential scanning calorimetry (DSC) analysis.

Publications

1. Cyclic Pentameric Puckered Hybrid Chloride–Water Cluster $[Cl_3(H_2O)_4]^{3-}$ in the Hydrophobic Architecture.
   Hoque, M. N.; Basu, A.; Das, G. *Cryst. Growth Des*. **2012**, *12*, 2153. ***(Communication)***
2. Structural Insight into the Anion–Water Cluster: Stabilized by Alcohol and Carboxylic Acid Containing Tripodal Ligand.
   Hoque, M. N.; Basu, A.; Das, G. *Supramol. Chem*. **2014**, *26*, 392.
3. Fluorescence Turn on Sensor for Sulfate Ion in Aqueous Medium Using Tripodal-Cu^{2+} Ensemble.
   Hoque, M. N.; Basu, A.; Das, G. *J. Fluo*. **2014**, *24*, 411.
4. Pyridine–Urea-Based Anion Receptor: Formation of Cyclic Sulfate–Water Hexamer and Dihydrogen Phosphate–Water Trimer in Hydrophobic Environment.
   Hoque, M. N.; Basu, A.; Das, G. *Cryst. Growth Des*. **2014**, *14*, 6. ***(Communication)***
5. Cationic Tripodal Receptor Assisted Formation of Anion and Anion–Water Clusters: Structural Interpretation of Dihydrogen Phosphate Cluster and Sulfate–Water Tetramer $[(SO_4)_2–(H_2O)_2]^{4-}$
   Hoque, M. N.; Das, G. *Cryst. Growth Des*. **2014**, *14*, 2962.
6. Hydrated Anion Glued Capsular and Non-capsular assembly of a Tripodal Host: Solid State Recognition of Bromide–Water $[Br_5–(H_2O)_6]^{5-}$ and Iodide–Water $[I_2–(H_2O)_4]^{2-}$ Clusters in Cationic Tripodal Receptor.
   Hoque, M. N.; Das, G. *CrystEngComm*. **2014**, *16*, 4447.
7. Anion Complexation with Cyanobenzoyl Substituted First and Second Generation Tripodal Amide Receptors: Crystal Structures and Solution Studies
   Hoque, M. N.; Gogoi, A.; Das, G. *Dalton Trans*. **2015**, *44*, 15220.
8. Encapsulation of Fluoride and Hydrogen Sulfate Dimer by Polyammonium Functionalized First and Second Generation Tripodal: Cavity Induced Anion Encapsulation
   Hoque, M. N.; U. Manna.; Das, G. *Supramol. Chem*. **DOI**: 10.1080/10610278.2015.1102259.
9. An Aggregation-induced Emission (AIE) Active Probe Renders Al(III) Sensing and Tracking of Subsequent Interaction with DNA.
   Samanta, S.; Goswami, S.; **Hoque, M. N**.; Ramesh, A.; Das, G. *Chem. Commun*. **2014**, *50*, 11833.
10. Implications of Hydrogen/Halogen-Bond in the Stabilization of Confined Water and Anion-Water Clusters by a Cationic Receptor.
    Hoque, M. N.; Das, G. *communicated.*
11. Discrepancy in Anion Coordination Directed by Isomeric Pyridine-Urea Receptors: Solid State Recognition of Hydrated Anions.
    Hoque, M. N.; Das, G. *communicated*.
12. An Upsurge in Solid State Recognition of Hydrated Anions: A Progress and Future Scope
    Hoque, M. N.; Das, G. *Manuscript under preparation*.

Conference

- ***New Directions in Chemical Science (NDCS),*** Indian Institute of Technology Delhi, New Delhi, Dec-2012.
- **Frontiers in Chemical Sciences (FICS),** Indian Institute of Technology Guwahati, Assam, India Dec-2014.